SYNTHESIS AND PHOTOPHYSICAL INVESTIGATIONS OF NOVEL DEEP BLUE TRIPLET EMITTERS BASED ON N-HETEROCYCLIC CARBENE PLATINUM(II) ACETYLIDE COMPLEXES FOR LIGHT EMITTING DEVICES

DISSERTATION

zur

Erlangung der naturwissenschaftlichen Doktorwürde
(Dr. sc. nat.)

vorgelegt der

Mathematisch-naturwissenschaftlichen Fakultät

der

Universität Zürich

von

YUZHEN ZHANG

aus

der V. R. China

Promotionskommittee

Prof. Dr. Heinz Berke (Vorsitz)

Dr. Koushik Venkatesan (Leitung)

Prof. Dr. Roger Alberto

Zürich 2013

SYNTHESIS AND PHOTOPHYSICAL INVESTIGATIONS OF NOVEL DEEP BLUE TRIPLET EMITTERS BASED ON N-HETEROCYCLIC CARBENE PLATINUM(II) ACETYLIDE COMPLEXES FOR LIGHT EMITTING DEVICES

DISSERTATION

zur

Erlangung der naturwissenschaftlichen Doktorwürde
(Dr. sc. nat.)

vorgelegt der

Mathematisch-naturwissenschaftlichen Fakultät

der

Universität Zürich

von

YUZHEN ZHANG

aus

der V. R. China

Promotionskommittee

Prof. Dr. Heinz Berke (Vorsitz)

Dr. Koushik Venkatesan (Leitung)

Prof. Dr. Roger Alberto

Zürich 2013

Die vorliegende Arbeit wurde von der Mathematisch-naturwissenschaftlichen Fakultät der Universität Zürich im Wintersemester 2013 als Dissertation angenommen.

Promotionskomitee: Prof. Dr. Heinz Berke (Vorsitz, Leitung der Dissertation)
Dr. Koushik Venkatesan
Prof. Dr. Roger Alberto

To My family

CONTENTS

List of abbreviations

2-MeTHF	2-methytetrahydrofuran
COD	cyclooctadiene
CV	cyclic voltammetry
dbim	N,N'-didodecyl-benzimidazoline-2-ylidene
DCM	dichloromethane
ddmi	N,N'-didodecyl-imidazoline-2-ylidene
DMF	N,N-dimethylformamide
DSC	differential scanning calorimetry
EL	electroluminescence
EQE	external quantum efficiency
ESI-MS	electrospray ionization mass spectroscopy
ETL	electron transport layer
GC-MS	gas chromatography mass spectroscopy
HOMO	highest occupied molecular orbital
HTL	hole transport layer
Hz	hertz
ibim	N,N'-diisopropyl-benzimidazoline-2-ylidene
IC	inter conversion
IQE	internal quantum efficiency
IR	infrared
ISC	intersystem crossing
LED	light emitting device
LF	ligand field
LMCT	ligand to metal charge transfer
LUMO	lowest unoccupied molecular orbital
Me	methane
MLCT	metal to ligand charge transfer

MO	molecular orbital
NHC	N-heterocyclic carbene
NMR	nuclear magnetic resonance
OLED	organic light-emitting diodes
PhOLEDs	phosphorescent organic light-emitting diodes
pimi	N,N'-dipentyl-imidazoline-2-ylidene
pm2tz	1,1’-dipentyl-3,3’-methylene-di-1,2,4-trizoline-5,5’-diylidene
pm3tz	1,1’-dipentyl-3,3’-methylene-di-1,3,4-trizoline-5,5’-diylidene
pmdb	1,1’-dipentyl-3,3’-methylene-dibenzimidazoline-2,2’-diylidene
pmim	1,1’-dipentyl-3,3’-methylene-diimidazoline-2,2’-diylidene
PMMA	poly(methyl methacrylate)
ppbim	3-pentyl-1-picolylbenzimidazoline-2-ylidene
ppim	3-pentyl-1-picolylimidazoline-2-ylidene
ppm	parts per million
ptrz	N,N'-dipentyl-trizoline-2-ylidene
QY	quantum yield
RT	room temperature
SOC	spin orbital coupling
SOMO	single occupied molecular orbital
TBAP	*tert*-butyl ammonium phosphorate
TCSPC	time correlated single photon counting
TD-DFT	time-dependent density functional theory
TGA	thermogravimetric analysis
UV-Vis	ultraviolet-visible (spectroscopy)
ZFS	zero-field splitting
ν	frequency

Overview of Dissertation

This thesis reports the scientific results done by the author during the four years doctoral studies in the Inorganic Chemistry Institute, University of Zurich. The Chapter 1 provides a short introduction of the history, structures and working principle of phosphorescent organic light-emitting diodes (PhOLEDs). Following this part several examples of triplet blue emitters based on different metals has been reviewed. The last part of this chapter serves up the motivation for the research and the formulation of goals for the thesis. Following this introduction are four subprojects summarized in the format of a mansucript for publication. Chapter 2 illustrates the photophysical investigation of chelated bis-N-heterocyclic carbene (NHC) Pt(II) acetylide complexes. This is the first report on such kind of molecular structures and four of these complexes exhibited triplet blue emission in fluid solution. Encouraged by the interesting results, we probed the influence of *cis* and *trans* configuration of the NHC Pt(II) acetylide complexes on the photophysical properties. Eight triplet blue emitters were obtained and one among them exhibited as high as 80% quantum yield in 10 wt% PMMA film. Elucidation of the mechanism involved in the *cis* to *trans* isomerization under mild reaction conditions and harsh thermal conditions were also carried out. Chapter 4 is focused on evaluation of the electronic influence of the NHC ligand on the quantum efficiencies of triplet blue emitter. After the syntheses and investigation of five group triplet blue emitters bearing electronically different NHCs ligands, we concluded that the electronic of the NHC ligand is crucial to harvest phosphorescence from Pt(II) acetyldie complexes by avoiding the low-lying d-d non-radiative decay. Based on the previous results, Chapter 5 describes our efforts devoted to the design and synthesis of triplet blue emitters with high quantum yields. Ten *cis* and *trans* NHC Pt(II) acetylide complexes bearing N,N'-dipentyl-trizoline-2-ylidene, N,N'-dipentyl-imidazoline-2-ylidene and N,N'-didodecyl-imidazoline-2-ylidene were synthesized and two *trans* isomers bearing N,N'-dipentyl-trizoline-2-ylidene exhibited blue emission with a quantum yield of 82%. All the results are summarized in Chapter 6 and the thesis is concluded with acknowledgements in Chapter 8.

Chapter 1 Introduction

1.0 Overview of PhOLEDs

Since the discovery of organic electroluminescence (EL) phenomenon from anthracene by Pope and coworkers in 1963,[1] the pursuit of highly efficient and durable OLEDs have never ceased because of their attractive advantages of self emitting, low drive voltage, high brightness, full-color emission, rapid response, and easy fabrication of potentially large-area, flexible thin-film devices.[2-7] In this chapter, the history of OLEDs development will be summarized followed by a short introduction of PhOLEDs structure and emitting principle. Afterward the phosphorescent blue emitters will be reviewed and this chapter will be closed with the research motivations of this thesis.

1.1 History of PhOLEDs

Electroluminescence (EL) is one phenomenon of light emission which relies on electrical excitation to release energy in the form of photons or visible light. This phenomenon was first discovered from silicon carbide (SiC) by Henry Joseph Round in 1907.[8] In his letter to Electrical World, Round wrote “On applying a potential of 10 Volts between two points on a crystal of carborundum, the crystal gave out a yellowish light.”[9, 10] This discovery didn’t attract much attention and after 16 years later, Russian scientist Oleg Vladimirocich Losev reported the same behavior of SiC in a Russian journal.[8, 11] In the next years, this research gradually started to gain attention and with the efforts of many scientists and inventors, significant progresses have been made. In late 1950s, Vlasenko and Popkow fabricated the first thin film EL with the inorganic material of zinc sulfide doped with manganese. Although those devices are still unreliable for commercial use, they provided a new strategy for utilization. Another breakthrough was made by Aron Vecht who first demonstrated a direct current (DC) powered EL panel using powdered phosphors in 1968.[8]

In 1963, only five years before Aron Vecht demonstrated direct current powered

EL panel,[8] Pope and coworkers reported the observation of EL from anthracene, an organic molecule. In this paper, both 400 Volt direct current and alternating current were applied to the 10 to 20 μm thick anthracene single crystals and electronic luminescence were observed with the current through the crystal more than 1 μA.[1] This breakthrough did not attract much interest because of the high excitation voltage and in the following few decades most of the efforts had still been focused on inorganic materials.[12] The breakthrough of organic electroluminescence happened in 1987 with the report of an EL device with a thin film structure and requiring low bias voltage by Tang and VanSlyke. The EL device consisted of two thin organic layers of *tris*(8-hydroxyquionline) aluminum (Alq_3) (Figure 1.1) and N,N'-diphenyl-N,N'-bis(3-methylpheyl)-1,1'-4,4'-diamine (TPD) (Figure 1.1) and it exhibited a "High external quantum efficiency (1% photon/electron), luminous efficiency (1.5 lm/W), and brightness (> 1000 cd/m^2) at a driving voltage below 10 V."[13] Burroughes and coworkers reported the light-emitting diodes based on conjugated polymers polyparaphenylenevinylene (PPV) in 1990. That device was fabricated through a solution process. The polymer PPV was dissolved in MeOH and the mixed solution was spin-coated on suitable substrates. After thermal annealing in *vacuo* at $\geqslant$ 250 ^oC for 10 h, the PPV films with 100 nm thick were homogenous, dense and uniform. The electroluminescence studies were performed on this device and around 8% quantum yield was obtained in green-yellow range with charge injection voltage below 14 V.[14]

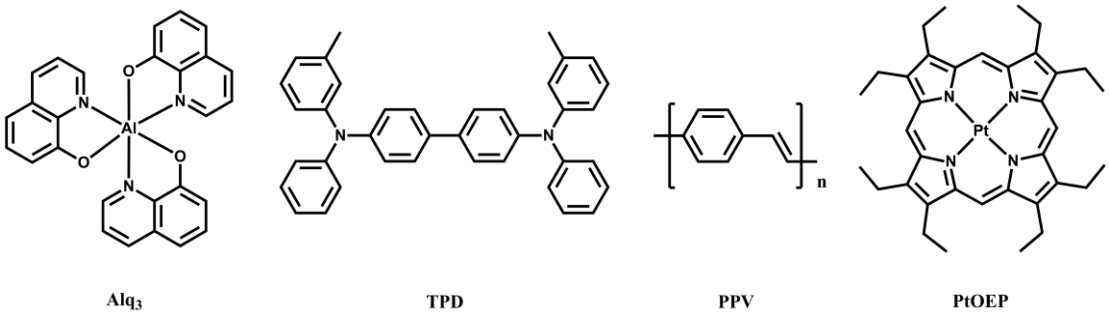

Figure 1.1. Structures of Alq_3, TPD, PPV and PtOEP

Highly efficient phosphorescent organic light-emitting diodes (PhOLEDs) were reported by Thompson, Forrest and coworkers in 1998.[15] They reported the

observation and harvesting of electro-phosphorescence rather than regular florescence as in a pure organic light-emitting device. Moreover, as high as 90% energy transfer efficiency was obtained from both the singlet and triplet states with the maximum emission wavelength of 650 nm. In this device the host material was doped with 2,3,7,8,12,13,17,18-octaethyl-21H,23H-porphine platinum(II) (PtOEP) as the triplet emitter (Figure 1.1). Since the first report of this high efficient device, intensive efforts were provoked on PhOLEDs and a large number of triplet organometallic emitters were synthesized. As PhOLEDs are self-emitting displays, and the color can be generated by combination of three primary colors of red, green and blue, the research efforts were focused on inventing red, green and blue triplet emitters and a great progress has been achieved for red and green emitter.[16, 17] However, due to the high energy difference between the HOMO and LUMO, efficient and reliable triplet blue candidate is still lacking.[2]

1.2 Structure and Emitting Principle of PhOLEDs

Since the working basis of PhOLEDs is still electroluminescence, the principle and light-emitting mechanism of electroluminescence can still be applied to PhOLEDs.[18] Figure 1.2 illustrated a simple scheme of light emitting device (LED) structure from inorganic p-n semiconductors junction.[19] Although there are some detail differences between PhOLEDs and inorganic LED, the principle and light-emitting mechanism are still the same. When bias is applied to the

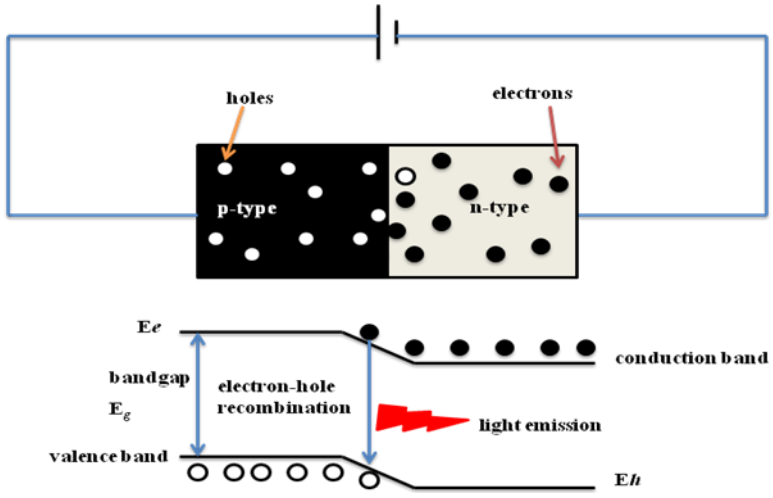

Figure 1.2. Simple LED device structure from inorganic p-n semiconductors.[19]

semiconductors, the positive holes and negative electrons move and encounter each other. Consequently, the light will be generated by the recombination of electrons and holes.

In comparison to inorganic LEDs, the difficulties of PhOLEDs are the electrical charge injection, transport and recombination. The solution for this problem is to create a hole transport layer (HTL) and an electron transport layer (ETL) on both sides of emitting layers. Moreover, due to the diffusive nature of the triplet excited state with long life time two blocking layers were also created for blocking the diffusion of electrons and holes. (Figure 1.3)[19]

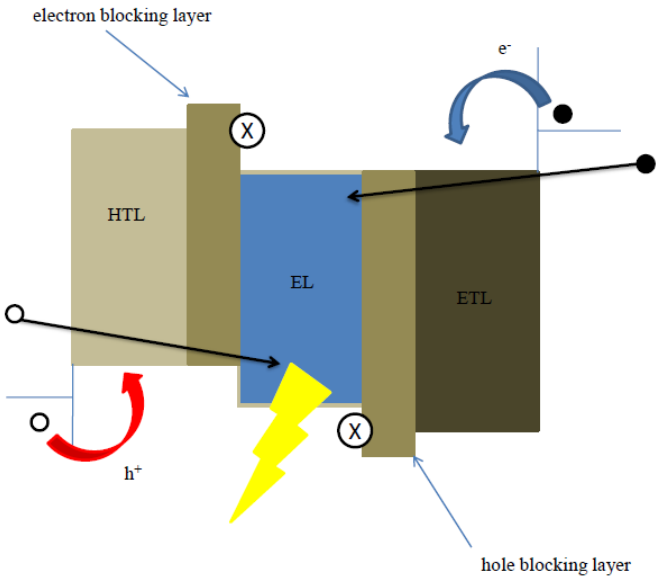

Figure 1.3. Typical PhOLED structure with the hole transport layer (for hole injection/transport), electron transport layer (for electron injection/transport), hole and electron blocking layers and emissive layer.[19]

The emission principle is easy to understand through the PhOLEDs structures. As show in Figure 1.4, on the anode side, when the holes are injected to the HTL with the application of a bias, those positive holes go through the HTL and BL and finally reach the emission layer (EL). On the cathode side, also with the same application of a bias, the electrons go through the ETL and BL and reach to the emission layer. As positive holes and negative electrons encounter with each other in the emissive layer, the recombination happens and the light can be generated by the formation of excitons.

Although there is no difficulty in understanding the emission mechanism, but for practical purposes, the difficulties are associated with controlling the turn-on voltage of the device which is influenced by the charge injection and transport in the organic layers and increasing device efficiency which is affected by the hole and electron leakage as well as charge carrier supply.[18]

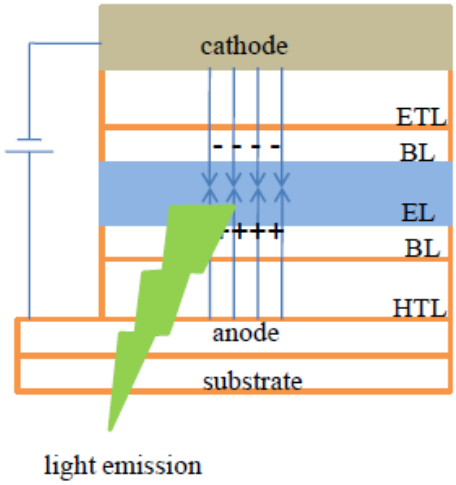

Figure 1.4. Light emitting process of PhOLEDs.[18]

1.3 Advantage and Disadvantage of PhOLEDs[10, 12]

In view of the high efficiency and high definition, PhOLEDs is considered to be the next generation display and it is also expected to replace the liquid crystal display (LCD). In comparison of nowadays used LCD, the three most advantages could be high efficiency, self-emitting and easy fabrication of large-area devices. The utilization of both phosphorescence from the excited triplet state and florescence from exited singlet state raise the ideal quantum efficiency to 100% theoretically and this provides high possibility to cut down the energy consumption. And due to the self-emitting properties, the PhOLEDs can be fabricated on all kind of substrates and this provides the opportunity to make transparent and flexible displays. Moreover the demand of large-area display can also be satisfied by the easy fabrication on large scale substrates.

There are also some disadvantages of PhOLEDs and the first one could be the still high price of PhOLEDs display due to the high cost of complicated

manufacturing process. The second one is the device instability and short lifetime. Those devices are very sensitive to O_2 and the reason is the triplet emission quenching by trace of O_2 which is also a triplet. The third one is the lack of efficient blue emitters. Blue emitter is one of the primary colors materials besides red and green emitters. Although the research of red and green emitters have made a great progress and there is no technical problem for red and green emitters to apply in a industry setting, due to high energy level between the HOMO and LUMO, the research of durable and efficient blue emitter is still undergoing.

1.4 PhOLEDs Emitting Materials

1.4.1 Introduction of PhOLEDs

Since the first report of the red PhOLED device in 1998, triplet emitting organo-transition metal complexes have attracted much interest due to their potential applications in PhOLEDs. Phosphorescence is one type of luminescence, which emits photons from the excited triplet state. Jablonski energy diagram is illustrated in Figure 1.5 and one can clearly see the principle of phosphorescence.[20] When compounds are excited from the ground state, the electrons will be excited to singlet excited states (S_1, S_2 ⋯) in 10^{-15} seconds and immediately the electrons fall back to S_1 through internal conversion (IC) and vibrational relaxation in time range of 10^{-14} to 10^{-11} seconds. When electrons fall back to ground state in a manner of radiative decay, photons can be generated in the form of fluorescence. During this process, due to some influences of solvent effects and so on, non-radiative decay which releases the energy in the way of heating from excited singlet state to ground state can also happen. If the electrons in the excited state undergoes intersystem crossing (IC) from excited singlet states to excited triplet states via spin orbital coupling (SOC), the electron spin orientation will change and generation of phosphorescence occurs during the process of electron relaxation from the excited triplet state to the ground state. Although there is

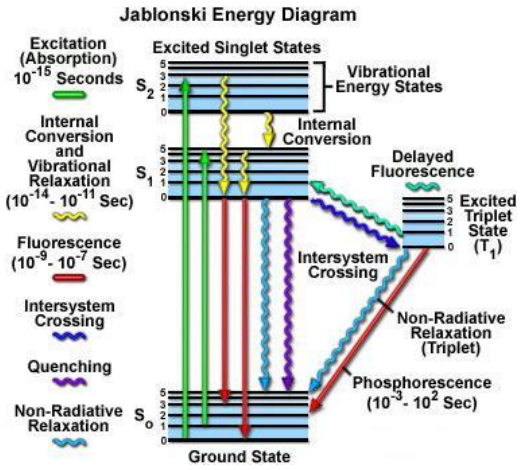

Figure 1.5. Jabloski energy diagram of florescence and phosphorescence. [20]

no significant difference for calculating the quantum yield of florescence and phosphorescence in light excited emission, the influence on electroluminescence quantum yield is significant. In OLED devices the electroluminescence is generated by recombination of electrons and holes in emission layer. (Figure 1.6) Due to the different spin orientations of holes and electrons, only 25% excitons can form singlet state statistically and the rest 75% excitons are in a triplet state.[21, 22] Subsequently, the florescence is generated by the 25% excitons and the rest 75% emission harvest are really dependent on the specific devices. If the emitting layer consists of pure organic molecules, the emission will be released in a way of non-radiative decay. But the situation can be changed by applying organo-transition metal complexes in the emitting layer due to the harvesting of triplet emission through the spin orbital coupling of the transition metal. In Comparison to the organo-transition metal emitters based devices and the pure organic emitter devices, the maximum internal quantum efficiency (IQE) is only 25% for organic emitter devices rather than organo-transition metal emitters with the maximum of 100% in harvesting both singlet and triplet emission.

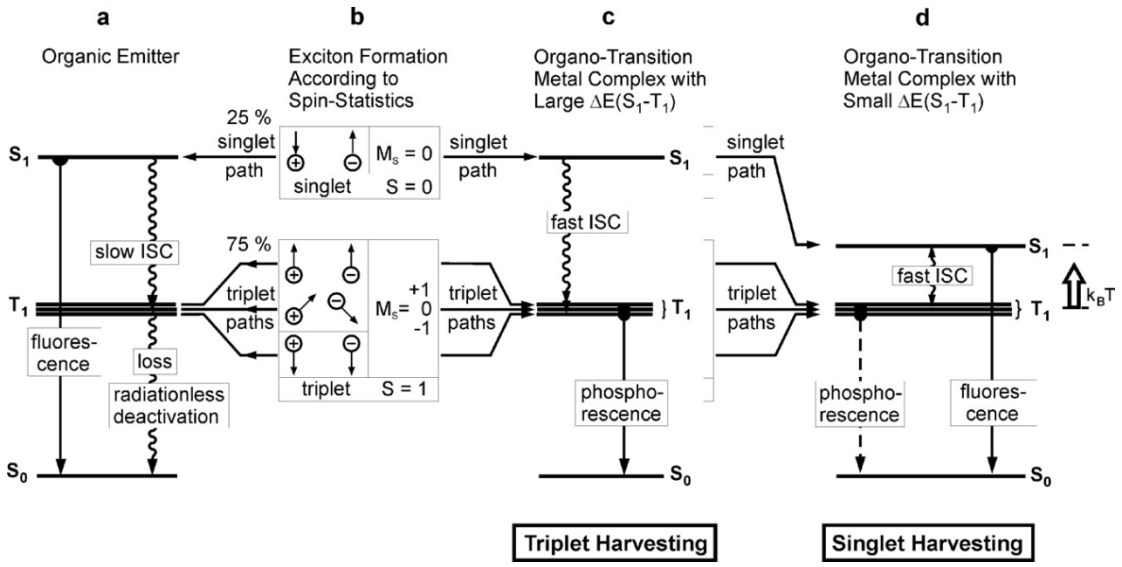

Figure 1.6. Electro-lumiescence excitation processes for organic and organo-transition metal emitters.[22]

Triplet emissions of organo-transition complexes can be classified into four different types based on their emission parentage. Figure 1.7 illustrates the molecular orbital (MO) descriptions of difference emission of MC, MLCT, LC and LMCT on octahedral complex.[23]

The MOs can be classified to six types according to the proportions of atomic orbital. σ_L orbital is a strong bonding which is dominated by ligand centered σ orbitals and the π_L is also predominately a ligand centered π orbital. π_M orbital is a metal-centered d orbital with t_{2g} symmetry and the orbital of σ_M^* has a symmetry of e_g. The antibonding σ_M^* and π_L^* are dominated by ligand π* orbital and metal-centered s and p orbitals. The various electronic transitions is displayed in Figure 1.7. While Metal to ligand transition (MC) and ligand to ligand transition can be assigned to $\pi_M \rightarrow \sigma_M^*$ and $\pi_L \rightarrow \pi_L^*$ respectively, ligand to metal charge transfer (LMCT) and metal to ligand charge transfer (MLCT) can be assigned to $\pi_L \rightarrow \sigma_M^*$ and $\pi_M \rightarrow \pi_L^*$ respectively.

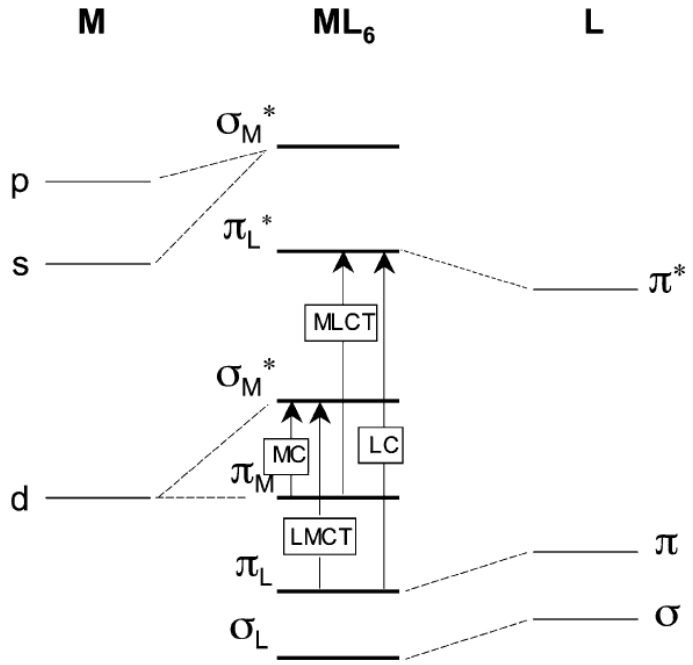

Figure 1.7. Molecular orbital diagram for an octahedral complex of a transition metal.[23]

Transition metal is crucial for harvesting triplet emission by changing electrons spin with the aid of SOC. But on the other hand, the triplet emission can also be quenched by the low-lying metal centered d-d non-radiative decay. This can be presented in a simplified way in Figure 1.8 for a square planar d^8 complex.[24] The d-d excited states lie on the certain energy level. When the electrons get excited from the ground state, the d-d excited state is populated through light absorption, and then the molecule will undergo a significant distortion on formation of the excited state and increasing of Pt-L bond lengths. This unfavorable scenario for luminescence can occur due to the thermal accessibility of isoenergetic crossing point where non-radiative decay or intersystem crossing to the ground state. This d-d excited state can somehow quench the emission by competing with the radiative decay of LC and MLCT due to the energy gap ΔE (Figure 1.8 b). In order to maximum harvest radiative decay, one can push the d-d state to higher energy level to generate large energy gap ΔE between the d-d state and radiative decay state with the strong ligand field strength ligand like phosphine and polypyridine.

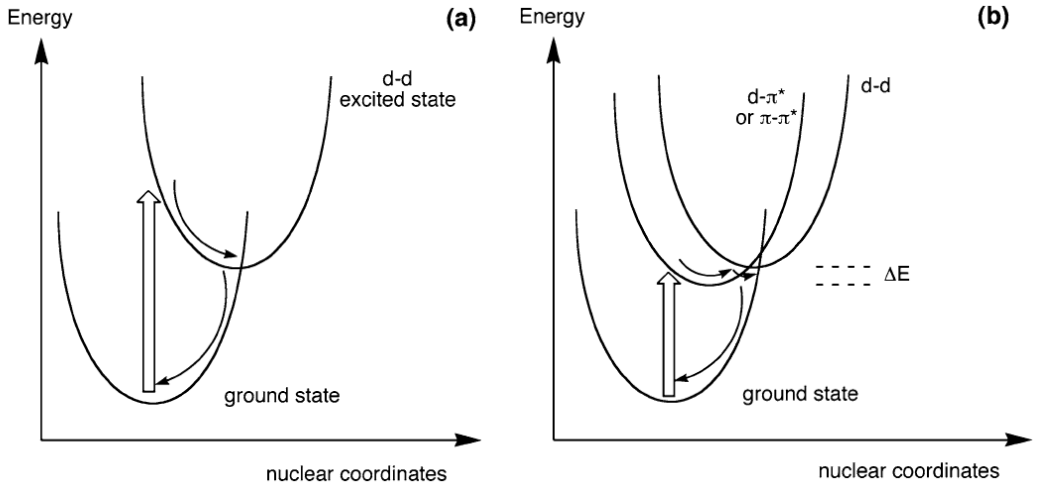

Figure 1.8. a Potential energy surface for the d-d excited state in square planar d^8 complexes. **b** thermal activated non-radiative decay pathway of d-d excited state.[24]

The excited triplet state can be splits into three substrates and the parameter of zero-field splitting (ZFS) can be utilized to classify the origin (LC or MCLT) of the triplet emission.[21] Based on experimental data, the total ZFS [ΔE(ZFS)] represents a valuable parameter to assess or even predict the parentage of the triplet emission. The value of ΔE(ZFS) more than 1-2 cm^{-1} is connected with $^{1,3}d\pi^*$ components. In other words, the larger value of ΔE(ZFS), the more ^{1,3}MLCT components involved. Figure 1.9 listed the complexes with increasing ΔE(ZFS) and different components.

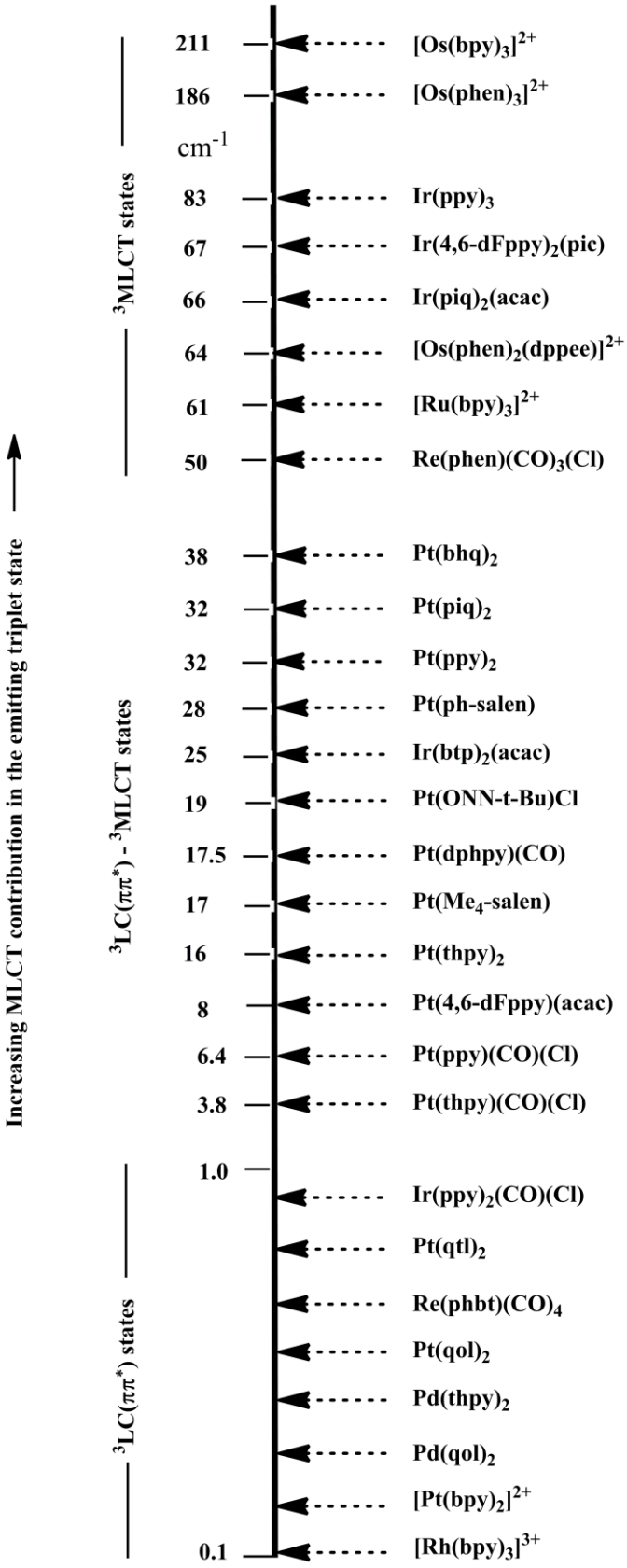

Figure 1.9. The compounds are arranged according to an increasing splitting of the emitting triplet state into substates (zero-field splitting, ZFS).[21]

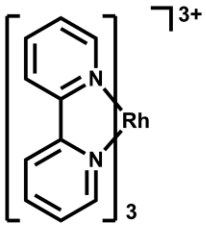

$[Rh(bpy)_3]^{3+}$

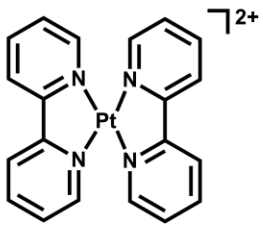

$[Pt(bpy)_2]^{2+}$

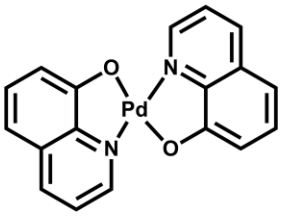

$Pd(qol)_2$

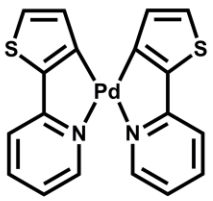

$Pd(thpy)_2$

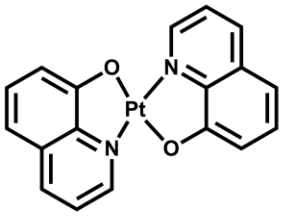

$Pt(qol)_2$

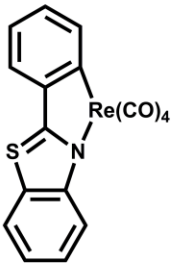

$Re(phbt)(CO)_4$

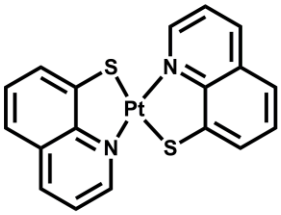

$Pt(qtl)_2$

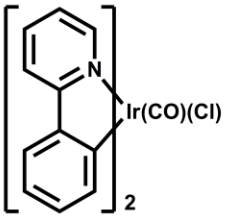

$Ir(ppy)_2(CO)(Cl)$

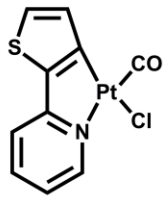

$Pt(thpy)(CO)(Cl)$

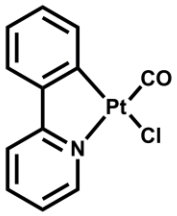

$Pt(ppy)(CO)(Cl)$

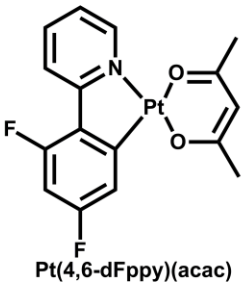

$Pt(4,6\text{-}dFppy)(acac)$

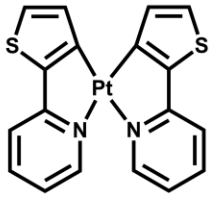

$Pt(thpy)_2$

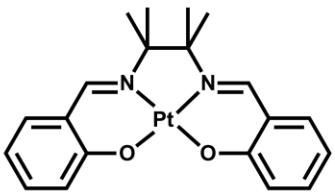

$Pt(Me_4\text{-}salen)$

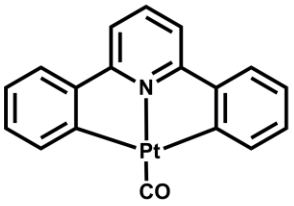

$Pt(dphpy)(CO)$

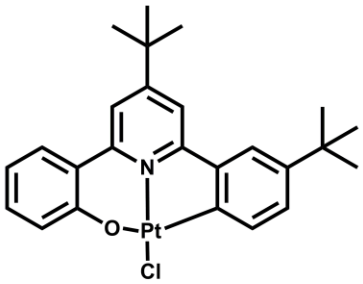

$Pt(ONN\text{-}t\text{-}Bu)Cl$

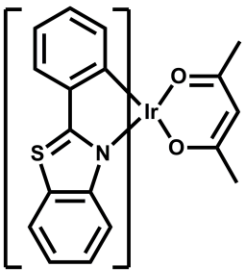

$Ir(btp)_2(acac)$

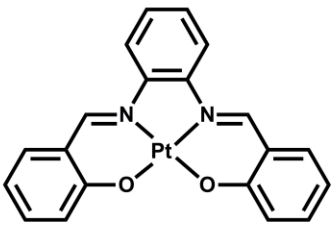

$Pt(ph\text{-}salen)$

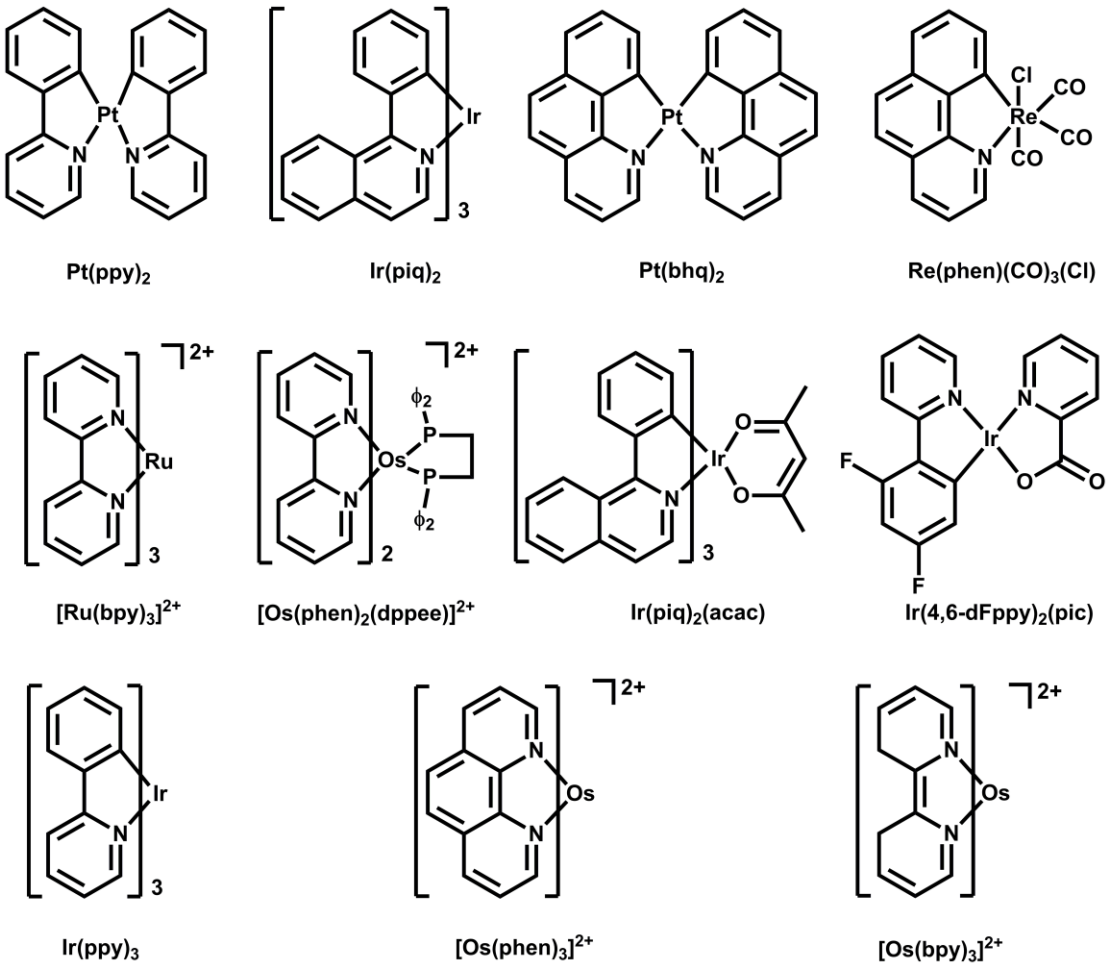

Figure 1.10. Complexes structures of Figure 1.9.[21]

1.4.2 Review of Blue Phosphorescent Materials

The requirement of blue phosphorescent emitters for OLEDs has accelerated the research both in academic and industry. The triplet emitters can be classified into polymer emitters and small molecular emitters. Polymer emitters normally use solution process to fabricate the devices while the vapor deposition process is used in the case of small molecular emitters. The polymer emitters are synthesized by introducing the metal emitting unit to the organic polymer and this method is used for most of the red and green polymer triplet emitters like poly(2,2'-bipyridine-5,5'-diyl) **P1**,[25] and Iridium polymer **P2**.[26] Due to the conjugation of organic polymers, polymer based on a triplet blue emitter has never been reported. Normally there are two type of polymers based on the side chain and main chain polymer unit.[27] The polymers **P1** and **P2** belong to the category of main chain polymers and polymer **P3**[28]

and **P4**[29] with different metals are examples of side chain polymers as illustrated in Figure 1.11. Also the synthesis of side chain and main chain polymers provide new opportunity to fabricate OLEDs in a solution process. In most of the cases, the way to harvest triplet emission based on polymers is carried out by doping the small molecular emitters into the host conjugated organic polymers and good efficiency devices can be produced by adjusting the composition of different polymers and triplet emitters.[27, 30]

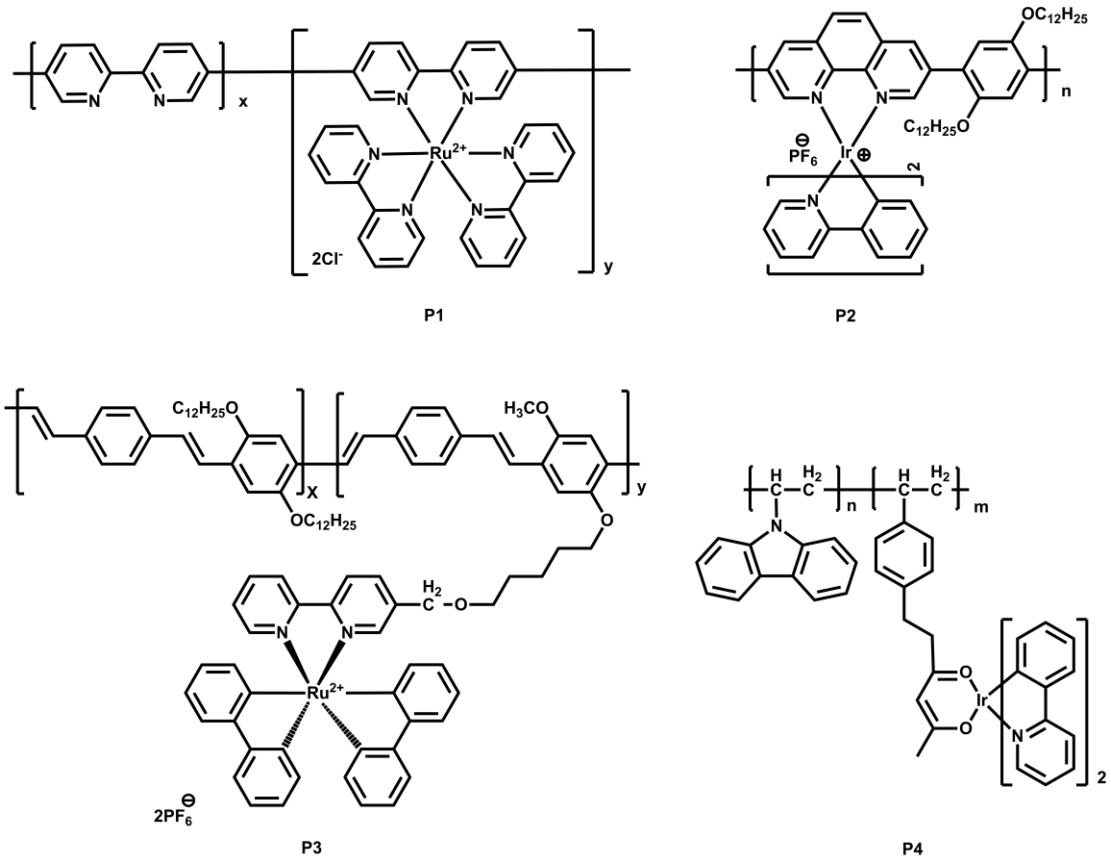

Figure 1.11. Structure of Polymer emitters.

1.4.2.1 Small molecular emitters based on Iridium

In comparison to the polymer based emitters, small molecule triplet emitters are easy to produce especially in the case of red and green emitters. Due to the high energy gap between HOMO and LUMO, durable and efficient blue emitters are still the bottleneck, which hinders the commercialization of OLEDs. Due to the strong demand for triplet blue emitters, research progress has been intensified since early 2000s. The first successful blue emitter Iridium(II)bis((4,6-di-fluorophenyl)-

pyridinato-$N,C^{2'}$)picolinate (FIrpic **S1)** was reported by Thompson and coworkers in 2001.[16] The emitter is a neutral cyclometalated Iridium complex bearing electron-withdrawing fluorine groups. The emission wavelength maximum is 475 nm with a quantum yield of 50-60% in solution. The device was fabricated with a 6% FIrpic in the host material of 4,4'-*N*,*N*'-dicarbazole-biphenyl (CBP) and the maximum external quantum efficiency achieved was η_{ext} = (5.7±0.3)% with the luminous power efficiency (η_p) of (6.3±0.3) lm/W. In view of the difficulty to achieve highly efficient triplet blue emitters, attempts to change host materials, device configuration and even change in fabrication process were carried out with the same emitter and the required improvements are not remarkable.[31, 32]

After the investigation of the first triplet blue emitter FIrpic **S1**, a new iridium complex was reported by the same group. Ir(III) complex **S2** still consists of bis((4,6-di-fluorophenyl)-pyridinato-$N,C^{2'}$), but the picolinate ligand was changed to tetrakis(1-pyrazolyl)borate. The triplet emission of complex **S2** is at 457 nm with an unreported quantum yield. But the external electroluminescent quantum yield and power efficiencies were η_{ext} = (8.8±0.9)% and (11.6±1.2) lm/W for the device.[33] In their report of the deep blue devices using a fluorine-free emitter, two isomers of *fac* and *mer*-tris(phenyl-methyl-benzimidazlyl)iridium(III) **S3** were synthesized with their triplet emission at 389 nm and 395 nm respectively. The external quantum efficiencies and power efficiencies for both isomers were η_{ext} = (2.6±0.3)%; η_p = (0.5±0.1) lm/W and η_{ext} = (5.8±0.6)%; η_p = (1.7±0.2) lm/W respectively. In comparison with their previously reported **S1** and **S2**, this system did not perform well.[34]

Emitter **S4** was reported by Chi and coworkers by substituting the picolinate fragment to stronger electron-withdrawing pyridyl-tetrazolate group in 2005. This emitter exhibited blue emission at 460 nm and the device showed a improved electroluminescent efficiencies of η_{ext} = 9.4% and 7.2 lm/W with the host material of 3,5-bis(9-carbazolyl)tetraphenylsiliane (**SimCP**).[35] The modifications on this model molecule **S4** are still going on and a series of triplet blue emitters such as **S5**, **S6**, **S7** and **S8** have been reported.[36, 37] After many modifications on the picolinate bound

fragment, research groups started to explore ways of changing the (4,6-di-fluorophenyl)-pyridinato-*N*,*C*^{2}, and a series of new molecules such as **S9**,[38] **S10**,[39] **S11**[40] and **S12**[40] were synthesized.

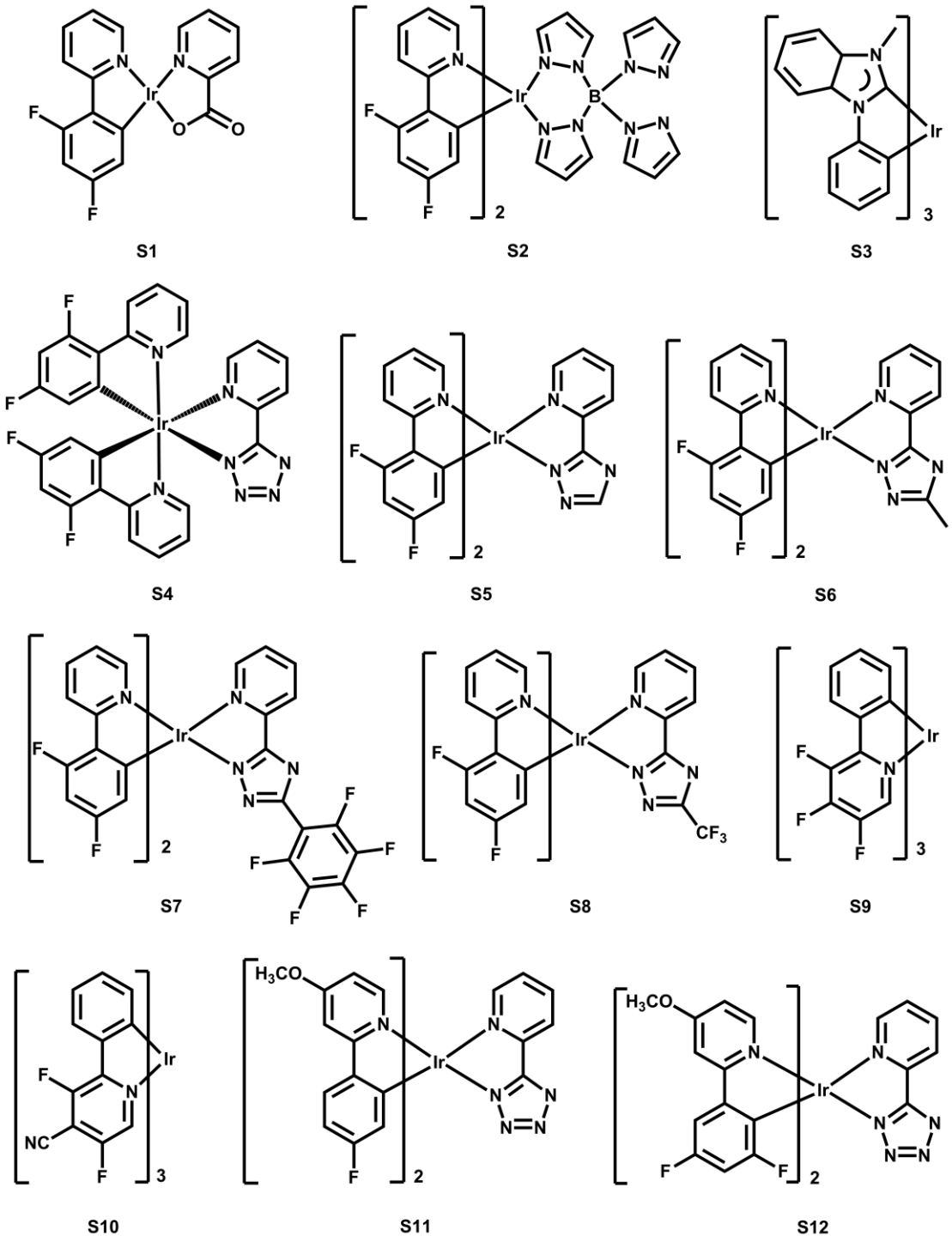

Figure 1.12. Structure of small molecules S1-S12.

It is worth noting that the device fabricated with *fac-tris*((3',4',5',6'-tetrafluorophenyl)pyridine)iridium(III) **S9** using **mCP** as host material gave a high

external quantum efficiency of η_{ext} = 19.2% and η_p = 19 lm/w which is the highest reported.[41] In 2007 Ir(III) complex **S13** bearing 2-(2,4-difluorophenyl)pyridine and 5-(2-pyridyl)-3-trifluoromethylpyrazole ligands was reported. Although the structure is still consists of a cyclometalation and the ligands still contain nitrogen heterocycle, the breakthrough could achieved by avoiding the use of model molecule FIrpic. This molecule emits at 450 nm with 50% quantum yield and the device measurement reveals a low turn-on voltage of less than 4 V along with η_{ext} = 8.5% and η_p = 8.5 lm/w.[42] The following molecules **S14**, **S15** and **S16** were obtained by subsequent ligand modification on **S1**3 with emissions of 451 nm, 447 nm, 449 nm and a quantum yield of 80%, 58% and 68% respectively. The electroluminescent efficiencies of **S14** (11%, 12.8 lm/W), **S15** (13%, 14.1 lm/W) and **S16** (13.7%, 14 lm/W) were significantly improved in comparison to the model molecule **S13**.[43]

Besides the nitrogen linked cyclometalating molecules, phosphine ligated blue emitters based on Ir(III) have also been reported. As described in the introduction, the stronger the ligand field strength the easier to harvest triplet emission by pushing the low-lying d-d excited state to high energy level. In comparison to nitrogen heterocycles, phosphine ligands are more electron rich and it is hoped that this character could be efficient to improve the quantum yields of triplet emitters.[2]

Blue iridium emitters bearing benzyldiphenylphosphine and difluorinated phenylpyridine ligands were reported by Chi, Chou and Wu in 2009. The target complexes were obtained by treating difluorobenzyldiphenylphosphine with the Ir(III) dimer $[(dfppy)_2Ir(\mu\text{-}Cl)]_2$ dfppy = difluorophenylpridyl. By changing the substitutents on the ligands, three complexes **S17-S19** were obtained with the emission at 457, 456 and 469 nm.[44] The quantum yields were recorded in degassed DCM and only complex **S17** gave the highest quantum yield of 67%. This complex **S17** fabricated into a device gave a 10.24% external quantum efficiency with power efficiency of 10.07 lm/W. Based on this result, the same group explored a new phosphine linked Ir(III) complexes **S20**-**22**. These three complexes possess an emission wavelength maxima at 451, 454 and 448 nm with solid state quantum yields of 97%, ≈100% and 41%. Inspite of the so high quantum yields in solid state, the produced devices

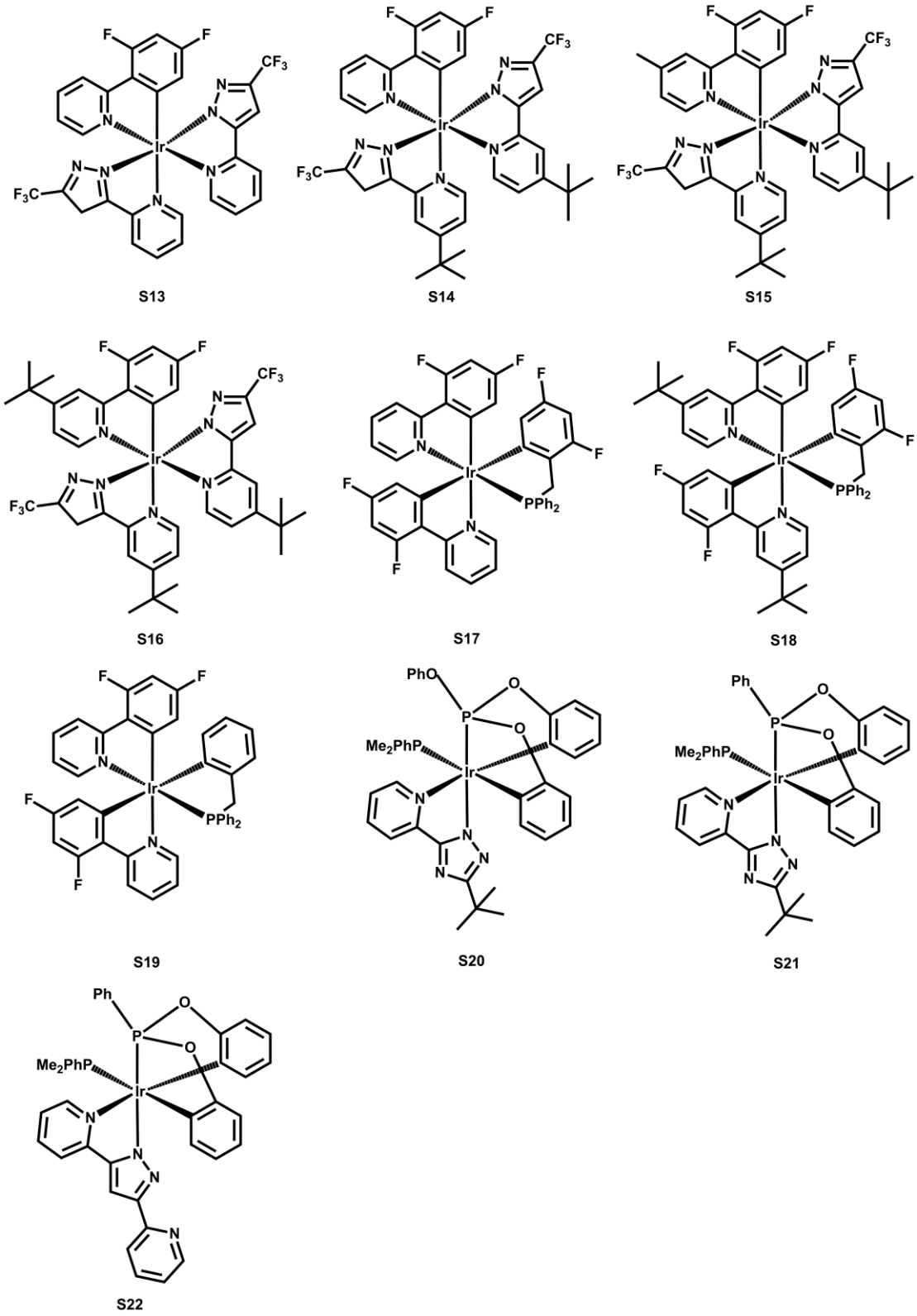

Figure 1.13. Structure of small molecules S13-S22

showed EQE of η_{ext} = 11% and η_p = 16.7 lm/w (**S20**); η_{ext} = 8.4% and η_p = 13.2 lm/w (**S21**); η_{ext} = 8.7% and η_p = 10.8 lm/w (**S22**), respectively.[45]

1.4.2.2 Small molecular emitters based on Platinum and other metals

Although most of the triplet blue emitters are based on iridium, Pt(II) triplet emitters attracted much more attention since they are reported with good quantum efficiencies. In comparison to iridium, platinum has a high spin orbital coupling constant of ζ = 4481 cm^{-1}.[46] Moreover, due to the large crystal field stabilization energy of platinum, platinum complexes exhibit square planar coordination pattern that provide the possibility to form Pt-Pt interaction. Jabbour and coworkers reported the efficient blue emitting electrophosphorescent devices based on Pt(II) [1,3,-difluoro-4,6-di(2-pyridinyl)benzene] chloride **S23**.[47] In this case the tridentate biphenyl pyridine ligand was still used to form the cyclometalated Pt complex and the emission wavelength maximum was around 465-470 nm with a quantum yield of 46%. The devices fabricated with this emitter showed an external quantum efficiency is η_{ext} = 8.6%. As the photophysical properties can be affected by electronic factors of different substitutes, blue emitters **S24-26** are synthesized with different heterocyclic ligand. The emissions of complexes **S24-26** are 470, 448 and 430 nm respectively. Although the internal quantum yields were not reported, the external quantum yields for **S24-26** were 18.1%, 0.7% and 10.1%. Almost at the same time Strassner and coworkers reported the tetracarbene Pt(II) complexes which possessed an emission wavelength maximum of 386 nm with the quantum yield of 45%. Unfortunately, those tetra carbene complexes are charged complexes and this restricts their applications in OLEDs.[48] A series of neutral cyclometalated phenyl-carbene Pt(II) complexes were reported bearing different substitutents by the same group in 2010. Among all the six complexes, **S27** exhibited a blue emission at 463 nm with a quantum yield of 90% in 2 wt% PMMA film. The device of complexes **S27** was also fabricated and the external quantum efficiency was obtained with 6.2%.[49] Che and coworkers reported another type of cyclometalated carbene Pt(II) complexes **S28-31**.[50] These emitters showed blue emission in the range of 443-461 with the quantum yield from 24-29%. Very recently, Wang group reported two Pt blue emitters bearing boron ligand and the quantum yield of those two complexes are 86% and 90% with the emission

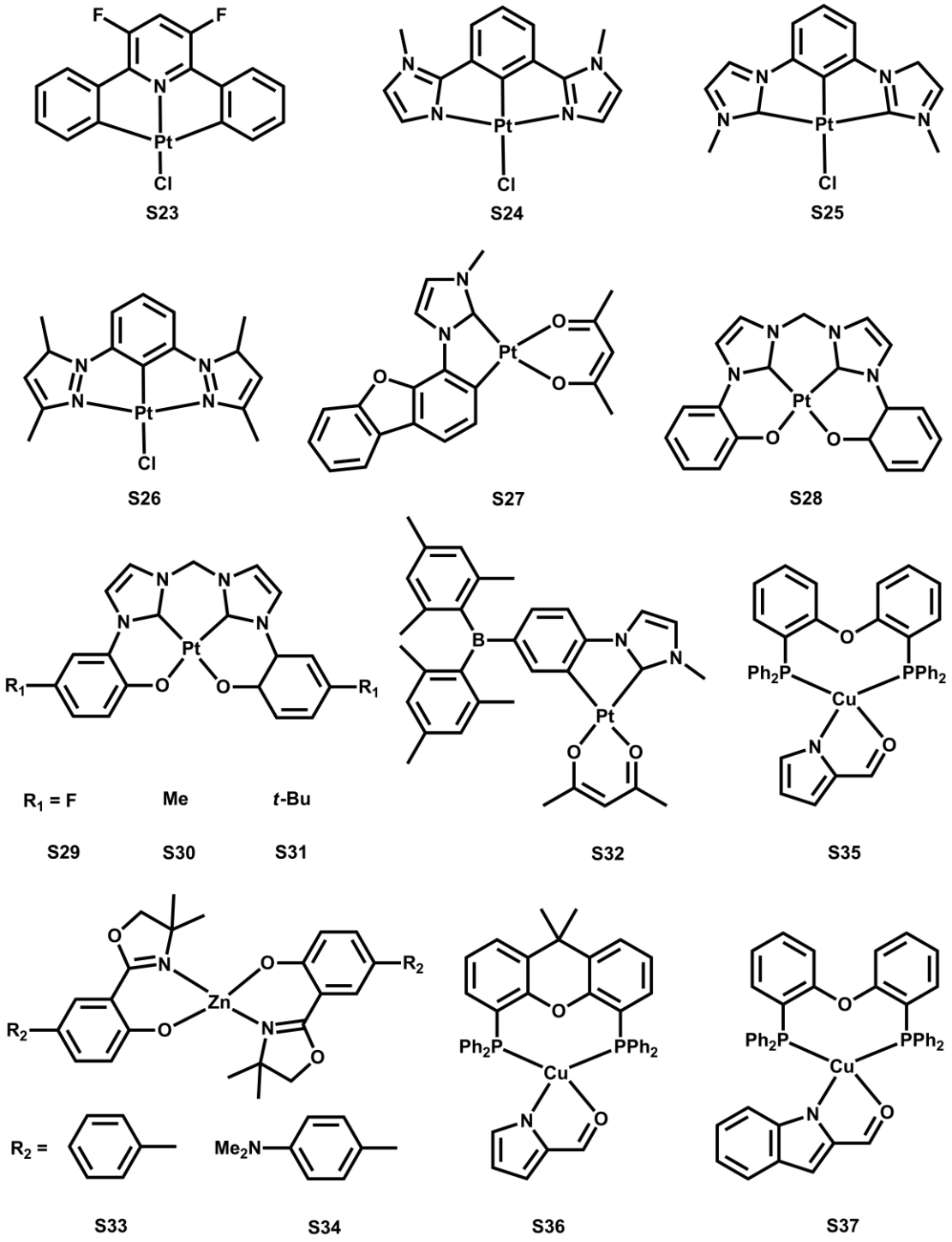

Figure 1.14. Structure of small molecules S23-S37

wavelength maximum at 478 nm and 462 nm. The external quantum efficiency of 17.9% for complex **S32** is the highest reported until now.[51]

Iridium and platinum are all noble metals and the exploitation of triplet blue emitters based on cheap metals such as zinc and copper have also been reported. **S33** and **S34** bearing oxazolyl-phenylated ligand exhibited blue emissions of 463 nm and

449 nm with quantum yield of 8% and 16% but the device of **S33** was found to be extremely poor.[52] Copper blue emitters such as **S35-37** were reported by Yersin in 2011 with the emission wavelength maximum of 436, 447 and 464 nm. Although the quantum yield were as good as 90% for both **S36** and **S37**, the long life times of 22 μs and 13μs and their delayed fluorescence restrict their current application in OLEDs.[53]

1.5 Motivation of the thesis

From the preceding literature overview, the importance of triple blue emitters in PhOLEDs is obvious and also many efforts have been pursued on the design and development of efficient and durable triplet blue emitters. In view of the difficulty to obtain blue triplet emitters, our intent in this thesis was to prove the efficacy of a new design approach to the molecules that display blue emission with high quantum efficiency.

There are four primary reasons that formed the basis to focus our work on the development the NHC Pt(II) acetylide triplet emitters. In comparison to Ir, Ru and Rh, platinum has two merits: i) a big spin-orbit coupling constant of $\zeta = 4481$ cm^{-1}; and ii square planar coordination. The spin-orbit coupling constant can promote rapid intersystem crossing (ISC) from singlet to triplet excited states; and the square planar conformation provides with less distortions in the excited state. Besides the core of platinum, acetylene is the second factor. Acetylene group with sp hybridization carbon is widely utilized to form metal-acetylide complexes due to its linear geometry, structural rigidity and strong electron-donating properties. As a strong field ligand the insertion of acetylene into the Pt coordination sphere will create strong interaction via pπ - dπ overlap which would raise the metal-centered d-d energy by lowering the HOMO-LUMO energy gap. In terms of σ-alkynyl based platinum complexes bearing phosphine and polypyridyl ancillary ligand, the photophysical investigation have been performed and while the phosphine Pt(II) acetylide complexes show weak or non-emission, the Pt(II)-acetylide complexes bearing polypyridyl mostly exhibit low energy emission of green or red. We considered the Pt(II) acetylide to act as a good

chromophore and the problem for their inefficiency is due to the competing radiative and non-radiative excited states in the case of pyridyl and phosphine bound complexes. This inefficiency was expected to be solved by the introduction of a strong ligand field (LF) strength ligand by reducing the competition by pushing the d-d non-radiative excited state to higher energy. NHCs are strong Lewis bases that have large ligand field (LF) strength in addition to the strong σ-donation which should enable triplet emission by changing the metal-centered d-d energy gap intensively.

Its well known until now that molecular configuration consisting of cyclometalation is the only successful design motif that has been utilized to obtain triplet blue emitters and minor modifications of cyclometalating ligands do not influence the emission energy and efficiency drastically. Based on the above reasons we thought that a bottom-up approach requiring the entire modification of the basic framework would pave way to achieve triplet blue emitters with high quantum efficiencies. In the scope of this thesis, we dedicated our efforts towards the synthesis of highly efficient triplet blue emitter based on NHC Pt(II) acetylide complexes devoid of cyclometalation.

1.6 References

[1] M. Pope, H. P. Kallmann, P. Magnante, *J. Chem Phys.* **1963**, *38*, 2042.

[2] C.-L. Ho, W.-Y. Wong, *New J. Chem.*, **2013**, *37*, 1665.

[3] G. Zhou, W.-Y. Wong, X. Yang, *Chem.–Asian. J.*, **2011**, *6*, 1706.

[4] Z. H. Kafafi, *Organ electroluminescence*, CRC, Taylor & Francis, Boca Raton, Fla. **2005**.

[5] S. Miyata, H. S. Nalwa, *Organic electroluminescent materials and devices*, Gordon and Breach Publishers, Amsterdam, **1997**.

[6] T. Tsujimura, *OLED Displays*, John Wiley & Sons, Hoboken, **2011**.

[7] Y. H. Kim, C.-S. Ha, *Advances in organic light-emitting devices*, Trans Tech Publications, Stafa-Zuerich, United Kingdom, **2008**.

[8] flashwear.com/flashwear_information/history_of_electroluminescence.cfm

[9] H. J. Round, *Electrical world* **1907**, *49*, 309.

[10] http://en.wikipedia.org/wiki/OLED

[11] N. Zheludev, *Nat Photon*, **2007**, *1*, 189.

[12] B. Choudhury, Iowa State University, **2005**.

[13] C. W. Tang, S. A. VanSlyke, *Appl. Phys. Lett.*, **1987**, *51*, 913.

[14] J. H. Burroughes, D. D. C. Bradley, A. R. Brown, R. N. Marks, K. Mackay, R. H. Friend, P. L. Burns, A. B. Holmes, *Nature* **1990**, *347*, 539.

[15] M. A. Baldo, D. F. O'Brien, Y. You, A. Shoustikov, S. Sibley, M. E. Thompson, S. R. Forrest, *Nature* **1998**, *395*, 151.

[16] C. Adachi, R. C. Kwong, P. Djurovich, V. Adamovich, M. A. Baldo, M. E. Thompson, S. R. Forrest, *Appl. Phys. Lett.*, **2001**, *79*, 2082.

[17] D. F. O'Brien, M. A. Baldo, M. E. Thompson, S. R. Forrest, *Appl. Phys. Lett.* **1999**, *74*, 442.

[18] J.-X. H. X.-W. Chen, *OLED: you ji dian ji fa guang cai liao yu yuan jian = OLED: organic electroluminescent materials & devices*, Wu nan, Tai bei shi, **2005**.

[19] L. Pereira, *Organic light emitting diodes: the use of rare earth and transition*

metals, Pan Stanford ; Eurospan, Singapore; London, **2012**.

[20] http://www.olympusmicro.com/primer/java/jablonski/jabintro/

[21] H. Yersin, W. J. Finkenzeller, in *Highly Efficient OLEDs with Phosphorescent Materials*, Wiley-VCH Verlag GmbH & Co. KGaA, **2008**, pp. 1.

[22] H. Yersin, A. F. Rausch, R. Czerwieniec, T. Hofbeck, T. Fischer, *Coord. Chem. Rev.*, **2011**, *255*, 2622.

[23] V. Balzani, S. Campagna, G. Bergamini, F. Puntoriero, in *Photochemistry and Photophysics of Coordination Compounds I, Vol. 280*, Springer Berlin Heidelberg, **2007**, pp. 1.

[24] V. Balzani, S. Campagna, J. A. G. Williams, in *Photochemistry and Photophysics of Coordination Compounds II, Vol. 281*, Springer Berlin Heidelberg, **2007**, pp. 205.

[25] T. Yamamoto, Y. Yoneda, T. Maruyama, *J. Chem. Soc., Chem. Commun.* **1992**, 1652.

[26] T. Yasuda, I. Yamaguchi, T. Yamamoto, *Adv. Mater.*, **2003**, *15*, 293.

[27] Q. Zhao, S.-J. Liu, W. Huang, *Macromol. Rapid Commun.*, **2010,** *31*, 794.

[28] C. T. Wong, W. K. Chan, *Adv. Mater.*, **1999**, *11*, 455.

[29] S. Tokito, M. Suzuki, F. Sato, M. Kamachi, K. Shirane, *Org. Electron.*, **2003**, *4*, 105.

[30] C. S. K. Mak, W. K. Chan, in *Highly Efficient OLEDs with Phosphorescent Materials*, Wiley-VCH Verlag GmbH & Co. KGaA, **2008**, pp. 329.

[31] N. Chopra, L. Jaewon, J. Xue, F. So, *Electron Devices, IEEE Trans.*, **2010**, *57*, 101.

[32] M.-T. Lee, J.-S. Lin, M.-T. Chu, M.-R. Tseng, *Appl. Phys. Lett.*, **2009**, *94*, 083506.

[33] R. J. Holmes, B. W. D'Andrade, S. R. Forrest, X. Ren, J. Li, M. E. Thompson, *Appl. Phys. Lett.*, **2003**, *83*, 3818.

[34] R. J. Holmes, S. R. Forrest, T. Sajoto, A. Tamayo, P. I. Djurovich, M. E. Thompson, J. Brooks, Y. J. Tung, B. W. D'Andrade, M. S. Weaver, R. C. Kwong, J. J. Brown, *Appl. Phys. Lett.*, **2005**, *87*, 243507.

[35] S. J. Yeh, M. F. Wu, C. T. Chen, Y. H. Song, Y. Chi, M. H. Ho, S. F. Hsu, C. H. Chen, *Adv. Mater.*, **2005**, *17*, 285.

[36] X. Zhang, C. Jiang, Y. Mo, Y. Xu, H. Shi, Y. Cao, *Appl. Phys. Lett.*, **2006**, *88*, 051116.

[37] E. Orselli, G. S. Kottas, A. E. Konradsson, P. Coppo, R. Frohlich, L. De Cola, A. van Dijken, M. Buchel, H. Borner, *Inorg. Chem.*, **2007**, *46*, 11082.

[38] R. Ragni, E. A. Plummer, K. Brunner, J. W. Hofstraat, F. Babudri, G. M. Farinola, F. Naso, L. De Cola, *J. Mater. Chem.*, **2006**, *16*, 1161.

[39] S. H. Kim, J. Jang, S. J. Lee, J. Y. Lee, *Thin Solid Films* **2008**, *517*, 722.

[40] L.-L. Wu, C.-H. Yang, I. W. Sun, S.-Y. Chu, P.-C. Kao, H.-H. Huang, *Organometallics* **2007**, *26*, 2017.

[41] S. O. Jeon, K. S. Yook, C. W. Joo, J. Y. Lee, *Adv. Mater.*, **2010**, *22*, 1872.

[42] C.-H. Yang, Y.-M. Cheng, Y. Chi, C.-J. Hsu, F.-C. Fang, K.-T. Wong, P.-T. Chou, C.-H. Chang, M.-H. Tsai, C.-C. Wu, *Angew. Chem. Int. Ed.*, **2007**, *46*, 2418.

[43] C.-H. Chang, C.-C. Chen, C.-C. Wu, C.-H. Yang, Y. Chi, *Org. Electron.*, **2009**, *10*, 1364.

[44] J.-Y. Hung, Y. Chi, I. H. Pai, Y.-C. Yu, G.-H. Lee, P.-T. Chou, K.-T. Wong, C.-C. Chen, C.-C. Wu, *Dalton Trans.*, **2009**, 6472.

[45] C.-H. Lin, Y.-Y. Chang, J.-Y. Hung, C.-Y. Lin, Y. Chi, M.-W. Chung, C.-L. Lin, P.-T. Chou, G.-H. Lee, C.-H. Chang, W.-C. Lin, *Angew. Chem.*, **2011**, *123*, 3240.

[46] M. Montalti, A. Credi, L. Prodi, M. T. Gandolfi, *Handbook of Photochemistry*, Taylor & Francis Group: Broken Sound Parkway NW, **2006**.

[47] X. Yang, Z. Wang, S. Madakuni, J. Li, G. E. Jabbour, *Adv. Mater.*, **2008**, *20*, 2405.

[48] Y. Unger, A. Zeller, S. Ahrens, T. Strassner, *Chem. CommUN.* **2008**, 3263.

[49] Y. Unger, D. Meyer, O. Molt, C. Schildknecht, I. Münster, G. Wagenblast, T. Strassner, *Angew. Chem. Int. Ed.*, **2010**, *49*, 10214.

[50] K. Li, X. Guan, C.-W. Ma, W. Lu, Y. Chen, C.-M. Che, *Chem. Commun.*,

2011, *47*, 9075.

[51] Z. M. Hudson, C. Sun, M. G. Helander, Y.-L. Chang, Z.-H. Lu, S. Wang, *J. Am. Chem. Soc.*, **2012**, *134*, 13930.

[52] H.-J. Son, W.-S. Han, J.-Y. Chun, B.-K. Kang, S.-N. Kwon, J. Ko, S. J. Han, C. Lee, S. J. Kim, S. O. Kang, *Inorg. Chem.*, **2008**, *47*, 5666.

[53] R. Czerwieniec, J. Yu, H. Yersin, *Inorg. Chem.*, **2011**, *50*, 8293.

Chapter 2 Synthesis and Luminescent Properties of *cis* Bis-N-Heterocyclic Carbene Platinum(II) Bis-Arylacetylide Complexes

Publication 1. *Inorganic chemistry* **2011**, *50*, 1220-1228.

Yuzhen Zhang, Jai Anand Garg, Clement Michelin, Thomas Fox, Olivier Blacque,* and Koushik Venkatesan*

Institute of Inorganic Chemistry, University of Zurich, Winterthurerstrasse 190, CH-8057, Zurich, Switzerland

1220 *Inorg. Chem.* **2011**, *50*, 1220–1228
DOI: 10.1021/ic101632v

Inorganic Chemistry
Article

Synthesis and Luminescent Properties of *cis* Bis-*N*-Heterocyclic Carbene Platinum(II) Bis-Arylacetylide Complexes

Yuzhen Zhang, Jai Anand Garg, Clement Michelin, Thomas Fox, Olivier Blacque,* and Koushik Venkatesan*

Institute of Inorganic Chemistry, University of Zürich, Winterthurerstrasse 190, CH-8057, Zürich, Switzerland

Received August 11, 2010

A series of luminescent *N*-heterocyclic carbene platinum(II) complexes, [(pmim)Pt(C≡C−R)$_2$] (R = C_6H_5 (**2**), C_6H_4OMe (**3**), $C_6H_2(OMe)_3$ (**4**), $C_6H_4NMe_2$ (**5**), C_4H_3S (**6**), $C_6H_4C{\equiv}CC_6H_5$ (**7**), 1-pyrenyl (**8**), and C_6H_4F (**9**)), were successfully synthesized using the precursor (pmim)PtI_2, **1** (pmim = 1,1′-dipentyl-3,3′-methylene-diimidazoline-2,2′-diylidene). The X-ray crystal structures of **1**, **4**, **5**, and **7** have been determined. These complexes showed long-lived emission in solution at room temperature. The emission origin of the complexes is tentatively assigned to be from triplet states of predominantly intraligand (IL) character with some mixing of metal-to-ligand charge-transfer (MLCT) character. TD-DFT and DFT calculations have been performed on most of the complexes to ascertain the nature of the excited state. Changes in the alkynyl ligands lead to a change in the absorption and emission maxima seen for these complexes in a potentially predictable way.

Introduction

During the past two decades, heavy metal complexes that display room temperature phosphorescence[1−3]have been actively probed due to their application in phosphorescent organic light-emitting devices (PhOLED).[4,5] Most commonly used heavy metal complexes are based on Pt and Ir.[6−13] In this context, *cis*-platinum σ-acetylide complexes bearing either diimine or phosphine as ancillary ligands (Figure 1) have evoked a lot of recent interest.[14−24] Moreover, devices based on α-diimine bis-(arylacetylide)platinum(II) complexes have also been successfully fabricated and have been shown as promising materials for application in devices.[25] Following the utility of *N*-heterocyclic carbenes as good σ-donating neutral ligands in organometallic chemistry,[26−32] their effect on varying photophysical properties when

*To whom correspondence should be addressed. E-mail: oblacque@aci.uzh.ch (O.B.), venkatesan.koushik@aci.uzh.ch (K.V.).

(1) Bulovic, V.; Gu, G.; Burrows, P. E.; Forrest, S. R.; Thompson, M. E. *Nature* **1996**, *380*, 29–29.
(2) Sun, Y. R.; Giebink, N. C.; Kanno, H.; Ma, B. W.; Thompson, M. E.; Forrest, S. R. *Nature* **2006**, *440*, 908–912.
(3) Yersin, H. *Highly efficient OLEDs with Phosphorescent Materials*; Wiley-VCH: Weinheim, Germany, 2008.
(4) Baldo, M. A.; O'Brien, D. F.; You, Y.; Shoustikov, A.; Sibley, S.; Thompson, M. E.; Forrest, S. R. *Nature* **1998**, *395*, 151–154.
(5) Baldo, M. A.; Thompson, M. E.; Forrest, S. R. *Nature* **2000**, *403*, 750–753.
(6) Brooks, J.; Babayan, Y.; Lamansky, S.; Djurovich, P. I.; Tsyba, I.; Bau, R.; Thompson, M. E. *Inorg. Chem.* **2002**, *41*, 3055–3066.
(7) Furuta, P. T.; Deng, L.; Garon, S.; Thompson, M. E.; Frechet, J. M. J. *J. Am. Chem. Soc.* **2004**, *126*, 15388–15389.
(8) Hirani, B.; Li, J.; Djurovich, P. I.; Yousufuddin, M.; Oxgaard, J.; Persson, P.; Wilson, S. R.; Bau, R.; Goddard, W. A.; Thompson, M. E. *Inorg. Chem.* **2007**, *46*, 3865–3875.
(9) Ma, B. W.; Djurovich, P. I.; Thompson, M. E. *Coord. Chem. Rev.* **2005**, *249*, 1501–1510.
(10) Ma, B. W.; Li, J.; Djurovich, P. I.; Yousufuddin, M.; Bau, R.; Thompson, M. E. *J. Am. Chem. Soc.* **2005**, *127*, 28–29.
(11) You, Y.; Park, S. Y. *Dalton Trans.* **2009**, 1267–1282.
(12) Lamansky, S.; Djurovich, P.; Murphy, D.; Abdel-Razzaq, F.; Lee, H. E.; Adachi, C.; Burrows, P. E.; Forrest, S. R.; Thompson, M. E. *J. Am. Chem. Soc.* **2001**, *123*, 4304–4312.
(13) Tamayo, A. B.; Alleyne, B. D.; Djurovich, P. I.; Lamansky, S.; Tsyba, I.; Ho, N. N.; Bau, R.; Thompson, M. E. *J. Am. Chem. Soc.* **2003**, *125*, 7377–7387.
(14) Hissler, M.; Connick, W. B.; Geiger, D. K.; McGarrah, J. E.; Lipa, D.; Lachicotte, R. J.; Eisenberg, R. *Inorg. Chem.* **2000**, *39*, 447–457.
(15) Miskowski, V. M.; Houlding, V. H.; Che, C. M.; Wang, Y. *Inorg. Chem.* **1993**, *32*, 2518–2524.
(16) Chan, C. W.; Cheng, L. K.; Che, C. M. *Coord. Chem. Rev.* **1994**, *132*, 87–97.
(17) Yam, V. W. W.; Lo, K. K. W.; Wong, K. M. C. *J. Organomet. Chem.* **1999**, *578*, 3–30.
(18) Sacksteder, L.; Baralt, E.; Degraff, B. A.; Lukehart, C. M.; Demas, J. N. *Inorg. Chem.* **1991**, *30*, 2468–2476.
(19) Yam, V. W. W.; Yeung, P. K. Y.; Chan, L. P.; Kwok, W. M.; Phillips, D. L.; Yu, K. L.; Wong, R. W. K.; Yan, H.; Meng, Q. J. *Organometallics* **1998**, *17*, 2590–2596.
(20) Whittle, C. E.; Weinstein, J. A.; George, M. W.; Schanze, K. S. *Inorg. Chem.* **2001**, *40*, 4053–4062.
(21) Pomestchenko, I. E.; Luman, C. R.; Hissler, M.; Ziessel, R.; Castellano, F. N. *Inorg. Chem.* **2003**, *42*, 1394–1396.
(22) Castellano, F. N.; Pomestchenko, I. E.; Shikhova, E.; Hua, F.; Muro, M. L.; Rajapakse, N. *Coord. Chem. Rev.* **2006**, *250*, 1819–1828.
(23) Hua, F.; Kinayyigit, S.; Cable, J. R.; Castellano, F. N. *Inorg. Chem.* **2005**, *44*, 471–473.
(24) Hua, F.; Kinayyigit, S.; Cable, J. R.; Castellano, F. N. *Inorg. Chem.* **2006**, *45*, 4304–4306.
(25) Chan, S. C.; Chan, M. C. W.; Wang, Y.; Che, C. M.; Cheung, K. K.; Zhu, N. Y. *Chem.—Eur. J.* **2001**, *7*, 4180–4190.
(26) Arnold, P. L.; Casely, I. J. *Chem. Rev.* **2009**, *109*, 3599–3611.
(27) Doyle, M. P.; Duffy, R.; Ratnikov, M.; Zhou, L. *Chem. Rev.* **2010**, *110*, 704–724.
(28) Hindi, K. M.; Panzner, M. J.; Tessier, C. A.; Cannon, C. L.; Youngs, W. J. *Chem. Rev.* **2009**, *109*, 3859–3884.

 Published on Web 01/18/2011 © 2011 American Chemical Society

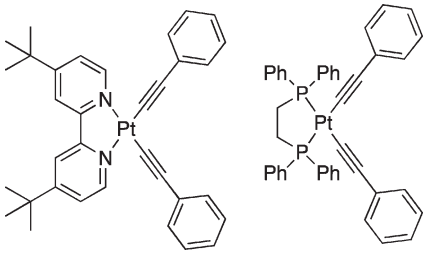

Figure 1. Platinum(II) dialkynyl complexes bearing diimine and bis-phosphine ligands.

compared to diimine or phosphine ligands is of current interest. Developments in bidentate bis-(imidaozolin-2-ylidenes) based metal complexes have been reviewed recently.[33]

Phosphorescence of iridium(III) *N*-heterocyclic carbene and platinum(II) tetracarbene in the ultra/near-UV region and blue region of the spectrum have also been reported.[34−37] While compared to the platinum(II) tetracarbene dicationic complexes, the platinum(II) bis-(imidazolin-2-ylidenes) diiodide complexes do not show any luminescence at RT. It was hypothesized that substitution of the halides with strong field ligands such as alkynes would sufficiently destabilize the metal centered (MC) transition states to higher energies, thereby creating an appropriate metal−ligand environment for effective mixing of singlet−triplet states and radiative relaxation from the triplet manifold. Examples of bis-carbene platinum(II) complexes bearing σ-acetylide ligands *cis* to each other are unprecedented. Together with the aim of achieving emmisivity at RT, an emission tunabilty could also be expected upon varying the electronic properties of the alkyne ligands. Herein, we report the synthesis and spectroscopic properties of a series of platinum(II) bis-(imidazolin-2-ylidenes) bis-(arylacetylide) complexes along with DFT and TD-DFT (time-dependent DFT) calculations to elucidate the photophysical nature of the complexes.

Results and Discussion

Synthesis and Characterization. The preparation of the 1,1′-dipentyl-3,3′-methylene-diimidazoline-2,2′-diylidene (pmim) salt **A** was accomplished in good yield upon reaction of *N*-pentylimidazole with diiodomethane by using a previously reported procedure (see the Supporting Information for details).[36a,37] The bis-carbene Pt(II) diiodide complex **1** (Scheme 1) was obtained in 62% yield following a literature procedure.[36b] Single crystal X-ray

Scheme 1

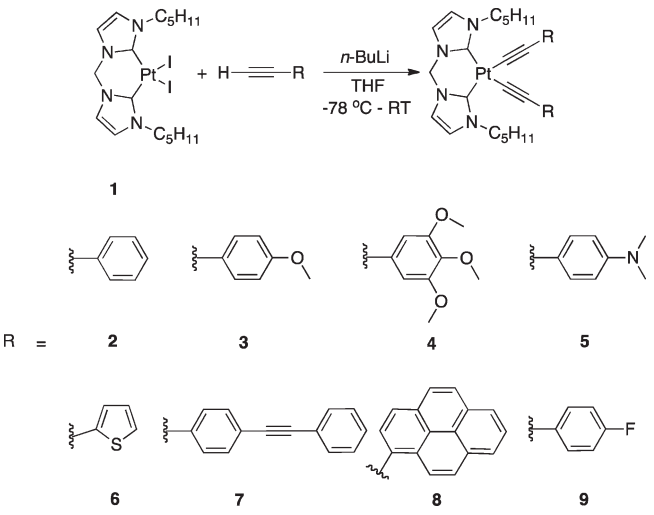

diffraction studies further confirmed the molecular structure of **1**. Our initial attempts to synthesize the diacetylide complex **2** by reaction of **1** with phenylacetylene involving a CuI-catalyzed iodide-to-alkyne metathesis using CH_2Cl_2/$HNiPr_2$ did not proceed in the same fashion as has been reported for the diimine complexes;[25] instead it afforded a mixture of inseparable products. Lithium phenylacetylide in THF was added to complex **1** in THF at −80 °C, and the reaction mixture was stirred at RT for 12 h. Subsequent workup and column chromatography on silica gel gave complex **2** in 54% yield. A total of eight platinum(II) complexes bearing different acetylide ligands were synthesized in moderate to good yields of 36−84% using similar reaction conditions. Scheme 1 shows the general procedure for the synthesis of complexes **2**−**9**.

All of the complexes were fully characterized; the various spectroscopic data (^{1}H NMR, ^{13}C NMR, IR) supported the assignmnent of a square planar platinum(II) center accommodating two *cis*-acetylide and bis-carbene ligands in the coordination sphere. Single crystal X-ray diffraction structures of complexes **4**, **5**, and **7** were also obtained. It is worth noting here that complexes bearing a combination of bidentate *N*-heterocyclic carbene and acetylide ligands are unknown so far. The perspective views of **1**, **4**, **5**, and **7** are shown in Figure 2. As expected, the Pt(II) atom adopted a distorted square planar environment; the Pt−$C_{carbene}$ bond lengths observed in **4**, **5**, and **7** varied between 2.001(11) and 2.041(2) Å and were marginally longer than those of 1.977(4) and 1.984(4) in [Pt(pmim)$_2$I$_2$]. These slight elongations reflect the greater *trans* influence of the phenylacetylide ligands in comparison with the iodide. The bond lengths between the acetylenic carbon atoms in the range 1.194(14)−1.209(15) were similar to those found in platinum(II) diimine bisacetylide complexes.[25] Further, the molecular packing in the crystal structures of these complexes showed no Pt···Pt interactions; the shortest intermolecular Pt···Pt distance was 5.228 Å in **7**. Concentration dependent absorption studies of all of the complexes in CH_2Cl_2 ($c \approx 10^{-6}$−10^{-4} mol dm^{-3}) showed neither a change of the peak maxima nor generation of an additional low energy band, confirming the absence of Pt···Pt interactions in solution and also precluding any excimeric (MMLCT) transitions.

(29) Lin, J. C. Y.; Huang, R. T. W.; Lee, C. S.; Bhattacharyya, A.; Hwang, W. S.; Lin, I. J. B. *Chem. Rev.* **2009**, *109*, 3561–3598.
(30) Mizuhata, Y.; Sasamori, T.; Tokitoh, N. *Chem. Rev.* **2010**, *110*, 3850–3850.
(31) Poyatos, M.; Mata, J. A.; Peris, E. *Chem. Rev.* **2009**, *109*, 3677–3707.
(32) Vougioukalakis, G. C.; Grubbs, R. H. *Chem. Rev.* **2010**, *110*, 1746–1787.
(33) Schuster, O.; Yang, L. R.; Raubenheimer, H. G.; Albrecht, M. *Chem. Rev.* **2009**, *109*, 3445–3478.
(34) Sajoto, T.; Djurovich, P. I.; Tamayo, A.; Yousufuddin, M.; Bau, R.; Thompson, M. E.; Holmes, R. J.; Forrest, S. R. *Inorg. Chem.* **2005**, *44*, 7992–8003.
(35) Unger, Y.; Meyer, D.; Strassner, T. *Dalton Trans.* **2010**, *39*, 4295–4301.
(36) (a) Unger, Y.; Zeller, A.; Taige, M. A.; Strassner, T. *Dalton Trans.* **2009**, 4786–4794. (b) Ahrens, S.; Strassner, T. *Inorg. Chim. Acta* **2006**, *359*, 4789–4796.
(37) Unger, Y.; Zeller, A.; Ahrens, S.; Strassner, T. *Chem. Commun.* **2008**, 3263–3265.

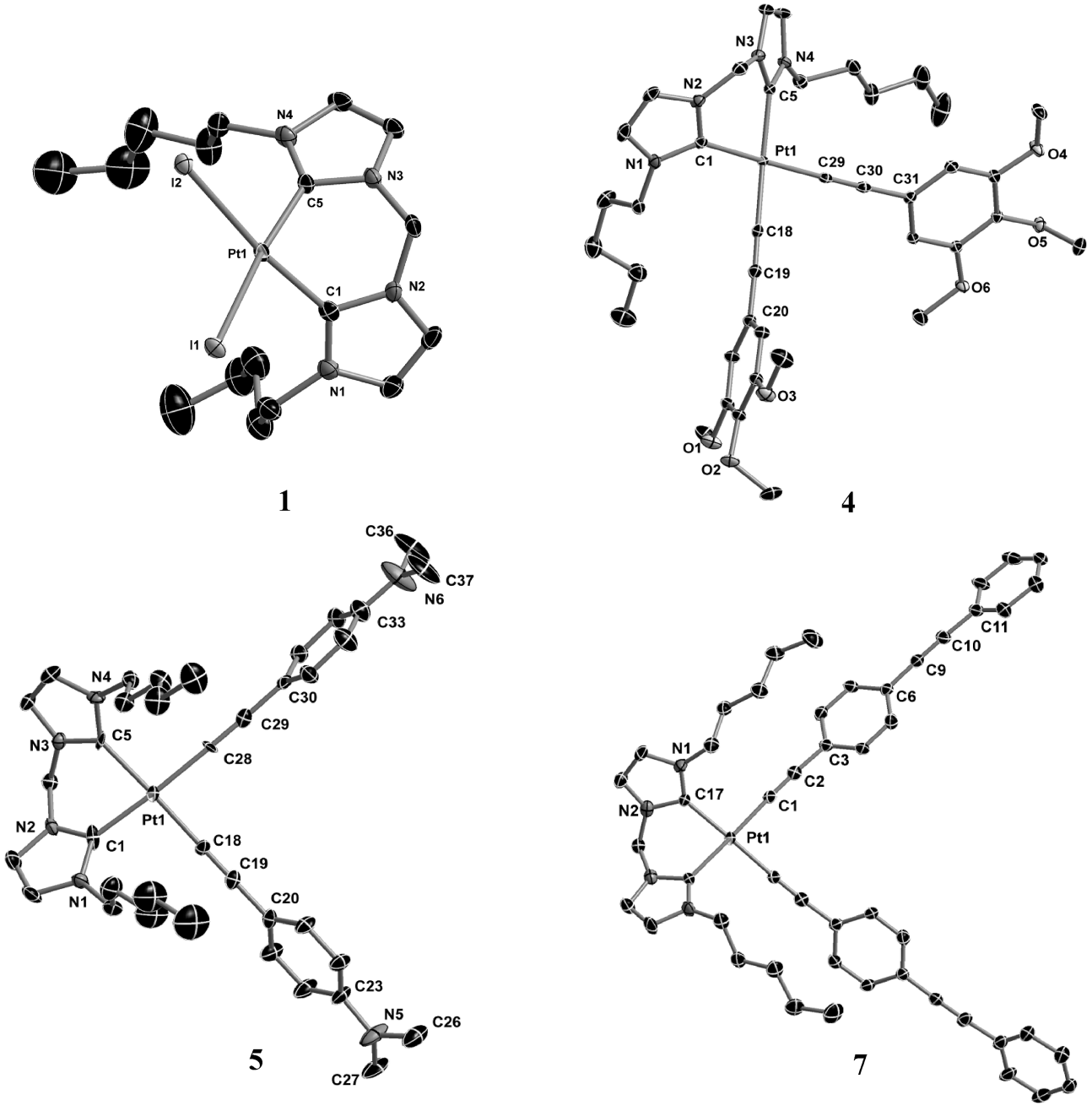

Figure 2. Molecular structures of **1** (top left), **4** (top right), **5** (bottom left), and **7** (bottom right) with a selective atomic numbering scheme. Thermal ellipsoids are drawn at the 30% probability level. Hydrogen atoms and dichloromethane solvent molecules are omitted for clarity.

Photophysical Properties. Figure 3 shows the absorption and emission spectra for complexes **2**−**7** and **9**; for clarity, the absorption spectrum of **8** is shown in the Supporting Information (Figure S3). The dependence of the absorption maxima at *ca.* 325 nm in relation to the acetylide ligands was studied. While the difference in the absorption maxima is barely discernible for **2** and **9**, the band exhibits a significant shift to lower energies for compounds **3**−**8**. Moreover, this systematic bathochromic shift was in line with the increasing electron donating nature of the acetylide ligands (F < H < OMe < $(OMe)_3$ < NMe_2). In addition to this phenomenon, a similar trend was observed with an increase in π-conjugation (**6** < **7** < **8**). The band around 325 nm in the absorption spectra of the complexes showed slight solvatochromic behavior along with the other higher energy bands, which corresponds to the carbene ligand and acetylide-based intraligand transitions (ILCT; see Figure S1 in the Supporting Information). As the electron donating nature of arylacetylide increases, it is expected that the energies of nonbonding and weakly π bonding metal orbitals will increase, leading to the observed red shifts in the complexes.[14]

The RT emissions of all compounds were broad and structureless, while the 77 K spectrum for these compounds showed resolvable vibronic components of the emission (see the Supporting Information). The influence of acetylide variation on the emission energies is evident from Table 1. The extent of observed shifts is greater than those seen in the absorption spectra with trends that are exactly similar. The observed bathochromic trends, both

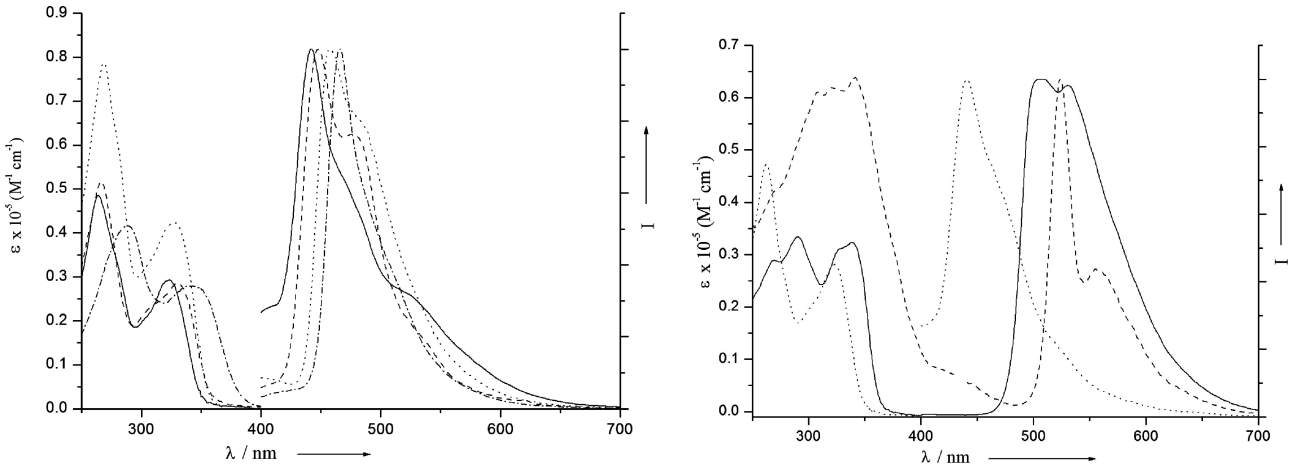

Figure 3. (Left) Electronic absorption spectra of **2** (—), **3** (----), **4** (· · · ·), and **5** (-·-·-·) and normalized emission spectra of **2** (—), **3** (----), **4** (· · · ·), and **5** (-·-·-) in degassed CH_2Cl_2 at 298 K. (Right) Electronic absorption spectra of **6** (—), **7** (----), and **9** (· · · ·) and normalized emission spectra of **6** (—), **7** (----), and **9** (· · · ·), in degassed CH_2Cl_2 at 298 K.

Table 1. Photophysical Properties of Complexes **2**−**9**

	room temperature solution (CH_2Cl_2)						77 K glass[b]
complex	absorption λ_{max}[nm] (ε_{max}/[dm^3 mol^{-1}cm^{-1}])	emission λ_{max} [nm]	τ [ns]	Φ_{em}[a]	k_r [s^{-1}] × 10^3	K_{nr} [s^{-1}] × 10^5	(2-MeTHF)
2	264(48600), 324(29400)	442, 482 sh	27.1	2.4×10^{-3}	88.6	368.1	437, 456 sh
3	266(51700), 330(28600)	447, 475 sh	44.0	1.8×10^{-3}	40.9	226.9	440, 484 sh
4	269(78700), 327(42500)	458, 482 sh	963.7	4.8×10^{-3}	5.0	10.3	444, 478 sh
5	288(41600), 341(27900)	465	844.1	3.4×10^{-2}	40.3	11.4	454, 481 sh
6	290(33400), 340(32400)	506, 530 sh	6335.1	1.1×10^{-2}	1.7	1.6	493, 508 sh
7	341(63800)	524, 555 sh	28982.0	1.9×10^{-2}	0.7	0.3	520, 553 sh
8	290(67400), 369(66500), 399(64700)	664, 725 sh	*c*	1.8×10^{-3}			659, 677 sh
9	263(47200), 323(28100)	440, 475 sh	27.2	8.2×10^{-3}	301.5	364.6	429, 455 sh

[a] Photoluminescence quantum yield determined with quinine sulfate as standard at 298 K. [b] Vibronic structured emission bands. [c] Multiexponential decay.

with increasing σ-donicity and greater conjugation, are consistent with a mainly metal-based HOMO and a π^* acetylide LUMO. All the Pt(II) complexes **2**−**9** displayed moderate phosphorescence intensity with quantum yields of emission between 1.8×10^{-3} and 3.4×10^{-2} in RT deoxygenated fluid solution and exhibited weak solvatochromic behavior (see Figure S2 in the Supporting Information). At 77 K, a rigidochromic shift of 4−14 nm was observed (see Figure S4 in the Supporting Information). The rigid glass does not allow the reorganization of the solvent dipoles upon generation of excited states and gives strongly blue-shifted spectra of complexes that emit from charge-transfer states. The above observed trend along with the vibronically structured nature of emission at 77 K suggests that the origin of emission occurs from admixed MLCT and interligand $\pi-\pi^*$ states. Stokes shifts of the lower lying emission in the range of 115−265 nm and lifetimes in the nanosecond to sub-microsecond regime, together with the observation of a 5- to 10-fold decrease in PL intensities upon exposure to molecular dioxygen, further support the phosphorescent nature of the emission.

Table 2. Electrochemical Data for Complexes **1**−**9**[a]

complex	E_{ox} (V)
1	+0.28
2	+0.58
3	+0.47
4	+0.46
5	−0.05
6	+0.50
7	+0.67
8	+0.33
9	+0.60

[a] Scan rate = 100 mV s^{-1} in 0.1 M [nBu$_4$][PF$_6$] (Au elelctrode; E vs $Fc^{0/+}$; 20 °C; CH_2Cl_2).

The cyclic voltammograms of all complexes showed similar redox profiles. In DCM/0.1 M TBAP, all complexes show an irreversible oxidation wave between +0.67 and −0.05 V (Table 2). A qualitative relationship between the oxidation potential of the alkynes and their respective emission energy was observed. In general, the oxidation potential was in decreasing order (**9** > **2** > **3** > **4** > **5**) with the increasing electron richness of the arylacetylide

(38) Frisch, M. J.; Trucks, G. W.; Schlegel, H. B.; Scuseria, G. E.; Rob, M. A.; Cheeseman, J. R.; Montgomery, J. A., Jr.; Vreven, T.; Kudin, K. N.; Burant, J. C.; Millam, J. M.; Iyengar, S. S.; Tomasi, J.; Barone, V.; Mennucci, B.; Cossi, M.; Scalmani, G.; Rega, N.; Petersson, G. A.; Nakatsuji, H.; Hada, M.; Ehara, M.; Toyota, K.; Fukuda, R.; Hasegawa, J.; Ishida, M.; Nakajima, T.; Honda, Y.; Kitao, O.; Nakai, H.; Klene, M.; Li, X.; Knox, J. E.; Hratchian, H. P.; Cross, J. B.; Bakken, V.; Adamo, C.; Jaramillo, J.; Gomperts, R.; Stratmann, R. E.; Yazyev, O.; Austin, A. J.; Cammi, R.; Pomelli, C.; Ochterski, J. W.; Ayala, P. Y.; Morokuma, K.; Voth, G. A.; Salvador, P.; Dannenberg, J. J.; Zakrzewski, V. G.; Dapprich, S.; Daniels, A. D.; Strain, M. C.; Farkas, O.; Malick, D. K.; Rabuck, A. D.; Raghavachari, K.; Foresman, J. B.; Ortiz, J. V.; Cui, Q.; Baboul, A. G.; Clifford, S.; Cioslowski, J.; Stefanov, B. B.; Liu, G.; Liashenko, A.; Piskorz, P.; Komaromi, I.; Martin, R. L.; Fox, D. J.; Keith, T.; Al-Laham, M. A.; Peng, C. Y.; Nanayakkara, A.; Challacombe, M.; Gill, P. M. W.; Johnson, B.; Chen, W.; Wong, M. W.; Gonzalez, C.; Pople, J. A. *Gaussian 03*, Gaussian, Inc.: Wallingford, CT, 2003.

Table 3. Comparison between Selected DFT Optimized and X-Ray Bond Distances (Å) and Angles (deg)

	compd	symm	Pt−C_{carb}	Pt−C_{alk}	$(-C\equiv C-)_n$	≡C−R	C_{carb}−Pt−C_{carb}	C_{alk}−Pt−C_{alk}
1	X-ray	C_1	1.984(4)				83.91(16)	
			1.977(4)					
	DFT	Cs	1.974				85.6	
2	DFT	Cs	2.028	1.985	1.228	1.425	85.9	88.4
3	DFT	Cs	2.027	1.986	1.228	1.425	86.0	88.2
5	X-ray	C_1	2.001(11)	1.993(11)	1.194(14)	1.451(16)	83.4(5)	88.8(4)
			2.020(10)	1.990(9)	1.205(14)	1.460(15)		
	DFT	C_s	2.026	1.986	1.228	1.424	86.0	88.4
6	DFT	C_s	2.028	1.981	1.229	1.407	85.9	89.0
7	X-ray	C_s	2.026(11)	1.999(11)	1.209(15) (n = 1)	1.440(16)	85.4(6)	88.6(6)
					1.203(17) (n = 2)			
	DFT	C_s	2.028	1.984	1.228 (n = 1)	1.421	85.9	88.7
					1.218 (n = 2)			
8	DFT	C_1	2.028	1.983	1.229	1.420	86.0	87.8
			2.029	1.983	1.229	1.420		
9	DFT	Cs	2.028	1.986	1.228	1.425	85.9	88.2

Table 4. Selected Singlet−Singlet (S_n) and Singlet−Triplet (T_1) Excited States with TDDFT/CPCM Vertical Excitation Energies (nm), Transition Coefficients, Orbitals Involved in the Transitions, and Oscillator Strengths for Compounds **2**−**9**

	2	**3**	**5**	**6**	**7**	**8**	**9**
				absorption			
exp λ_{abs}	264, 324	266, 330	288, 341	290, 340	341	290, 369, 399	262, 323
calc λ_{abs} [a]	289, 329	281, 344	286, 370	291, 354	372	410	277, 330
S_0-S_n	n = 1	n = 1	n = 1	n = 1	n = 1	n = 1	n = 1
	337 (0.481)	350 (0.496)	378 (0.534)	363 (0.561)	356 (1.565)	428 (0.833)	336 (0.458)
	H→L (0.68)	H→L (0.68)	H→L (0.68)	H→L (0.68)	H→L (0.65)	H→L (0.65)	H→L (0.68)
S_0-S_n	n = 2	n = 2	n = 2	n = 2	n = 2	n = 2	n = 2
	335 (0.376)	343 (0.434)	363 (0.563)	346 (0.478)	372 (1.258)	408 (0.533	334 (0.392)
	H-1→L (0.67)	H-1→L (0.68)	H-1→L (0.68)	H-1→L (0.67)	H-1→L (0.65)	H-1→L (0.66)	H-1→L (0.67)
S_0-S_n	n = 3	n = 3	n = 7	n = 5	n = 3	n = 3	n = 3
	304 (0.172)	302 (0.118)	290 (0.182)	290 (0.218)	342 (0.655)	389 (0.363)	302 (0.151)
	H-2→L (0.67)	H-2→L (0.68)	H→L+4 (0.53)	H→L+1 (0.59)	H→L+1 (0.65)	H→L+1 (0.66)	H-2→L (0.67)
S_0-S_n	n = 5	n = 5	n = 8	n = 6	n = 4	n = 4	n = 7
	282 (0.055)	286 (0.066)	284 (0.577)	287 (0.239)	340 (0.346)	382 (0.200)	275 (0.060)
	H-4→L (0.66)	H→L+2 (0.53)	H→L+1 (0.58)	H-1→L+1 (0.61)	H-1→L+1 (0.65)	H-1→L+1 (0.67)	H-4→L (0.66)
S_0-S_n	n = 6	n = 8	n = 9	n = 7	n = 10	n = 10	n = 8
	282 (0.358)	280 (0.409)	282 (0.352)	282 (0.049)	285 (0.067)	321 (0.090)	274 (0.312)
	H-1→L+1 (0.62)	H-1→L+1 (0.47)	H→L+5 (0.43)	H-4→L (0.65)	H-3→L+1 (0.53)	H-1→L+2 (0.52)	H→L+1 (0.65)
S_0-S_n	n = 7	n = 9	n = 10				n = 11
	279 (0.280)	278 (0.446)	282 (0.069)				273 (0.352)
	H→L+1 (0.65)	H-2→L+1 (0.43)	H-1→L+4 (0.51)				H-1→L+1 (0.57)
				Emission			
exp λ_{emiss}	442	447	465	506	524	664	440
calc λ_{emiss} [b]	454	461	485	546	562	683	453
S_0-T_1	437	442	464	504	549	698	436
	H→L (0.57)	H→L (0.58)	H→L (0.60)	H→L (0.61)	H→L (0.57)	H→L (0.53)	H→L (0.57)

[a] The calculated values are obtained from the TDDFT/CPCM UV−vis spectra drawn by Gaussview. [b] Solvent-corrected energy difference between the optimized ground state and the lowest-lying triplet state.

ancillary ligands. The correlation exemplifies the similarity between the electrochemical and spectroscopic trend. However, it should be noted here that complexes **6**−**8** did not obey the above tendency. Oxidation of the [(pmim)Pt-(C≡C−R)$_2$] was not observed in most cases up to +1.5 V. This result is comparable to the behavior observed in Pt(diimine)(C≡C−R)$_2$ complexes.

DFT and TD-DFT Calculations. In order to support the photophysical assignments from experimental observations, TD-DFT and DFT calculations were carried out for most of the studied complexes (**1** - **3** and **5** − **9**). All calculations were performed with the Gaussian03 program package[38] using the hybrid functional PBE1PBE[39] in conjunction with the Stuttgart/Dresden effective core potentials (SDD) basis set[40] for the Pt center augmented with one f-polarization function (exponent α = 0.993) and the standard 6-31+G(d) basis set[41] for the remaining atoms. For computational ease, the *n*-pentyl chain was replaced by a methyl group and the details about the DFT-optimized geometries are presented in Supporting Information. The main geometric parameters of the calculated complexes, especially the bond distances and angles around the Pt metal center and the C≡C triple bond distances, obtained with the combination PBE1PBE/SDD:6-31+g(d) were in a good agreement with those from the X-ray structures (Table 3).

(39) Adamo, C.; Barone, V. *J. Chem. Phys.* **1999**, *110*, 6158–6170.

(40) Dunning, T. H., Jr.; Hay, P. J. *Modern Theoretical Chemistry*; Plenum: New York, 1976; Vol. *3*.

(41) Ditchfie, R.; Hehre, W. J.; Pople, J. A. *J. Chem. Phys.* **1971**, *54*, 724.

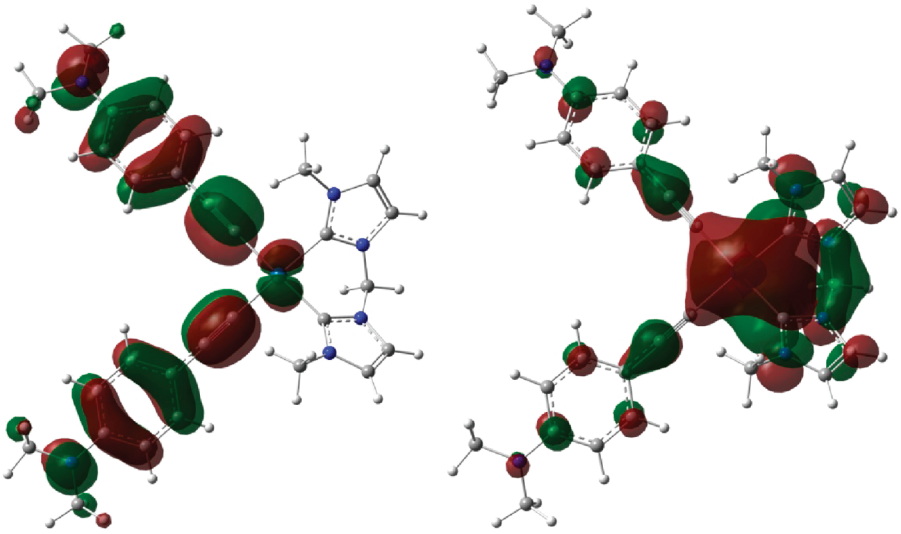

Figure 4. HOMO (left) and LUMO (right) of **5**.

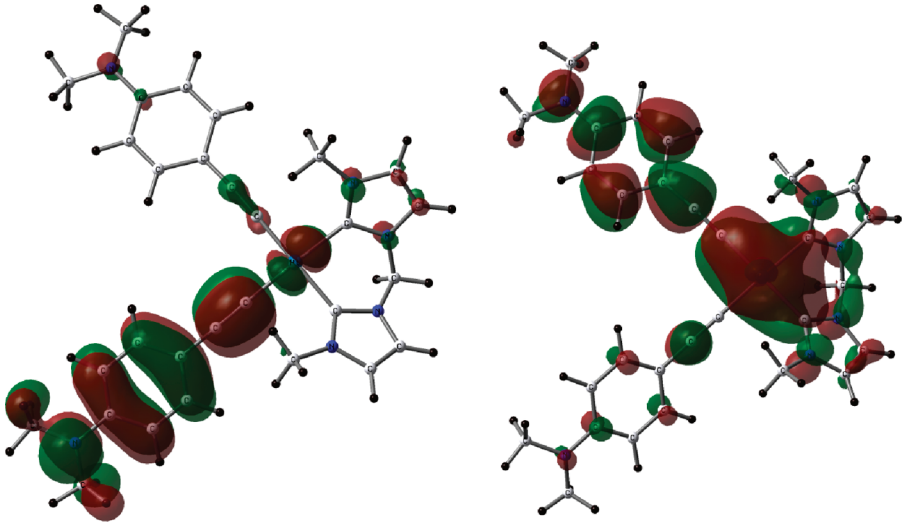

Figure 5. Lower- (left) and higher-energy SOMO (right) of the triplet excited state of **5**.

The main geometric parameters of the calculated complexes, especially the bond distances and angles around the Pt metal center and the C≡C triple bond distances, obtained with the combination PBE1PBE/SDD:6-31+g(d) are in a good agreement with those from the X-ray structures (Table 3). The calculated UV−vis spectra of the studied compounds also mimic the experimental results very well with two sharp and distinct absorption bands in the region of 250−450 nm for **2** and **3**, **5** and **6**, and **8** and **9**, and only one band for **7** in the same UV−visible region (Table 4). Although the vertical singlet−triplet transitions ($S_0 \rightarrow T_1$) calculated on the ground state geometries were very satisfactory for estimating the emission maxima of the studied compounds since $\Delta\lambda_{max}$ is for five complexes as low as 2−5 nm (overall $2 < \Delta\lambda_{max} < 33$ nm, Table 3), we thought that emission maxima calculated from the energy differences between the ground- and triplet-excited states would be more relevant theoretically. For this purpose, solvent effects (dichloromethane) were included by single-point calculations on the optimized gas-phase geometries. The corresponding solvent-corrected energy differences calculated for the studied compounds are reported in Table 3 as calc λ_{emiss}. Surprinsigly, these new values exhibit a larger overestimation of the emission maxima ($13 < \Delta\lambda < 42$ nm, Table 3); however, the tendency is still correct from one compound to another (Supporting Information).

It appeared from the TD-DFT calculations that the HOMO−LUMO gap and consequently the shape of these frontier orbitals play a major role in the absorption and emission properties of our complexes. Taking **5** as an exemplary molecule, the most red band of the absorption spectrum corresponds to H → L and H-1 → L; the HOMO is of π character mainly based on the C≡C−R π orbitals (93%) in an out-of-phase combination with the Pt $5d_{xy}$ orbital (6%). The participation of the *N*-heterocyclic dicarbene in the HOMO is very weak (1%). The LUMO is clearly delocalized over the whole molecule with 32% on the alkyne ligands, 35% on the dicarbene ligand, and 33% on the empty Pt $6p_y$ metal (Figure 4). The shape of the LUMO exhibits a bonding interaction between the p_y atomic orbitals of the Pt and C_{alk} atoms and an antibonding interaction between the p_y atomic orbitals of the triply bonded C atoms of the alkyne ligands. Consequently,

the red-shifted band of the UV−vis spectrum can be assigned to an admixture of metal-perturbed intraligand ^{1}ILCT ($\pi_{alk} \rightarrow \pi^*_{alk}$), metal-perturbed ligand-to-ligand ^{1}LLCT ($\pi_{alk} \rightarrow \pi^*_{carb}$), and metal-to-ligand ^{1}MLCT transitions. The blue-shifted band appears to get its origins from different occupied frontier orbitals and the only LUMO+1. Since H and L+1 are both composed at 93 and 88% of π orbitals of the alkyne atoms (only 6 and 4% of Pt), the absorption band can easily be assigned as a metal-perturbed intraligand ^{1}ILCT ($\pi_{alk} \rightarrow \pi^*_{alk}$).

The transition responsible for the emission band of **5** involves the migration of one electron from the HOMO to the LUMO, leading to the two singly occupied molecular orbitals (SOMOs) of the triplet excited state. Both SOMOs have contributions mainly from only one of the alkyne ligands (also with participation of the carbene and the metal center): the lower-energy SOMO is localized on one alkyne, and the higher-energy SOMO involves the other one (Figure 5). The modifications of the geometrical parameters of the optimized triplet state relative to the ground state structure confirm this observation. Indeed, the main changes occur for only one alkyne ligand in which the Pt−C and the C−C_{ring} are shortened and the C≡C bond is elongated, a consequence of the π-bonding and π-antibonding interactions seen in the higher-energy SOMO (Figure 5) derived from the former LUMO of the ground state. The unchanged alkyne is the one which does not participate in the higher-energy SOMO. This provides a clear indication that the triplet excited state of **5** contains mainly the metal-perturbed ligand-to-ligand ^{3}LLCT ($\pi_{alk} \rightarrow \pi^*_{alk}$) character and to a lesser extent the ^{3}MLCT (d $\rightarrow \pi^*_{alk}$). Since the calculations revealed a similar behavior for all compounds, we can extend this conclusion to all of them.

Conclusions

A series of luminescent platinum(II) alkynyl complexes of the type [(pmim)Pt(C≡C−R)$_2$] (R = C_6H_5, C_6H_4OMe, $C_6H_2(OMe)_3$, $C_6H_4NMe_2$, C_4H_3S, $C_6H_4C{\equiv}CC_6H_5$, 1-pyrenyl, and C_6H_4F) were successfully synthesized starting from the corresponding diiodide complex [(pmim)PtI$_2$]. These complexes are found to be emissive at room temperature with their lowest lying emissive states tunable and assigned from predominantly metal-perturbed ligand-to-ligand ^{3}LLCT ($\pi_{alk} \rightarrow \pi^*_{alk}$) character and to a lesser extent the ^{3}MLCT (d $\rightarrow \pi^*_{alk}$). Through further rational design and synthetic methodologies, these new alkynyl complexes can be utilized for the buildup of luminescent functional materials.

Experimental Section

General Procedure. All manipulations requiring an inert atmosphere were carried out using standard Schlenk techniques under dinitrogen. ^{1}H, ^{13}C{^{1}H}, and ^{19}F NMR spectra were recorded on Bruker AV2-300 (300 MHz) or AV-500 (500 MHz) spectrometers. Chemical shifts (δ) are reported in parts per million (ppm) referenced to tetramethylsilane (δ 0.00) ppm using the residual protio solvent peaks as internal standards (^{1}H NMR experiments) or the characteristic resonances of the solvent nuclei (^{13}C NMR experiments). ^{19}F NMR was referenced to $CFCl_3$ (δ 0.00) ppm. Coupling constants (J) are quoted in Hertz (Hz), and the following abbreviations are used to describe the signal multiplicities: s (singlet), d (doublet), t (triplet), q (quartet), m (multiplet), and dm (doublet of multiplet). Proton and carbon assignments have been made using routine one- and two-dimensional NMR spectroscopies where appropriate. Infrared (IR) spectra were recorded on a Perkin-Elmer 1600 Fourier Transform spectrophotometer using KBr pellets with frequencies (ν_{max}) quoted in wavenumbers (cm^{-1}). Elemental microanalysis was carried out with a Leco CHNS-932 analyzer. Mass spectra were run on a Finnigan-MAT-8400 mass spectrometer. TLC analysis was performed on precoated Merck Silica Gel 60F_{254} slides and visualized by luminescence quenching either at (short wavelength) 254 nm or (long wavelength) 365 nm. Chromatographic purification of products was performed on a short column (length 15.0 cm, diameter 1.5 cm) using silica gel 60 and 230−400 mesh using a forced flow of eluent. UV−vis measurements were carried out on a Perkin-Elmer Lambda 19 UV/vis spectrophotometer. Emission spectra were acquired on a Perkin-Elmer spectrophotometer using 450 W xenon lamp excitation by exciting at the longest-wavelength absorption maxima. All samples for emission spectra were degassed by at least three freeze−pump−thaw cycles in an anaerobic cuvette and were pressurized with N_2 following each cycle. The 77 K emission spectra were acquired in frozen 2-methyltetrahydrofuran (2-MeTHF) glass. Luminescence quantum yields of ϕ were determined at 298 K (estimated uncertainty ±15%) using standard methods; wavelength-integrated intensities (I) of the corrected emission spectra were compared to iso-absorptive spectra of the quinine sulfate standard (ϕ_r = 0.54 in 1N H_2SO_4 air-equilibrated solution) and were corrected for the solvent refractive index. Phosphorescence lifetime measurements were performed on an Edinburgh FLS920 spectrophotometer, using nF900 with a 30 000 Hz frequency, with 15 nm excitation and 15 nm emission slit widths.

All starting materials were purchased from commercial sources and used as received unless stated otherwise. The solvents used for synthesis were of analytical grade. The compounds 4-methoxyphenylacetylene, 2-ethynylthiophene, 2,3,4-trimethoxyphenylacetylene, and 4-(phenylethynyl)phenylacetylene were prepared according to literature methods.

[Pt(pmim)$_2$I$_2$] (1). Platinum(II) acetylacetonate (Pt(acac)$_2$) (0.197 g, 0.5 mmol) was dissolved in DMSO (3 mL) and heated to 100 °C. The ligand pmim (0.272 g, 0.5 mmol) dissolved in DMSO (20 mL) was slowly added to the hot solution of Pt(acac)$_2$ for a period of 10 h. The reaction mixture was then stirred at 100 °C for another 2 h, and the DMSO was removed *in vacuo*. The resulting product was purified by column chromatography over silica gel with the acetone/*n*-hexane (v/v 4:5) as the eluent. The pure compound was isolated as a white powder. Crystals suitable for X-ray were obtained from a mixture of dichloromethane and pentane. (Crystallographic data for compounds **1**, **4**, **5**, and **7** are giving in Table 5.) Yield: 62%. ^{1}H NMR (500 MHz, CD_2Cl_2, 20 °C): δ (ppm) 7.31 (d, 2H, ^3J = 2.5 Hz, NC*H*=CHN), 6.91 (d, 2H, ^3J = 2.0 Hz, NCH=C*H*N), 6.23 (d, H, ^2J = 13.0 Hz, NCH_2N), 5.80 (d, H, ^2J = 13.0 Hz, NCH_2N), 4.73 (m, 2H, NCH_2CH$_2$), 4.08 (m, 2H, NCH_2CH$_2$), 1.84 (m, 4H, NCH$_2$CH_2CH$_2$), 1.27 (m, 8H, CH$_2$CH_2CH_2CH$_3$), 0.86 (t, 6H, ^3J = 2.0 Hz, CH$_2$CH_3). ^{13}C{^{1}H} NMR (125.8 MHz, CD_2Cl_2, 20 °C), δ (ppm) = 151.3 ($J_{Pt=C}$ = 1373 Hz), 121.1 and 120.3 (NC*H*=*C*HN), 63.6 (N*C*H$_2$N), 52.3, 31.0, 28.6, 22.5, 14.0 (C on the (CH$_2$)$_4$CH$_3$). ESI$^+$ MS m/z: 687.5 (M$^+$). Elemental analysis calcd for $C_{17}H_{30}I_2N_4Pt$: C, 27.60; H, 4.09; N, 7.58. Found: C, 27.81; H, 4.03; N, 7.58.

General Procedure for the Synthesis of Complexes 2−9. All manipulations were performed under a N_2 atmosphere. Two equivalents of *n*-BuLi were added to the flask containing 2 equiv of the ligand in THF (10 mL) at −78 °C, and the reaction mixture was stirred for 30 min at this temperature. The temperature was then gradually raised to room temperature and stirred for another 30 min. The reaction mixture was then transferred to a flask containing starting material (**1**) dissolved in THF (10 mL) at −78 °C and stirred for 30 min at this temperature. The

Table 5. Crystallographic Data for Compounds **1**, **4**, **5**, and **7**[a]

	1	**4**	**5**	**7**
empirical formula	$2(C_{17}H_{28}I_2N_4Pt)$, $5(CH_2Cl_2)$	$C_{39}H_{50}N_4O_6Pt$, CH_2Cl_2	$2(C_{37}H_{48}N_6Pt)$, $3(CH_2Cl_2)$	$C_{49}H_{46}N_4Pt$, CH_2Cl_2
fw (g mol^{-1})	1899.26	950.84	1798.57	970.90
temp (K)	183(2)	183(2)	183(2)	183(2)
wavelength (Å)	0.71073	0.71073	0.71073	0.71073
cryst syst, space group	monoclinic, *C*2/*c*	monoclinic, $P2_1/n$	monoclinic, *C*2/*c*	orthorhombic, *Pnma*
a (Å)	31.7153(11)	14.7205(2)	25.9714(6)	10.2966(3)
b (Å)	9.0519(3)	20.6676(2)	10.0221(2)	36.5438(9)
c (Å)	21.9061(18)	15.2338(2)	31.4262(7)	11.4905(2)
α (deg)	90	90	90	90
β (deg)	102.644(5)	117.138(1)	90.715(2)	90
γ (deg)	90	90	90	90
volume (Å^3)	6136.4(6)	4124.46(9)	8179.2(3)	4323.61(18)
Z, density (calcd) (Mg m^{-3})	4, 2.056	4, 1.531	4, 1.461	4, 1.492
abs coefficient (mm^{-1})	7.037	3.581	3.661	3.408
F(000)	3576	1920	3624	1952
cryst size (mm^3)	0.48 × 0.33 × 0.07	0.32 × 0.11 × 0.05	0.17 × 0.07 × 0.03	0.16 × 0.11 × 0.03
θ range (deg)	2.6 to 30.5	2.5 to 30.5	2.5 to 25.0	2.7 to 25.7
reflns collected	27259	59674	32595	19026
reflns unique	9355/R_{int} = 0.0355	12584/R_{int} = 0.0417	7199/R_{int} = 0.0852	4048/R_{int} = 0.0568
completeness to *θ* (%)	99.9	99.9	99.9	97.0
absorption correction	analytical	analytical	analytical	analytical
max/min transmission	0.632 and 0.128	0.839 and 0.583	0.912 and 0.661	0.906 and 0.672
data/restraints/params	6910/62/308	9450/15/486	5024/53/443	3136/0/272
goodness-of-fit on F^2	0.983	0.915	1.109	1.180
final R_1 and wR_2 indices [$I > 2\sigma(I)$]	0.0344, 0.0713	0.0253, 0.0531	0.0764, 0.1272	0.0699, 0.1625
R_1 and wR_2 indices (all data)	0.0571, 0.0752	0.0396, 0.0545	0.1327, 0.1417	0.0887, 0.1670

[a] The unweighted *R* factor is $R_1 = \sum(F_o - F_c)/\sum F_o$, $I > 2\,\sigma(I)$, and the weighted *R* factor is $wR_2 = \{\sum w(F_o^2 - F_c^2)^2/\sum w(F_o^2)^2\}^{1/2}$.

temperature was gradually raised to room temperature and stirred for another 1 h. After H_2O (10 mL) was added, the product was extracted with CH_2Cl_2 (3 × 10 mL). The organic layer was separated and dried over $MgSO_4$. The solvent was evaporated to dryness, and the compound was purified by column chromatography over silica gel.

[Pt(pmim)$_2$(C≡C−C$_6$H$_5$)$_2$] (2). EtOAc/CH_2Cl_2 (3:7 v/v) was used as the eluent. Yield: 52%. ^{1}H NMR (500 MHz, CD_2Cl_2, 20 °C): *δ* (ppm) 7.28 (d, 2H, ^3J = 1.5 Hz, NC*H*=CHN), 7.24 (d, 4H, ^3J = 10.0 Hz, *o*-Phenyl H), 7.16 (t, 4H, ^3J = 6.0 Hz, *m*-Phenyl H), 7.06 (t, 2H, ^3J = 6.5 Hz, *p*-Phenyl H), 6.79 (d, ^3J = 1.5 Hz, NCH=C*H*N), 5.95 (s, 2H, NCH_2N), 4.96 (m, 2H, NCH_2CH$_2$), 4.18 (m, 2H, NCH_2CH$_2$), 1.76 (m, 4H, NCH$_2$-CH_2CH$_2$), 1.21 (m, 8H, CH$_2$CH_2CH_2CH$_3$), 0.78 (t, 6H, ^3J = 7.5 Hz, CH$_2$CH_3). ^{13}C{^{1}H} NMR (125.8 MHz, CD_2Cl_2, 20 °C): *δ* (ppm) 167.8 (*C*=Pt), 131.1, 128.1, 124.9 (C on Phenyl ring), 129.1 (C≡*C*−Pt), 120.3 and 120.2 (N*C*H=*C*HN), 108.9 and 106.8 (Ph*C*≡*C*−Pt), 63.2 (N*C*H$_2$N), 50.8, 31.3, 28.9, 22.6, 13.9 (C on the (CH$_2$)$_4$CH$_3$). ESI$^+$ MS *m*/*z*: 687.5 (M$^+$). IR (ATR, cm^{-1}) $\nu_{C\equiv C}$ = 2098. Elemental analysis calcd for $C_{33}H_{40}N_4Pt$: C, 57.63; H, 5.86; N, 8.15. Found: C, 57.79; H, 5.89; N, 8.20.

[Pt(pmim)$_2$(C≡C−C$_6$H$_4$−OCH$_3$)$_2$] (3). EtOAc/CH_2Cl_2 (2:8 v/v) was used as the eluent. Yield: 74%. ^{1}H NMR (500 MHz, CD_2Cl_2, 20 °C): *δ* (ppm) = 7.23 (d, 4H, ^3J = 10.0 Hz, *o*-Phenyl H), 7.15 (d, 2H, ^3J = 2.0 Hz, *H*C=CH), 6.88 (d, 2H, ^3J = 2.0 Hz, HC=C*H*), 6.73 (d, 4H, ^3J = 10.0 Hz, m-Phenyl H), 6.09 (d, 1H, ^2J = 12.5 Hz, NCH_2N), 5.62 (d, 1H, ^2J = 13.0 Hz, NCH_2N), 4.98 (m, 2H, NCH_2CH$_2$), 4.24 (m, 2H, NCH_2CH$_2$), 3.74 (s, 6H, OCH_3), 1.81 (m, 4H, NCH$_2$CH_2CH$_2$), 1.21 (m, 8H, CH$_2$CH_2CH_2CH$_3$), 0.78 (t, 6H, ^3J = 7.0 Hz, CH$_2$CH_3). ^{13}C-{^{1}H} NMR (125.8 MHz, CD_2Cl_2, 20 °C), *δ* (ppm) 168.4 (C=Pt), 157.3, 132.3, 121.7, and 113.5 (C on Phenyl ring), 120.7 and 119.7 (N*C*=*C*N), 108.1 and 103.5 (Ph*C*=*C*−Pt), 63.5 (N*C*H$_2$N), 55.4 (O−*C*H$_3$), 50.9, 31.3, 29.0, 22.6, 14.0 (C on the (CH$_2$)$_4$CH$_3$). ESI$^+$ MS *m*/*z*: 746.4 (M$^+$). IR (ATR, cm^{-1}) $\nu_{C\equiv C}$ = 2107. Elemental analysis calcd (%) for $C_{35}H_{44}N_4O_2Pt$: C, 56.21; H, 5.94; N, 7.49. Found: C, 56.38; H, 6.01; N, 7.34.

[Pt(pmim)$_2$(C≡C−C$_6$H$_2$(OCH$_3$)$_3$)$_2$] (4). EtOAc was used as the eluent. Yield: 84%. ^{1}H NMR (500 MHz, CD_2Cl_2, 20 °C): *δ* (ppm) 7.18 (d, 2H, ^3J = 1.5 Hz, *H*C=CH), 6.89 (d, 2H, ^3J = 2.0 Hz, HC=C*H*), 6.55 (s, 4H, *o*-Phenyl H), 6.09 (d, 1H, ^2J = 12.5 Hz, NCH_2N), 5.69 (d, 1H, ^2J = 11.5 Hz, NCH_2N), 4.93 (m, 2H, NCH_2CH$_2$), 4.28 (m, 2H, NCH_2CH$_2$), 3.7 (m, 12H, OCH_3), 3.71(m, 6H, OCH_3), 1.79 (m, 4H, NCH$_2$CH_2CH$_2$), 1.21 (m, 8H, CH$_2$CH_2CH_2CH$_3$), 0.77 (t, 6H, ^3J = 7.0 Hz, CH$_2$CH_3). ^{13}C-{^{1}H} NMR (125.8 MHz, CD_2Cl_2, 20 °C): *δ* (ppm) 171.7 (*C*=Pt), 153.0, 136.4, 124.5, 108.3, and 105.5 (C on the phenyl ring), 120.7 and 119.7 (N*C*=*C*N), 110.1 (*C*-Pt), 63.5 (N*C*H$_2$N), 60.7 and 56.1 (O-*C*H$_3$), 51.0, 33.6, 31.4, 23.7, 14.0 (C on the (CH$_2$)$_4$CH$_3$). ESI$^+$ MS *m*/*z*: 866.5 (M$^+$). IR(ATR, cm^{-1}) $\nu_{C\equiv C}$ = 2096. Elemental analysis calcd for $C_{39}H_{52}N_4O_6Pt$: C, 53.97; H, 6.04; N, 6.46. Found: C, 53.74; H, 6.10; N, 6.54.

[Pt(pmim)$_2$(C≡C−C$_6$H$_4$−N(CH$_3$)$_2$)$_2$] (5). EtOAc/CH_2Cl_2 (1:9 v/v) was used as the eluent. Single crystals suitable for X-ray diffraction studies were obtained from a mixture of dichloromethane and pentane. Yield: 43%. ^{1}H NMR (500 MHz, CD_2Cl_2, 20 °C): *δ* (ppm) 7.19 (d, 4H, ^3J = 9.0 Hz, *o*-Phenyl H), 7.09 (d, 2H, ^3J = 2.0 Hz, NC*H*CHN), 6.90 (d, 2H, ^3J = 1.5 Hz, NC*H*CHN), 6.60 (d, 4H, ^2J = 4.5 Hz, *m*-phenyl H), 6.13 (d, 1H, ^2J = 12.5 Hz, NCH_2N), 5.52 (d, H, ^2J = 12.5 Hz, NCH_2N), 5.13 (m, 2H, NCH_2CH$_2$), 4.17 (m, 2H, NCH_2CH$_2$), 2.89 (s 12H, N(CH$_3$)$_2$), 1.80 (m, 4H, CH$_2$CH_2CH$_2$), 1.23 (m, 8H, CH$_2$CH_2CH_2CH$_3$), 0.80 (t, 6H, ^3J = 7.0 Hz, CH$_2$CH_3). ^{13}C{^{1}H} NMR (125.8 MHz, CD_2Cl_2, 20 °C): *δ* 169.0 (*C*=Pt), 148.5, 132.2, 117.7, and 112.5 (C on the phenyl ring), 120.6 and 119.4 (N*C*=*C*N), 108.9 and 102.0 (Ph*C*=*C*−Pt), 63.6 (N*C*H$_2$N), 40.7 (C on the N(*C*H$_3$)$_2$), 50.9, 31.4, 29.0, 22.7, 14.0 (C on the (CH$_2$)$_4$CH$_3$). ESI$^+$ MS *m*/*z*: 772.5 (M$^+$). IR (ATR, cm^{-1}) $\nu_{C\equiv C}$ = 2098. Elemental analysis calcd for $C_{37}H_{50}N_6Pt$: C, 57.42; H, 6.51; N, 10.86. Found: C, 57.69; H, 6.40; N, 10.63.

[Pt(pmim)$_2$(C≡C−Ph−C≡C−Ph)$_2$] (6). EtOAc/CH_2Cl_2 (1:9 v/v) was used as the eluent. Single crystals suitable for X-ray diffraction studies were obtained from a mixture of dichloromethane and diethyl ether. Yield: 36%. ^{1}H NMR (500 MHz, CD_2Cl_2, 20 °C): *δ* (ppm) 7.51 (m, 4H, Phenyl H), 7.34 (m, 10H, phenyl H), 7.26 (m, 4H, phenyl H), 7.24 (d, 2H, ^3J = 2.0 Hz, NCHC*H*N), 6.86 (d, ^3J = 2.0 Hz, NCHC*H*N), 6.06 (d, 2H, ^2J = 13.0 Hz, NCH_2N), 5.84 (d, 2H, ^2J = 13.0 Hz, NCH_2N), 4.90 (m, 2H, NCH_2CH$_2$), 4.24 (m, 2H, NCH_2CH$_2$), 1.81 (m, 4H, NCH$_2$CH_2CH$_2$), 1.23 (m, 8H, CH$_2$CH_2CH_2CH$_3$), 0.79 (t, 6H,

^3J = 7.0 Hz, CH_2CH_3). $^{13}C\{^1H\}$ NMR (125.8 MHz, CD_2Cl_2, 20 °C): δ (ppm) 167.6 (*C*═Pt), 131.6, 131.3, 131.2, 129.3, 128.6, 128.3, 123.7, and 119.2 (C on the phenyl ring), 120.6 and 120.0 (N*C*═*C*N), 110.4 (C≡*C*−Pt), 109.1 (*C*≡C−Pt), 90.1 and 89.8 (Ph*C*≡*C*Ph), 63.4 (N*C*H_2N), 50.9, 31.3, 29.0, 22.6, and 14.0 (C on the $(CH_2)_4CH_3$). ESI^+ MS *m*/*z*: 886.5 (M^+). IR (ATR, cm^{-1}) $\nu_{C\equiv C}$ = 2094. Elemental analysis calcd for $C_{49}H_{48}N_4Pt$: C, 66.27; H, 5.45; N, 6.31. Found: C, 65.95; H, 5.66; N, 6.16.

[Pt(pmim)$_2$(C≡C−2-thienyl)$_2$] (7). EtOAc/CH_2Cl_2 (1:9 v/v) was used as the eluent. Yield: 55%. ^1H NMR (500 MHz, CD_2Cl_2, 20 °C): δ (ppm) 7.28 (d, 2H, ^3J = 1.5 Hz, NC*H*CHN), 6.95 (d, 2H, ^3J = 1.5 Hz, NCHC*H*N), 6.84 (m, 6H, H on thienyl), 5.95 (d, H, ^2J = 13.0 Hz, NCH_2N), 5.88 (d, H, ^2J = 13.0 Hz, NCH_2N), 4.90 (m, 2H, NCH_2CH_2), 4.16 (m, 2H, NCH_2CH_2), 1.78 (m, 4H, $NCH_2CH_2CH_2$), 1.22 (m, 8H, $CH_2CH_2CH_2CH_3$), 0.86 (t, 6H, ^3J = 3.5, CH_2CH_3). $^{13}C\{^1H\}$ NMR (125.8 MHz, CD_2Cl_2, 20 °C): δ (ppm) 167.2 (*C*═Pt), 129.9, 127.6, 126.7, and 122.7 (C on thienyl ring), 120.5 (N*C*═CN), 120.2 (NC═*C*N), 111.9 (C≡*C*−Pt), 100.5 (*C*≡C−Pt), 63.4 (N*C*H_2N), 50.9, 31.3, 28.9, 22.6, 14.0 (C on the $(CH_2)_4CH_3$)). ESI^+ MS *m*/*z*: 698.3 (M^+). IR (ART, cm^{-1}) $\nu_{C\equiv C}$ = 2090. Elemental analysis calcd for $C_{29}H_{36}N_4S_2Pt$: C, 49.77; H, 5.18; N, 8.01. Found: C, 49.69; H, 5.25; N, 8.04.

[Pt(pmim)$_2$(C≡C-2-Pyrenyl)$_2$] (8). EtOAc/CH_2Cl_2 (1:3 v/v) was used as the eluent. Yield: 46%. ^1H NMR (500 MHz, CD_2Cl_2, 20 °C): δ 9.04 (d, 1H, ^3J = 10.0 Hz, H on the pyrenyl), 8.1, 8.0, 7.9, 7.8 (m, 8H, H on the pyrenyl), 7.18 (d, ^3J = 1.5 Hz, NCHC*H*N), 6.95 (d, ^3J = 1.5 Hz, NC*H*CHN), 6.29 (d, 1H, ^2J = 13.0 Hz, NCH_2N), 5.70 (d, 1H, ^2J = 13.0 Hz, NCH_2N), 5.18 (m, 2H, NCH_2CH_2), 4.40 (m, 2H, NCH_2CH_2), 1.90 (m, 4H, $NCH_2CH_2CH_2$), 1.21 (m, 8H, $CH_2CH_2CH_2CH_3$), 0.78 (t, 6H, ^3J = 7.5 Hz, CH_2CH_3). $^{13}C\{^1H\}$ NMR (125.8 MHz, CD_2Cl_2, 20 °C), δ (ppm) 168.3 (*C*═Pt), 131.9, 131.8, 131.7, 129.0, 125.0, and 125.0 (C on the pyrenyl ring without H), 129.5, 127.8, 127.8, 127.2, 126.5, 126.0, 124.8, 124.7, and 124.6 (C on the pyrenyl ring with H), 120.8 (N*C*═CN), 119.9 (NC═*C*N), 114.7 (C≡*C*−Pt), 108.0 (*C*≡C−Pt), 63.7 (N*C*H_2N), 51.3, 31.4, 28.9, 22.6, 13.9 (C on the $(CH_2)_4CH_3$)). ESI^+ MS *m*/*z*: 934.5 (M^+). IR (ATR,cm^{-1}) $\nu_{C\equiv C}$ = 2080. Elemental analysis calcd for $C_{53}H_{48}N_4Pt$: C, 68.01; H, 5.17; N, 5.99. Found: C, 67.91; H, 5.38; N, 5.83.

[Pt(pmim)$_2$(C≡C-4-C_6H_4F)$_2$] (9). EtOAc/CH_2Cl_2 (2:8 v/v) was used as an eluent. Yield: 76%. ^1H NMR (500 MHz, CD_2Cl_2, 20 °C): δ (ppm) 7.47 (d, 4H, ^3J = 8.0 Hz, Phenyl H), 7.09 (d, 2H, ^3J = 1.5 Hz, NC*H*═CHN), 6.92 (m, 4H, Phenyl H), 6.75 (d, 2H, ^3J = 1.5 Hz, NCH═C*H*N), 6.15 (d, 1H, ^2J = 13.0 Hz, NCH_2N), 5.67 (d, 1H, ^2J = 13.0 Hz, NCH_2N), 4.94 (m, 2H, NCH_2CH_2), 4.31 (m, 2H, NCH_2CH_2), 1.85 (m, 4H, $NCH_2CH_2CH_2$), 1.26 (m, 8H, $CH_2CH_2CH_2CH_3$), 0.83 (t, 6H, ^3J = 5.0 Hz, CH_2CH_3). $^{13}C\{^1H\}$ NMR (125.8 MHz, CD_2Cl_2, 20 °C): δ (ppm) 167.8 (*C*═Pt), 161.4, 159.5 (J_{F-C} = 240 Hz), 132.4, 114.5 (C on Phenyl ring), 125.1 (C≡*C*−Pt), 120.4 and 120.2 (N*C*H═*C*HN), 107.2 and 105.0 (Ph*C*≡*C*−Pt), 63.4 (N*C*H_2N), 50.7, 31.0, 28.6, 22.7, 13.9 (C on the $(CH_2)_4CH_3$). ^{19}F NMR (188.3 MHz, CD_2Cl_2, 20 °C): δ (ppm) −115.8;. ESI^+ MS *m*/*z*: 721.3 (M^+). IR (ART, cm^{-1}) $\nu_{C\equiv C}$ = 2104. Elemental analysis calcd for $C_{33}H_{40}N_4Pt$: C, 54.92; H, 5.03; N, 7.76. Found: C, 55.31; H, 4.90; N, 7.39.

Computational Details. All calculations were performed with the Gaussian 03 program package[38] using the hybrid functional PBE1PBE[39] in conjunction with the Stuttgart/Dresden effective core potentials (SDD) basis set[40] for the Pt center augmented with one f-polarization function (exponent α = 0.993) and the standard 6-31+G(d) basis set[41] for the remaining atoms. Geometry optimizations were performed in the gas phase for both the singlet ground states and the lowest triplet excited states of all complexes. The optimized molecular structures were confirmed to be potential energy minima by vibrational frequency calculations at the same level of theory, as no imaginary frequency was found. The first 10 singlet−singlet and singlet−triplet transition energies were computed at the optimized S_0 geometries by using the time-dependent DFT (TDDFT) methodology.[42−44] Solvent effects were taken into account using the conductor-like polarizable continuum model (CPCM)[45,46] with dichloromethane as a solvent for single-point calculations on all optimized gas-phase geometries.

X-Ray Diffraction Analyses. Intensity data were collected at 183(2) K on an Oxford Xcalibur diffractometer (4-circle kappa platform, Ruby CCD detector, and a single wavelength Enhance X-ray source with MoK_α radiation, λ = 0.71073 Å).[47] The selected suitable single crystals were mounted using polybutene oil on the top of a glass fiber fixed on a goniometer head and immediately transferred to the diffractometer. Pre-experiment, data collection, data reduction, and analytical absorption corrections[48] were performed with the Oxford program suite *CrysAlisPro*.[49] The crystal structures were solved with SHELXS-97[50] using direct methods. The structure refinements were performed by full-matrix least-squares on F^2 with SHELXL-97.[50] All programs used during the crystal structure determination process are included in the WINGX software.[51] The program PLATON[52] was used to check the results of the X-ray analyses. CCDC 787595−787598 contain the supplementary crystallographic data (excluding structure factors) for this paper. These data can be obtained free of charge from The Cambridge Crystallographic Data Centre via www.ccdc.cam.ac.uk/data_request/cif.

Acknowledgment. We thank S. V. Rocha and Dr. N. Finney for help with excited-state lifetime measurements. K.V. is grateful to the University of Zürich and Prof. H. Berke for generous support.

Supporting Information Available: Synthetic protocol of ligand **A**, absorbance spectra of **3** in different solvents, emission spectra of **3** in different solvents, absorbance and emission spectra of **8**, 77 K emission spectra of all complexes, cyclic voltammogram of **8**, and energies and Cartesian coordinates from DFT calculations. This material is available free of charge via the Internet at http://pubs.acs.org.

(42) Bauernschmitt, R.; Ahlrichs, R. *Chem. Phys. Lett.* **1996**, *256*, 454–464.
(43) Casida, M. E.; Jamorski, C.; Casida, K. C.; Salahub, D. R. *J. Chem. Phys.* **1998**, *108*, 4439–4449.
(44) Stratmann, R. E.; Scuseria, G. E.; Frisch, M. J. *J. Chem. Phys.* **1998**, *109*, 8218–8224.
(45) Barone, V.; Cossi, M. *J. Phys. Chem. A* **1998**, *102*, 1995–2001.
(46) Cossi, M.; Rega, N.; Scalmani, G.; Barone, V. *J. Comput. Chem.* **2003**, *24*, 669–681.
(47) *Xcalibur CCD System*; Oxford Diffraction Ltd: Abingdon, England, 2007.
(48) Clark, R. C.; Reid, J. S. *Acta Crystallogr.* **1995**, *51*, 887–897.
(49) *CrysAlisPro*, versions 1.171.32334d-55; Oxford Diffraction Ltd: Abingdon, Oxfordshire, England.
(50) Sheldrick, G. M. *Acta Crystallogr.* **2008**, *64*, 112–122.
(51) Farrugia, L. J. *J. Appl. Crystallogr.* **1999**, *32*, 837.
(52) Spek, A. L. *J. Appl. Crystallogr.* **2003**, *36*, 7–13.

Supporting Information

Synthesis and Luminescent Properties of *cis* Bis-*N*-Heterocyclic Carbene Platinum(II) Bis-Arylacetylide Complexes

Yuzhen Zhang, Jai Anand Garg, Clement Michelin, Thomas Fox, Olivier Blacque and Koushik Venkatesan*[a]*

Institute of Inorganic Chemistry, University of Zürich, Winterthurerstrasse 190, CH-8057, Zürich, Switzerland

Table of contents

Synthesis of 1,1'- dipentyl - 3,3' – methylene - diimidazolium diiodide ($pmimI_2$)

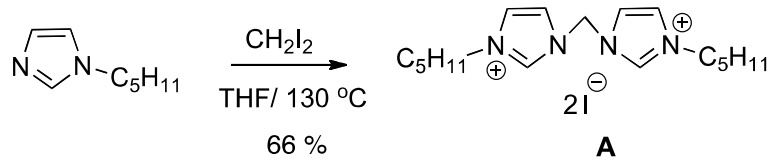

In a schlenk tube, *N*-pentylimidazole (0.55 g, 4 mmol) and diiodomethane (0.55 g, 2 mmol) were dissolved in THF (5 mL) and heated to 130 °C for 10 h. After cooling the reaction mixture to room temperature, precipitate was filtered off and washed with cold THF. The product was dried *in vacuo*. Yield 1.08 g (66%). ^{1}H NMR (300 MHz, CD_2Cl_2, 20 °C): δ (ppm) = 10.92 (s, 2H, NC*H*N), 9.07 (d, 2H, NCH=C*H*N), 7.52 (d, 2H, NCH=C*H*N), 7.36 (d, 2H, NCH_2N), 4.27 (t, 4H, NCH_2CH$_2$), 2.01 (m, 4H, NCH$_2$CH_2CH$_2$), 1.41 (m, 8H, CH$_2$CH_2CH_2CH$_3$), 0.69 (t, 6H, CH$_2$CH_3); ^{13}C{^{1}H} NMR (125.8 MHz, CD_2Cl_2, 20 °C), δ (ppm) = 137.5 (N*C*HN), 123.6 and 122.3 (N*C*H=*C*HN), 56.6 (N*C*H$_2$N), 50.8, 31.0, 29.2, 28.3, 22.0 (C on the (CH$_2$)$_4$CH$_3$); ESI$^+$ MS *m/z* : 289.4 (M$^+$).

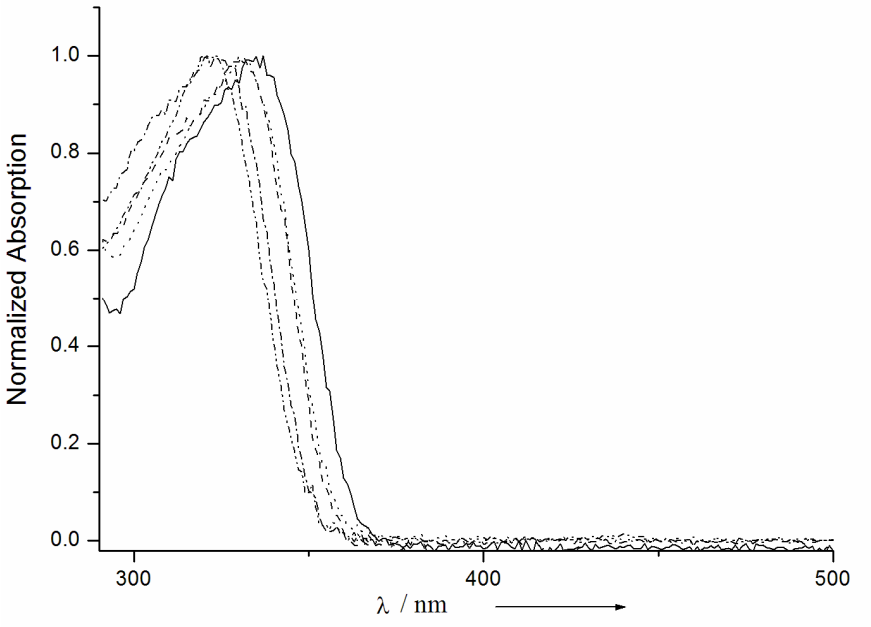

Figure S1. Normalized absorption spectra of complex **3** in toluene solid (―); THF dash (-- --); CH_2Cl_2 dot (····) , acetonitrile dash dot (-·-·); MeOH dash dot dot (-···).

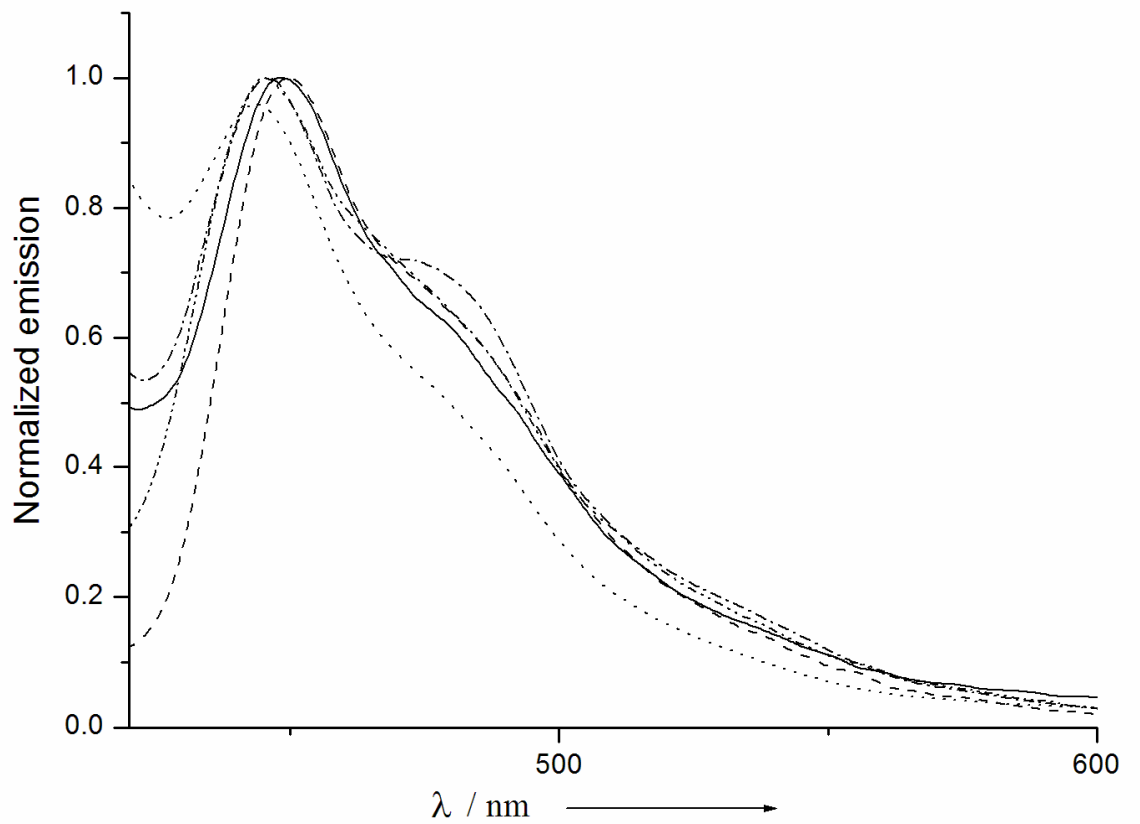

Figure S2. Normalized emission spectra of complex **3** in toluene solid (─); CH_2Cl_2 dash (-- --); THF dot (····); acetonitrile dash dot (-·-·); MeOH dash dot dot (-···).

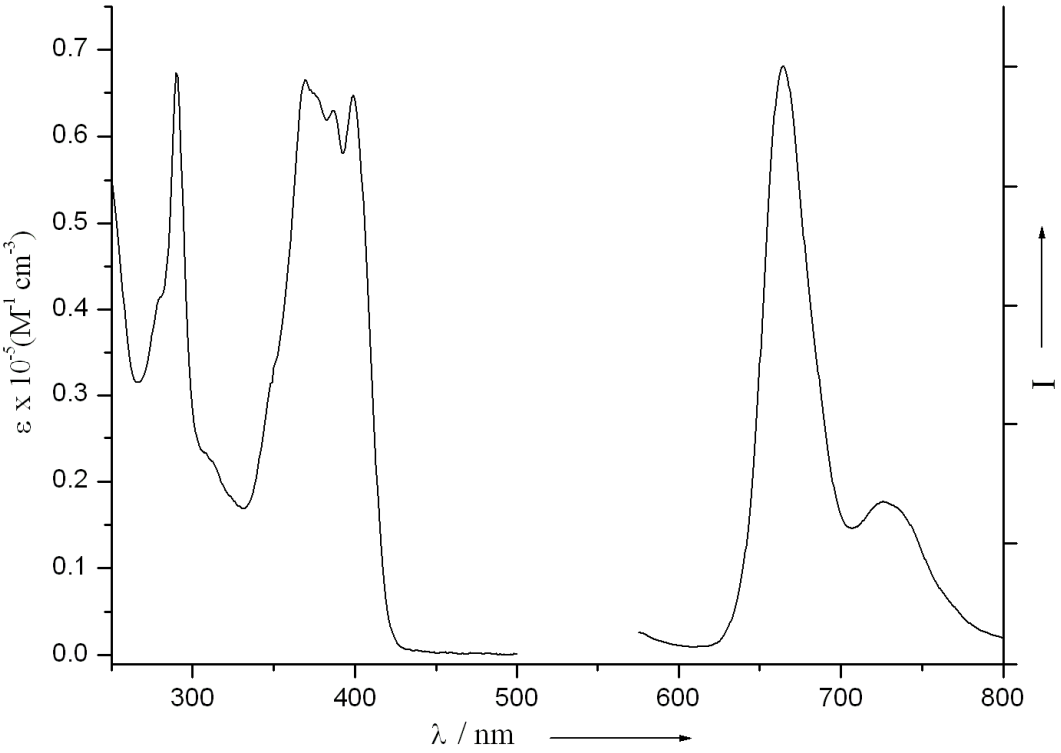

Figure S3. Absorption and emission spectra at room temperature in CH_2Cl_2 for complex **8**.

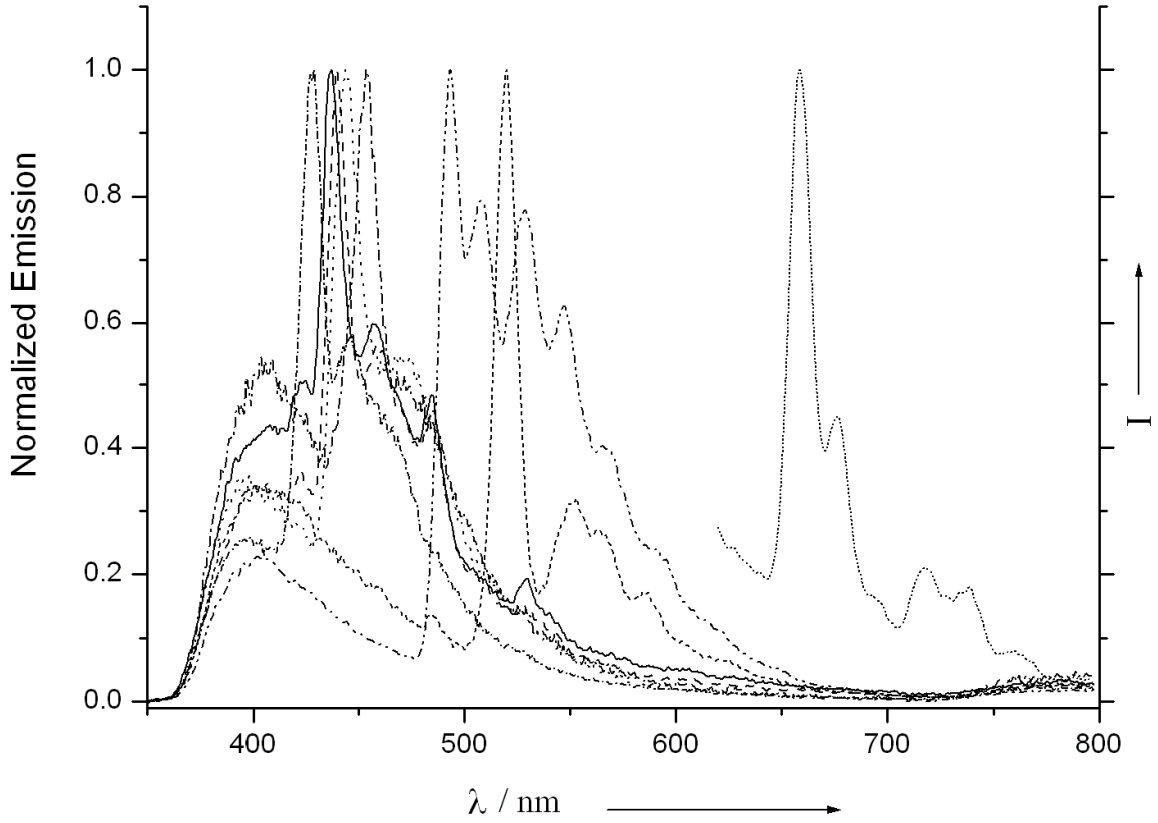

Figure S4. Emission spectra (77 K) in 2-MeTHF for all complexes. **2** solid (—), **3** dash (-- --), **4** dot (····), **5** dash dot (-·-·), **6** dash dot dot (- ··) **7** short dash (- - - -), **8** short dot (····), **9** short dash dot (-··)

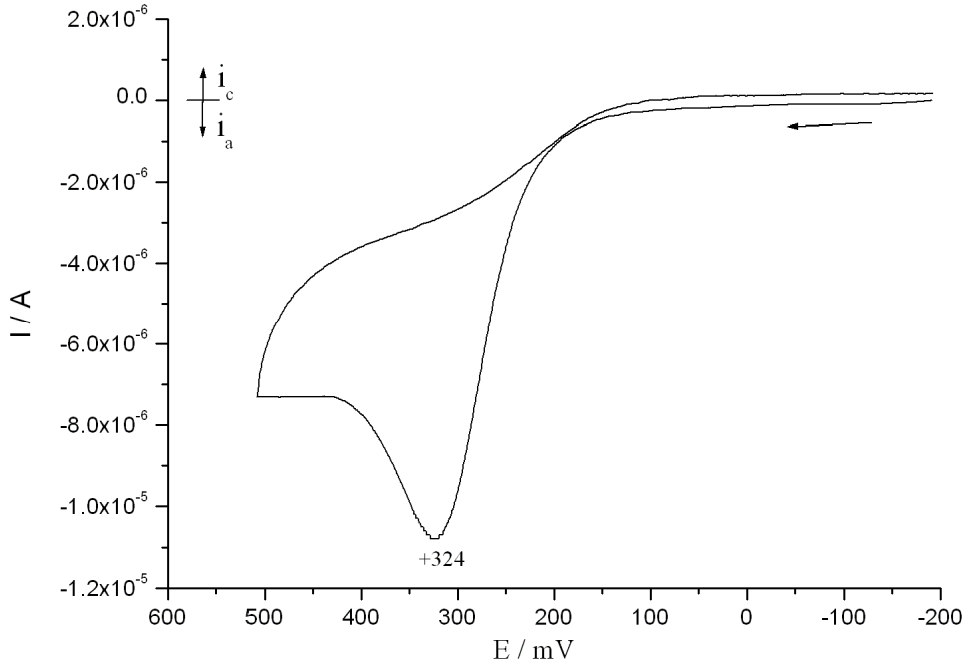

Figure S5. Cyclic voltammogram of **8** in 0.1 M [nBu_4][PF_6] (Au elelctrode; E vs $Fc^{0/+}$; 20 ^{o}C; CH_2Cl_2).

Energies and cartesian coordinates of the optimized ground-state structure of 1

C	0.91116500	1.81163400	3.02700000	H	3.31007800	0.74149500	-3.91204200
C	0.91116500	1.81163400	-3.02700000	H	4.30830300	-1.23868300	2.25243400
C	2.91412400	0.31872000	3.00078300	H	4.30830300	-1.23868300	-2.25243400
C	2.91412400	0.31872000	-3.00078300	H	3.52640500	-2.15838900	0.00000000
C	1.42026400	0.04435000	1.34079900	H	1.74435700	-2.35399400	0.00000000
C	1.42026400	0.04435000	-1.34079900	N	1.71283000	0.74002300	2.46132200
C	3.40602900	-0.64886900	2.18951800	N	1.71283000	0.74002300	-2.46132200
C	3.40602900	-0.64886900	-2.18951800	N	2.47468600	-0.80463200	1.18149300
C	2.56852500	-1.63545500	0.00000000	N	2.47468600	-0.80463200	-1.18149300
H	1.57087100	2.64213700	3.29470800	Pt	-0.02809200	0.06855100	0.00000000
H	1.57087100	2.64213700	-3.29470800	H	0.36857200	1.45486300	3.90554600
H	0.18552900	2.13326800	2.28076800	H	0.36857200	1.45486300	-3.90554600
H	0.18552900	2.13326800	-2.28076800	I	-1.89077100	-0.18767500	1.93924600
H	3.31007800	0.74149500	3.91204200	I	-1.89077100	-0.18767500	-1.93924600

Zero-point correction= 0.215314 (Hartree/Particle)
Thermal correction to Energy= 0.232386
Thermal correction to Enthalpy= 0.233330
Thermal correction to Gibbs Free Energy= 0.167032
Sum of electronic and zero-point Energies= -710.639457
Sum of electronic and thermal Energies= -710.622385
Sum of electronic and thermal Enthalpies= -710.621441
Sum of electronic and thermal Free Energies= -710.687739

Energies and cartesian coordinates of the optimized ground-state structure of 2

C	1.49693600	1.61197600	3.17309100	H	1.89007800	2.62583200	-3.04677900
C	1.49693600	1.61197600	-3.17309100	H	-5.79170200	0.93310800	3.82718200
C	-4.83925700	0.44043300	4.00959400	H	-5.79170200	0.93310800	-3.82718200
C	-4.83925700	0.44043300	-4.00959400	H	0.52233700	1.51951000	2.69164000
C	-3.84596200	0.48602500	3.03714200	H	0.52233700	1.51951000	-2.69164000
C	-3.84596200	0.48602500	-3.03714200	H	-4.01536200	1.00670000	2.09877500
C	-4.62288800	-0.23585800	5.21101700	H	-4.01536200	1.00670000	-2.09877500
C	-4.62288800	-0.23585800	-5.21101700	H	3.98188000	0.72259800	4.03049800
C	3.63610700	0.32421400	3.08824100	H	3.98188000	0.72259800	-4.03049800
C	-2.60344800	-0.14330300	3.24511800	H	-3.22154000	-1.40363800	6.35991000
C	3.63610700	0.32421400	-3.08824100	H	-3.22154000	-1.40363800	-6.35991000
C	-2.60344800	-0.14330300	-3.24511800	H	-1.44927500	-1.32148900	4.62943700
C	-1.58237000	-0.08865600	2.25262000	H	5.18347400	-1.03330800	2.25470400
C	-1.58237000	-0.08865600	-2.25262000	H	5.18347400	-1.03330800	-2.25470400
C	-0.71642900	-0.02626100	1.38448400	H	-1.44927500	-1.32148900	-4.62943700
C	-0.71642900	-0.02626100	-1.38448400	H	4.49347000	-1.94506600	0.00000000
C	-3.39888800	-0.86881400	5.42935000	H	2.73957400	-2.30164300	0.00000000
C	-3.39888800	-0.86881400	-5.42935000	N	2.40032200	0.65164200	2.56278600
C	2.18857200	0.02548000	1.38204000	N	2.40032200	0.65164200	-2.56278600
C	2.18857200	0.02548000	-1.38204000	N	3.32642700	-0.70033600	1.18683100
C	-2.40062200	-0.82335000	4.46137200	N	3.32642700	-0.70033600	-1.18683100
C	-2.40062200	-0.82335000	-4.46137200	Pt	0.70471400	0.04599200	0.00000000
C	4.22878300	-0.52976600	2.21855600	H	-5.40227900	-0.27237000	5.96819800
C	4.22878300	-0.52976600	-2.21855600	H	-5.40227900	-0.27237000	-5.96819800
C	3.49284900	-1.50857800	0.00000000	H	1.39304100	1.38659900	4.23775600
H	1.89007800	2.62583200	3.04677900	H	1.39304100	1.38659900	-4.23775600

After PCM corrections, the SCF energy is -1302.86151853 a.u.

Zero-point correction= 0.416108 (Hartree/Particle)
Thermal correction to Energy= 0.443925
Thermal correction to Enthalpy= 0.444869
Thermal correction to Gibbs Free Energy= 0.351688
Sum of electronic and zero-point Energies= -1302.401933
Sum of electronic and thermal Energies= -1302.374116
Sum of electronic and thermal Enthalpies= -1302.373172
Sum of electronic and thermal Free Energies= -1302.466353

Energies and cartesian coordinates of the optimized triplet-state structure of 2

C	1.43587300	1.49119000	3.21084500	C	-1.58100200	0.01800200	2.17945500
C	1.55728200	1.60741100	-3.21337800	C	-1.55868600	-0.04998000	-2.29656200
C	-4.82217400	0.61257400	3.94484200	C	-0.70278700	0.06238400	1.32160300
C	-4.97196400	-0.10185400	-3.70939400	C	-0.64740800	0.05751700	-1.41339400
C	-3.83030100	0.64155700	2.97067600	C	-3.40780200	-0.73407500	5.35543400
C	-3.95937100	0.00118300	-2.79354400	C	-3.35278300	-0.54487900	-5.49655000
C	-4.61859500	-0.07377300	5.14303200	C	2.18750900	-0.00120700	1.35601800
C	-4.69670900	-0.37113400	-5.07470800	C	2.23901300	0.03340000	-1.40592200
C	3.57043400	0.20138400	3.13078700	C	-2.41111900	-0.70657700	4.38561000
C	-2.60046000	-0.01623900	3.17177800	C	-2.31791700	-0.44767800	-4.60566500
C	3.71161600	0.34803000	-3.09063200	C	4.18993400	-0.61683100	2.24505600
C	-2.56695900	-0.16001500	-3.19814200	C	4.29349500	-0.50907100	-2.21671800

C	3.51535900	-1.51648800	-0.02378200	H	5.14281000	-1.12292300	2.29122700
H	2.00253900	2.31085800	3.66253900	H	5.25511300	-1.00007100	-2.23655900
H	2.12639900	2.45685200	-3.60247800	H	-1.28906400	-0.59086500	-4.92523700
H	-5.76348800	1.12796400	3.76721700	H	4.51062600	-1.96486600	-0.01139100
H	-6.00350400	0.02123300	-3.38713200	H	2.74745100	-2.29903400	-0.05316600
H	0.75323300	1.87540600	2.45346300	N	2.36200600	0.57228200	2.57486500
H	0.84093300	1.94844500	-2.46470000	N	2.46900600	0.67374000	-2.58022100
H	-3.98972200	1.17414300	2.03713600	N	3.33058400	-0.72865100	1.17014900
H	-4.16301200	0.20105400	-1.74559700	N	3.37694400	-0.69136200	-1.19978500
H	3.88691200	0.55450500	4.10102300	Pt	0.72980000	0.08415200	-0.05179900
H	4.07363700	0.75494200	-4.02310900	H	-5.39691100	-0.09663700	5.90176800
H	-3.24022300	-1.27748300	6.28285200	H	-5.50865300	-0.44991500	-5.79158500
H	-3.14576900	-0.76250500	-6.54216600	H	0.84642100	0.97604200	3.97397400
H	-1.47229000	-1.22987300	4.54842100	H	1.01022000	1.12237300	-4.02645400

After PCM corrections, the SCF energy is -1302.75728916 a.u.

b1m_t.com.log: Zero-point correction= 0.412302 (Hartree/Particle)
b1m_t.com.log- Thermal correction to Energy= 0.440607
b1m_t.com.log- Thermal correction to Enthalpy= 0.441551
b1m_t.com.log- Thermal correction to Gibbs Free Energy= 0.346901
b1m_t.com.log- Sum of electronic and zero-point Energies= -1302.305474
b1m_t.com.log- Sum of electronic and thermal Energies= -1302.277169
b1m_t.com.log- Sum of electronic and thermal Enthalpies= -1302.276225
b1m_t.com.log- Sum of electronic and thermal Free Energies= -1302.370875

Energies and cartesian coordinates of the optimized ground-state structure of 3

C	1.96852000	1.73721600	3.13831100	H	0.98721700	1.57579800	-2.73550600
C	1.97279600	1.61381600	-3.20260900	H	-3.62223700	1.37636300	1.96568200
C	-4.50851500	0.93783900	3.86869100	H	-3.61954600	1.29871300	-2.02436600
C	-4.50326900	0.78645700	-3.91006700	H	4.39486100	0.71344800	4.01672700
C	-3.48839600	0.90120100	2.93336600	H	4.40029300	0.55671000	-4.03725500
C	-3.48441300	0.78626400	-2.97264900	H	-2.99882000	-0.82773300	6.36278200
C	-4.34839000	0.31950500	5.11457500	H	-2.99025900	-1.07477600	-6.33153800
C	-4.34148000	0.12012100	-5.13073200	H	-1.19933900	-0.87785900	4.69112700
C	4.02441300	0.31795300	3.08264000	H	5.48484200	-1.14897100	2.27805800
C	-2.26596900	0.25132900	3.20523900	H	5.48788000	-1.23662400	-2.22597300
C	4.02857500	0.19784700	-3.08898800	H	-1.19303500	-1.05977800	-4.65677400
C	-2.26163700	0.12633900	-3.21738400	H	4.73555300	-2.06520200	0.04251400
C	-1.22052200	0.22197500	2.23717500	H	2.96148100	-2.30614400	0.04600600
C	-1.21749700	0.13469900	-2.24750200	N	2.81050600	0.70966800	2.55021200
C	-0.34404300	0.21500300	1.37725400	N	2.81396200	0.60994900	-2.57384100
C	-0.34217900	0.16121200	-1.38678000	N	3.65078300	-0.72456700	1.20260600
C	-3.15002100	-0.33473200	5.40766000	N	3.65238300	-0.77074600	-1.17032100
C	-3.14273500	-0.54499100	-5.39652500	Pt	1.08277200	0.16451800	-0.00334200
C	2.55972100	0.07428700	1.38165300	H	1.86869700	1.55320800	4.21134400
C	2.56158400	0.02050800	-1.38178600	H	1.87441500	1.38819500	-4.26780400
C	-2.12737400	-0.36154600	4.45954300	O	-5.40885900	0.40821200	5.96440300
C	-2.12136800	-0.53487000	-4.44670400	O	-5.40080000	0.17566900	-5.98479700
C	4.56292400	-0.58845400	2.23092200	C	-5.29041600	-0.49750300	-7.21521300
C	4.56591300	-0.67472200	-2.20192400	H	-5.13721200	-1.57604500	-7.07193500
C	3.76544600	-1.56456000	0.03211700	H	-6.23688700	-0.33449300	-7.73451700
H	2.41310100	2.72395200	2.97300100	H	-4.46969600	-0.09328200	-7.82394600
H	2.41718000	2.60624800	-3.07521600	C	-5.30015200	-0.21657600	7.22022600
H	-5.44873000	1.43851900	3.65392100	H	-6.24731700	-0.03350900	7.73151700
H	-5.44376000	1.29509000	-3.71620700	H	-5.14678200	-1.29987100	7.11922700
H	0.98357000	1.68102700	2.67171300	H	-4.48024200	0.21104500	7.81387700

After PCM corrections, the SCF energy is -1531.66474144 a.u.

Zero-point correction= 0.482265 (Hartree/Particle)
Thermal correction to Energy= 0.515129
Thermal correction to Enthalpy= 0.516073
Thermal correction to Gibbs Free Energy= 0.411466
Sum of electronic and zero-point Energies= -1531.135927
Sum of electronic and thermal Energies= -1531.103063
Sum of electronic and thermal Enthalpies= -1531.102119
Sum of electronic and thermal Free Energies= -1531.206726

Energies and cartesian coordinates of the optimized triplet-state structure of 3

C	1.99100700	1.65590100	3.16919200	C	4.08203500	0.20975400	-3.09043000
C	2.01374100	1.60604100	-3.21251500	C	-2.21997800	0.08850100	-3.14217900
C	-4.52096100	1.04910700	3.78027700	C	-1.22728500	0.30017600	2.17316600
C	-4.62211900	0.27228300	-3.61613900	C	-1.19301000	0.15906800	-2.25610500
C	-3.49301400	1.00759400	2.85372300	C	-0.32814800	0.27267600	1.33564200
C	-3.59271600	0.33712700	-2.72792900	C	-0.26953700	0.22260800	-1.38601000
C	-4.37899500	0.42048700	5.02326400	C	-3.18977000	-0.24805800	5.32233700
C	-4.38231000	-0.04699300	-4.98676200	C	-3.06715800	-0.30686500	-5.43014100
C	4.01411000	0.20185300	3.10611900	C	2.57461500	0.02601400	1.37089400
C	-2.27998500	0.34082400	3.13033000	C	2.60334900	0.01059700	-1.39168400

C	-2.15958900	-0.28110600	4.38325200	H	-1.00480700	-0.45751000	-4.88371600
C	-2.01539100	-0.24579100	-4.54683900	H	4.74657300	-2.11418300	0.01672500
C	4.56545400	-0.67332600	2.23030200	H	2.96084200	-2.31736700	-0.00123400
C	4.61426100	-0.67200500	-2.20921600	N	2.80909700	0.61593100	2.57402900
C	3.78658900	-1.59432500	0.00464500	N	2.86618400	0.62066800	-2.57718700
H	2.45273400	2.63587900	3.00474000	N	3.67203100	-0.77108400	1.18182900
H	2.63638000	2.40137800	-3.63331100	N	3.69439600	-0.78459000	-1.18535200
H	-5.45279300	1.56364300	3.56152800	Pt	1.11195900	0.17869600	-0.02975800
H	-5.64768500	0.45634800	-3.30767200	H	1.89415900	1.47087700	4.24255100
H	1.00256300	1.62494100	2.70886900	H	1.41208800	1.14733600	-4.00206100
H	1.34219200	2.01660100	-2.45675100	O	-5.44623100	0.51419000	5.86471000
H	-3.61230800	1.49541000	1.89027200	O	-5.48558300	-0.07731200	-5.77301000
H	-3.77292400	0.57310500	-1.68335400	C	-5.32893300	-0.40016600	-7.13595600
H	4.37288200	0.56263400	4.05877400	H	-4.91050400	-1.40745700	-7.26227800
H	4.46356800	0.58062300	-4.03018400	H	-6.32992100	-0.36779000	-7.56961100
H	-3.05179300	-0.74830000	6.27573400	H	-4.68717000	0.32897000	-7.64810600
H	-2.87442300	-0.56160900	-6.46807700	C	-5.35317700	-0.11982200	7.11710400
H	-1.23967700	-0.80973900	4.61919200	H	-6.30281600	0.06801500	7.62207500
H	5.48521400	-1.23773900	2.27299300	H	-5.20816800	-1.20369600	7.00998300
H	5.54270400	-1.22324700	-2.22896800	H	-4.53436600	0.29657000	7.72017500

After PCM corrections, the SCF energy is -1531.56200197 a.u.

Zero-point correction=	0.478459 (Hartree/Particle)
Thermal correction to Energy=	0.511883
Thermal correction to Enthalpy=	0.512828
Thermal correction to Gibbs Free Energy=	0.406722
Sum of electronic and zero-point Energies=	-1531.041291
Sum of electronic and thermal Energies=	-1531.007867
Sum of electronic and thermal Enthalpies=	-1531.006923
Sum of electronic and thermal Free Energies=	-1531.113029

Energies and cartesian coordinates of the optimized ground-state structure of 5

C	2.48238200	1.60374100	3.17057500	H	4.93608900	0.62737500	-4.02809900
C	2.48238200	1.60374100	-3.17057500	H	-2.27904300	-0.94182900	6.45121100
C	-4.00841700	0.44582500	3.87320600	H	-2.27904300	-0.94182900	-6.45121100
C	-4.00841700	0.44582500	-3.87320600	H	-0.50883300	-0.89768200	4.78147100
C	-2.98959800	0.46352200	2.93135800	H	6.07354700	-1.17043100	2.25223200
C	-2.98959800	0.46352200	-2.93135800	H	6.07354700	-1.17043100	-2.25223200
C	-3.79050700	-0.04062400	5.17888900	H	-0.50883300	-0.89768200	-4.78147100
C	-3.79050700	-0.04062400	-5.17888900	H	5.34439200	-2.06427500	0.00000000
C	4.57532200	0.24081400	3.08650100	H	3.57641900	-2.34932400	0.00000000
C	-1.69693000	-0.00498300	3.22543700	N	3.35059200	0.61010200	2.56293100
C	4.57532200	0.24081400	-3.08650100	N	3.35059200	0.61010200	-2.56293100
C	-1.69693000	-0.00498300	-3.22543700	N	4.22737000	-0.77434100	1.18667100
C	-0.65934300	0.01848700	2.24970900	N	4.22737000	-0.77434100	-1.18667100
C	-0.65934300	0.01848700	-2.24970900	Pt	1.63564300	0.06901800	0.00000000
C	0.21173500	0.05365700	1.38439500	H	2.38908800	1.39762000	4.24022800
C	0.21173500	0.05365700	-1.38439500	H	2.38908800	1.39762000	-4.24022800
C	-2.50181100	-0.53114100	5.47213800	N	-4.79807900	-0.02496500	-6.13767500
C	-2.50181100	-0.53114100	-5.47213800	N	-4.79807900	-0.02496500	6.13767500
C	3.11511900	-0.00863800	1.38194800	C	-4.61587100	-0.80271200	7.33985900
C	3.11511900	-0.00863800	-1.38194800	H	-4.48531000	-1.88073400	7.14040500
C	-1.48932800	-0.50572900	4.52200300	H	-3.74348300	-0.45295800	7.90388400
C	-1.48932800	-0.50572900	-4.52200300	H	-5.48985400	-0.67545900	7.98334200
C	5.13696600	-0.63385900	2.21668500	C	-6.15679600	0.20063800	5.70424100
C	5.13696600	-0.63385900	-2.21668500	H	-6.25726100	1.18288100	5.22875300
C	4.36196500	-1.58802400	0.00000000	H	-6.51463600	-0.56310500	4.99200900
H	2.90018900	2.60496300	3.02291900	H	-6.81515300	0.19360100	6.57636600
H	2.90018900	2.60496300	-3.02291900	C	-6.15679600	0.20063800	-5.70424100
H	-4.98554700	0.81419000	3.57963000	H	-6.51463600	-0.56310500	-4.99200900
H	-4.98554700	0.81419000	-3.57963000	H	-6.25726100	1.18288100	-5.22875300
H	1.49855600	1.52920900	2.70375600	H	-6.81515300	0.19360100	-6.57636600
H	1.49855600	1.52920900	-2.70375600	C	-4.61587100	-0.80271200	-7.33985900
H	-3.19143200	0.84195300	1.93288600	H	-3.74348300	-0.45295800	-7.90388400
H	-3.19143200	0.84195300	-1.93288600	H	-4.48531000	-1.88073400	-7.14040500
H	4.93608900	0.62737500	4.02809900	H	-5.48985400	-0.67545900	-7.98334200

After PCM corrections, the SCF energy is -1570.48373494 a.u.

Zero-point correction=	0.563572 (Hartree/Particle)
Thermal correction to Energy=	0.600048
Thermal correction to Enthalpy=	0.600992
Thermal correction to Gibbs Free Energy=	0.486765
Sum of electronic and zero-point Energies=	-1569.873292
Sum of electronic and thermal Energies=	-1569.836816
Sum of electronic and thermal Enthalpies=	-1569.835872
Sum of electronic and thermal Free Energies=	-1569.950100

Energies and cartesian coordinates of the optimized triplet-state structure of 5

C	2.44482100	1.46227500	3.20571600	H	5.16858800	0.68851500	-3.98523200
C	2.65669000	1.59103000	-3.21091900	H	-2.31156300	-0.95392300	6.26688300
C	-3.93667200	0.64389200	3.74432800	H	-2.28469700	-0.51113300	-6.50318500
C	-3.99901700	0.15399100	-3.60211100	H	-0.52883000	-0.93955300	4.61253500
C	-2.91029900	0.64606000	2.81055100	H	6.10842800	-1.22565100	2.32805900
C	-2.94369300	0.20788400	-2.73682500	H	6.28620000	-1.09056500	-2.18363700
C	-3.75851700	0.08926700	5.02858700	H	-0.40278300	-0.41988600	-4.97461400
C	-3.81139000	-0.08727300	-5.00010200	H	5.47382100	-2.06621600	0.01804300
C	4.55032800	0.12469800	3.15266700	H	3.69654700	-2.33927900	-0.04919300
C	-1.64679000	0.09218300	3.08925400	N	3.35557200	0.52018200	2.58517300
C	4.78193500	0.28685300	-3.06030500	N	3.53733600	0.63547200	-2.57110000
C	-1.57615800	0.02316100	-3.18510000	N	4.31652300	-0.79738400	1.18686500
C	-0.60061300	0.09940300	2.12678600	N	4.39629800	-0.75237500	-1.17825700
C	-0.53126500	0.08464800	-2.31360600	Pt	1.74946400	0.09241700	-0.06641500
C	0.29765700	0.11956000	1.28694900	H	1.79007400	0.95625400	3.92026400
C	0.38291200	0.13663700	-1.43829100	H	2.05891000	1.10937600	-3.98990900
C	-2.50233400	-0.48710400	5.30630200	N	-4.87785400	-0.09685100	-5.87461800
C	-2.47275900	-0.29592100	-5.45619500	N	-4.77185700	0.12311400	5.98315100
C	3.18276300	-0.04714500	1.35894500	C	-4.64414400	-0.71872200	7.14869100
C	3.27296100	-0.00360000	-1.39860200	H	-4.57936800	-1.79292100	6.90090000
C	-1.48173000	-0.47777900	4.36507200	H	-3.75454100	-0.44959100	7.72953600
C	-1.40759400	-0.24428700	-4.60030600	H	-5.51162200	-0.56636900	7.79568600
C	5.16527700	-0.70255500	2.27194500	C	-6.11370100	0.42884000	5.54715700
C	5.33297800	-0.58299600	-2.17883700	H	-6.16223400	1.43034600	5.10506200
C	4.49412400	-1.58463500	-0.00564500	H	-6.50137800	-0.29214600	4.80605800
H	3.02770300	2.23783900	3.71210900	H	-6.78002300	0.42445700	6.41335300
H	3.25691100	2.39599800	-3.64598900	C	-6.22754400	-0.08352700	-5.35732600
H	-4.88820600	1.08185500	3.46195000	H	-6.45456800	-0.97585300	-4.75208900
H	-4.99960100	0.28973100	-3.20479500	H	-6.40183000	0.80442100	-4.73963600
H	1.82068900	1.90371800	2.42841300	H	-6.92999600	-0.04657700	-6.19233900
H	1.98031100	1.99402900	-2.45484600	C	-4.68331400	-0.53549800	-7.23752100
H	-3.08209800	1.08355600	1.83056500	H	-3.93040000	0.07921300	-7.74358600
H	-3.11085000	0.38233800	-1.67806200	H	-4.36777400	-1.58964700	-7.29993300
H	4.86293600	0.46873500	4.12749200	H	-5.62088700	-0.42482900	-7.78592100

After PCM corrections, the SCF energy is -1570.38608973 a.u.

Zero-point correction=	0.560004 (Hartree/Particle)
Thermal correction to Energy=	0.597084
Thermal correction to Enthalpy=	0.598029
Thermal correction to Gibbs Free Energy=	0.482873
Sum of electronic and zero-point Energies=	-1569.782113
Sum of electronic and thermal Energies=	-1569.745033
Sum of electronic and thermal Enthalpies=	-1569.744089
Sum of electronic and thermal Free Energies=	-1569.859245

Energies and cartesian coordinates of the optimized ground-state structure of 6

C	1.43518300	1.60512900	3.18449400	N	2.31492300	0.62895500	2.56504800
C	1.43518300	1.60512900	-3.18449400	N	2.31492300	0.62895500	-2.56504800
C	3.53696000	0.26007100	3.09538100	N	3.20552300	-0.74550700	1.18724900
C	3.53696000	0.26007100	-3.09538100	N	3.20552300	-0.74550700	-1.18724900
C	-1.66360000	-0.02496500	2.26758700	Pt	0.60639500	0.07157600	0.00000000
C	-1.66360000	-0.02496500	-2.26758700	H	1.18724400	1.28640500	4.20059800
C	-0.80603600	0.02841100	1.38893500	H	1.18724400	1.28640500	-4.20059800
C	-0.80603600	0.02841100	-1.38893500	C	-2.64173400	-0.07536000	3.27733800
C	2.08938600	0.01286700	1.38194500	C	-4.00875800	0.09541500	3.18080100
C	2.08938600	0.01286700	-1.38194500	S	-2.20136600	-0.38402600	4.94211500
C	4.10748800	-0.60714100	2.22412700	C	-4.68275300	-0.01780300	4.42460000
C	4.10748800	-0.60714100	-2.22412700	H	-4.49372500	0.29485500	2.23178400
C	3.35019100	-1.55752500	0.00000000	C	-3.83529300	-0.27435900	5.46989300
H	1.92918000	2.58145300	3.21135800	H	-5.75692000	0.08466200	4.54207300
H	1.92918000	2.58145300	-3.21135800	H	-4.08476000	-0.41020700	6.51483300
H	0.51739800	1.65994400	2.59884100	C	-2.64173400	-0.07536000	-3.27733800
H	0.51739800	1.65994400	-2.59884100	C	-4.00875800	0.09541500	-3.18080100
H	3.89044100	0.64359100	4.04094400	S	-2.20136600	-0.38402600	-4.94211500
H	3.89044100	0.64359100	-4.04094400	C	-4.68275300	-0.01780300	-4.42460000
H	5.04749200	-1.13751500	2.26107100	H	-4.49372500	0.29485500	-2.23178400
H	5.04749200	-1.13751500	-2.26107100	C	-3.83529300	-0.27435900	-5.46989300
H	4.33877200	-2.02052400	0.00000000	H	-5.75692000	0.08466200	-4.54207300
H	2.57595100	-2.33026500	0.00000000	H	-4.08476000	-0.41020700	-6.51483300

After PCM corrections, the SCF energy is -1944.26204703 a.u.

Zero-point correction=	0.348823 (Hartree/Particle)
Thermal correction to Energy=	0.375969
Thermal correction to Enthalpy=	0.376913
Thermal correction to Gibbs Free Energy=	0.284792
Sum of electronic and zero-point Energies=	-1943.871238
Sum of electronic and thermal Energies=	-1943.844092
Sum of electronic and thermal Enthalpies=	-1943.843148
Sum of electronic and thermal Free Energies=	-1943.935269

Energies and cartesian coordinates of the optimized triplet-state structure of 6

C	1.39148000	1.58245200	3.20991900	N	2.29083800	0.63013100	2.58178000
C	1.40468000	1.56997100	-3.19352400	N	2.28611100	0.60280300	-2.56391600
C	3.50941900	0.26105600	3.11933800	N	3.19347300	-0.74034400	1.20590300
C	3.50772000	0.23247100	-3.09275000	N	3.19265000	-0.74555200	-1.16707400
C	-1.66971500	-0.01991700	2.30324700	Pt	0.58726100	0.07797300	0.01680900
C	-1.69215700	-0.00327100	-2.24275200	H	0.87172800	1.12037200	4.05348500
C	-0.79785100	0.04958400	1.39218400	H	1.10169100	1.21024900	-4.18073600
C	-0.82739100	0.04689800	-1.37043300	C	-2.59198100	-0.08064300	3.27711900
C	2.07358100	0.01295500	1.39631300	C	-4.05076600	0.04782700	3.16067300
C	2.06880500	0.00314400	-1.36823400	S	-2.16255600	-0.33847400	5.01231300
C	4.08845800	-0.60125900	2.24860300	C	-4.70233200	-0.04075500	4.35858400
C	4.08789000	-0.61734000	-2.21083800	H	-4.51467700	0.19856600	2.19304900
C	3.34038000	-1.55350200	0.02061000	C	-3.84560400	-0.24011400	5.46735700
H	1.96783900	2.44635000	3.55387300	H	-5.77963900	0.03262300	4.47186700
H	1.92269700	2.52940500	-3.29027600	H	-4.13640900	-0.33846600	6.50541900
H	0.65262400	1.89481600	2.47205500	C	-2.67232200	-0.05277900	-3.24944200
H	0.51593200	1.68041900	-2.57263500	C	-4.03917400	0.12293400	-3.15079500
H	3.85705100	0.64354900	4.06744300	S	-2.23655300	-0.36939200	-4.91418500
H	3.85581000	0.60436900	-4.04496500	C	-4.71578300	0.00744700	-4.39265200
H	5.03317300	-1.12300200	2.28657800	H	-4.52203000	0.32801200	-2.20189900
H	5.03176600	-1.14104000	-2.24354000	C	-3.87137300	-0.25566400	-5.43889800
H	4.32929900	-2.01570800	0.02131600	H	-5.78981000	0.11323100	-4.50842800
H	2.56433100	-2.32613500	0.02363800	H	-4.12337500	-0.39412400	-6.48286200

After PCM corrections, the SCF energy is -1944.17498543 a.u.

Zero-point correction=	0.345307 (Hartree/Particle)
Thermal correction to Energy=	0.373109
Thermal correction to Enthalpy=	0.374053
Thermal correction to Gibbs Free Energy=	0.279882
Sum of electronic and zero-point Energies=	-1943.789792
Sum of electronic and thermal Energies=	-1943.761990
Sum of electronic and thermal Enthalpies=	-1943.761046
Sum of electronic and thermal Free Energies=	-1943.855217

Energies and cartesian coordinates of the optimized ground-state structure of 7

C	-7.49169100	0.52727500	8.93755300	C	6.36339300	-0.65998400	2.22123200
C	-7.49169100	0.52727500	-8.93755300	C	6.36339300	-0.65998400	-2.22123200
C	-6.51498700	0.55445900	7.94820600	C	5.58495700	-1.59943000	0.00000000
C	-6.51498700	0.55445900	-7.94820600	H	-8.43204500	1.04885800	8.77762200
C	-7.27017600	-0.16428500	10.12879400	H	-8.43204500	1.04885800	-8.77762200
C	-7.27017600	-0.16428500	-10.12879400	H	-6.68531300	1.09268800	7.02018600
C	-5.29171900	-0.11421500	8.13637200	H	-6.68531300	1.09268800	-7.02018600
C	-5.29171900	-0.11421500	-8.13637200	H	-8.03569300	-0.18318100	10.90016900
C	-6.06035600	-0.83142600	10.32467800	H	-8.03569300	-0.18318100	-10.90016900
C	-6.06035600	-0.83142600	-10.32467800	H	4.24398800	2.56707600	3.21399400
C	-4.28720700	-0.08420700	7.13011800	H	4.24398800	2.56707600	-3.21399400
C	-4.28720700	-0.08420700	-7.13011800	H	-3.54896500	1.20845800	3.91164000
C	-5.07832300	-0.80937600	9.34087900	H	-3.54896500	1.20845800	-3.91164000
C	3.73246000	1.59987200	3.18458800	H	-5.88105300	-1.37326600	11.24998500
C	3.73246000	1.59987200	-3.18458800	H	2.81559100	1.67123600	2.59946600
C	-5.07832300	-0.80937600	-9.34087900	H	2.81559100	1.67123600	-2.59946600
C	-2.61645300	0.67181900	4.06375700	H	-5.88105300	-1.37326600	-11.24998500
C	-2.61645300	0.67181900	-4.06375700	H	-1.79420500	1.24655700	2.16480900
C	-3.43083300	-0.06746300	6.26417500	H	-1.79420500	1.24655700	-2.16480900
C	-3.43083300	-0.06746300	-6.26417500	H	-4.13548100	-1.32744200	9.49117900
C	-1.63459800	0.69455800	3.08655700	H	-4.13548100	-1.32744200	-9.49117900
C	-1.63459800	0.69455800	-3.08655700	H	6.17299000	0.59859100	4.03590100
C	-2.42585900	-0.04386100	5.26044500	H	6.17299000	0.59859100	-4.03590100
C	-2.42585900	-0.04386100	-5.26044500	H	-1.05727900	-1.30015200	6.35489400
C	5.81090600	0.21930700	3.09194000	H	-1.05727900	-1.30015200	-6.35489400
C	-0.41731100	0.00559800	3.26046900	H	0.69402600	-1.25859000	4.60537900
C	5.81090600	0.21930700	-3.09194000	H	7.29299700	-1.20846800	2.25736200
C	-0.41731100	0.00559800	-3.26046900	H	7.29299700	-1.20846800	-2.25736200
C	0.59164100	0.03596600	2.25998300	H	0.69402600	-1.25859000	-4.60537900
C	0.59164100	0.03596600	-2.25998300	H	6.56408100	-2.08216500	0.00000000
C	1.45457700	0.07164000	1.38676200	H	4.79578300	-2.35686400	0.00000000
C	1.45457700	0.07164000	-1.38676200	N	4.59451500	0.60897700	2.56362300
C	-1.21499900	-0.73879800	5.43788200	N	4.59451500	0.60897700	-2.56362300
C	-1.21499900	-0.73879800	-5.43788200	N	5.45635700	-0.78467600	1.18729100
C	4.35490800	-0.00507600	1.38224600	N	5.45635700	-0.78467600	-1.18729100
C	4.35490800	-0.00507600	-1.38224600	Pt	2.87295000	0.08425700	0.00000000
C	-0.23405700	-0.71252400	4.45971000	H	3.47859100	1.28362500	-4.19990400
C	-0.23405700	-0.71252400	-4.45971000	H	3.47859100	1.28362500	4.19990400

After PCM corrections, the SCF energy is -1916.58110964 a.u.

Zero-point correction= 0.598982 (Hartree/Particle)

Thermal correction to Energy= 0.640690
Thermal correction to Enthalpy= 0.641634
Thermal correction to Gibbs Free Energy= 0.511246
Sum of electronic and zero-point Energies= -1915.928555
Sum of electronic and thermal Energies= -1915.886847
Sum of electronic and thermal Enthalpies= -1915.885903
Sum of electronic and thermal Free Energies= -1916.016291

Energies and cartesian coordinates of the optimized triplet-state structure of 7

C	0.54392400	-7.61825200	-8.77020100	C	-0.72346600	6.37586400	-2.18733300
C	0.15363300	-7.67711100	8.63245400	C	-0.66680900	6.34536100	2.25779200
C	0.57125600	-6.61984800	-7.80311000	C	-1.62521600	5.57495000	0.03974700
C	0.19166300	-6.68870500	7.66263400	H	1.05052200	-8.56162700	-8.58202500
C	-0.12889000	-7.41467500	-9.97535700	H	0.42445600	-8.69660500	8.36829500
C	-0.22962500	-7.37488100	9.94441100	H	1.09394500	-6.77649000	-6.86377200
C	-0.07894400	-5.39278600	-8.02771700	H	0.48859600	-6.92374800	6.64446700
C	-0.15789300	-5.34957100	7.98252300	H	-0.14855300	-8.19760500	-10.72909900
C	-0.77705300	-6.20122800	-10.20755600	H	-0.25757800	-8.15525400	10.70010600
C	-0.57722100	-6.05994500	10.27536600	H	2.54700500	4.23472700	-3.08333400
C	-0.05371800	-4.36898200	-7.04090100	H	2.54875000	4.30163600	3.33706200
C	-0.12289700	-4.34790000	7.01207100	H	1.19078100	-3.59881900	-3.81366400
C	-0.75488300	-5.19747800	-9.24586900	H	0.58611800	-3.78156100	3.56397400
C	1.55749100	3.78016200	-3.19574600	H	-1.30399600	-6.03583000	-11.14406400
C	1.63272400	3.72834100	3.16536700	H	1.53554800	2.79945600	-2.71916500
C	-0.54473800	-5.05915700	9.31813200	H	1.82853700	2.90243500	2.48194500
C	0.67614200	-2.65853700	-3.99173500	H	-0.87648700	-5.81827700	11.29252500
C	0.32393100	-2.75907500	3.82093700	H	1.22380500	-1.81891600	-2.09250100
C	-0.03226400	-3.49343000	-6.19441100	H	0.63837800	-2.00350900	1.85981000
C	-0.09291900	-3.45615900	6.14562400	H	-1.25949500	-4.25207900	-9.42417300
C	0.69534500	-1.66284800	-3.02857900	H	-0.81522600	-4.03885800	9.57509500
C	0.35306800	-1.78041000	2.88423500	H	0.50635700	6.20943400	-4.02345400
C	-0.00898100	-2.47235300	-5.20721900	H	0.62022700	6.15485400	4.05188700
C	-0.06262900	-2.47549000	5.19614100	H	-1.21137100	-1.09577100	-6.35115600
C	0.14597300	5.83651800	-3.07622600	H	-0.72597300	-0.87713300	6.53702100
C	0.03448800	-0.43527600	-3.23689900	H	-1.17433500	0.68118800	-4.62830600
C	0.23100500	5.79505500	3.11102300	H	-1.28095600	7.30052500	-2.20933400
C	0.00590600	-0.40662000	3.20443200	H	-1.22122600	7.27072200	2.30867600
C	0.05977000	0.58650400	-2.24947600	H	-0.67153500	0.88980700	4.82532500
C	0.04760000	0.58334600	2.25111500	H	-2.11809100	6.54881100	0.05132900
C	0.08945400	1.46013000	-1.38641800	H	-2.37379300	4.77673700	0.04396300
C	0.09903200	1.46851600	1.36996900	N	0.55337200	4.61930200	-2.56453500
C	-0.67412600	-1.25047500	-5.41930600	N	0.62892900	4.58907300	2.56466400
C	-0.42319900	-1.10119200	5.51785100	N	-0.82249400	5.46204800	-1.15661400
C	-0.03664700	4.36784600	-1.37250000	N	-0.79561700	5.44699500	1.21660700
C	-0.00138200	4.35360300	1.39068200	Pt	0.09119400	2.87839500	0.00165000
C	-0.65092400	-0.25528600	-4.45546300	H	1.26480800	3.32332200	4.11196900
C	-0.38969300	-0.12974900	4.57369100	H	1.32180000	3.66824000	-4.25729000

After PCM corrections, the SCF energy is -1916.49713142 a.u.

Zero-point correction= 0.596149 (Hartree/Particle)
Thermal correction to Energy= 0.637934
Thermal correction to Enthalpy= 0.638879
Thermal correction to Gibbs Free Energy= 0.509102
Sum of electronic and zero-point Energies= -1915.849074
Sum of electronic and thermal Energies= -1915.807288
Sum of electronic and thermal Enthalpies= -1915.806344
Sum of electronic and thermal Free Energies= -1915.936121

Energies and cartesian coordinates of the optimized ground-state structure of 8

C	2.99015900	4.00122000	1.09975300	H	-3.72777200	5.92369100	-0.11197600
C	-2.95504500	2.04275800	2.28969800	H	-1.59955700	6.00794300	-1.47179800
C	2.00990800	6.05264100	0.06680700	H	-1.16015900	4.35677300	-2.00225500
C	-3.77109100	4.14510200	1.21664600	N	1.94898700	4.70573800	0.37129600
C	2.64643200	0.77615400	-0.60378500	N	-2.84482100	3.12462100	1.32556300
C	-1.53581000	-0.53129500	0.11363400	N	0.10766500	5.21239200	-0.59444800
C	1.61290400	1.38372800	-0.33515500	N	-2.10934600	4.48169400	-0.15712700
C	-0.96808900	0.55807900	0.13286300	Pt	-0.07498700	2.32877400	0.10284600
C	0.77612200	4.16517600	-0.03209600	H	3.95799100	4.19348100	0.62913400
C	-1.80639500	3.31473900	0.47915300	H	-3.92842300	1.55570900	2.18597800
C	0.84441300	6.37945000	-0.54259500	C	-2.17571500	-1.79895800	0.09907400
C	-3.30807700	5.00959900	0.28125700	C	-3.56667300	-1.92054400	-0.16288900
C	-1.21642100	5.03824700	-1.14844500	C	-1.43019600	-2.96634600	0.35112900
H	3.01095400	4.34089100	2.14010100	C	-4.17757100	-3.20586200	-0.15065200
H	-2.84459600	2.43891300	3.30409400	C	-4.38144700	-0.77929200	-0.45164300
H	2.77858700	2.93237300	1.05384000	C	-2.02568100	-4.21646300	0.36065100
H	-2.17099400	1.31492400	2.07941200	H	-0.36425200	-2.86613100	0.53503900
H	2.87255000	6.65618000	0.30715200	C	-5.57402600	-3.33561600	-0.40841200
H	-4.67322000	4.16598200	1.80993600	C	-3.39945400	-4.36764200	0.11682000
H	0.49273100	7.31601600	-0.94943900	C	-5.71450500	-0.90190700	-0.69951800

H	-3.89446200	0.19226700	-0.48152500	C	5.88387400	-0.22784400	-2.16144900
H	-1.42213000	-5.10050800	0.55691600	H	4.49068500	1.38683800	-2.41349700
C	-6.36113800	-2.18090500	-0.68383200	C	5.61754400	-3.07664200	0.24019100
C	-6.18804700	-4.62211800	-0.39482600	C	6.20482400	-1.40853800	-1.47508500
C	-4.04188700	-5.64671600	0.12326900	C	3.53478400	-2.81327100	1.51458400
H	-6.31501300	-0.02246000	-0.92541300	H	2.32915600	-1.11636700	1.04037300
C	-7.73244400	-2.33141300	-0.93584800	H	6.55877500	0.13578000	-2.93406300
C	-7.56295400	-4.72485100	-0.65149700	C	4.73010900	-3.55671100	1.24526700
C	-5.37544900	-5.77089700	-0.12012800	C	6.81112600	-3.79860000	-0.05283000
H	-3.43613800	-6.52736100	0.32761300	C	7.39544800	-2.15431900	-1.75004800
C	-8.32433500	-3.59088300	-0.91882300	H	2.85576900	-3.18471900	2.27984200
H	-8.33205600	-1.44860900	-1.14866800	C	5.05095900	-4.73594400	1.93341500
H	-8.03124300	-5.70693300	-0.64119800	C	7.09088500	-4.97319600	0.66006300
H	-5.84872400	-6.75053400	-0.11228400	C	7.68766200	-3.29716100	-1.07085400
H	-9.38876500	-3.69021300	-1.11725600	H	8.06919100	-1.78587400	-2.52129800
C	3.82549700	0.03522100	-0.88321600	C	6.21888500	-5.43428600	1.64218700
C	4.11892000	-1.16156200	-0.17559900	H	4.37219900	-5.10194900	2.70103200
C	4.72661800	0.47580700	-1.87035400	H	8.00189900	-5.52446800	0.43616900
C	5.31186300	-1.87901000	-0.47053700	H	8.59669600	-3.85281400	-1.29172200
C	3.24188600	-1.67031000	0.83562800	H	6.45170600	-6.34722400	2.18496400

After PCM corrections, the SCF energy is -2069.05240320 a.u.

Zero-point correction=	0.630695 (Hartree/Particle)
Thermal correction to Energy=	0.669552
Thermal correction to Enthalpy=	0.670496
Thermal correction to Gibbs Free Energy=	0.554587
Sum of electronic and zero-point Energies=	-2068.372365
Sum of electronic and thermal Energies=	-2068.333509
Sum of electronic and thermal Enthalpies=	-2068.332565
Sum of electronic and thermal Free Energies=	-2068.448474

Energies and cartesian coordinates of the optimized triplet-state structure of 8

C	-2.97469100	-4.09244700	1.10875000	H	3.83795300	-0.19754400	-0.45285300
C	2.95937500	-2.03989600	2.25497300	H	1.32749900	5.09654800	0.48270500
C	-1.96601000	-6.11929500	0.05669000	C	6.29685900	2.18402500	-0.64893700
C	3.79866700	-4.11783100	1.15355300	C	6.10893800	4.62769500	-0.39251500
C	-2.71126500	-0.85945100	-0.54381600	C	3.95109200	5.64893800	0.08191500
C	1.47066600	0.52131100	0.10869500	H	6.26320600	0.02288200	-0.86672300
C	-1.65057700	-1.45138300	-0.29046600	C	7.67085800	2.33766600	-0.88382800
C	0.91765500	-0.57547000	0.13739500	C	7.48682100	4.73354900	-0.63122900
C	-0.76208900	-4.21252700	-0.03450100	C	5.28747700	5.77608200	-0.14386200
C	1.80986900	-3.31798300	0.44818900	H	3.33861400	6.52932700	0.26617200
C	-0.80277900	-6.42094600	-0.56977400	C	8.25690600	3.59991600	-0.87399200
C	3.33853900	-4.98432100	0.21853900	H	8.27723000	1.45509600	-1.07756600
C	1.22992000	-5.04009600	-1.18484500	H	7.95055200	5.71781700	-0.62653100
H	-3.13703200	-4.59094000	2.06923800	H	5.75625600	6.75788900	-0.14164200
H	2.88593200	-2.44994700	3.26720100	H	9.32354200	3.70171600	-1.05876100
H	-2.66875600	-3.05854700	1.26679900	C	-3.87531800	-0.13824900	-0.77387600
H	2.14938200	-1.33337800	2.07274000	C	-4.07149700	1.18017800	-0.14530800
H	-2.81585000	-6.73922600	0.30088500	C	-4.90438600	-0.64463600	-1.62063200
H	4.70880900	-4.12691500	1.73479100	C	-5.27674200	1.89818200	-0.39790200
H	-0.43996600	-7.34837300	-0.98761200	C	-3.11160400	1.74109600	0.69280700
H	3.76915500	-5.88817600	-0.18634200	C	-6.05255200	0.05314100	-1.85875700
H	1.62620000	-5.99999900	-1.52118300	H	-4.74417700	-1.61284900	-2.08833000
H	1.15025000	-4.35231900	-2.03202300	C	-5.48285100	3.16884800	0.20414200
N	-1.92085400	-4.77571600	0.37893200	C	-6.28379700	1.35239900	-1.25453800
N	2.85629200	-3.11474400	1.28220000	C	-3.31390700	2.99154800	1.28828800
N	-0.08416700	-5.24248300	-0.61641500	H	-2.19219400	1.19026900	0.87607300
N	2.12477900	-4.47540100	-0.20034500	H	-6.81925700	-0.35286500	-2.51476000
Pt	0.05430600	-2.36157200	0.10697500	C	-4.48519500	3.72351800	1.06145400
H	-3.89900300	-4.10041000	0.52474800	C	-6.68946200	3.89472500	-0.04717200
H	3.91492600	-1.52274100	2.13279800	C	-7.44779700	2.07627800	-1.48496600
C	2.10293000	1.79247100	0.08334400	H	-2.54844200	3.40508100	1.94219600
C	3.49677000	1.91716600	-0.16219000	C	-4.71709800	5.00593400	1.65837000
C	1.34851600	2.95975900	0.30777100	C	-6.86996100	5.17039500	0.57289800
C	4.10160800	3.20535600	-0.15841700	C	-7.65339700	3.33023200	-0.89275300
C	4.32031600	0.77640600	-0.42679800	H	-8.21132500	1.65930700	-2.13868900
C	1.93795400	4.21270800	0.30819300	C	-5.89137200	5.70183300	1.40831500
H	0.28027300	2.85773400	0.47666600	H	-3.95461100	5.42431700	2.31105900
C	5.50087400	3.33832400	-0.39854700	H	-7.78787800	5.72082700	0.38052600
C	3.31455200	4.36694200	0.08277100	H	-8.57287600	3.87728000	-1.08954500
C	5.65603500	0.90211600	-0.65846000	H	-6.04970500	6.67396000	1.86949800

After PCM corrections, the SCF energy is -2068.98556953 a.u.

Zero-point correction could not be calculated due to the limitation of G03 on 32 bit machines…

Energies and cartesian coordinates of the optimized ground-state structure of 9

C	1.84225100	1.61566700	3.16869800	C	1.84225100	1.61566700	-3.16869800

C	-4.56359700	0.47965800	3.93749100	H	-5.52465200	0.95326400	3.76009100
C	-4.56359700	0.47965800	-3.93749100	H	-5.52465200	0.95326400	-3.76009100
C	-3.54992400	0.51398600	2.98607000	H	0.86487700	1.53185300	2.69129100
C	-3.54992400	0.51398600	-2.98607000	H	0.86487700	1.53185300	-2.69129100
C	-4.33232600	-0.18180300	5.13440900	H	-3.71120800	1.02127000	2.03948600
C	-4.33232600	-0.18180300	-5.13440900	H	-3.71120800	1.02127000	-2.03948600
C	3.96428800	0.29943100	3.08548200	H	4.31639200	0.69548000	4.02638700
C	-2.30567200	-0.10246500	3.22086900	H	4.31639200	0.69548000	-4.02638700
C	3.96428800	0.29943100	-3.08548200	H	-2.98719000	-1.32071500	6.35542800
C	-2.30567200	-0.10246500	-3.22086900	H	-2.98719000	-1.32071500	-6.35542800
C	-1.27101300	-0.05456100	2.24250200	H	-1.16826300	-1.25383900	4.64235800
C	-1.27101300	-0.05456100	-2.24250200	H	5.49304900	-1.07971500	2.25336000
C	-0.39704400	0.00109100	1.38220700	H	5.49304900	-1.07971500	-2.25336000
C	-0.39704400	0.00109100	-1.38220700	H	-1.16826300	-1.25383900	-4.64235800
C	-3.12599700	-0.80825900	5.40800800	H	4.78925400	-1.98624800	0.00000000
C	-3.12599700	-0.80825900	-5.40800800	H	3.03067100	-2.31873700	0.00000000
C	2.51137600	0.01569800	1.38144000	N	2.73217500	0.64154400	2.56056500
C	2.51137600	0.01569800	-1.38144000	N	2.73217500	0.64154400	-2.56056500
C	-2.11863300	-0.76405600	4.44948200	N	3.63922500	-0.72538800	1.18668900
C	-2.11863300	-0.76405600	-4.44948200	N	3.63922500	-0.72538800	-1.18668900
C	4.54487900	-0.56401000	2.21702700	Pt	1.02733600	0.05540300	0.00000000
C	4.54487900	-0.56401000	-2.21702700	H	1.74062500	1.39798800	4.23519900
C	3.79474500	-1.53612000	0.00000000	H	1.74062500	1.39798800	-4.23519900
H	2.24613400	2.62431600	3.03500400	F	-5.31449400	-0.21908800	6.06304700
H	2.24613400	2.62431600	-3.03500400	F	-5.31449400	-0.21908800	-6.06304700

After PCM corrections, the SCF energy is -1501.16880348 a.u.

Zero-point correction=	0.399754 (Hartree/Particle)
Thermal correction to Energy=	0.429222
Thermal correction to Enthalpy=	0.430166
Thermal correction to Gibbs Free Energy=	0.332679
Sum of electronic and zero-point Energies=	-1500.726162
Sum of electronic and thermal Energies=	-1500.696694
Sum of electronic and thermal Enthalpies=	-1500.695750
Sum of electronic and thermal Free Energies=	-1500.793237

Energies and cartesian coordinates of the optimized triplet-state structure of 9

C	1.45434900	1.49432400	3.20835000	H	2.14927200	2.48401700	-3.57406100
C	1.57827200	1.62642600	-3.20610600	H	-5.78188400	1.14487300	3.74902000
C	-4.83803100	0.63064700	3.90452300	H	-6.02586800	-0.01560800	-3.35094400
C	-4.98876100	-0.12350300	-3.65532700	H	0.76863200	1.87545100	2.45217200
C	-3.83069200	0.65614100	2.94631900	H	0.85207000	1.95285700	-2.46044700
C	-3.96172700	-0.01471600	-2.75782300	H	-3.97979700	1.20003500	2.01811100
C	-4.62275800	-0.07234200	5.08073300	H	-4.15611300	0.18065300	-1.70787100
C	-4.69285400	-0.38681300	-5.00818400	H	3.90128300	0.54563100	4.09817900
C	3.58271300	0.19423000	3.12799900	H	4.09198300	0.76760700	-4.01718400
C	-2.60710200	-0.01182600	3.15217800	H	-3.31050600	-1.29341700	6.25758700
C	3.72689100	0.35717600	-3.08744800	H	-3.21039300	-0.76879800	-6.52935600
C	-2.57111200	-0.16301100	-3.18095500	H	-1.50457900	-1.24675300	4.53187100
C	-1.57830100	0.02400100	2.16975700	H	5.14902200	-1.13623100	2.28706500
C	-1.55441700	-0.04466000	-2.29114500	H	5.26408800	-1.00071500	-2.23774400
C	-0.69458700	0.06919400	1.31784000	H	-1.30990900	-0.58425000	-4.92668900
C	-0.63860900	0.06701100	-1.41382100	H	4.51330100	-1.97235700	-0.01717500
C	-3.43748600	-0.74899500	5.32645500	H	2.74876700	-2.29899800	-0.06039500
C	-3.37438300	-0.55443200	-5.47707400	N	2.37552200	0.57044000	2.57270100
C	2.19830400	-0.00158600	1.35362900	N	2.48440000	0.68444100	-2.57752000
C	2.25042100	0.03909200	-1.40681400	N	3.33799400	-0.73386400	1.16695400
C	-2.43638300	-0.71456400	4.36139400	N	3.38526700	-0.69081200	-1.20252100
C	-2.33460100	-0.44861700	-4.59340500	Pt	0.74036100	0.09029100	-0.05364900
C	4.19827500	-0.62609400	2.24154600	H	0.86842900	0.98429800	3.97767400
C	4.30422900	-0.50632700	-2.21692000	H	1.04315000	1.15372600	-4.03435300
C	3.51995900	-1.51979800	-0.02876700	F	-5.59924300	-0.10076000	6.01587600
H	2.02416300	2.31571400	3.65284800	F	-5.71007800	-0.48846800	-5.88794800

After PCM corrections, the SCF energy is -1501.06417557 a.u.

Zero-point correction=	0.395782 (Hartree/Particle)
Thermal correction to Energy=	0.425858
Thermal correction to Enthalpy=	0.426802
Thermal correction to Gibbs Free Energy=	0.327633
Sum of electronic and zero-point Energies=	-1500.629347
Sum of electronic and thermal Energies=	-1500.599271
Sum of electronic and thermal Enthalpies=	-1500.598327
Sum of electronic and thermal Free Energies=	-1500.697496

Chapter 3 Highly Efficient Deep Blue Emitters Based on *cis* and *trans* *N*-Heterocyclic Carbene Pt^{II} Acetylide Complexes: Syntheses, Photophysical Properties and Mechanistic Studies

Publication 2. *Chemistry – A European Journal*, **2013**, *19*, 15689-15701.

Yuzhen Zhang, Olivier Blacque, and Koushik Venkatesan*

Institute of Inorganic Chemistry, University of Zurich, Winterthurerstrasse 190, CH-8057, Zurich, Switzerland

DOI: 10.1002/chem.201302196

Highly Efficient Deep-Blue Emitters Based on *cis* and *trans* N-Heterocyclic Carbene Pt^{II} Acetylide Complexes: Synthesis, Photophysical Properties, and Mechanistic Studies

Yuzhen Zhang, Olivier Blacque, and Koushik Venkatesan*[a]

Abstract: We have synthesized *cis* and *trans* N-heterocyclic carbene (NHC) platinum(II) complexes bearing σ-alkynyl ancillary ligands, namely [Pt(dbim)$_2$(C≡CR)$_2$] [DBIM = *N*,*N*′-didodecylbenzimidazoline-2-ylidene; R = C_6H_4F (**4**), C_6H_5 (**5**), $C_6H_2(OMe)_3$ (**6**), C_4H_3S (**7**), and $C_6H_4C{\equiv}CC_6H_5$ (**8**)] and [Pt(ibim)$_2$(C≡CC_6H_5)$_2$] (**9**) (ibim = *N*,*N*′-diisopropylbenzimidazoline-2-ylidene), starting from [Pt(cod)(C≡CR)$_2$] (COD = cyclooctadiene) and 2 equivalents of [dbimH]Br ([ibimH]Br for complexes **9**) in the presence of *t*BuOK and THF. Mechanistic investigations aimed at uncovering the *cis* to *trans* isomerization reaction have been performed on the representative *cis* complex **5a** [Pt(dbim)$_2$(C≡CC_6H_5)$_2$] and revealed the isomerization to progress smoothly in good yield when **5a** was treated with catalytic amounts of [Pt(cod)(C≡CR)$_2$] at 75 °C in THF or when **5a** was heated at 200 °C in the solid state under an inert atmosphere. Detailed examination of the reactions points to the possible involvement, in a catalytic fashion, of a solvent-stabilized Pt^{II} dialkyne complex in the former case and a Pt^0 NHC complex in the latter case, for the transformation of the *cis* isomer to the corresponding *trans* complex. Thermal stability and the isomerization process in the solid state have been further investigated on the basis of TGA and DSC measurements. X-ray diffraction studies have been carried out to confirm the solid-state structures of **4b**, **5a**, **5b**, and **9b**. All of the synthesized dialkyne complexes **4**–**9** exhibit phosphorescence in solution, in the solid state at room temperature (RT), and also in frozen solvent glasses at 77 K. The emission wavelengths and quantum yields have been found to be highly tunable as a function of the alkynyl ligand. In particular, the *trans* isomer of complex **9** in a spin-coated film (10 wt % in poly(methyl methacrylate), PMMA) exhibits a high phosphorescence quantum yield of 80 %, which is the highest reported for Pt^{II}-based deep-blue emitters. Experimental observations and time-dependent density functional theory (TD-DFT) calculations are strongly indicative of the emission being mainly governed by metal-perturbed interligand (^{3}IL) charge transfer.

Keywords: acetylides · isomerization · N-heterocyclic carbenes · OLEDs · phosphorescence · platinum

Introduction

Small-molecule triplet emitters and polymers based on platinum(II) complexes have received considerable attention due to their potential applications in phosphorescent organic light-emitting devices (PhOLEDs),[1] chemosensors,[2] nonlinear optical (NLO) materials,[3] photocatalysts,[4] optical limiting materials,[5] and photovoltaic devices.[6] This wide range of applications can be attributed to platinum's spin-orbit coupling constant of 4481 cm^{-1},[7] which promotes efficient intersystem crossing (ISC) from singlet to triplet excited states. When the fast ISC rates of Pt complexes are combined with a strong field ligand like an alkyne, it creates a strong interaction through pπ–dπ overlap and raises the metal-centered d–d energy states, which in turn lowers the HOMO–LUMO energy gap resulting in emissive complexes.[1i,8]

Since the time of the first report of a phosphine-ligated Pt^{II} acetylide complex, *trans*-[Pt(PEt$_3$)$_2$(C≡CPh)$_2$], by Chatt and Shaw in 1959,[9] intensive research investigations have been carried out on the photophysical properties of these complexes (Figure 1, top). Studies of the phosphorescent emission properties of small molecules,[10] oligomers,[11] dendrimers,[3c,12] and polymers[1b,13] based on phosphine Pt^{II} acetylide fragments have indicated moderate to low quantum yields with emission only in the low-energy part of the visible spectrum. The bipyridine Pt^{II} acetylide complexes first reported by Che and co-workers showed a metal–ligand charge transfer (^{3}MLCT) [5d(Pt)→π*$_{phen}$]-centered emission in fluid solution at RT.[14] Subsequently, the groups of Eisenberg,[4a,15] Schanze,[16] Castellano,[4b,8a,17] and Yam[3b,c,8b,12,18] carried out extensive investigations on similar molecular entities and in due course expanded their diversity with the use of polypyridine-type ligands [Pt(N^N^N)(C≡CR)]$^+$ [4a,4c,5b,15f,19] and [Pt(N^N^C)(C≡CR)] (Figure 1, bottom).[5a,20] The origin of the triplet emission in diimine Pt^{II} ace-

[a] Y. Zhang, Dr. O. Blacque, Dr. K. Venkatesan
Inorganic Chemistry, University of Zürich,
Winterthurerstrasse 190, 8057 Zürich (Switzerland)
Fax: (+41) 44 6356803
E-mail: venkatesan.koushik@aci.uzh.ch

Supporting information for this article is available on the WWW under http://dx.doi.org/10.1002/chem.201302196.

 © 2013 Wiley-VCH Verlag GmbH & Co. KGaA, Weinheim

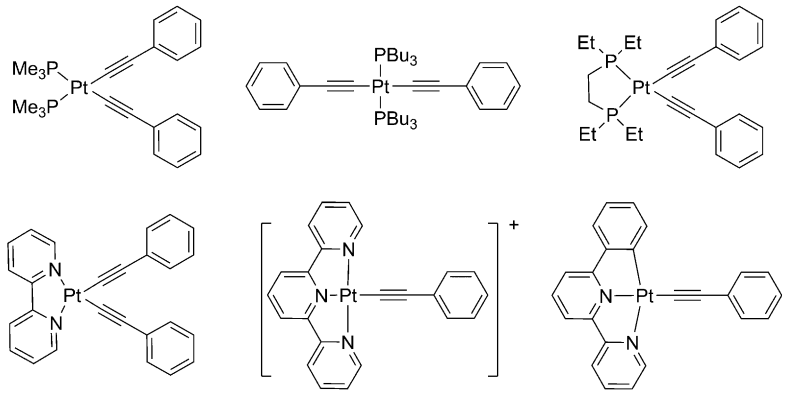

Figure 1. Platinum(II) dialkynyl complexes bearing phosphine ligands (top) and nitrogen ligands (bottom).

tylide complexes has been ascribed to a mixture of intraligand charge transfer $^3[\pi\rightarrow\pi^*(C{\equiv}CR)]$ (^{3}IL) and metal–ligand charge transfer $^3[5d(Pt)\rightarrow\pi^*(NN)]$ (^{3}MLCT) giving rise to moderate to good emission properties, albeit only at longer wavelengths.[21]

Since phosphine- and diimine-bound Pt^{II} acetylide small molecules show mostly moderate to good emission properties in the low-energy part of the visible spectrum, the development of highly emissive and stable small-molecule emitters at the high-energy end of the spectrum is highly desirable. Such systems could serve as key building blocks for the construction of new polymers and dendrimers that meet the demands of a number of applications.[16,17b,c,22] N-Heterocyclic carbene (NHC) ligands are considered as an interesting alternative to phosphine and pyridine ligands. Given that NHCs are strong σ-donors, their strong Lewis basicity would be expected to result in stronger Pt^{II}–ligand bonds, which would significantly reduce the likelihood of nonradiative deactivation of the excited states through dissociation of the ligand upon excitation.[1f,7c,23] In addition, the strong σ-donation of the NHC ligands is expected to be effective in preventing thermal access to metal-centered d–d states by pushing these to higher energies.[1h,24] The versatile coordination modes of NHCs would further allow the preparation of molecules with large conformational diversity.[13c] Exquisite control of the steric environment and electronic properties can be achieved by rational modification of the substituents on the nitrogen atoms and the NHC framework.[25] Following the report of Strassner and co-workers on dicationic blue-light-emitting tetra-NHC Pt^{II} complexes,[1d,26] we recently described the preparation and photophysical investigation of a series of neutral bis-NHC Pt^{II} acetylide and bis-NHC Pd^{II} acetylide complexes.[27] Some of the bis-NHC Pt^{II}-acetylides displayed blue emission at room temperature and the luminescent properties were found to be tunable by changing the functional group on the alkyne.[28] TD-DFT calculations revealed that the emission was dominated by intraligand charge transfer $^3[\pi\rightarrow\pi^*(C{\equiv}CR)]$ (^{3}IL), with limited participation of the metal center in the excited state. In view of the observed intriguing phosphorescence emission properties of the *cis* NHC Pt^{II} dialkyne complexes in solution and the solid state, the *trans* NHC Pt^{II} dialkyne complexes were expected to be suitable candidates as novel building blocks for the preparation of linear organometallic oligomers, dendrimers, macrocycles, and polymers. NHC ligands bearing dodecyl chains have been used to enhance the solubility of the final complexes.

In this context, we report herein detailed investigations on the synthesis, solid-state structures, and luminescent properties of new *trans* bis-NHC Pt^{II} bisacetylide complexes. Different reaction conditions have been employed to prepare the *trans* complexes in high yields, and studies have been carried out aimed at elucidating the mechanism underpinning their formation. Since the electronic properties of the alkyne ligands were expected to strongly influence the luminescent properties, complexes bearing different alkyne ligands were targeted, and experimental and theoretical investigations were carried out to analyze the nature of the excited states. The remarkable quantum yields of the *trans* complexes of **4** and **5** in the solid state are the highest reported for deep-blue emitters. The readily tunable emission properties hold great promise for the potential use of this fragment in the construction of light-emitting macromolecules for varied applications.

Results and Discussion

Synthesis and characterization: Transition metal alkynyl complexes are mostly synthesized by well-known transmetallation procedures involving copper acetylides, alkynyl stannanes, or lithium acetylides starting from the readily accessible metal halide complexes. However, previous studies have shown that *trans* $[Pt(dbim)_2Br_2]$[29] (DBIM = *N*,*N*′-diisopropylbenzimidazoline-2-ylidene), particularly bearing nonsterically demanding substituents at the nitrogen atoms, can only be generated in a dismal yield (3%), and hence this approach was discarded. $[Pt(cod)(C{\equiv}CR)_2]$ (cod = cyclooctadiene) was considered as a suitable precursor, since the labile COD ligand was expected to be readily displaced in the presence of the NHC ligand due to the strong *trans* effect of the alkynyl ligand. Based on an earlier literature protocol, the precursor complexes of the type $[Pt(cod)(C{\equiv}CR)_2]$ (R = C_6H_4F (**1**), C_6H_5 (reported),[30a] $C_6H_2(OCH_3)_3$ (**2**), 2-thienyl (**3**), and $C_6H_4C{\equiv}CC_6H_5$ (reported)[30b]) were obtained in good to moderate yields by treating $[Pt(cod)Cl_2]$ with the corresponding sodium acetylides in ethanol.[31] Subsequent treatment of $[Pt(cod)(C{\equiv}CC_6H_5)_2]$ with 2 equivalents of DBIM in THF at 75 °C resulted in a mixture of two

 © 2013 Wiley-VCH Verlag GmbH & Co. KGaA, Weinheim

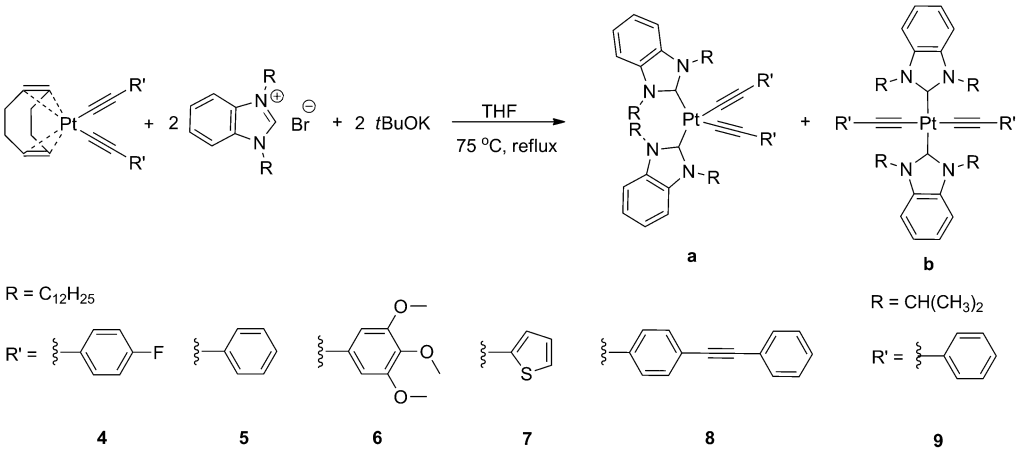

Scheme 1.

complexes. The ^{1}H NMR spectrum of the mixture featured three multiplets at $\delta = 4.89$, 4.86, and 4.38 ppm, characteristic resonances of the -CH_2 protons bound to the α-C connected to the benzimidazole nitrogen ($NCH_2C_{11}H_{23}$). ESI-MS analysis of the mixture gave a peak at m/z 1330.0 $[M+Na]^+$. Based on detailed NMR studies, the multiplets at $\delta = 4.89$ and 4.38 ppm were assigned to the *cis* isomer **5a** and that at $\delta = 4.86$ ppm to the *trans* isomer **5b** (Figure 2).

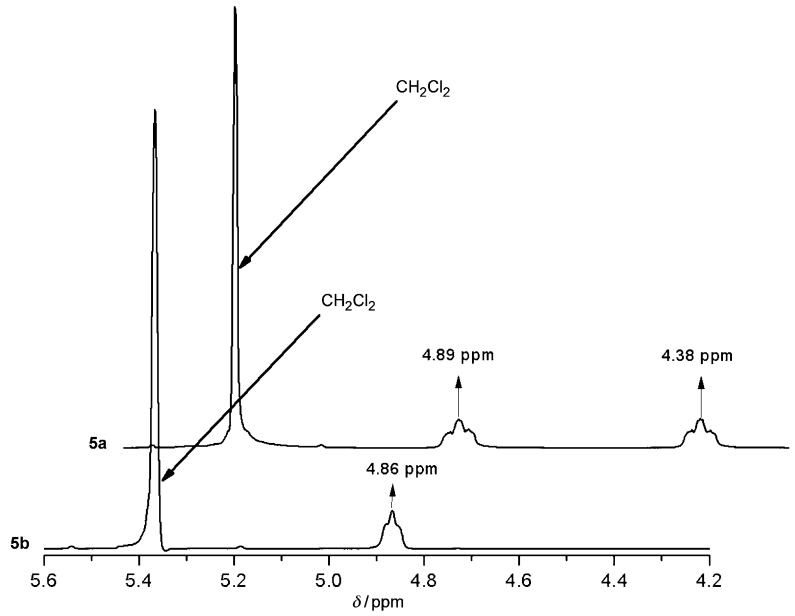

Figure 2. ^{1}H NMR spectra of *cis* complex **5a** and *trans* complex **5b**.

The two products were obtained in yields of 27 and 24%, respectively, after separation by column chromatography on silica gel. Single-crystal X-ray diffraction studies further confirmed the structures of **5a** and **5b**. Analogously, various *cis* and *trans* complexes of the type $[Pt(dbim)_2(C{\equiv}CR)_2]$ (R = C_6H_4F (**4a**,**b**); C_6H_5 (**5a**,**b**); $C_6H_2(OCH_3)_3$ (**6a**,**b**); 2-thienyl (**7a**,**b**); $C_6H_4C{\equiv}CC_6H_5$ (**8a**,**b**)) and $[Pt(ibim)_2(C{\equiv}CR)_2]$ (R = C_6H_5 (**9a**,**b**)) were synthesized (Scheme 1). The isolated yields were between 9 and 42% for the *cis* isomers and between 4 and 27% for the *trans* isomers, depending on the alkyne substituents. All of the *cis* and *trans* complexes were characterized by ^{1}H NMR, ^{13}C NMR, and IR spectroscopy, as well as ESI-MS. The structure of **4b** was also confirmed by a single-crystal X-ray diffraction study. In order to improve the yield of the highly desired *trans* product and to account for the observation of both *cis* and *trans* product during the reaction, further investigations were carried out. When the reaction was performed at room temperature by using 3.0 equivalents of the NHC ligand instead of the original 2.0 equivalents, a near-quantitative yield of **5a** was obtained with only a trace of the *trans* isomer. Significant improvements in the yields (47–90%) of the respective *cis* isomers were accomplished when 3.0 equivalents of the NHC were used in the reaction.

Single-crystal X-ray diffraction analysis: Single crystals suitable for X-ray diffraction were grown by slow evaporation of the solvent from a concentrated solution of the compound in a mixture of MeOH and CH_2Cl_2. The molecular structures of complexes **4b**, **5a**, **5b**, and **9b** are shown in Figure 3. Crystallographic parameters are summarized in Table S1 in the Supporting Information and selected bond lengths and angles are listed in Table 1. The four complexes exhibit distorted square-planar coordination geometries about the Pt^{II} core. The $Pt{-}C_{carb}$ distances in the complexes range from

 © 2013 Wiley-VCH Verlag GmbH & Co. KGaA, Weinheim

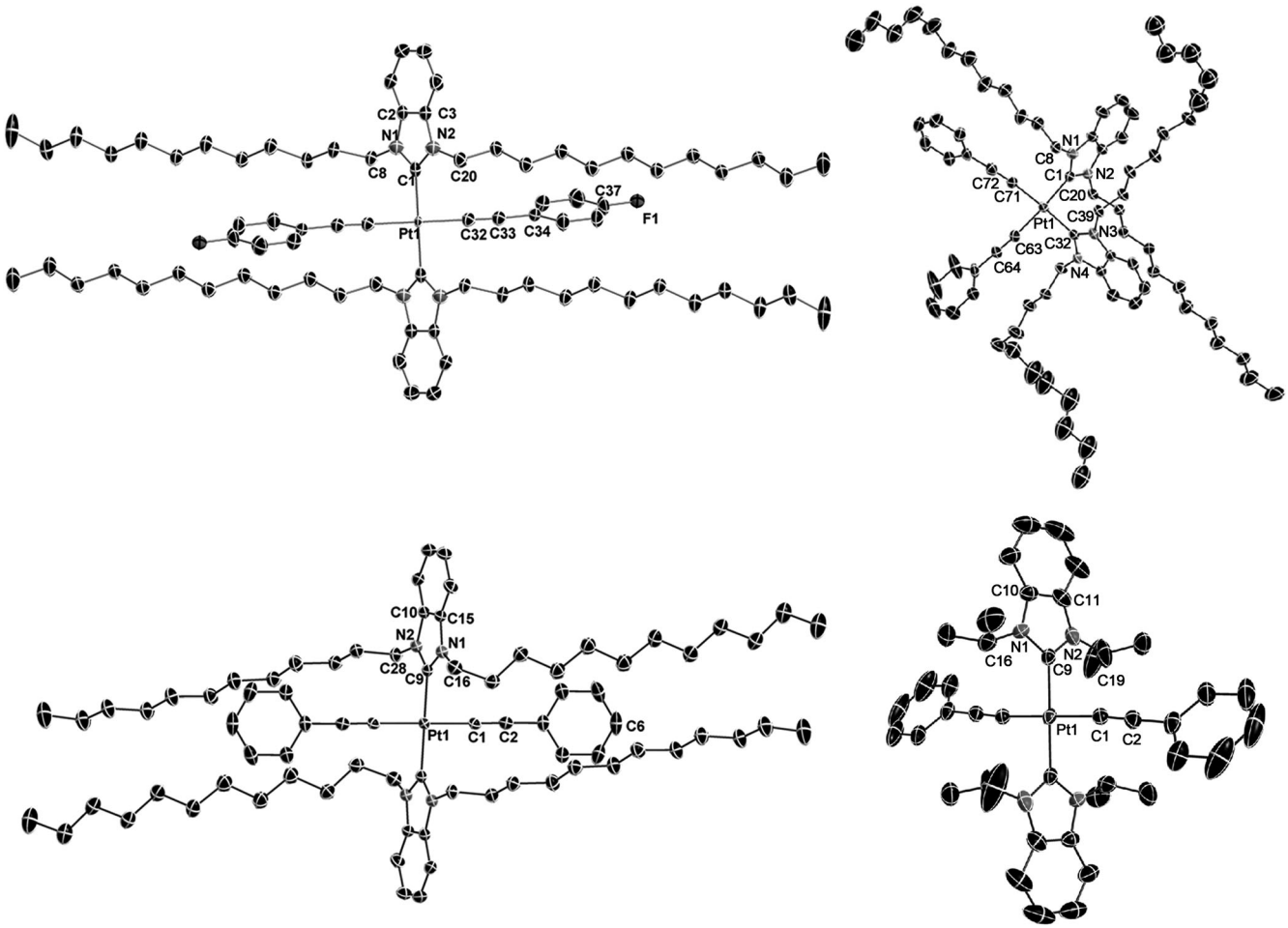

Figure 3. Molecular structures of **4b**, **5a**, **5b**, and **9b** showing selected atomic numbering. Ellipsoids are set at the 50% probability level. Hydrogen atoms and solvent molecules are omitted for clarity

2.0168(18) to 2.029(3) Å and the Pt–C_{alk} distances from 1.996(3) to 2.0092(18) Å. The Pt–C_{carb} distances in the current complexes are longer than those in previously reported analogous structures, which may be due to the *trans* influence of the strongly electron-donating acetylene ligands.[29,32] The Pt–C_{alk} distances are shorter than those in reported [Pt(phosphine)$_2$(C≡CR)$_2$] complexes,[33] but 0.04 Å longer than those in [Pt(bipyridine)(C≡CR)$_2$] complexes.[15a,21] The Pt–C_{carb} distance in **5a** is 0.01 Å longer than that in **5b**, but the reverse is true for the Pt–C_{alk} distances. The shortest Pt···Pt distance in these structures was found to be 8.6169(2) Å, and hence any intermolecular Pt···Pt interaction in the solid state can be ruled out.

UV/Vis absorption and emission: The UV/Vis absorption spectra of complexes **4**–**9** in solution at 298 K are shown in Figure 4 and Figure S1 in the Supporting Information. All ten complexes exhibit similar spectra, with an intense absorption band at 284–300 nm and an additional shoulder band (low-energy absorption bands) at 305–358 nm. The molar absorption coefficients (ε) for the intense absorption bands are in the range 2.0×10^4 to $6.0\times10^4\,M^{-1}cm^{-1}$, and are thus comparable to those of reported [Pt(diimine)(C≡CR)$_2$] complexes. In comparison with the spectra of our previously reported bidentate NHC Pt^{II} acetylide complexes, the low-energy absorption bands are hypsochromically shifted by approximately 40 nm and overlap with the high-energy bands. Varying the solvent in further UV/Vis studies on these complexes showed no significant shifts in the absorption wavelengths.

Based on the spectroscopic studies and the DFT and TD-DFT calculations, the low-energy absorption bands in these ten complexes are assigned to a mixture of metal-perturbed ligand-to-ligand ^{1}LLCT ($\pi_{alk}\rightarrow\pi^*_{carb}$) and metal-to-ligand ^{1}MLCT (5d(Pt)$\rightarrow\pi^*_{carb}$) transitions.[15a,21] The high-energy absorption bands that display the characteristic $\pi\rightarrow\pi^*$ transition are assigned to metal-perturbed intraligand ^{1}LLCT ($\pi_{alk}\rightarrow\pi^*_{alk}$) transitions.[16,18b,20a] There are no significant differences in the patterns of the absorption bands and absorption maxima for complexes **4**–**7** and **9**. However, in the case of complexes **8a** and **8b** bearing the conjugated ligand C≡CC_6H_4C≡CC_6H_5, the absorption bands are further redshifted to 343 and 353 nm, respectively. The observed redshifts in the absorptions of **8a** and **8b** in comparison to those of the

 © 2013 Wiley-VCH Verlag GmbH & Co. KGaA, Weinheim

Table 1. Selected bond lengths [Å] and angles [°] of complexes **4b**, **5a**, **5b**, and **9b**.

	Distance [Å]	Angle [°]	
Complex **4b**			
C(1)−Pt(1)	2.020(2)	C(1)-Pt(1)-C(32)	88.85(8)
C(32)−Pt(1)	2.0092(18)	C(1)-Pt(1)-C(32)^{i}	91.15(8)
Complex **5a**			
C(1)−Pt(1)	2.026(3)	C(63)-Pt(1)-C(71)	84.14(13)
C(32)−Pt(1)	2.029(3)	C(71)-Pt(1)-C(1)	91.42(12)
C(63)−Pt(1)	1.996(3)	C(63)-Pt(1)-C(32)	92.16(12)
C(71)−Pt(1)	2.006(3)	C(1)-Pt(1)-C(32)	92.37(11)
Complex **5b**			
C(1)−Pt(1)	2.0043(19)	C(1)-Pt(1)-C(9)	88.60(7)
C(9)−Pt(1)	2.0168(18)	C(1)-Pt(1)-C(9)^{i}	91.40(7)
Complex **9b**			
C(1)−Pt(1)	2.008(2)	C(1)-Pt(1)-C(9)	93.03(8)
C(9)−Pt(1)	2.027(2)	C(8)-Pt(1)-C(1)	86.97(8)

[i] $-x, -y, -z$.

other eight complexes reflect the smaller HOMO–LUMO gaps arising from the increased conjugation of the alkyne ligand. Comparison of the UV/Vis absorption bands between the isomers revealed those of the *trans* isomers to be slightly bathochromically shifted with lower molar absorption coefficients than those of the corresponding *cis* isomers.

All of the synthesized dialkyne complexes were found to be emissive both in solution and the solid state. The emission spectra of the complexes recorded in CH_2Cl_2 featured bands in the range 431–530 nm (Table 2). The large Stokes shifts ($\approx$150 nm), along with emission lifetimes of the order of microseconds and rapid quenching of the emission in air, are highly indicative of emission from a triplet manifold. The emission wavelengths of the *cis* complexes **4a**–**6a** are bathochromically shifted with increasing electron-donating character ($F < H < (OMe)_3$) of the substituents on the alkynes. A similar trend was seen for the *trans* isomers **4b**–**6b**. All of the *trans* isomers show a 3–6 nm redshift in their emission maxima compared to the corresponding *cis* isomers. This can be attributed to the efficient charge delocalization in the highly symmetrical *trans* isomer, resulting in a decrease in the HOMO–LUMO gap. Complexes **7a** and **7b** exhibit broad bands along with a strong vibronic progression due to the thienyl group. Their emission maxima are also bathochromically shifted by about 70 nm compared to those of complexes **6a** and **6b**. In accordance with the different electron donicities and electron delocalization of the alkynyl substituents, the emission maxima of complexes **8a** and **8b** bearing $C{\equiv}CC_6H_4C{\equiv}CC_6H_5$ are significantly redshift-

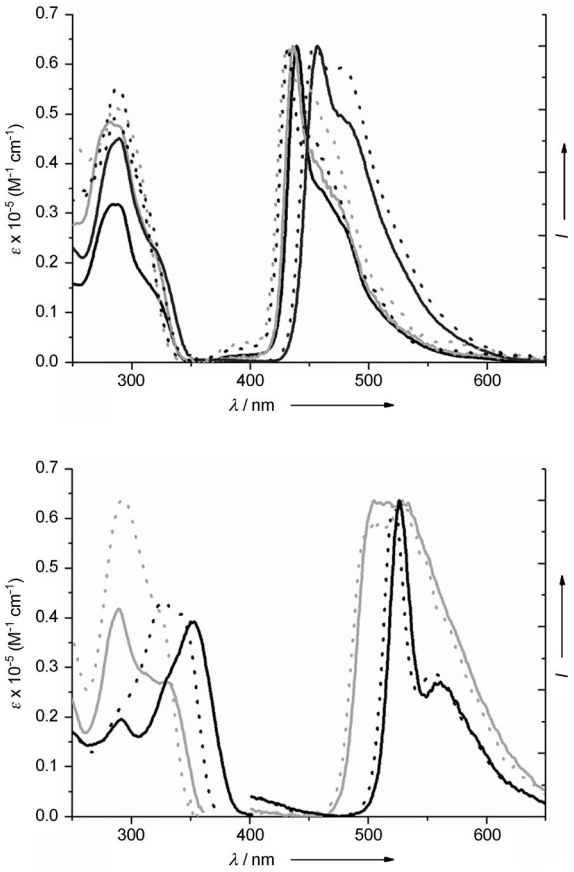

Figure 4. Top) Electronic absorption and normalized emission spectra of **4a** (light-gray dotted line), **4b** (light-gray solid line), **5a** (black dotted line), **5b** (black solid line), **6a** (dark-gray dotted line), **6b** (dark-gray solid line) in CH_2Cl_2 at RT. Bottom) Electronic absorption and normalized emission spectra of **7a** (light-gray dotted line), **7b** (light-gray solid line), **8a** (black dotted line), and **8b** (black solid line) in CH_2Cl_2 at RT.

Table 2. Photophysical properties of complexes **4a**–**9a** and **4b**–**9b**.

	Room temperature solution (CH_2Cl_2)								77 K Glass	10 wt % PMMA Film	
	Absorption λ_{max} [nm] (ε_{max}/[dm^{3}mol^{-1}cm^{-1}])	Emission λ_{max} [nm] Solution	Solid state	τ [μs]	$\phi_{em}\times10^{-2}$ CH_2Cl_2	Solid	k_r [$\times10^3$ s^{-1}]	k_{nr} [$\times10^5$s^{-1}]	(2-MeTHF) Emission λ_{max} [nm]	Emission λ_{max} [nm]	$\phi_{em}\times10^{-2}$
4a	284 (51634), 293 (50335)	431, 462 sh	432, 450 sh, 472 sh	0.22	0.4	7.1	19	45	422, 440 sh	429, 449	65.1
5a	285 (49082), 300 (39978)	432, 465 sh	430, 450 sh, 475 sh	0.24	0.9	1.6	36	41	425, 447 sh	431, 449	60.8
6a	289 (55406), 310 (33877)	454, 478 sh	454, 471 sh, 505 sh	3.48	1.2	0.2	3.4	2.8	442, 475 sh	454, 484	7.5
7a	293 (64198), 322 (41740)	529, 533 sh	496, 511, 531, 550	7.90	0.4	0.5	0.4	1.3	488, 503	506, 531	5.0
8a	327 (43462), 343 (40726)	522, 554 sh	526, 558, 573 sh	6.80	0.4	3.4	0.5	1.4	516, 548 sh	523, 558	5.2
9a	285 (47827), 302 (34208)	432, 465 sh	432, 450 sh, 460 sh	0.10	0.1	0.8	10	9.9	420, 448 sh	431, 450	53.6
4b	281 (48381), 311 (26955)	436, 471 sh	416, 431 sh, 457 sh	0.37	2.6	44.5	70	26	426, 445 sh	434, 457 sh	52.6
5b	288 (31751), 315 (15709)	439, 461 sh	443, 465 sh, 487 sh	3.58	1.0	46.6	2.7	2.8	430, 451 sh	440, 460 sh	44.7
6b	289 (45128), 318 (23190)	457, 498 sh	463, 481 sh, 523 sh	2.52	1.9	0.2	7.5	3.9	440, 473 sh	453, 484	7.7
7b	289 (41746), 333 (26741)	505 sh, 534	502, 516, 538, 556	2.41	0.3	0.4	1.4	4.1	488, 504	511, 535	1.5
8b	291 (19531), 353 (39222)	527, 561	529, 561, 576 sh	5.30	0.8	5.7	1.4	1.8	522, 555	525, 563	6.9
9b	283 (34110), 310 (18219)	439, 455 sh	438, 451 sh	1.11	0.9	4.1	8.1	8.9	423, 450 sh	436, 456	80.0

 © 2013 Wiley-VCH Verlag GmbH & Co. KGaA, Weinheim

ed to 522 and 527 nm, respectively. The triplet emissions are assigned to the metal-perturbed ligand-to-ligand ($\pi_{alk} \rightarrow \pi^*_{alk}$) transition. An increase in ligand donicity raises the alkynyl-based HOMO energy level, thereby decreasing the energy gap between the HOMO and LUMO, which in turn results in a bathochromic shift of the emission. The solution quantum yields of complexes **4**–**9** were found to lie in the range 1.0×10^{-3} to 2.6×10^{-2} by using quinine sulfate as a reference ($\phi_{em}=0.55$). These are comparable to those of known [Pt(diimine)(C≡CR)$_2$] complexes and our previously reported chelating NHC Pt acetylide complexes.

In a rigidified glass medium (2-methyltetrahydrofuran, 2-MeTHF) at 77 K, the spectra of **4**–**9** are well-resolved, as shown in Figures S2 and S3 in the Supporting Information. The emission maxima of the complexes are in the wavelength range 422–522 nm, shifted by 5–58 nm compared with those at RT. Unlike the broad and unsymmetrical emission profiles at room temperature, the spectra at 77 K exhibit a rigidochromic shift and resolvable vibronic components of the emission. The vibrational progressional spacings of **7a** are 650 and 1450 cm^{-1}, which can be assigned to the characteristic skeletal vibration of the thienyl ring, and 2041 cm^{-1}, which can be assigned to the $\tilde{\nu}_{(C\equiv C)}$ stretching vibration of (Figure S4 in the Supporting Information). Complex **7b** was found to exhibit similar behavior to that of **7a**. The vibrational progressional spacings of complex **8b** are 1106, 1613, and 2092 cm^{-1}, which can be assigned to the C–N stretching vibration, the skeletal vibration of the phenyl ring, and the $\tilde{\nu}_{(C\equiv C)}$ stretching vibration, respectively (Figure S4 in the Supporting Information). Complex **8a** exhibits a similar behavior. The rest of the complexes display features like those of **4b** (Figure S5 in the Supporting Information), comprising two vibrational progressional spacings of 1100 cm^{-1} (C–N stretching vibration of benzimidazole) and 2100 cm^{-1} ($\tilde{\nu}_{(C\equiv C)}$ stretching vibration). These vibronic emission peaks further support the involvement of the alkynyl ligand in the triplet emission. At 77 K, the emission maxima of the *trans* isomers show moderate redshifts with respect to those of the corresponding *cis* isomers, although for complex **6b** the redshift is only 2 nm relative to the maximum for **6a**. This difference is also reflected in the oxidation potentials of the complexes derived from the CV measurements of the *cis* and *trans* complexes (see below). All of the synthesized complexes **4**–**9** show emission in the solid state. The absolute quantum yields of all of the *cis* and *trans* complexes in pure crystalline form were measured. Interestingly, the maxima of the triplet emissions of all the complexes appear at different wavelengths in different media due to the effects of the solvent environment and molecular aggregation (Figures S6–S8 in the Supporting Information). These influences also extend to the luminescent efficiencies of the complexes. The quantum yields of most of the complexes in fluid solution were found to lie in a low range from 0.1 to 2.6%, but increased to 47% in the case of complex **5b**. Moreover, when the complexes were dispersed at 10 wt% in poly(methyl methacrylate) (PMMA) films, their quantum yields were found to be significantly enhanced, to 80% in the case of complex **9b**. The absorption and emission spectra of complexes **9a** and **9b** were the same as those of complexes **5a** and **5b**. However, the quantum yields of **5b** and **9b** at 10 wt% in PMMA differed significantly.

Based on the above results, we can conclude that increased molecular rigidity and weaker intermolecular interactions in the solid state lead to a significant enhancement in quantum efficiency in molecules of this type. The development of blue-emitting Pt^{II} complexes has been notoriously difficult, and only recently have quantum yields of 90 and 86% with $\lambda_{em}=464$ nm been reported by the groups of Strassner[1d] and Wang[1f] by using cyclometalated ligands. To the best of our knowledge, the emission quantum yield of 80% for **9b** with $\lambda_{em}=436$ nm is the highest reported for a deep-blue emitter in this range. This work provides further impetus to the design of highly emissive deep-blue emitters devoid of a cyclometalating ligand.

Electrochemistry: Cyclic voltammograms of complexes **4**–**8** were measured in DMF by using [nBu$_4$N][PF$_6$] (0.1 M) as supporting electrolyte. The electrochemical data are listed in Table 3. There is only one irreversible oxidation wave for each complex and no observable reduction wave on scanning up to −2.57 V (Figure S9 in the Supporting Information). This behavior is consistent with the stronger σ-donating nature of the NHC ligand and quite closely resembles that of analogous [Pt(phosphine)$_2$(C≡CR)$_2$] complexes. However, it differs from that of [Pt(diimine)(C≡CR)$_2$] complexes, which show one or more reversible reduction waves associated with the diimine ligand. For complexes **4**, **5**, and **6**, the oxidation potential decreases with increasing donor ability of the alkynyl functional group (F < H < (OMe)$_3$). Comparing the oxidation potentials of the respective pairs of *cis* and *trans* isomers, that of the *cis* isomer is about 50–110 mV higher than that of the *trans* isomer, except in the case of compounds **6a** and **6b**. This abnormal behavior of **6a** and **6b** is consistent with the emission maxima observed at 77 K, with **6b** emitting at a higher energy than **6a**. The oxidation waves observed for all of the complexes are tentatively assigned to oxidation of the alkynyl ligand rather than a Pt^{II}/Pt^{III} process given the low oxidation potential (< +1.0 V) and since the HOMO (93%) is mainly located on the C≡CR π orbital, according to DFT calculations.

Table 3. Electrochemical potentials for **4a**–**9a** and **4b**–**9b**.[a]

Complex	E_{ox} [V]	Complex	E_{ox} [V]
4a	+0.86	**4b**	+0.79
5a	+0.84	**5b**	+0.77
6a	+0.58	**6b**	+0.66
7a	+0.86	**7b**	+0.75
8a	+0.94	**8b**	+0.83
9a	+0.85	**9b**	+0.78

[a] Scan rate = 100 mV s^{-1} in 0.1 M [nBu$_4$N][PF$_6$] (Au electrode; E vs Fc$^+$/Fc; 20 °C; DMF).

© 2013 Wiley-VCH Verlag GmbH & Co. KGaA, Weinheim

DFT calculations: In order to study the luminescent properties of our *cis* and *trans* N-heterocyclic carbene Pt^{II} acetylide complexes, we performed DFT and TD-DFT calculations on **5a** and **5b** with the Gaussian 03 program package.[34] The hybrid functional PBE1PBE (also known as PBE0)[35] in conjunction with the Stuttgart/Dresden effective core potentials (SDD) basis set[36] for the Pt center, augmented with one f-polarization function (exponent = 0.993), and the standard 6-31+G(d) basis set[37] for the remaining atoms were applied for all calculations. Full geometry optimizations without symmetry constraints, but with a C_2H_5 model instead of the long $C_{12}H_{25}$ chain of the carbene ligands in **5a** and **5b**, were carried out in the gas phase for the singlet ground states (S_0) and the lowest triplet states (T_1). The optimized geometries were confirmed to be potential energy minima by vibrational frequency calculations at the same level of theory, as no imaginary frequency was found. The first ten singlet–singlet and singlet–triplet transition energies were computed for the optimized S_0 geometries, by using the time-dependent DFT (TD-DFT) methodology. Solvent effects were taken into account by using the conductor-like polarizable continuum model (CPCM) with dichloromethane (absorption/emission) or toluene (mechanistic study) as solvent for single-point calculations on all of the optimized gas-phase geometries.

The experimental UV/Vis absorption spectra of complexes **5a** and **5b** in solution (dichloromethane) at 298 K exhibit similar absorption patterns with intense absorption bands at 285 and 288 nm and shoulder absorption bands at 300 and 315 nm, respectively. Based on the spectroscopic studies, the low-energy absorption bands in these complexes are assigned to a mixture of metal-perturbed ligand-to-ligand ^{1}LLCT ($\pi_{alk}\rightarrow\pi^*_{carb}$) and metal-to-ligand ^{1}MLCT ($5d(Pt)\rightarrow\pi^*_{carb}$) transitions. The high-energy absorption bands, which show the characteristics of $\pi\rightarrow\pi^*$ transitions, are assigned to metal-perturbed intraligand ^{1}ILCT ($\pi_{alk}\rightarrow\pi^*_{alk}$) transitions. TD-DFT calculations carried out on the ground-state structures of **5a** and **5b** confirmed the experimental analyses. In the ground-state geometry, the lowest significant singlet excited states S_1, S_3, and S_8 ($f>0.05$) of **5b** are calculated to give rise to discrete HOMO→LUMO, HOMO→LUMO+1, and HOMO−1→LUMO+3 excitations at 327 ($f=0.238$), 301 ($f=0.860$), and 278 nm ($f=0.597$), respectively (Table S2 in the Supporting Information). The LUMO is of π^* character with the electron density delocalized over both carbene ligands (82%) in an out-of-phase combination with a Pt 5d orbital (11%). On the contrary, the HOMO is located mainly on one alkyne ligand (77%) and on the metal center (23%) and has no contribution from the carbene ligands (Figure 5 and Table S3 in the Supporting Information). The HOMO−1 is almost degenerate with the HOMO, showing a main contribution from the other alkyne ligand. The participation of the metal is slightly greater in the HOMO than in the HOMO−1 (23 vs. 16%), which destabilizes the former orbital and accounts for the energy gap between these two orbitals ($\Delta E_{H-1/H}=0.17$ eV). The electron densities in the LUMO+1 and LUMO+3 are located mainly on the same alkyne ligand as the HOMO and HOMO−1, respectively. We can therefore surmise that the intense absorption band observed experimentally at 288 nm arises from overlap of the TD-DFT-calculated $S_0\rightarrow S_3$ and $S_0\rightarrow S_8$ singlet–singlet transitions and shows, in agree-

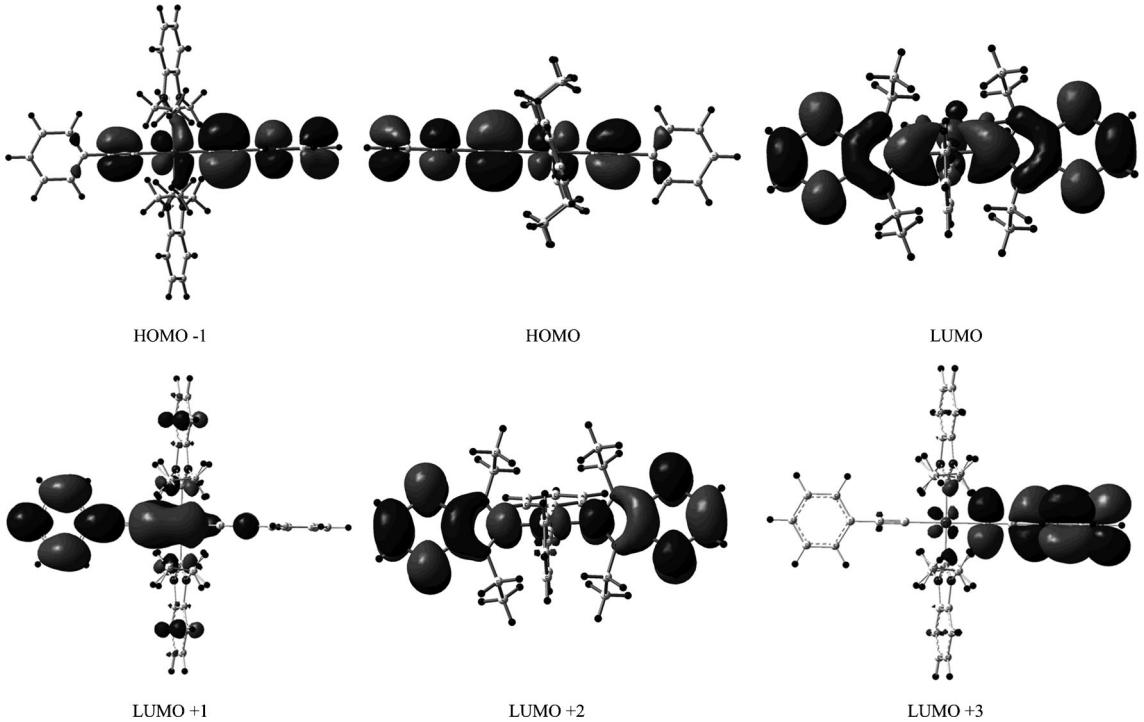

Figure 5. Spatial plots of selected frontier orbitals of the DFT-optimized ground state of **5b**.

 © 2013 Wiley-VCH Verlag GmbH & Co. KGaA, Weinheim

ment with the experimental indications, intraligand ^{1}ILCT ($\pi_{alk}\rightarrow\pi^*_{alk}$) charge-transfer character. The low-energy absorption band, observed as a shoulder in the experimental UV/Vis spectrum, corresponds to the single HOMO→LUMO excitation assigned to an admixture of ligand-to-ligand ^{1}LLCT ($\pi_{alk}\rightarrow\pi^*_{carb}$) and metal-to-ligand ^{1}MLCT ($5d\rightarrow\pi^*_{carb}$) characteristics.

For complex **5a**, the assignment of the experimental bands and lowest-energy transitions is not as trivial as in the case of **5b**. Indeed, TD-DFT calculations showed only three singlet–singlet transitions (among the ten lowest transitions calculated) with an oscillator strength $f>0.1$ for **5b**, whereas no fewer than six transitions with $f>0.2$ were computed for **5a**. Furthermore, one transition exhibits a large oscillator strength of 0.860 for **5b**, whereas all transitions of **5a** are more or less equivalent ($f=0.204$–0.380). In the ground-state geometry, the lowest significant singlet excited states S_1 and S_2 of **5a** are calculated to give rise to HOMO→LUMO and HOMO−1→LUMO excitations at 320 ($f=0.357$) and 307 nm ($f=0.380$), respectively. In the HOMO and HOMO−1, the electron density is mainly located on both alkyne ligands (81–85%) in an out-of-phase combination with a Pt 5d orbital (15–16%). The bonding (HOMO−1) and antibonding orbitals (HOMO) of **5a** and **5b** differ in the through-space interactions between the alkyne ligands (Figure 6). The main difference compared to **5b** is that the unoccupied orbital involved in the one-electron excitation, here the LUMO, is delocalized over the whole molecule: 46% on the carbene ligands, 40% on the alkyne ligands, and 14% on the metal center. Considering that the low-energy absorption band (observed as a shoulder in the UV/Vis spectrum) is produced by the overlap of these two transitions, this energy absorption predominately arises from excited states with a ligand-to-ligand ^{1}LLCT ($\pi_{alk}\rightarrow\pi^*_{carb}$) charge transfer, as in **5b**, but with sizable amounts of metal-to-ligand ^{1}MLCT ($5d\rightarrow\pi^*_{carb}$) and intraligand ^{1}ILCT ($\pi_{alk}\rightarrow\pi^*_{alk}$) character. At higher energies, four transitions overlap to produce the intense experimental band at 285 nm ($S_0\rightarrow S_5$, 292 nm, $f=0.204$; $S_0\rightarrow S_8$, 282 nm, $f=0.298$; $S_0\rightarrow S_9$, 278 nm, $f=0.326$; $S_0\rightarrow S_{10}$, 277 nm, $f=0.292$). All frontier orbitals in the range HOMO−2 to LUMO+3 play a role in the single excitations of these four transitions, leading to an unclear assignment of the band.

The lowest singlet–triplet vertical excitation (T_1–S_0) energies obtained by TD-DFT calculations on the ground-state structures of **5a** and **5b** are 431 and 437 nm, which are consistent with the experimental emissions at 425 and 430 nm, respectively. The transitions responsible for the emission bands comprise the HOMO↔LUMO ($a_i=0.438$) and HOMO−1↔LUMO+3 ($a_i=0.417$) single excitations for **5a**, and the HOMO↔LUMO+1 excitation for **5b**. As already mentioned, the HOMO and HOMO−1 are mainly located on both alkyne ligands in an out-of-phase combination with a Pt 5d orbital, whereas the LUMO is delocalized over the whole molecule. The LUMO+3 is 98% localized on both alkyne ligands. The promotion of one electron to an unoccupied orbital leads to a singlet excited state, and then a spin-orbit interaction between excited states operates to induce S→T intersystem crossing to form the corresponding triplet excited state. Geometry relaxation of the latter leads to the lowest-energy triplet state, the optimized structure of which can be determined by DFT calculations. Careful analysis of the molecular orbital diagrams of the optimized triplet states of **5a** and **5b** revealed that the highest singly occupied molecular orbitals (SOMOs) are located almost exclusively on the alkyne ligands (Table S2 in the Supporting Informa-

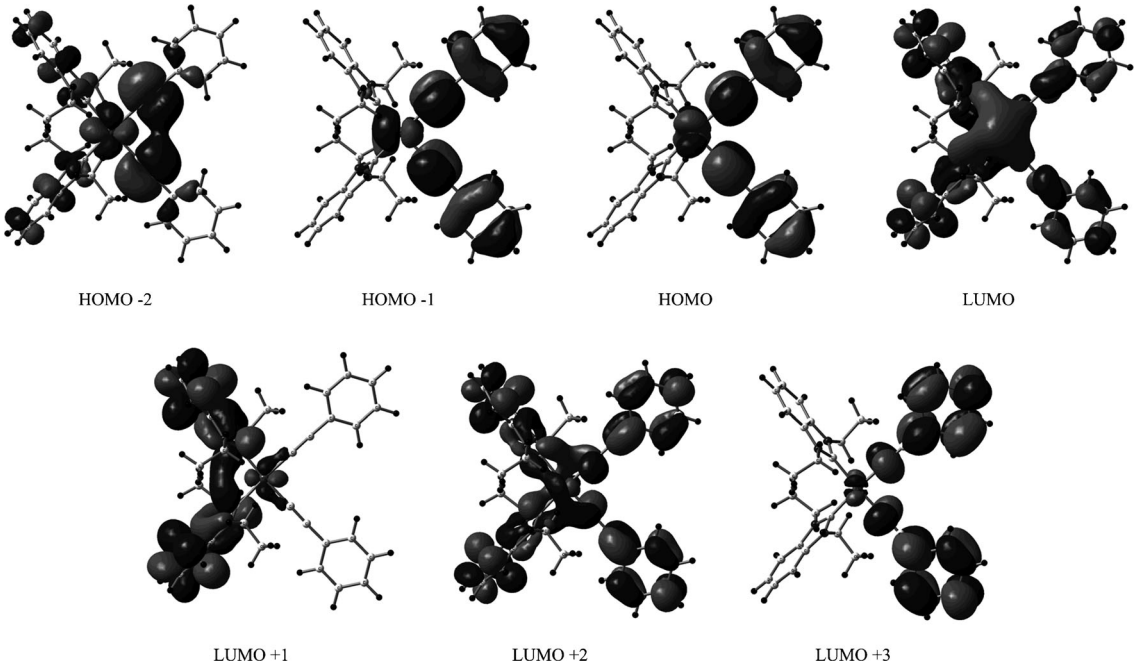

Figure 6. Spatial plots of selected frontier orbitals of the DFT-optimized ground state of **5a**.

 © 2013 Wiley-VCH Verlag GmbH & Co. KGaA, Weinheim

tion). The highest SOMO, from which the emission is produced, is localized at 95 (**5a**) and 93% (**5b**) on one alkyne ligand and 5 (**5a**) and 7% (**5b**) on the metal center, whereas the second highest SOMO, called SOMO−1, to which the excited electron should return, is localized at 85% on the other alkyne ligand and 13% on the metal center (both **5a** and **5b**). The spin density surfaces of **5a** and **5b**, which take into account the electron density on all singly occupied orbitals and not only the SOMOs, visually identify the emission from a transition with mainly intraligand ^{3}ILCT ($\pi^*_{alk}\rightarrow\pi_{alk}$) character and minor ligand-to-ligand ^{3}LLCT character (Figure S10 in the Supporting Information).

Mechanistic investigations: Investigations of the *cis* to *trans* isomerization of square-planar Pt^{II} complexes have been carried out since the 1950s.[9,38,39] The mechanisms of isomerization in this class of complexes can be divided into two major categories. The first involves consecutive displacement, consisting of ligand dissociation resulting in the formation of a three-coordinate intermediate, whereas the second involves pseudorotation, consisting of an intramolecular rearrangement accompanied by formation of a five-coordinate intermediate.[39d,40] In spite of extensive mechanistic studies on this class of complexes, mechanisms for the photochemically and thermally induced isomerizations still remain elusive.[39e]

In order to determine the optimal conditions for obtaining the *trans* complexes in high yields, we set out to elucidate the possible intermediates involved in the *cis* to *trans* isomerization process. The dependence of product formation on stoichiometry was first examined by varying the ratio of NHC and precursor in [D_8]THF at 75°C (Figure S11 in the Supporting Information). The results revealed initial formation of the *cis* isomer and the *cis* isomer was found to scale up with increase in the stoichiometry of the NHC ligand. When the reaction was closely monitored by ^{1}H NMR spectroscopy with a 1:2 stoichiometry of precursor to NHC ligand, resonances attributable to the *cis* isomer were first detected, along with signals of both COD bound to the Pt^{II} center in a monodentate fashion and unbound COD.[41] The proton resonances of the bound monodentate COD appeared further downfield than those of the free COD.

Additional 1D-TOCSY NMR experiments further confirmed the presence of the intermediate (Figure S12 in the Supporting Information). Based on this observation, a plausible mechanism involving stepwise substitution with the two NHC ligands is proposed in Scheme 2. The *trans* isomer was confirmed to be the thermodynamically more stable product, since resonances in the ^{1}H NMR spectrum corresponding to this isomer started to appear when the reaction mixture containing the *cis* complex was further heated to 75°C.

Precursor-catalyzed isomerization: After carrying out several reactions in different reactant combinations,[42] we found a notable *cis* to *trans* conversion only when **4a** was treated with a stoichiometric amount of [Pt(cod)(C≡CC_6H_5)$_2$] in THF at 75°C for 24 h. The yield of **4b** was 71% (see the Supporting Information). This finding is consistent with the formation of a small amount of the *trans* isomer when only 2.0 equivalents of the NHC ligand is used, whereas little or none of the *trans* isomer was observed when using 3.0 equivalents of the NHC ligand. The conversion of **5a** to **5b** in a similar yield of 64% was accomplished by treating only 10% of the precursor complex [Pt(cod)(C≡CC_6H_5)$_2$], but the reaction proceeded very slowly (see the Supporting Information). This can be rationalized by the hypothesis that the initially formed *cis* isomer reacts with an intermediate COD-free solvent-stabilized Pt^{II} complex [(S)$_2$Pt(C≡CC_6H_5)$_2$] (S = THF).[43] The interaction between the two fragments takes place through the binding of the platinum to the alkyne in an η^2 fashion and additional support may be provided through a Pt–Pt interaction. Binuclear complexes showing similar kinds of interactions have been reported previously.[22] Through this interaction, the COD-free platinum(II) fragment acting as a fifth ligand on the *cis* platinum complex **5a** could then undergo pseudorotation followed by expulsion, resulting in the formation of the *trans* complex. The fact that only *trans* **4b** and no *trans* **5b** was obtained corroborates the participation of the [Pt(cod)(C≡CC_6H_5)$_2$] precursor in the conversion of the *cis* to the *trans* isomer. Although we were able to obtain the desired *trans* compound by treating the *cis* isomer with the precursor, the thermally induced isomerization reaction was pursued with a view to obtaining the *trans* compound in good yield.

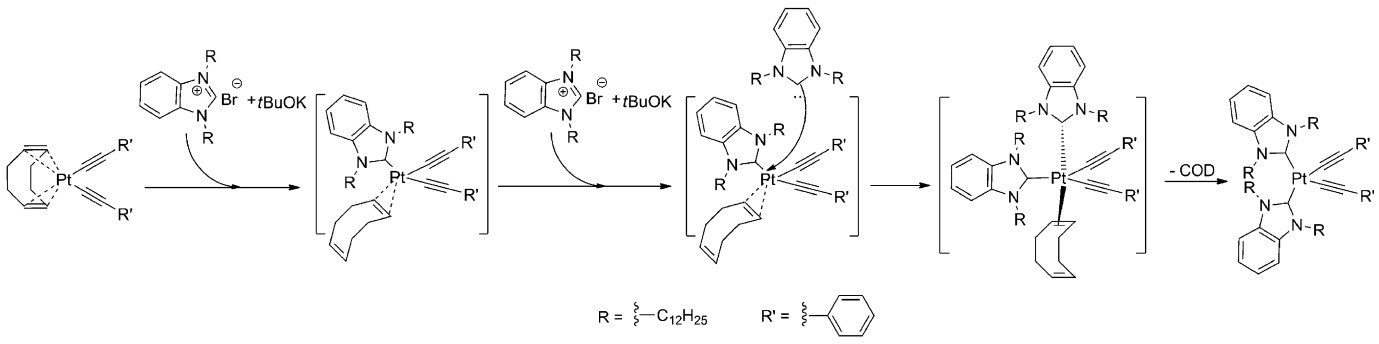

Scheme 2. Proposed reaction path for the formation of *cis* complex **5a**.

 © 2013 Wiley-VCH Verlag GmbH & Co. KGaA, Weinheim

Thermally induced isomerization: In order to test the propensity of our complexes to undergo thermally induced isomerization,[39e,44] thermogravimetric analysis (TGA) and differential scanning calorimetry (DSC) measurements were carried out on complexes **5a** and **5b** (Figures S14–S16 in the Supporting Information). The data from these measurements revealed the isomerization to progress at high temperatures around 200 °C and, based on these experiments, we were also able to obtain an isomerization enthalpy ΔH_{isom} of $-4.5\ kcal\,mol^{-1}$ by using $RbNO_3$ as a calibration standard (Figure S17 in the Supporting Information). This value is in good accordance with the relative thermodynamic stability of the *trans* isomer **5b** over the *cis* isomer **5a**, estimated as $-6.0\ kcal\,mol^{-1}$ by DFT calculations (see the Supporting Information).

The results from the DSC studies were further verified by heating the neat complex **5a** in a J. Young NMR tube at 200 °C for 6 h under an inert atmosphere. The black-brown residue obtained after the reaction was chromatographed on silica gel to obtain a colorless product, which was confirmed as the *trans* complex **5b** based on ^1H NMR studies. The yield of **5b** was found to be 64 %. Investigation of one of the fractions collected during chromatography showed it to contain a trace amount of diphenylbutadiyne (confirmed on the basis of GC-MS analysis). Although one could attribute the formation of this molecule to reductive elimination from the *cis* complex, it still does not entirely clarify the conversion process. Previous mechanistic studies on platinum complexes bearing phosphine or pyridine ligands have suggested that *cis–trans* isomerization either proceeds by a dissociative mechanism that involves loss of the phosphine, pyridine, or halide ligands leading to a three-coordinate T-shaped complex intermediate, or by an associative mechanism that involves coordination of the phosphine or pyridine ligand leading to a five-coordinate intermediate.[45] We found that the conversion of complex **5a** to **5b** proceeded efficiently when **5a** was heated in [D_8]toluene at 200 °C for 2 days in a J. Young NMR tube to give an isolated yield of 73 %. The reaction was found to proceed more slowly than that carried out in the neat solid. Performing the reaction in the presence of the free carbene ligand and *t*BuOK neither accelerated nor retarded formation of the product.

Furthermore, when complex **5a** was heated in the presence of the carbene ligand IBIM and *t*BuOK, no incorporation of IBIM in the final *trans* product was found. This observation disfavors dissociation of the carbene ligand during the isomerization process and is consistent with the theoretical study since the calculated carbene dissociation enthalpy was as high as $54.6\ kcal\,mol^{-1}$ (see the Supporting Information). Considering the temperature at which the reaction was performed, such dissociation can be ruled out. The observation of a small amount of diphenylbutadiyne, as mentioned above, may be attributed to reductive elimination of the alkyne ligands from the *cis* complex. This would generate the corresponding biscarbene Pt^0 complex, which is isolobal with a carbene ligand. The in situ generated small amount of Pt^0 complex could then associate with a molecule of the four-coordinate *cis* complex to form a pentacoordinate complex stabilized through a Pt^0–Pt^{II} interaction. This could then undergo pseudorotation, resulting in expulsion of the Pt^0 complex and leading to formation of the desired *trans* Pt^{II} complex. Acting like a catalyst, the Pt^0 complex could coordinate to another *cis* complex and could repeat the same process over and over again to transform all of the *cis* complex into the corresponding *trans* complex. In this way, the Pt^0 complex would only be required in catalytic amounts, which would be consistent with the small amount of diphenylbutadiyne expelled during the entire reaction and the obtained high yield of the *trans* complex. The need for such elevated temperatures for the isomerization to proceed is further corroborated by the DFT-calculated energy of activation of $34.9\ kcal\,mol^{-1}$ (see the optimized transition state in the Supporting Information) required for reductive elimination of the alkyne ligands. It is important to note that, although rare, well-defined Pt^0 species bearing carbene ligands have recently been isolated and characterized by Braunschweig and co-workers.[46] In order to further confirm our hypothesis, we performed a scrambling experiment between two *cis* complexes bearing different carbene ligands. To this end, we synthesized complex **9a** bearing the IBIM ligand instead of the DBIM ligand as in the case of complex **5a**. For comparison, complex **9b** was also synthesized and characterized separately. A 1:1 mixture of **5a** and **9a** in toluene was heated at 200 °C for 2 days, and subsequent workup gave complexes **5b** and **9b** as the major products. We were also able to isolate and characterize the new complex **10**, in which both IBIM and DBIM are ligated to the Pt^{II} center. The structure of **10** was confirmed by various NMR and MS studies. The formation of **10** is supportive of scrambling of the NHC ligand during the *cis* to *trans* conversion, although our earlier experiments suggested no dissociation of the free carbene ligand. We presume that transfer of the ligand proceeds through bridging of the carbene ligand between the two platinum centers, which could well facilitate the scrambling without the need for complete dissociation of the carbene ligand. Based on the above experimental observations, a preliminary mechanism is proposed in Scheme 3.

Conclusion

We have presented the synthesis and characterization of a new class of triplet emitter molecules based on NHC-ligated platinum(II) acetylide complexes. A viable synthetic route for a series of *cis* and *trans* complexes of the type [Pt(dbim)$_2$(C≡CR)$_2$] is reported. Although the yields of *trans* isomers obtained by a direct approach were very low, we have demonstrated that they can be significantly improved by employing different reaction conditions starting from the readily available *cis* NHC Pt^{II} acetylide complexes. Experimental and theoretical studies of the photophysical properties of the complexes have revealed very interesting luminescent properties, with two of the complexes displaying the

 © 2013 Wiley-VCH Verlag GmbH & Co. KGaA, Weinheim

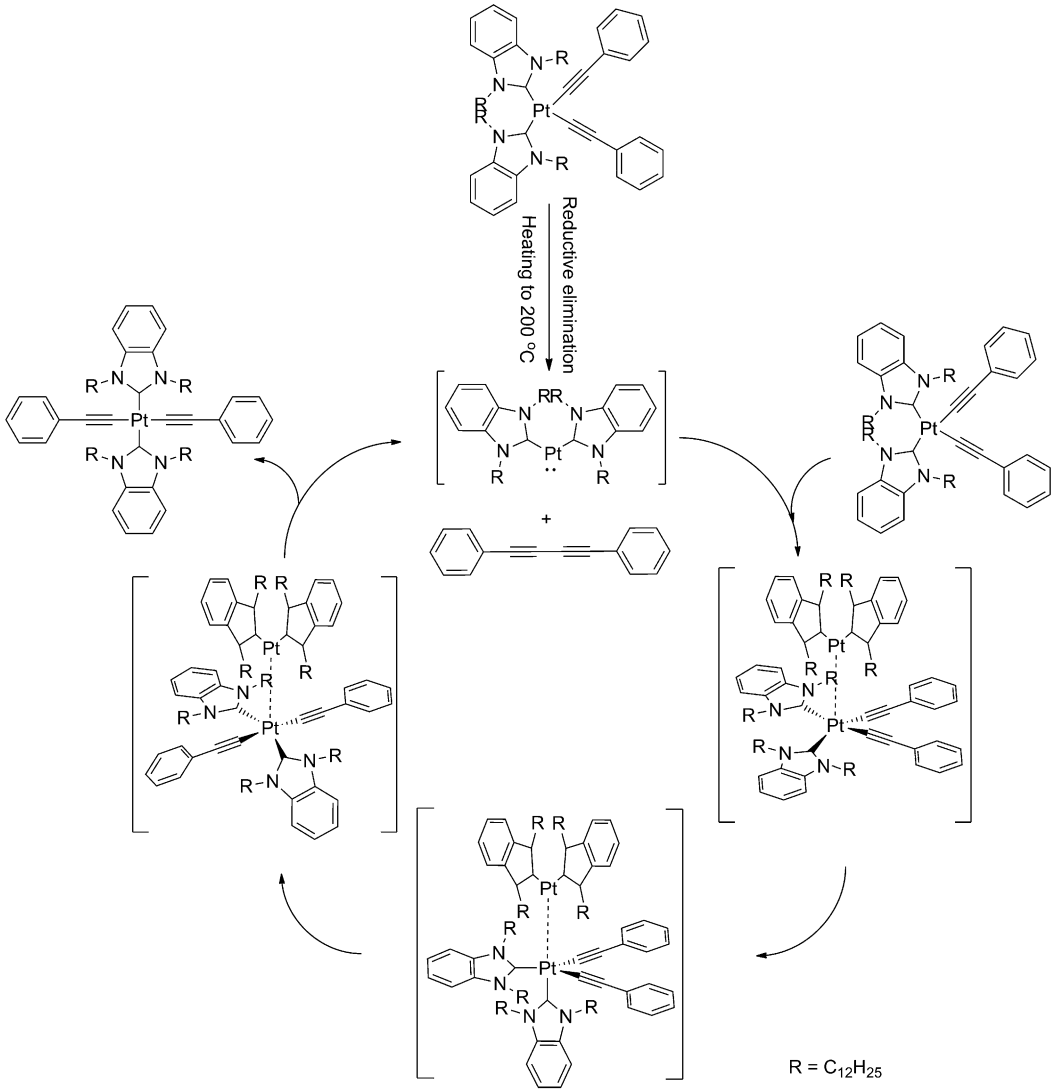

Scheme 3. Proposed isomerization path from **5a** to **5b**.

highest quantum yields hitherto reported for deep-blue emitters in the solid state. The properties of the NHC-bearing Pt^{II} acetylide complexes are very different to those of the non-emissive complex $[Pt(PBu_3)_2(C{\equiv}CC_6H_5)_2]$ and the mostly green-emitting $[Pt(diimine)_2(C{\equiv}CC_6H_5)_2]$ complexes. Experimental results coupled with DFT and TD-DFT calculations have indicated that the emission is intrinsically a mixture of metal-perturbed ^{3}IL with a small contribution from ^{3}MLCT. Close examination of the synthetic reaction revealed the *cis* complexes to be the kinetically favored isomers and the *trans* complexes to be the more thermodynamically stable isomers. Detailed investigations have been carried out with a view to improving the yield of the *trans* products. The *cis* to *trans* isomerization was found to be strongly influenced by temperature, light, and the precursor complex $[Pt(cod)(C{\equiv}CR)_2]$. Based on preliminary mechanistic studies, a solvent-stabilized Pt^{II} dialkyne complex and a bis-NHC Pt^0 species serving as a catalyst are invoked as being involved in the key transformation of the *cis* to the *trans* isomer. DSC measurements have further confirmed the *trans* isomer as the thermodynamically stable product and the isomerization enthalpy (ΔH_{isom}) was found to be 4.5 kcal mol^{-1}. The novel structural and electronic features of the presented complexes, coupled with their interesting luminescent properties in solution, at 10 wt% in PMMA films, and in the solid state, opens up new opportunities for studying a wide range of optical and electronic (or electrochemical) properties.

Acknowledgements

The authors wish to thank Prof. Heinz Berke for scientific discussions, Dr. Thomas Fox for help with NMR studies, and Dr. Ferdinand Wild for DSC and TGA measurements. Financial support from the Swiss National Science Foundation (Grant no. 200021-135488) and the University of Zürich is gratefully acknowledged.

 © 2013 Wiley-VCH Verlag GmbH & Co. KGaA, Weinheim

[1] a) M. E. Thompson, *MRS Bull.* **2007**, *32*, 694; b) W.-Y. Wong, P. D. Parvey, *Macromol. Rapid Commun.* **2010**, *31*, 671; c) H. Yersin, A. F. Rausch, R. Czerwieniec, T. Hofbeck, T. Fischer, *Coord. Chem. Rev.* **2011**, *255*, 2622; d) Y. Unger, D. Meyer, O. Molt, C. Schildknecht, I. Münster, G. Wagenblast, T. Strassner, *Angew. Chem.* **2010**, *122*, 10412; *Angew. Chem. Int. Ed.* **2010**, *49*, 10214; e) K. Li, G. Cheng, C. Ma, X. Guan, W.-M. Kwok, Y. Chen, W. Lu, C.-M. Che, *Chem. Sci.* **2013**, *4*, 2630; f) Z. M. Hudson, C. Sun, M. G. Helander, Y.-L. Chang, Z.-H. Lu, S. Wang, *J. Am. Chem. Soc.* **2012**, *134*, 13930; g) H.-F. Xiang, S.-W. Lai, P. T. Lai, C.-M. Che in *Highly Efficient OLEDs with Phosphorescent Materials* (Ed.: H. Yersin), Wiley-VCH, Weinheim, **2008**, pp. 259; h) J. A. G. Williams, *Topics in Current Chemistry, Vol. 281, Photochemistry and Photophysics of Coordination Compounds: Platinum*, Springer, Heidelberg, **2007**; i) Y. Chi, P.-T. Chou, *Chem. Soc. Rev.* **2010**, *39*, 638; j) S.-Y. Chang, J.-L. Chen, Y. Chi, Y.-M. Cheng, G.-H. Lee, C.-M. Jiang, P.-T. Chou, *Inorg. Chem.* **2007**, *46*, 11202; k) H. Yersin, W. Finkenzeller in *Highly Efficient OLEDs with Phosphorescent Materials* (Ed.: H. Yersin), Wiley-VCH, Weinheim, **2008**, p. 15.

[2] a) S. W. Thomas, K. Venkatesan, P. Müller, T. M. Swager, *J. Am. Chem. Soc.* **2006**, *128*, 16641; b) Z. M. Hudson, C. Sun, K. J. Harris, B. E. G. Lucier, R. W. Schurko, S. Wang, *Inorg. Chem.* **2011**, *50*, 3447; c) C.-S. Lee, R. R. Zhuang, S. Sabiah, J.-C. Wang, W.-S. Hwang, I. J. B. Lin, *Organometallics* **2011**, *30*, 3897; d) Q.-Z. Yang, L.-Z. Wu, H. Zhang, B. Chen, Z.-X. Wu, L.-P. Zhang, C.-H. Tung, *Inorg. Chem.* **2004**, *43*, 5195; e) L.-Y. Zhang, L.-J. Xu, X. Zhang, J.-Y. Wang, J. Li, Z.-N. Chen, *Inorg. Chem.* **2013**, *52*, 5167.

[3] a) R. Zieba, C. Desroches, F. Chaput, M. Carlsson, B. Eliasson, C. Lopes, M. Lindgren, S. Parola, *Adv. Funct. Mater.* **2009**, *19*, 235; b) C. K. M. Chan, C.-H. Tao, H.-L. Tam, N. Zhu, V. W.-W. Yam, K.-W. Cheah, *Inorg. Chem.* **2009**, *48*, 2855; c) C. K. M. Chan, C.-H. Tao, K.-F. Li, K. M.-C. Wong, N. Zhu, K.-W. Cheah, V. W.-W. Yam, *Dalton Trans.* **2011**, *40*, 10670; d) R. Liu, A. Azenkeng, D. Zhou, Y. Li, K. D. Glusac, W. Sun, *J. Phys. Chem. A* **2013**, *117*, 1907.

[4] a) P. Du, J. Schneider, P. Jarosz, R. Eisenberg, *J. Am. Chem. Soc.* **2006**, *128*, 7726; b) X. Wang, S. B. Goeb, Z. Ji, N. A. Pogulaichenko, F. N. Castellano, *Inorg. Chem.* **2011**, *50*, 705; c) M. N. Roberts, J. K. Nagle, M. B. Majewski, J. G. Finden, N. R. Branda, M. O. Wolf, *Inorg. Chem.* **2011**, *50*, 4956.

[5] a) G.-J. Zhou, W.-Y. Wong, *Chem. Soc. Rev.* **2011**, *40*, 2541; b) F. Guo, W. Sun, Y. Liu, K. Schanze, *Inorg. Chem.* **2005**, *44*, 4055.

[6] a) M. J. Currie, J. K. Mapel, T. D. Heidel, S. Goffri, M. A. Baldo, *Science* **2008**, *321*, 226; b) W. Wu, J. Zhang, H. Yang, B. Jin, Y. Hu, J. Hua, C. Jing, Y. Long, H. Tian, *J. Mater. Chem.* **2012**, *22*, 5382; c) W.-Y. Wong, C.-L. Ho, *Acc. Chem. Res.* **2010**, *43*, 1246.

[7] M. Montalti, A. Credi, L. Prodi, M. T. Gandolfi, *Handbook of Photochemistry*, 3rd ed., Taylor & Francis Group, Boca Raton, **2006**.

[8] a) M. L. Muro, A. A. Rachfor, X. Wang, F. N. Castellano in *Topics in Organometallic Chemistry, Vol. 29, Photophysics of Organometallics* (Ed.: A. J. Lees), Springer Verlag, Berlin, **2010**, p. 159; b) V. W.-W. Yam, *Acc. Chem. Res.* **2002**, *35*, 555; c) T. Sajoto, P. I. Djurovich, A. Tamayo, M. Yousufuddin, R. Bau, M. E. Thompson, R. J. Holmes, S. R. Forrest, *Inorg. Chem.* **2005**, *44*, 7992.

[9] J. Chatt, B. L. Shaw, *J. Chem. Soc.* **1959**, 4020.

[10] a) M. N. Roberts, C.-J. Carling, J. K. Nagle, N. R. Branda, M. O. Wolf, *J. Am. Chem. Soc.* **2009**, *131*, 16644; b) G. Ramakrishna, T. Goodson, J. E. Rogers-Haley, T. M. Cooper, D. G. McLean, A. Urbas, *J. Phys. Chem. C* **2009**, *113*, 1060; c) K. Haskins-Glusac, I. Ghiviriga, K. A. Abboud, K. S. Schanze, *J. Phys. Chem. B* **2004**, *108*, 4969.

[11] a) K. Glusac, M. E. Köse, H. Jiang, K. S. Schanze, *J. Phys. Chem. B* **2007**, *111*, 929; b) T. Cardolaccia, Y. Li, K. S. Schanze, *J. Am. Chem. Soc.* **2008**, *130*, 2535; c) J. Stahl, J. C. Bohling, T. B. Peters, L. D. Quadras, J. A. Gladysz, *Pure Appl. Chem.* **2008**, *80*, 459; d) Q. Zheng, J. C. Bohling, T. B. Peters, A. C. Frisch, F. Hampel, J. A. Gladysz, *Chem. Eur. J.* **2006**, *12*, 6486; e) Y. Liu, S. Jiang, K. Glusac, D. H. Powell, D. F. Anderson, K. S. Schanze, *J. Am. Chem. Soc.* **2002**, *124*, 12412.

[12] C.-H. Tao, N. Zhu, V. W.-W. Yam, *Chem. Eur. J.* **2005**, *11*, 1647.

[13] a) W.-Y. Wong, C.-K. Wong, G.-L. Lu, A. W.-M. Lee, K.-W. Cheah, J.-X. Shi, *Macromolecules* **2003**, *36*, 983; b) K. Sonogashira, S. Takahashi, N. Hagihara, *Macromolecules* **1977**, *10*, 879; c) K. A. Williams, A. J. Boydston, C. W. Bielawski, *Chem. Soc. Rev.* **2007**, *36*, 729.

[14] C.-W. Chan, L.-K. Cheng, C.-M. Che, *Coord. Chem. Rev.* **1994**, *132*, 87.

[15] a) M. Hissler, W. B. Connick, D. K. Geiger, J. E. McGarrah, D. Lipa, R. J. Lachicotte, R. Eisenberg, *Inorg. Chem.* **2000**, *39*, 447; b) J. E. McGarrah, R. Eisenberg, *Inorg. Chem.* **2003**, *42*, 4355; c) T. J. Wadas, S. Chakraborty, R. J. Lachicotte, Q.-M. Wang, R. Eisenberg, *Inorg. Chem.* **2005**, *44*, 2628; d) J. Schneider, P. Du, P. Jarosz, T. Lazarides, X. Wang, W. W. Brennessel, R. Eisenberg, *Inorg. Chem.* **2009**, *48*, 4306; e) P. Jarosz, K. Lotito, J. Schneider, D. Kumaresan, R. Schmehl, R. Eisenberg, *Inorg. Chem.* **2009**, *48*, 2420; f) M. Hissler, J. E. McGarrah, W. B. Connick, D. K. Geiger, S. D. Cummings, R. Eisenberg, *Coord. Chem. Rev.* **2000**, *208*, 115.

[16] C. E. Whittle, J. A. Weinstein, M. W. George, K. S. Schanze, *Inorg. Chem.* **2001**, *40*, 4053.

[17] a) I. E. Pomestchenko, C. R. Luman, M. Hissler, R. Ziessel, F. N. Castellano, *Inorg. Chem.* **2003**, *42*, 1394; b) F. Hua, S. Kinayyigit, J. R. Cable, F. N. Castellano, *Inorg. Chem.* **2005**, *44*, 471; c) F. Hua, S. Kinayyigit, J. R. Cable, F. N. Castellano, *Inorg. Chem.* **2006**, *45*, 4304.

[18] a) W.-S. Tang, X.-X. Lu, K. M.-C. Wong, V. W.-W. Yam, *J. Mater. Chem.* **2005**, *15*, 2714; b) A. Y.-Y. Tam, W. H. Lam, K. M.-C. Wong, N. Zhu, V. W.-W. Yam, *Chem. Eur. J.* **2008**, *14*, 4562.

[19] a) V. W.-W. Yam, K. M.-C. Wong, N. Zhu, *J. Am. Chem. Soc.* **2002**, *124*, 6506; b) S. C. F. Kui, Y.-C. Law, G. S. M. Tong, W. Lu, M.-Y. Yuen, C.-M. Che, *Chem. Sci.* **2011**, *2*, 221; c) Q.-Z. Yang, L.-Z. Wu, Z.-X. Wu, L.-P. Zhang, C.-H. Tung, *Inorg. Chem.* **2002**, *41*, 5653; d) R. McGuire, Jr., M. C. McGuire, D. R. McMillin, *Coord. Chem. Rev.* **2010**, *254*, 2574; e) X. Han, L.-Z. Wu, G. Si, J. Pan, Q.-Z. Yang, L.-P. Zhang, C.-H. Tung, *Chem. Eur. J.* **2007**, *13*, 1231; f) H.-M. Wen, Y.-H. Wu, Y. Fan, L.-Y. Zhang, C.-N. Chen, Z.-N. Chen, *Inorg. Chem.* **2010**, *49*, 2210.

[20] a) R. Liu, Y. Li, Y. Li, H. Zhu, W. Sun, *J. Phys. Chem. A* **2010**, *114*, 12639; b) W. Lu, B.-X. Mi, M. C. W. Chan, Z. Hui, C.-M. Che, N. Zhu, S.-T. Lee, *J. Am. Chem. Soc.* **2004**, *126*, 4958; c) Z. Wang, E. Turner, V. Mahoney, S. Madakuni, T. Groy, J. Li, *Inorg. Chem.* **2010**, *49*, 11276; d) D. L. Rochester, S. Develay, S. Zalis, J. A. G. Williams, *Dalton Trans.* **2009**, 1728; e) P. Shao, Y. Li, A. Azenkeng, M. R. Hoffmann, W. Sun, *Inorg. Chem.* **2009**, *48*, 2407.

[21] S.-C. Chan, M. C. W. Chan, Y. Wang, C.-M. Che, K.-K. Cheung, N. Zhu, *Chem. Eur. J.* **2001**, *7*, 4180.

[22] S. Fernández, J. Fornies, B. Gil, J. Gomez, E. Lalinde, *Dalton Trans.* **2003**, 822.

[23] a) G. C. Vougioukalakis, R. H. Grubbs, *Chem. Rev.* **2010**, *110*, 1746; b) W. A. Herrmann, C. Köcher, *Angew. Chem.* **1997**, *109*, 2256; *Angew. Chem. Int. Ed. Engl.* **1997**, *36*, 2162; c) T. Fleetham, Z. Wang, J. Li, *Org. Electron.* **2012**, *13*, 1430.

[24] D. Bourissou, O. Guerret, F. P. Gabbaï, G. Bertrand, *Chem. Rev.* **2000**, *100*, 39.

[25] A. J. Boydston, K. A. Williams, C. W. Bielawski, *J. Am. Chem. Soc.* **2005**, *127*, 12496.

[26] a) Y. Unger, A. Zeller, S. Ahrens, T. Strassner, *Chem. Commun.* **2008**, 3263; b) Y. Unger, A. Zeller, M. A. Taige, T. Strassner, *Dalton Trans.* **2009**, 4786; c) Y. Unger, D. Meyer, T. Strassner, *Dalton Trans.* **2010**, *39*, 4295.

[27] M. Koch, J. A. Garg, O. Blacque, K. Venkatesan, *J. Organomet. Chem.* **2012**, *700*, 154.

[28] Y. Zhang, J. A. Garg, C. Michelin, T. Fox, O. Blacque, K. Venkatesan, *Inorg. Chem.* **2011**, *50*, 1220.

[29] Y. Han, H. V. Huynh, G. K. Tan, *Organometallics* **2007**, *26*, 4612.

[30] a) M. Herberhold, T. Schmalz, W. Milius, B. Wrackmeyer, *J. Organomet. Chem.* **2002**, *641*, 173; b) A. García, E. Lalinde, M. T. Moreno, *Eur. J. Inorg. Chem.* **2007**, 3553.

[31] Q.-X. Liu, F.-B. Xu, Q.-S. Li, H.-B. Song, Z.-Z. Zhang, *J. Mol. Struct.* **2004**, *697*, 131.

 © 2013 Wiley-VCH Verlag GmbH & Co. KGaA, Weinheim

[32] S. D. Adhikary, D. Bose, P. Mitra, K. D. Saha, V. Bertolasi, J. Dinda, *New J. Chem.* **2012**, *36*, 759.
[33] M. S. Khan, R. K. M. Al-Saadi, L. Male, P. R. Raithby, J. K. Bjernemose, *Acta Crystallogr. Sect. E* **2003**, *59*, m774.
[34] Gaussian 03, Revision D.01, M. J. Frisch, G. W. Trucks, H. B. Schlegel, G. E. Scuseria, M. A. Robb, J. R. Cheeseman, J. A. Montgomery, Jr., T. Vreven, K. N. Kudin, J. C. Burant, J. M. Millam, S. S. Iyengar, J. Tomasi, V. Barone, B. Mennucci, M. Cossi, G. Scalmani, N. Rega, G. A. Petersson, H. Nakatsuji, M. Hada, M. Ehara, K. Toyota, R. Fukuda, J. Hasegawa, M. Ishida, T. Nakajima, Y. Honda, O. Kitao, H. Nakai, M. Klene, X. Li, J. E. Knox, H. P. Hratchian, J. B. Cross, V. Bakken, C. Adamo, J. Jaramillo, R. Gomperts, R. E. Stratmann, O. Yazyev, A. J. Austin, R. Cammi, C. Pomelli, J. W. Ochterski, P. Y. Ayala, K. Morokuma, G. A. Voth, P. Salvador, J. J. Dannenberg, V. G. Zakrzewski, S. Dapprich, A. D. Daniels, M. C. Strain, O. Farkas, D. K. Malick, A. D. Rabuck, K. Raghavachari, J. B. Foresman, J. V. Ortiz, Q. Cui, A. G. Baboul, S. Clifford, J. Cioslowski, B. B. Stefanov, G. Liu, A. Liashenko, P. Piskorz, I. Komaromi, R. L. Martin, D. J. Fox, T. Keith, M. A. Al-Laham, C. Y. Peng, A. Nanayakkara, M. Challacombe, P. M. W. Gill, B. Johnson, W. Chen, M. W. Wong, C. Gonzalez, J. A. Pople, Gaussian, Inc., Wallingford CT, **2004**.
[35] C. Adamo, V. Barone, *J. Chem. Phys.* **1999**, *110*, 6158.
[36] T. H. Dunning, P. J. Hay in *Modern Theoretical Chemistry, Vol. 3* (Ed.: H. F. Schaefer), Plenum, New York, **1976**.
[37] R. Ditchfield, W. J. Hehre, J. A. Pople, *J. Chem. Phys.* **1971**, *54*, 724.
[38] a) J. Chatt, R. G. Wilkins, *J. Chem. Soc.* **1952**, 273; b) J. Chatt, R. G. Wilkins, *J. Chem. Soc.* **1952**, 4300.
[39] a) D. T. Rosevear, F. G. A. Stone, *J. Chem. Soc.* **1965**, 5275; b) D. A. Redfield, J. H. Nelson, *J. Am. Chem. Soc.* **1974**, *96*, 6219; c) W. J. Louw, *Inorg. Chem.* **1977**, *16*, 2147; d) R. Romeo, M. R. Plutino, L. I. Elding, *Inorg. Chem.* **1997**, *36*, 5909; e) J. H. Price, J. P. Birk, B. B. Wayland, *Inorg. Chem.* **1978**, *17*, 2245; f) J. Burgess, M. E. Howden, R. D. W. Kemmitt, N. S. Sridhara, *J. Chem. Soc. Dalton Trans.* **1978**, 1577; g) J. Vicente, A. Arcas, M.-D. Galvez-Lopez, P. G. Jones, *Organometallics* **2006**, *25*, 4247.
[40] G. K. Anderson, R. J. Cross, *Chem. Soc. Rev.* **1980**, *9*, 185, and references therein.
[41] N. Oberbeckmann, K. Merz, R. A. Fischer, *Organometallics* **2001**, *20*, 3265.
[42] The reactions of *cis* isomer **5a** with different combinations were probed by ^{1}H NMR studies involving: 1) THF, 2) [dbimH]Br, 3) [dbimH]Br and *t*BuOK, 4) KBr, 5) *t*BuOK, 6) *t*BuOH, and 7) cyclooctadiene (COD). No isomerization was detected.
[43] a) R. J. Puddephatt, P. J. Thompson, *J. Chem. Soc. Dalton Trans.* **1977**, 1219; b) C. Eaborn, K. J. Odell, A. Pidcock, *J. Chem. Soc. Dalton Trans.* **1978**, 1288.
[44] a) P. Haake, T. A. Hylton, *J. Am. Chem. Soc.* **1962**, *84*, 3774; b) R. Ellis, T. A. Weil, M. Orchin, *J. Am. Chem. Soc.* **1970**, *92*, 1078; c) J. R. Perumareddi, A. W. Adamson, *J. Phys. Chem.* **1968**, *72*, 414; d) B. Cetinkaya, E. Cetinkaya, M. F. Lappert, *J. Chem. Soc. Dalton Trans.* **1973**, 906.
[45] a) F. Yamashita, H. Kuniyasu, J. Terao, N. Kambe, *Inorg. Chem.* **2006**, *45*, 1399; b) W. Baratta, S. Stoccoro, A. Doppiu, E. Herdtweck, A. Zucca, P. Rigo, *Angew. Chem.* **2003**, *115*, 109; *Angew. Chem. Int. Ed.* **2003**, *42*, 105; c) E. Guido, G. D'Amico, N. Russo, E. Sicilia, S. Rizzato, A. Albinati, A. Romeo, M. R. Plutino, R. Romeo, *Inorg. Chem.* **2011**, *50*, 2224; d) S. Fantasia, H. Jacobsen, L. Cavallo, S. P. Nolan, *Organometallics* **2007**, *26*, 3286.
[46] J. Bauer, H. Braunschweig, P. Brenner, K. Kraft, K. Radacki, K. Schwab, *Chem. Eur. J.* **2010**, *16*, 11985.

Received: June 10, 2013
Revised: July 25, 2013
Published online: September 25, 2013

 © 2013 Wiley-VCH Verlag GmbH & Co. KGaA, Weinheim

CHEMISTRY
A EUROPEAN JOURNAL

Supporting Information

© Copyright Wiley-VCH Verlag GmbH & Co. KGaA, 69451 Weinheim, 2013

Highly Efficient Deep-Blue Emitters Based on *cis* and *trans* N-Heterocyclic Carbene Pt^{II} Acetylide Complexes: Synthesis, Photophysical Properties, and Mechanistic Studies

Yuzhen Zhang, Olivier Blacque, and Koushik Venkatesan*[a]

chem_201302196_sm_miscellaneous_information.pdf

Table of Contents

1. EXPERIMENTAL SECTION

1.1 General. All manipulations requiring inert atmosphere were carried out using standard schlenk techniques under dinitrogen. ^{1}H, $^{13}C\{1H\}$ and ^{19}F NMR spectra were recorded on Bruker AV2-300 (300 MHz), AV2-400 (400 MHz) or AV-500 (500 MHz) spectrometers. Chemical shifts (δ) are reported in parts per million (ppm) referenced to tetramethylsilane (δ 0.00) ppm using the residual protio solvent peaks as internal standards (^{1}H NMR experiments) or the characteristic resonances of the solvent nuclei (^{13}C NMR experiments). ^{19}F NMR was referenced to $CFCl_3$(δ 0.00) ppm. Coupling constants (*J*) are quoted in Hertz (Hz) and the following abbreviations are used to describe the signal multiplicities: s (singlet); d (doublet); t (triplet); q (quartet); m (multiplet); dm (doublet of multiplet). Proton and carbon assignments have been made using routine one and two dimensional NMR spectroscopies where appropriate. Infra-red (IR) spectra were recorded on a Perkin-Elmer 1600 Fourier Transform spectrophotometer using KBr pellet with frequencies (ν_{max}) quoted in wavenumbers (cm^{-1}). Elemental microanalysis was carried out with Leco CHNS-932 analyzer. Mass spectra were run on a Finnigan-MAT-8400 mass spectrometer. TLC analysis was performed on precoated Merck Silica Gel60F254 slides and visualized by luminescence quenching either at (short wavelength) 254 nm or (long wavelength) 365 nm. Chromatographic purification of products was performed on a short column (Length 15.0 cm: diameter 1.5 cm) using silica gel 60, 230–400 mesh using a forced flow of eluent. UV-Vis measurements were carried out on a Perkin-Elmer Lambda 19 UV/VIS spectrophotometer. Emission spectra were acquired on Perkin Elmer spectrophotometer using 450W Xenon lamp excitation by exciting at the longest-wavelength absorption maxima with the excitation slit width 5 nm and emission slit width 10 nm. All samples for emission spectra were degassed by at least three freeze-pump-thaw cycles in an anaerobic curette and were pressurized with N_2 following each cycle. 77 K emission spectra were acquired in frozen 2-methyltetrahydrofuran (2-MeTHF) glass. Luminescence quantum yields of ϕ was determined at 298 K (estimated uncertainty ± 15%) using standard methods, wavelength-integrated intensities (I) of the corrected emission spectra was compared to iso-absorptive spectra of quinine sulfate standard (ϕ_{ref} = 0.55 in 1N H_2SO_4 air-equilibrated solution) and was corrected for solvent refractive index.[1] The emission quantum yield was calculated by eqs. 1

$$\phi_x = (A_s/A_x)\,(F_x/F_s)\,(n_x/n_s)^2\,\phi_s \qquad (1)$$

where ϕ is the phosphorescent quantum yield, *A* is absorbance at excitation wavelength, *F* is the area under the corrected emission curve (expressed in number of photons), and *n* is the refractive index of the solvents used. Subscripts x and s refer to the sample and reference standard solution, respectively. Phosphorescence lifetimes were measured by time-correlate single-photon counting method (TCSPC) performed on an Edinburgh FLS920 spectrophotometer, using nF900 lamp source at 30 000 Hz frequency with 15 nm excitation and 15 nm emission slit widths. Absolute quantum yields were measured in the solid-state using an integrating sphere from Edinburgh Instruments. YAG:Ce (powder) was used as a calibration reference with ϕ = 97%. Thermo gravimetric analysis (TGA) and differential scanning calorimetry (DSC) were done using a NETZSCHSTA 449C instrument and a sample with known heat of fusion ($RbNO_3$; ΔH = 26.6 J/g). Cyclic voltammograms

(CV) were obtained with BAS 100 W voltammetric analyzer. The radiative and nonradiative rate constants were calculated using eqs. 2 and 3, respectively.[2]

$k_r = \phi_o \tau_o^{-1}$ (2)

$k_{nr} = k_r(\phi_0^{-1} - 1)$ (3)

k_r : nonradiative rat constant

k_{nr}: radiative rat constant

ϕ_o: luminescence quantum yield

τ_o: lifetime

All starting materials were purchased from commercial sources and used as received unless stated otherwise. The solvents used for synthesis were of analytical grade. The compounds 2, 3, 4-trimethoxyphenylacetylene,[3] 2-ethynylthiophene,[4] 4-(phenylethynyl)phenylacetylene,[5] [dbimH]Br (N,N'-diisopropyl-benzimidazolium bromide) and [ibimH]Br (N,N'-didodecyl-benzimidazolium bromide) and were prepared according to literature methods.[6]

1.2 [dbimH]Br. A mixture of benzimidazole (4.72 g, 40 mmol) and K_2CO_3 (6.08 g, 44 mmol) was suspended in CH_3CN (12 mL) and stirred at ambient temperature for 1 h. To the suspension was added dodecyl bromide (29.9 g, 120 mmol). The reaction mixture was stirred under reflux conditions for 24 h followed by a second addition of dodecyl bromide (29.9 g, 15 mmol). Stirring under reflux continued for an additional 72 h. After removing the volatiles in vacuo, CH_2Cl_2 (50 mL) was added to extract the organic compound. After filtering, the DCM solution was evaporated and light red solid was formed. The compound was washed with EtOAc and the light pink compound was formed (17.1 g, 80%). ^{1}H NMR (400 MHz, CD_2Cl_2, 25 ^{o}C): δ (ppm) = 11.50 (s, 1H, NC*H*N), 7.67 (d, 2H, phenyl), 7.63 (t, 2H, phenyl), 4.57 (t, 4H, ^3J = 8.0 Hz, NCH_2). 2.02 (m, 4H, NCH_2CH_2), 1.42 (m, 8H, $NCH_2CH_2CH_2CH_2$), 1.32 (m, 28H, $(CH_2)CH_3$), 0.83 (t, 6H, ^3J = 8.0 Hz, CH_3). ^{13}C{^{1}H} NMR (100.6 MHz, CD_2Cl_2, 25^{o}C): δ (ppm) = 143.40, (s, N*C*N), 131.94, 127.38, 113.57 (phenyl), 48.03, 32.39, 30.10, 29.89, 29.80, 29.70, 29.64, 29.54, 27.00, 23.16, 14.35. IR (ATR, cm^{-1}): 2919, 2850, 1560, 1466, 1425, 776, 721.

1.3 General Procedure for the synthesis of precursor complexes 1-3. A suspension of [Pt(COD)Cl_2] (374.0 mg, 1 mmol) in ethanol was maintained at 0 ^{o}C under nitrogen atmosphere, then a freshly prepared mixture of [HC≡C-R] (2.0 mmol) and sodium ethoxide (prepared from sodium (50.6 mg, 2.2 mmol) and ethanol) in ethanol (15 mL) was added dropwise with constant stirring. A light yellow solid was obtained after 1 h. The yellow solid was filtered and dried. The crude product was purified by column chromatography on silica gel with a suitable eluent. The product obtained was further washed with acetone.

[Pt(COD)(C≡C-$C_6H_4F)_2$] **1**. Yield: 409 mg, 71%. ^{1}H NMR (500 MHz, CD_2Cl_2, 25 ^{o}C): δ (ppm) = 7.33 (t, 4H, ^3J = 10.0 Hz, *o*-phenyl), 6.95 (t, 4H, ^3J = 10.0 Hz, *m*-phenyl), 5.64 (t, 4H, ^3J = 20.0 Hz, =C*H*, COD), 2.57 (s, 8H, -CH_2, COD). ^{13}C{^{1}H} NMR (125.8 MHz, CD_2Cl_2, 25^{o}C): δ (ppm) = 161.1 (d, $^1J_{F-C}$ = 245.0 Hz, C_6H_4F), 133.8, 123.1, 115.6 (d, $^3J_{F-C}$ = 7.6 Hz, $^4J_{F-C}$ = 2.5 Hz, $^2J_{F-C}$ = 22.5 Hz, C_6H_4), 108.8 (s, Pt-C≡C), 105.3 (t, $^1J_{Pt-C}$ = 76.2 Hz, C on COD), 95.6 (s, Pt-C≡*C*), 30.9

(s, C on COD). ^{19}F NMR (188.3 MHz, CD_2Cl_2, 25 ^oC), δ (ppm) = -115.4. ESI-MS *m/z*: 540.2 $[M]^+$ (M = $C_{24}H_{20}F_2Pt$). IR (ATR, cm^{-1}) $\tilde{\nu}_{C\equiv C}$ = 2126. Elemental analysis calcd (%) for $C_{24}H_{20}F_2Pt$: C 53.23, H 3.72; found: C 52.99, H 3.76.

[Pt(COD)(C≡C-$C_6H_2(OCH_3)_3)_2$] **2**. Yield: 520 mg, 77%. ^{1}H NMR (500 MHz, CD_2Cl_2, 25 ^oC): δ (ppm) = 6.60 (s, 4H, *o*-phenyl), 5.65 (t, 4H, ^3J = 25.0 Hz, =C*H*, COD), 3.80 (d, 12H, ^2J = 5.0 Hz, *m*-OCH_3), 3.74 (d, 6H, ^2J = 5.0 Hz, *p*-OCH_3), 2.58 (s, 8H, -CH_2, COD). ^{13}C{^{1}H} NMR (125.8 MHz, CD_2Cl_2, 25 ^oC): δ (ppm) = 153.5, 138.1, 122.0, 109.3 (C_6H_4), 108.3 (s, Pt-*C*≡C), 105.3 (t, $^1J_{Pt\text{-}C}$ = 80.0 Hz, C on COD), 95.0 (s, Pt-C≡*C*), 61.1 (s, *p*-O*C*H_3), 56.5 (s, *m*-O*C*H_3), 30.9 (s, C on COD). ESI-MS *m/z*: 708.2 $[M + Na]^+$ (M = $C_{30}H_{34}O_6Pt$). IR (ATR, cm^{-1}) $\tilde{\nu}_{C\equiv C}$ = 2131.

[Pt(COD)(C≡C-2-thienyl)$_2$] **3**. Yield: 120 mg, 28%. ^{1}H NMR (500 MHz, CD_2Cl_2, 25 ^oC): δ (ppm) = 7.13, 7.03, 6.92 (s, 6H, C_4H_3S), 5.67 (s, 4H, C*H*, COD), 2.57 (s, 8H, CH_2, COD). ^{13}C{^{1}H} NMR (125.8 MHz, CD_2Cl_2, 25 ^oC): δ (ppm) = 130.7, 129.1, 127.2, 125.7 (s, C_4H_3S), 105.5 (t, $^1J_{Pt\text{-}C}$ = 76.2 Hz, C on COD), 101.1 (s, Pt-*C*≡C), 100.0 (s, Pt-C≡*C*), 30.9 (s, C on COD). IR (ATR, cm^{-1}) $\tilde{\nu}_{C\equiv C}$ = 2117. Elemental analysis calcd (%) for $C_{20}H_{18}PtS_2$: C 46.41, H 3.51, found: C 46.09, H 3.31.

1.4 General procedure for the synthesis of *cis* complexes 4a-8a and 9a. All manipulations were performed under N_2 atmosphere. 3 equiv. of [dbimH]Br ([ibimH]Br for **9a**), 3 equiv. of *t*-BuOK and 1 equiv. of [Pt(COD)(C≡C-$R)_2$] were dissolved in dry THF (15 mL). The reaction mixture was stirred under reflux condition (75 ^oC) for 12-16 h. After the reaction mixture was allowed to cool down to room temperature H_2O (10 mL) was added. The product was extracted with CH_2Cl_2 (3 × 15 mL) and the organic layer was separated and dried over $MgSO_4$. The solvent was evaporated to dryness in vacuo and the compound was purified by column chromatography over silica gel.

cis-[Pt(dbim)$_2$(C≡C-$C_6H_4F)_2$] **4a**. Reflux time 14 h. A light red compound was obtained. EtOAc/ CH_2Cl_2/ Hexane (4:4:92 v/v/v) was used as the eluent. Yield: 150 mg, 86%. ^{1}H NMR (500 MHz, CD_2Cl_2, 25 ^oC): δ (ppm) = 7.36 (q, 4H, ^3J = 3.0 Hz, H on benzimidazole), 7.25 (q, 4H, ^3J = 3.0 Hz, H on benzimidazole), 7.20 (m, 4H, *o*-phenyl), 6.82 (m, 4H, *m*-phenyl), 4.83 (m, 4H, NC*H*HCH_2), 4.32 (m, 4H, NCH*H*CH_2), 2.13 (m, 4H, NCH_2CHHCH_2), 1.64 (m, 4H, NCH_2CHHCH_2), 1.46 (m, 4H, $NCH_2CH_2CHHCH_2$), 1.39 (m, 4H, $NCH_2CH_2CHHCH_2$), 1.30 (m, 64H, $CH_2(CH_2)_8CH_3$), 0.87 (m, 12H, CH_2CH_3). ^{13}C{^{1}H} NMR (125.8 MHz, CD_2Cl_2, 25 ^oC): δ (ppm) = 180.1 (*C*=Pt), 161.7 (d, $^1J_{F\text{-}C}$ = 242.0 Hz), 134.6 (s, C *p*-phenyl), 132.8 (d, $^2J_{F\text{-}C}$ = 7.8 Hz, *m*-phenyl), 125.5 (C on benzimidazole without H), 123.1, 111.2 (C on benzimidazole with H), 114.7 (d, $^3J_{F\text{-}C}$ = 21.4 Hz, *o*-phenyl), 105.5 (C≡*C*-Pt), 104.4 (*C*≡C-Pt), 49.1 (NCH_2CH_2), 32.3, 30.1, 30.0, 29.9, 29.7, 29.5, 27.6, 23.1 (C on $(CH_2)_{10}CH_3$), 14.3 (CH_3). ^{19}F NMR (188.3 MHz, CD_2Cl_2, 25 ^oC): δ (ppm) = -119.3. ESI-MS *m/z*: 1366.0 $[M + Na]^+$ (M = $C_{78}H_{118}N_4PtF_2$). IR (ATR, cm^{-1}) $\tilde{\nu}_{C\equiv C}$ = 2111. Elemental analysis calcd (%) for $C_{78}H_{118}N_4PtF_2$: C 69.76, H 8.71, N 4.17; found: C 69.58, H 8.85, N 3.98.

cis-[Pt(dbim)$_2$(C≡C-$C_6H_5)_2$] **5a**. Reflux time 14 h. A colorless compound was obtained. EtOAc/ Hexane (1:49 v/v) was used as the eluent. Yield: 107 mg, 59%. ^{1}H NMR (500 MHz, CD_2Cl_2, 25 ^oC): δ (ppm) = 7.36 (q, 4H, ^3J = 5.0 Hz, H on benzimidazole), 7.23 (q, 4H, ^3J = 3.0 Hz, H on benzimidazole), 7.21 (m, 4H, *o*-phenyl), 7.10 (m, 4H, *m*-phenyl), 7.01 (t, 2H, ^3J = 5.0 Hz, *p*-phenyl), 4.83 (m, 4H, NC*H*HCH_2), 4.34 (m, 4H, NCH*H*CH_2), 2.14 (m, 4H, NCH_2CHHCH_2), 1.64 (m, 4H, NCH_2CHHCH_2), 1.49 (m, 4H, $NCH_2CH_2CHHCH_2$), 1.40 (m, 4H, $NCH_2CH_2CHHCH_2$), 1.27 (m, 64H, $CH_2(CH_2)_8CH_3$), 0.89 (m, 12H, CH_2CH_3). ^{13}C{^{1}H} NMR (125.8 MHz, CD_2Cl_2, 25 ^oC): δ (ppm) = 180.5 (*C*=Pt), 134.8, 131.6, 129.5, 128.1 (C_6H_5),

125.0, 123.2, 111.4 (C on benzimidazole), 107.0 (C≡*C*-Pt), 105.4 (*C*≡C-Pt), 49.3 (N*C*H_2CH$_2$), 32.5, 30.2, 30.0, 29.9, 29.7, 27.8, 23.3 (C on -(*C*H_2)$_{10}$CH$_3$), 14.5 (*C*H$_3$). ESI-MS *m/z*: 1330.0 [M + Na]$^+$ (M = $C_{78}H_{116}N_4Pt$). IR (ATR, cm^{-1}) $\tilde{\nu}_{C\equiv C}$ = 2116. Elemental analysis calcd (%) for $C_{78}H_{116}N_4Pt$: C 71.68, H 9.10, N 4.29; found: C 71.35, H 9.11, N 4.10.

cis-[Pt(dbim)$_2$(C≡C-C_6H_2(OCH$_3$)$_3$)$_2$] **6a**. Reflux time 15 h. A white compound was obtained. EtOAc/ CH_2Cl_2/ Hexane (4:1:15 v/v/v) was used as the eluent. Yield: 102 mg, 47%. ^{1}H NMR (500 MHz, CD_2Cl_2, 25 ^{o}C): δ (ppm) = 7.36 (q, 4H, ^3J = 3.0 Hz, H on benzimidazole), 7.26 (q, 4H, ^3J = 3.0 Hz, H on benzimidazole), 6.47 (m, 4H, C$_6$*H*$_2$), 4.84 (m, 4H, NC*H*HCH$_2$), 4.34 (m, 4H, NCH*H*CH$_2$), 3.86 (s, 12H, H on OC*H*$_3$), 3.57 (s, 6H, H on OC*H*$_3$), 2.16 (m, 4H, NCH$_2$C*H*HCH$_2$), 1.63 (m, 4H, NCH$_2$CH*HC*H$_2$), 1.49 (m, 4H, NCH$_2$CH$_2$C*H*HCH$_2$), 1.43 (m, 4H, NCH$_2$CH$_2$CH*H*CH$_2$), 1.26 (m, 64H, CH$_2$(C*H*$_2$)$_8$CH$_3$), 0.88 (m, 12H, CH$_2$C*H*$_3$). ^{13}C{^{1}H} NMR (125.8 MHz, CD_2Cl_2, 25 ^{o}C): δ (ppm) = 180.3 (*C*=Pt), 153.2, 136.7, 134.7, 108.7 (*C*$_6$H$_2$), 124.8, 123.3, 111.4 (C on benzimidazole), 107.1 (C≡*C*-Pt), 104.1 (*C*≡C-Pt), 60.9, 56.3 (O*C*H$_3$), 49.3 (N*C*H$_2$CH$_2$), 32.5, 30.2, 30.0, 29.9, 29.7, 27.78, 23.3 (C on (*C*H$_2$)$_{10}$CH$_3$), 14.5 (*C*H$_3$). ESI-MS *m/z*: 1510.1 [M + Na]$^+$ (M = $C_{84}H_{130}N_4O_6Pt$). IR (ATR, cm^{-1}) $\tilde{\nu}_{C\equiv C}$ = 2100. Elemental analysis calc for $C_{84}H_{130}N_4O_6Pt$: C 67.85, H 8.81, N 3.77; found: C 67.63, H 8.86, N 3.58.

cis-[Pt(dbim)$_2$(C≡C-2-thienyl)$_2$] **7a**. Reflux time 16 h. A light red compound was obtained. EtOAc/ CH_2Cl_2/ Hexane (1:26:3 v/v/v) was used as the eluent. Yield: 138 mg, 90%. ^{1}H NMR (500 MHz, CD_2Cl_2, 25 ^{o}C): δ (ppm) = 7.34 (q, 4H, ^3J = 3.0 Hz, H on benzimidazole), 7.24 (q, 4H, ^3J = 3.0 Hz, H on benzimidazole), 6.88 (m, 2H, C$_4$*H*$_3$S), 6.81 (m, 2H, C$_4$*H*$_3$S), 6.66 (m, 2H, C$_4$*H*$_3$S), 4.79 (m, 4H, NC*H*HCH$_2$), 4.29 (m, 4H, NCH*H*CH$_2$), 2.09 (m, 4H, NCH$_2$C*H*HCH$_2$), 1.60 (m, 4H, NCH$_2$CH*HC*H$_2$), 1.46 (m, 4H, NCH$_2$CH$_2$C*H*HCH$_2$), 1.37 (m, 4H, NCH$_2$CH$_2$CH*H*CH$_2$), 1.25 (m, 64H, CH$_2$(C*H*$_2$)$_8$CH$_3$), 0.74 (m, 12H, CH$_2$C*H*$_3$). ^{13}C{^{1}H} NMR (125.8 MHz, CD_2Cl_2, 25 ^{o}C): δ (ppm) = 179.6 (*C*=Pt), 134.8, 130.3, 128.0, 126.7 (*C*$_4$H$_3$S), 123.3, 122.7, 111.5 (C on benzimidazole), 110.5 (C≡*C*-Pt), 98.7 (*C*≡C-Pt), 49.4 (N*C*H$_2$CH$_2$), 32.5, 30.2, 30.0, 29.9, 29.6, 27.8, 23.3 (C on (*C*H$_2$)$_{10}$CH$_3$), 14.5 (*C*H$_3$). ESI-MS *m/z*: 1341.9 [M + Na]$^+$ (M = $C_{74}H_{114}N_4PtS_2$). IR (ATR, cm^{-1}) $\tilde{\nu}_{C\equiv C}$ = 2096. Elemental analysis calcd (%) for $C_{74}H_{114}N_4PtS_2$: C 69.39, H 8.71, N 4.25; found: C 69.16, H 8.81, N 4.02.

cis-[Pt(dbim)$_2$(C≡C-C_6H_4-C≡C-C_6H_5)$_2$] **8a**. Reflux time 16 h. A light yellow compound was obtained. EtOAc/ CH_2Cl_2/ Hexane (1:2:17 v/v/v) was used as the eluent. Yield: 137 mg, 64%. ^{1}H NMR (500 MHz, CD_2Cl_2, 25^{o}C): δ (ppm) = 7.42, 7.40, 7.26, 7.25, 7.24, 7.22, 7.15, 7.14 (H on phenyl ring), 7.32 (q, 4H, ^3J = 3.0 Hz, H on benzimidazole), 7.19 (q, 4H, ^3J = 3.0 Hz, H on benzimidazole), 4.78 (m, 4H, NC*H*HCH$_2$), 4.26 (m, 4H, NCH*H*CH$_2$), 2.08 (m, 4H, NCH$_2$C*H*HCH$_2$), 1.60 (m, 4H, NCH$_2$CH*HC*H$_2$), 1.41 (m, 4H, NCH$_2$CH$_2$C*H*HCH$_2$), 1.34 (m, 4H, NCH$_2$CH$_2$CH*H*CH$_2$), 1.23 (m, 64H, CH$_2$(C*H*$_2$)$_8$CH$_3$), 0.80 (m, 12H, CH$_2$C*H*$_3$); ^{13}C{^{1}H} NMR (125.8 MHz, CD_2Cl_2, 25 ^{o}C): δ (ppm) = 180.1 (*C*=Pt), 134.8, 131.9, 131.7, 131.5, 129.8, 128.8, 128.5, 111.5 (C on phenyl ring), 124.2, 123.4, 119.5 (C on benzimidazole), 109.3 (C≡*C*-Pt), 107.3 (*C*≡C-Pt), 90.6, 90.0 (Ph-*C*≡*C*-Ph), 49.4 (N*C*H$_2$CH$_2$), 32.5, 30.2, 30.3, 30.0, 29.9, 29.6, 27.8, 23.3 (C on (*C*H$_2$)$_{10}$CH$_3$), 14.4 (*C*H$_3$). ESI-MS *m/z*: 1530.1 [M + Na]$^+$ (M = $C_{94}H_{126}N_4Pt$). IR (ATR, cm^{-1}) $\tilde{\nu}_{C\equiv C}$ = 2100.Elemental analysis calc for $C_{94}H_{126}N_4Pt$: C 74.91, H 8.43, N 3.72; found: C 74.58, H 8.19, N 3.42.

cis-[Pt(ibim)$_2$(C≡C-C_6H_5)$_2$] **9a**. Reflux time 16h. Colorless compound was obtained. Ether/ DCM/ Hexane (3:3:16 v/v/v) was used as the eluent. Yield: 88 mg, 56%. ^{1}H NMR (500 MHz, CD_2Cl_2, 25 ^{o}C): δ (ppm) = 7.54 (q, 4H, ^3J = 5.0 Hz, H on

benzimidazole), 7.17 (q, 4H, ^3J = 3.0 Hz, H on benzimidazole), 7.15 (m, 4H, *o*-phenyl), 7.05 (t, 4H,^3J= 10.0Hz, *m*-phenyl), 6.97 (t, 2H, ^3J = 5.0 Hz, *p*-phenyl), 6.03 (m, 4H, ^3J = 10.0 Hz, NC*H*$(CH_3)_2$), 1.71 (d, 12H,^3J = 10.0 Hz NCH(C$H_3)_2$), 1.31 (d, 12H, ^3J = 10.0 Hz, NCH(C$H_3)_2$). $^{13}C\{^1H\}$ NMR (125.8 MHz, CD_2Cl_2, 25 °C): δ (ppm) = 179.5 (*C*=Pt), 133.8, 131.6, 128.3, 125.1 (C on phenyl), 129.6, 122.7, 113.6 (C on benzimidazole), 106.9 (C≡*C*-Pt), 104.1 (*C*≡C-Pt), 53.6 (N*C*H(C$H_3)_2$), 21.5, 20.6 (*C*H_3). ESI-MS *m/z*: 1604.3 $[2M]^+$ (M = $C_{42}H_{46}N_4Pt$). IR (ATR, cm^{-1}) $\tilde{\nu}_{C\equiv C}$ = 2112.

1.5 General procedure for the synthesis of *trans* Complexes 4b–8b and 9b. All manipulations were performed under N_2 atmosphere. 2 equiv. of [dbimH]Br ([ibimH]Br for **9b**), 2 equiv. of *t*-BuOK, 1 equiv. of [Pt(COD)(C≡C-R)$_2$] were dissolved in dry THF (15 mL) and the reaction mixture was stirred under reflux conditions (75 °C) for 12-18 h. After allowing to cool down to room temperature, H_2O (10 mL) was added, and the product was extracted with CH_2Cl_2 (3 × 15 mL). The organic layer was separated and dried over $MgSO_4$. The solvent was evaporated to dryness in vacuo and the compound was purified by column chromatography over silica gel.

trans-[Pt(dbim)$_2$(C≡C-$C_6H_4F)_2$] **4b**. Reflux time 14 h. *cis* and *trans* isomers were separated after purification with column chromatography using Ether/ Pentane (5:95 v/v) as the eluent. Yield: *trans* 41 mg, 17%; *cis* 78 mg, 32%. ^1H NMR (500 MHz, CD_2Cl_2, 25 °C): δ (ppm) = 7.47 (q, 4H, ^3J = 3.0 Hz, H on benzimidazole), 7.30 (q, 4H, ^3J = 3.0 Hz, H on benzimidazole), 6.95 (m, 4H, *o*-phenyl), 6.71 (m, 4H, *m*-phenyl), 4.80 (m, 8H, NCH_2CH_2), 2.24 (m, 8H, $NCH_2CH_2CH_2$), 1.52 (m, 8H, $NCH_2CH_2CH_2$), 1.34 (m, 8H, $NCH_2CH_2CH_2CH_2$), 1.24 (m, 56H, $CH_2(CH_2)_7CH_3$), 0.87 (m, 12H, CH_2CH_3). $^{13}C\{^1H\}$ NMR (125.8 MHz, CD_2Cl_2, 25 °C): δ (ppm) = 182.0 (*C*=Pt), 161.7 (d, $^1J_{F\text{-}C}$ = 241.3 Hz), 135.1 (*p*-phenyl), 132.7 (d, $^2J_{F\text{-}C}$ = 8.8 Hz, *m*-phenyl), 125.8 (C on benzimidazole without H), 122.8, 111.0 (C on benzimidazole with H), 114.7 (d, $^3J_{F\text{-}C}$ = 22.5 Hz, *o*-phenyl), 105.4 (C≡*C*-Pt), 104.8 (*C*≡C-Pt), 48.9 (NCH_2CH_2), 32.5, 30.3, 30.2, 30.0, 29.9, 28.0, 23.3 (C on $(CH_2)_{10}CH_3$), 14.4 (CH_3). ^{19}F NMR (188.3 MHz, CD_2Cl_2, 25 °C): δ (ppm) = -119.6. ESI-MS *m/z*: 1342.0 $[M]^+$ (M = $C_{78}H_{118}N_4PtF_2$). IR (ATR, cm^{-1}) $\tilde{\nu}_{C\equiv C}$ = 2103. Elemental analysis calcd (%) for $C_{78}H_{118}N_4PtF_2$: C 69.76, H 8.71, N 4.17; found: C 69.90, H 8.29, N 3.82.

trans-[Pt(dbim)$_2$(C≡C-$C_6H_5)_2$] **5b**. Reflux time 14 h. *cis* and *trans* isomers were separated after purification with column chromatography using DCM/ Hexane (1:1 v/v) as the eluent. Yield: *trans* 72 mg, 27%; *cis* 24 mg, 9%. ^1H NMR (500 MHz, CD_2Cl_2, 25 °C): δ (ppm) = 7.46 (q, 4H, ^3J = 5.0 Hz, H on benzimidazole), 7.29 (q, 4H, ^3J = 3.0 Hz, H on benzimidazole), 7.00, 6.98, 6.93 (m, 10H, C_6H_5), 4.82 (m, 8H, NCH_2CH_2), 2.25 (m, 8H, $NCH_2CH_2CH_2$), 1.50 (m, 8H, $NCH_2CH_2CH_2CH_2$), 1.37 (m, 8H, $NCH_2CH_2CH_2CH_2$), 1.24 (m, 56H, $CH_2(CH_2)_7CH_3$), 0.86 (m, 12H, CH_2CH_3). $^{13}C\{^1H\}$ NMR (125.8 MHz, CD_2Cl_2, 25 °C): δ (ppm) = 180.5 (*C*=Pt), 135.1, 131.3, 129.7, 128.1 (C_6H_5), 124.7, 122.8, 111.0 (C on benzimidazole), 106.3 (C≡*C*-Pt), 106.2 (*C*≡C-Pt), 48.9 (NCH_2CH_2), 34.6, 32.5, 30.3, 30.2, 30.1, 30.028.0, 23.2, 22.9 (C on $(CH_2)_{10}CH_3$), 14.5 (CH_2CH_3). ESI-MS *m/z*: 1306.1 $[M + Na]^+$ (M = $C_{78}H_{118}N_4Pt$). IR (ATR, cm^{-1}) $\tilde{\nu}_{C\equiv C}$ = 2097. Elemental analysis calcd (%) for $C_{78}H_{118}N_4Pt$: C 71.68, H 9.10, N 4.29; found: C 71.97, H 9.06, N 4.10.

trans-[Pt(dbim)$_2$(C≡C-$C_6H_2(OCH_3)_3)_2$] **6b**. Reflux time 18 h. *cis* and *trans* isomers were separated after purification with column chromatography using EtOAc/ CH_2Cl_2/ Hexane (4:2:14 v/v/v) as the eluent. Yield: *trans* 9 mg, 4%; *cis* 90 mg, 41%. ^1H NMR (500 MHz, CD_2Cl_2, 25 °C): δ (ppm) = 7.41 (q, 4H, ^3J = 3.0 Hz, H on the benzimidazole), 7.24 (q, 4H, ^3J = 3.0 Hz,

H on benzimidazole), 6.13 (m, 4H, *o*-phenyl), 4.75 (m, 8H, NC*H*HCH$_2$), 3.55 (s, 18H, H on the OCH_3), 2.20 (m, 8H, NCH$_2$CH_2CH$_2$), 1.45 (m, 8H, NCH$_2$CH$_2$CH_2), 1.21 (m, 8H, NCH$_2$CH$_2$CH$_2$CH_2), 1.19 (m, 64H, -CH$_2$(CH_2)$_7$CH$_3$), 0.81 (m, 12H, CH$_2$CH_3). ^{13}C{^{1}H} NMR (125.8 MHz, CD_2Cl_2, 25 ^{o}C): δ (ppm) = 182.1 (*C*=Pt), 153.2, 136.7, 135.2, 108.7 (*C*$_6$H$_2$), 125.0, 122.9, 111.0 (C on benzimidazole), 106.3 (C≡*C*-Pt), 104.9 (*C*≡C-Pt), 60.9, 56.3 (O*C*H$_3$), 49.0 (N*C*H$_2$CH$_2$), 34.7, 32.5, 30.4, 30.3, 30.1, 30.0, 28.1, 28.0, 23.3 (C on (*C*H$_2$)$_{10}$CH$_3$), 14.4 (*C*H$_3$). ESI-MS *m/z*: 1510.1 [M + Na]$^+$ (M = $C_{84}H_{130}N_4O_6Pt$). IR (ATR, cm^{-1}) $\tilde{\nu}_{C\equiv C}$ = 2092. Elemental analysis calcd (%) for $C_{84}H_{130}N_4O_6Pt$: C 67.85, H 8.81, N 3.77; found: C 67.49, H 8.76, N 3.68.

trans-[Pt(dbim)$_2$(C≡C-2-thienyl)$_2$] **7b**. Reflux time 15 h. *cis* and *trans* isomers were separated after purification with column chromatography using EtOAc/ CH_2Cl_2/ Hexane (1:26:3 v/v/v) as the eluent. Yield: *trans* 58 mg, 22%; *cis* 38 mg, 15%. ^{1}H NMR (500 MHz, CD_2Cl_2, 25 ^{o}C): δ (ppm) = 7.40 (q, 4H, ^3J = 3.0 Hz, H on benzimidazole), 7.26 (q, 4H, ^3J = 3.0 Hz, H on benzimidazole), 6.75 (d, 2H, ^3J = 5.0 Hz, C$_4H_3$S), 6.61 (t, 2H,^3J = 5.0Hz, C$_4H_3$S), 6.56 (d, 2H,^3J = 3.0 Hz, C$_4H_3$S), 4.74 (t, 8H, ^3J = 10.0 Hz, NCH_2CH$_2$), 2.19 (m, 8H, NCH$_2$CH_2), 1.45 (m, 8H, NCH$_2$CH$_2$CH_2), 1.32 (m, 8H, NCH$_2$CH$_2$CH$_2$CH_2), 1.22 (m, 64H, CH$_2$(CH_2)$_7$CH$_3$), 0.84 (m, 12H, CH$_2$CH_3). ^{13}C{^{1}H} NMR (125.8 MHz, CD_2Cl_2, 25 ^{o}C): δ (ppm) = 180.7 (*C*=Pt), 134.4, 129.9, 126.8, 125.9 (*C*$_4$H$_3$S), 122.7, 121.8, 111.3 (C on benzimidazole), 110.6 (C≡*C*-Pt), 97.5 (*C*≡C-Pt), 48.9 (N*C*H$_2$CH$_2$), 31.9, 29.8, 29.6, 29.5, 29.0, 27.6, 22.7 (C on (*C*H$_2$)$_{10}$CH$_3$), 14.1 (*C*H$_3$). ESI-MS *m/z*: 1319.7 [M]$^+$ (M = $C_{74}H_{114}N_4PtS_2$). IR (ATR, cm^{-1}) $\tilde{\nu}_{C\equiv C}$ = 2091. Elemental analysis calcd (%) for $C_{74}H_{114}N_4PtS_2$: C 69.39, H 8.71, N 4.25; found: C 69.14, H 8.73, N 4.06.

trans-[Pt(dbim)$_2$(C≡C-C$_6$H$_4$-C≡C-C$_6$H$_5$)$_2$] **8b**. Reflux time 15 h. *cis* and *trans* isomers were separated after purification with column chromatography using Ether/ Hexane (1:7 v/v) as the eluent. Yield (based on 80 mg precursor): *trans* 10 mg, 6%; *cis* 70 mg, 42%. ^{1}H NMR (500 MHz, CD_2Cl_2, 25 ^{o}C): δ (ppm) = 7.41 (q, 4H, ^3J = 5.0 Hz, H on benzimidazole), 7.37 (q, 4H, ^3J = 5.0 Hz, H on benzimidazole), 7.25, 7.24, 7.12, 7.10, 6.90, 6.88 (H on phenyl ring), 4.82 (m, 8H, ^3J = 10.0 Hz, NCH_2CH$_2$), 2.25 (m, 8H, ^3J = 10.0 Hz, NCH$_2$CH_2CH$_2$), 1.52 (m, 8H, NCH$_2$CH$_2$CH_2), 1.38 (m, 4H, NCH$_2$CH$_2$CH$_2$CH_2), 1.24 (m, 56H, CH$_2$(CH_2)$_7$CH$_3$), 0.86 (m, 12H, CH$_2$CH_3). ^{13}C{^{1}H} NMR (100.6 MHz, CD_2Cl_2, 25 ^{o}C): δ (ppm) = 180.1 (*C*=Pt), 134.8, 131.9, 131.4, 128.9,122.9, 119.1, 111.0 (C one phenyl ring), 124.2, 123.4, 119.5 (C on benzimidazole), 108.0 (C≡*C*-Pt), 106.1 (*C*≡C-Pt), 90.6, 84.0 (Ph-*C*≡*C*-Ph), 49.4 (N*C*H$_2$CH$_2$), 32.5, 30.4, 30.3, 30.0, 29.9, 29.6, 27.8, 23.3 (C on (*C*H$_2$)$_{10}$CH$_3$), 14.4 (*C*H$_3$). ESI-MS *m/z*: 1530.4 [M + Na]$^+$ (M = $C_{94}H_{126}N_4Pt$). IR (ATR, cm^{-1}) $\tilde{\nu}_{C\equiv C}$ = 2095. Elemental analysis calcd (%) for $C_{94}H_{126}N_4Pt$: C 74.91, H 8.43, N 3.72; found: C 74.66, H 8.31, N 3.72.

trans-[Pt(ibim)$_2$(C≡C-C$_6$H$_5$)$_2$] **9b**. Reflux time 14 h. Colorless compound was obtained. Ether/ DCM/ Hexane (3:3:16 v/v/v) was used as the eluent. Yield: 21 mg, 13%. ^{1}H NMR (400 MHz, CD_2Cl_2, 25 ^{o}C): δ (ppm) = 7.71 (q, 4H, ^3J = 5.0 Hz, H on benzimidazole), 7.28 (q, 4H, ^3J = 3.0 Hz, H on benzimidazole), 7.06 (m, 4H, *o*-phenyl), 7.04 (m, 4H, *m*-phenyl), 6.98 (m, 2H, ^3J = 4.0 Hz, *p*-phenyl), 6.34 (m, 4H, ^3J = 8.0 Hz, NC*H*(CH$_3$)$_2$), 1.87 (d, 24H,^3J = 8.0 Hz, NCH(CH_3)$_2$). ^{13}C{^{1}H} NMR (125.8 MHz, CD_2Cl_2, 25 ^{o}C): δ (ppm) = 180.3 (*C*=Pt), 134.1, 131.3, 128.1, 124.6 (C on phenyl ring), 129.9, 122.2, 112.1 (C on benzimidazole), 105.9 (C≡*C*-Pt), 105.0 (*C*≡C-Pt), 53.4 (N*C*H(CH$_3$)$_2$), 21.1 (*C*H$_3$). ESI-MS *m/z*: 824.5 [M + Na]$^+$ (M = $C_{42}H_{46}N_4Pt$). IR (ATR, cm^{-1}) $\tilde{\nu}_{C\equiv C}$ = 2101.

trans-[Pt(ibim)(dbim)(C≡C-C_6H_5)$_2$] **10**. Method A: Complex **10** was obtained by heating the mixture of complexes **5a** (0.06 mmol, 78.4 mg) and **9a** (0.06 mmol, 48 mg) to 190 ^oC in toluene for 24 h. After removing the solvent, silica gel chromatography was use to isolated complexes 10. Method B: complexes **5a** and **9a** were mixed in a schlenk NMR tube and 4 mL deuterated benzene was added. The Schlenk NMR tube was sealed and exposed under UV-light for 55 min. after evaporating the solvent, checked by silica gel TLC and complexes 10 can be obtained. Ether/ Hexane (1:19 v/v) and Ether/ Hexane (2:18 v/v) were used as eluent. Yield: 5 mg. ^{1}H NMR (400 MHz, CD_2Cl_2, 25^oC): δ (ppm) = 7.67 (q, 2H, H on benzimidazole of **ibim**), 7.46 (q, 2H, H on benzimidazole of **dbim**), 7.30 (q, 2H, H on benzimidazole of **ibim**), 7.24 (q, 2H, H on benzimidazole of **dbim**), 7.01 (m, 4H, *o*-phenyl), 7.00 (m, 4H, *m*-phenyl), 6.95 (m, 2H, *p*-phenyl), 6.36 (m, 2H, NC*H*$(CH_3)_2$), 4.48 (t, 4H, ^3J = 8.0 Hz, NC$H_2(CH_2)_{10}$), 2.27 (m, 4H, $NCH_2CH_2(CH_2)_9$), 1.82 (d, 12H,^3J = 8.0 Hz, $NCH(CH_3)_2$), 1.60 (m, 4H, $NCH_2CH_2CH_2(CH_2)_8$), 1.27 (m 32H, $NCH_2CH_2CH_2(CH_2)_8$), 0.89 (t, 6H, $NCH_2(CH_2)_{10}CH_3$). ^{13}C{^{1}H} NMR (100.6 MHz, CD_2Cl_2, 25 ^oC): δ (ppm) = 183.3 (Pt=*C* of **dbim**), 180.3 (Pt=*C* of **ibim**), 130.7, 129.3, 127.5, 124.1 (C on phenyl), 134.5, 121.6, 110.2 (C on benzimidazole of **dbim**), 133.5, 122.2, 112.5 (C on benzimidazole of **ibim**), 105.6 (C≡*C*-Pt), 105.0 (*C*≡C-Pt), 53.4 (N*C*H$(CH_3)_2$ on **ibim**), 48.4 (NCH_2CH_2), 37.4, 31.9, 29.7, 29.6, 29.4, 27.5, 22.7 (C on $(CH_2)_{10}CH_3$), 20.6 (NCH(CH_3)$_2$ on **ibim**), 13.9 ($(CH_2)_{11}CH_3$). ESI-MS *m/z*: 1054.3 $[M]^+$ (M = $C_{60}H_{82}N_4Pt$).

1.6 Mechanistic reactions:

^{1}H-NMR experiments with varying ratio of NHC and precursor: Trial A: [Pt(COD)(C≡C-C_6H_5)$_2$] (10.1 mg, 0.02 mmol), **[dbimH]Br** (16.1 mg, 0.03 mmol) and *t*-BuOK (3.4 mg, 0.03 mmol) were placed in Schlenk NMR tube. THF-d_8 (0.5 mL) was then added and the reaction mixture was heated at 75 ^oC for 5 days even though the reaction was complete in 24 h (checked by ^{1}H-NMR). Trail B: [Pt(COD)(C≡C-C_6H_5)$_2$] (10.1 mg, 0.02 mmol), **[dbimH]Br** (21.4 mg, 0.04 mmol) and *t*-BuOK (4.5 mg, 0.04 mmol) were placed in Schlenk NMR tube, THF-d_8 (0.5 mL) was then added and the reaction mixture was heated at 75 ^oC for 5 days. Trial C: [Pt(COD)(C≡C-C_6H_5)$_2$] (10.1 mg, 0.02 mmol), **[dbimH]Br** (32.2 mg, 0.6 mmol) and *t*-BuOK (6.8 mg, 0.06 mmol) were placed in Schlenk NMR tube, THF-d_8 (0.5 mL) was then added and the reaction mixture was heated at 75 ^oC for 5 days.

Isomerization of 4a to 4b with stoichiometric amount [Pt(COD)(C≡C-C_6H_5)$_2$]: Complex **4a** (21.0 mg, 0.016 mmol) and **[Pt(COD)(C≡C-C_6H_5)$_2$]** (6.2 mg, 0.014 mmol) were mixed in 0.7 mL THF-d_8. After heating at 75 ^oC for 15 h, **4b** was isolated with the yield of 71% (15 mg) by column chromatography.

Isomerization of 5a to 5b with 10% [Pt(COD)(C≡C-C_6H_5)$_2$]: Complex **4a** (37.0 mg, 0.028 mmol) and **[Pt(COD)(C≡C-C_6H_5)$_2$]** (1.43 mg, 0.0027 mmol) were mixed in 1.0 mL THF-d_8. After heating at 75 ^oC for 7 days, complete conversion of **5a** to **5b** was achieved **(**probed by ^{1}H NMR). Isolated yield: 23.9 mg, 64%.

1.7 Computational details. All calculations were performed with the Gaussian 03 program package[7] using the hybrid functional PBE1PBE[8] in conjunction with the Stuttgart/Dresden effective core potentials (SDD) basis set[9] for the Pt center augmented with one *f*-polarization function (exponent = 0.993) and the standard 6-31+G(d) basis set[10] for the remaining atoms. Full geometry optimizations without symmetry constraints, but using the C_2H_5 model instead of the long $C_{12}H_{25}$ chain of the carbene, were carried out in the gas phase for the singlet ground states (S_0) and the lowest triplet excited states

(T_1). The optimized geometries were confirmed to be potential energy minima by vibrational frequency calculations at the same level of theory, as no imaginary frequency was found. The first 10 singlet-singlet and singlet-triplet transition energies were computed at the optimized S_0 geometries, by using the time-dependent DFT (TD-DFT) methodology.[11] Solvent effects were taken into account using the conductor-like polarizable continuum model (CPCM)[12] with dichloromethane (absorption/emission) or toluene (mechanistic study) as solvent for single-point calculations on all optimized gas-phase geometries.

1.8 X-ray diffraction analyses. Single-crystal X-ray diffraction data were collected at 183(2) K an Oxford Xcalibur diffractometer (4-circle kappa platform, Ruby CCD detector, and a single wavelength Enhance X-ray source with MoKa radiation, l= 0.71073 Å).[13] The selected suitable single crystals were mounted using polybutene oil on the top of a glass fiber fixed on a goniometer head and immediately transferred to the diffractometer. Pre-experiment, data collection, data reduction and analytical absorption corrections[14] were performed with the Oxford program suite *CrysAlis*^{Pro}.[15] The crystal structures were solved with SHELXS-97[15] using direct methods. The structure refinements were performed by full-matrix least-squares on F^2 with SHELXL-97.[16] All programs used during the crystal structure determination process are included in the WINGX software.[17] The program PLATON[18] was used to check the result of the X-ray analyses. For more details about the refinements, see the *refine_special_details* and *iucr_refine_instructions_details* sections in the Crystallographic Information files (Supporting Information). CCDC-916258 (for **4a**), CCDC-916259 (for **5a**), CCDC-916260 (for **5b**) and CCDC-916261 (for **9b**) contain the supplementary crystallographic data (excluding structure factors) for this paper. These data can be obtained free of charge from The Cambridge Crystallographic Data Centre via www.ccdc.cam.ac.uk/data_request/cif.

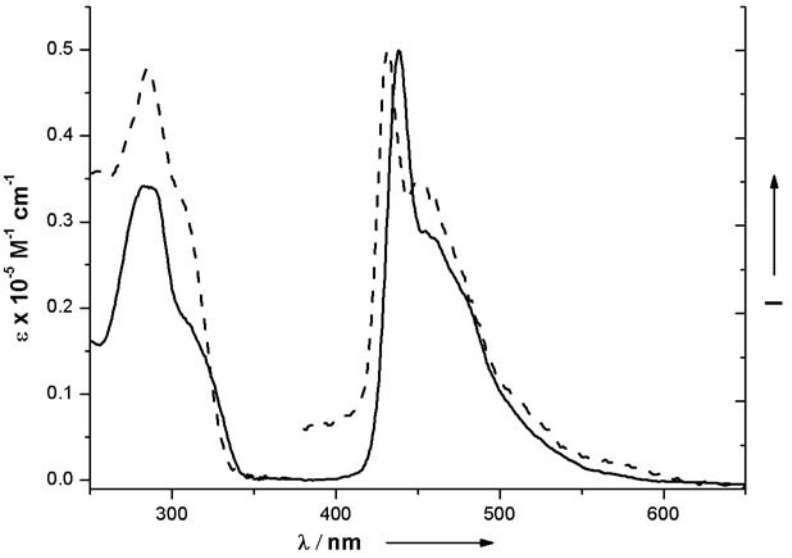

Figure S1. Electronic absorption and normalized emission spectra of **9a** (black dot), **9b** (black solid) in CH_2Cl_2 at RT.

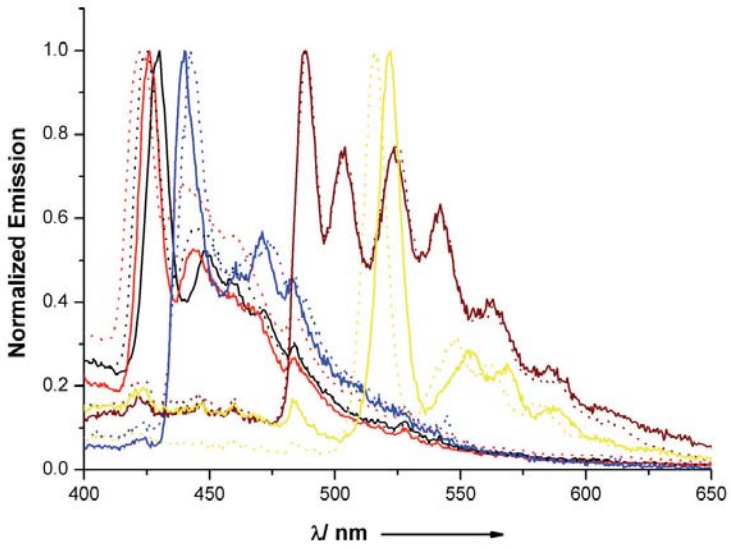

Figure S2. Emission spectra of complexes **4a** (red dot), **4b** (red solid), **5a** (black dot), **5b** (black solid), **6a** (blue dot), **6b** (blue solid), **7a** (wine dot), **7b** (wine solid), **8a** (yellow dot), **8b** (yellow solid) in 2-Me-THF at 77 K.

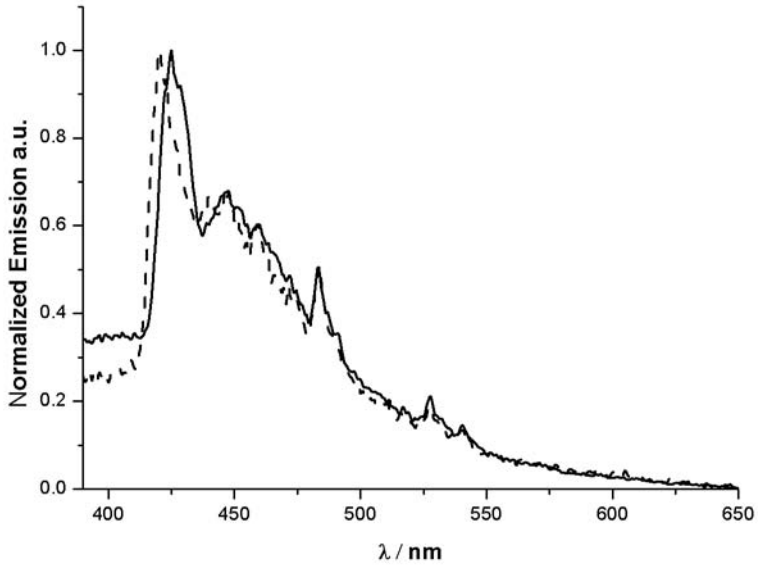

Figure S3. Emission spectra of complexes **9a** (black dot), **9b** (black solid) in 2-Me-THF at 77 K

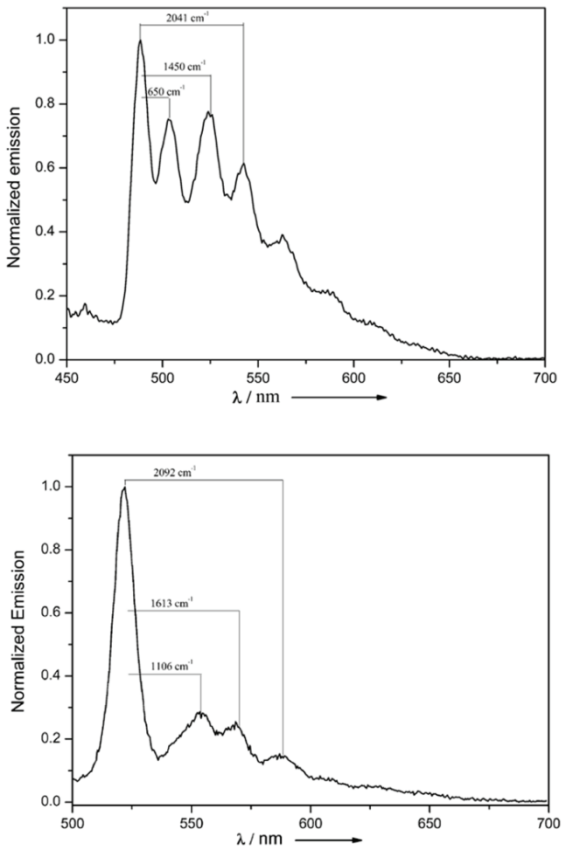

Figure S4. Emission spectra of **7a** (Top) and **8b** (Bottom) in 2-MeTHF at 77 K.

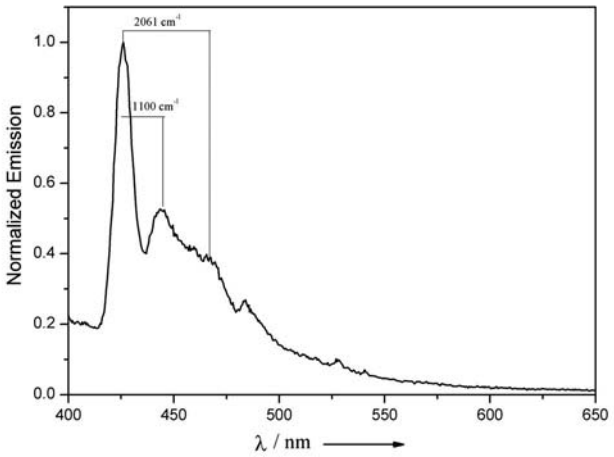

Figure S5. Emission spectra of **4b** in 2-MeTHF at 77 K.

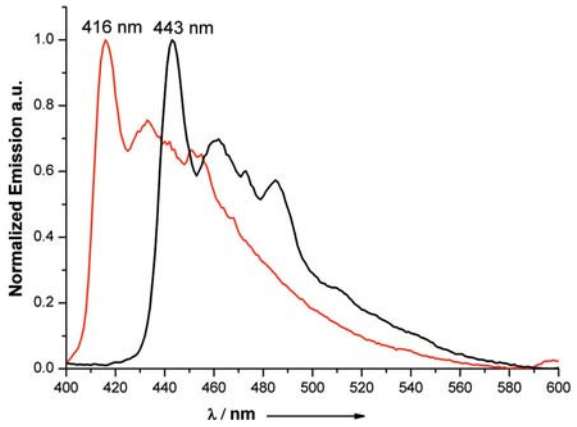

Figure S6. Solid state emission of complexes **4b** (red line) and **5b** (black line).

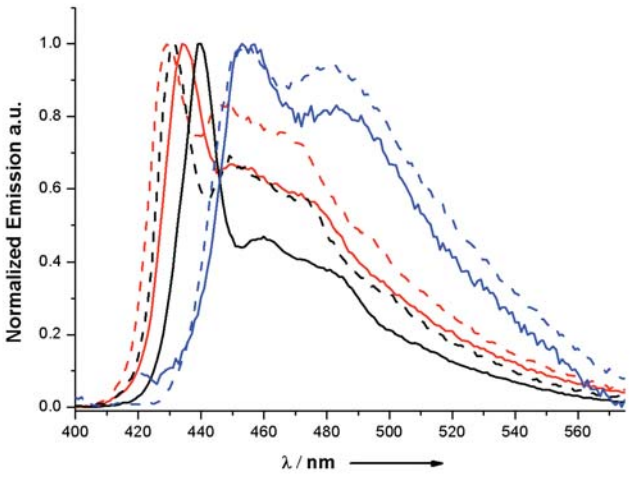

Figure S7. Normalized emission spectra of **4a** (red dot), **4b** (red solid), **5a** (black dot), **5b** (black solid), **6a** (blue dot), **6b** (blue solid) in 10% PMMA.

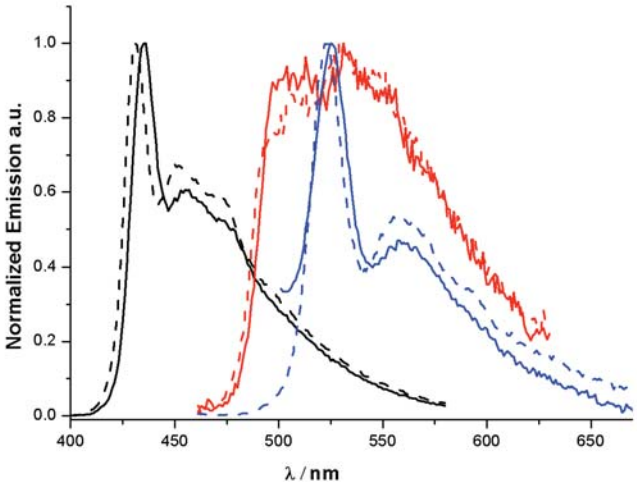

Figure S8. Normalized emission spectra of **7a** (red dot), **7b** (red solid), **8a** (blue dot), **8b** (blue solid), **9a** (black dot), **9b** (black solid) in 10% PMMA.

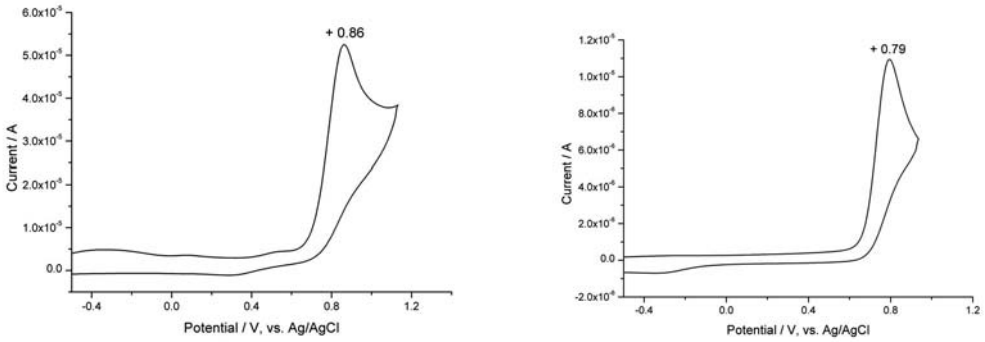

Figure S9. Cyclic voltammograms of complexes **4a** and **4b**.

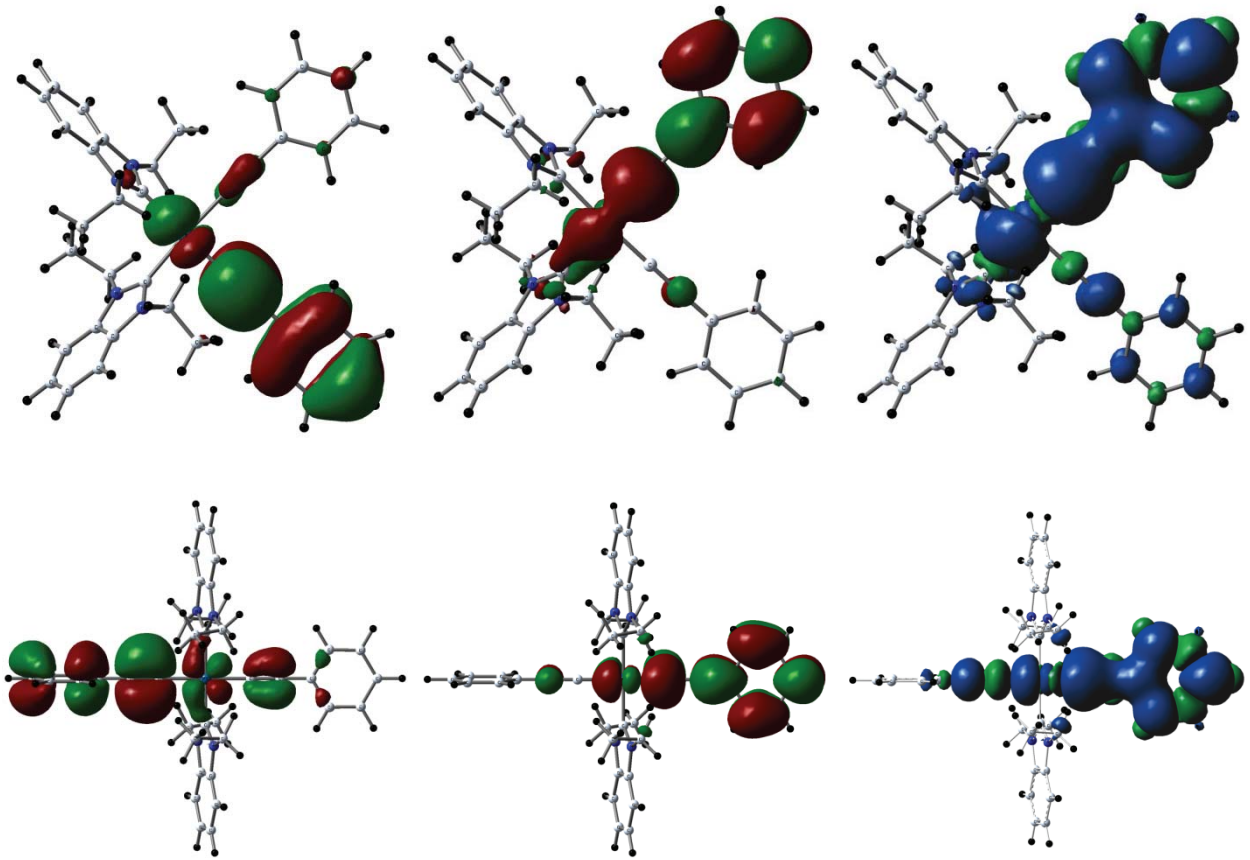

Figure S10. Singly occupied molecular orbitals of the lowest triplet state of **5a** (top) and **5b** (bottom): SOMO -1 (left), SOMO (middle), and triplet spin density surface (right, the positive spin densities are shown in blue and the negative ones are in green).

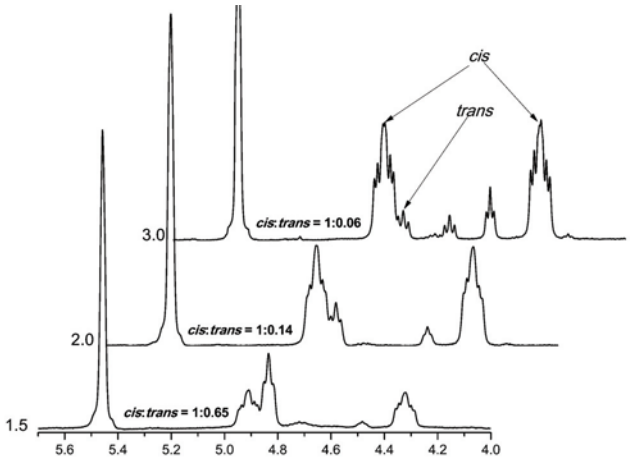

Figure S11. ^{1}H NMR spectra of reaction of precursor complex with 1.5, 2.0 and 3.0 equivalents NHC.

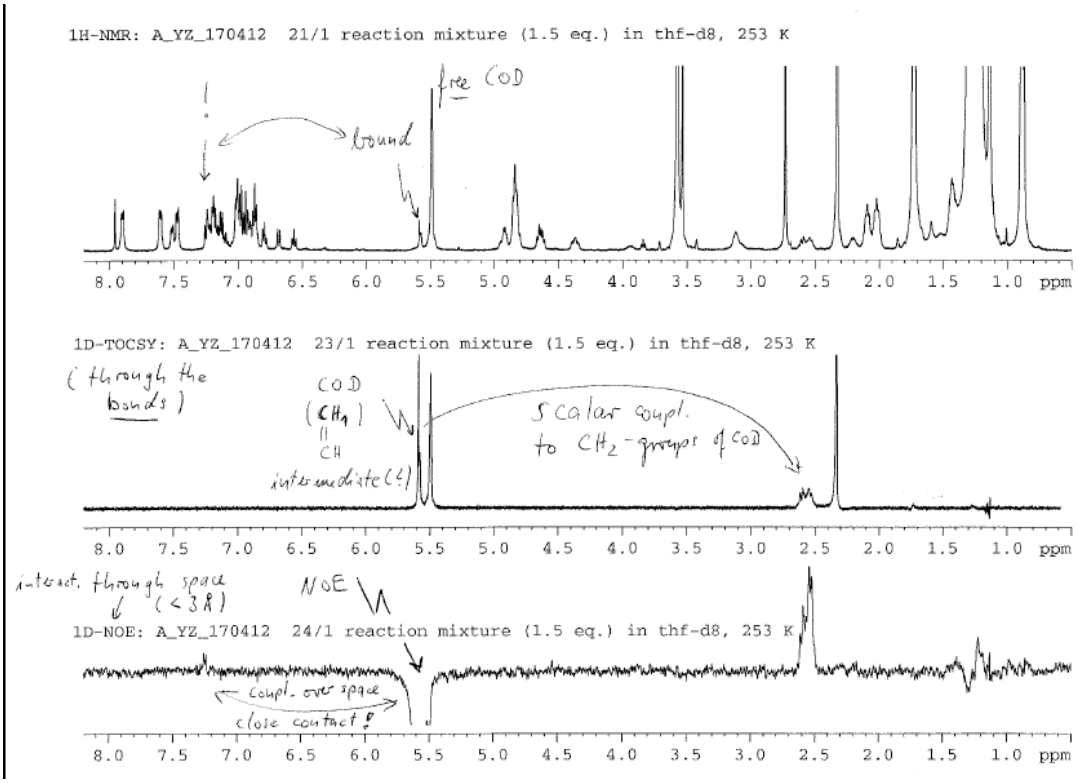

Figure S12. 1D-TOCSY of tracing the formation of complex **5a**.

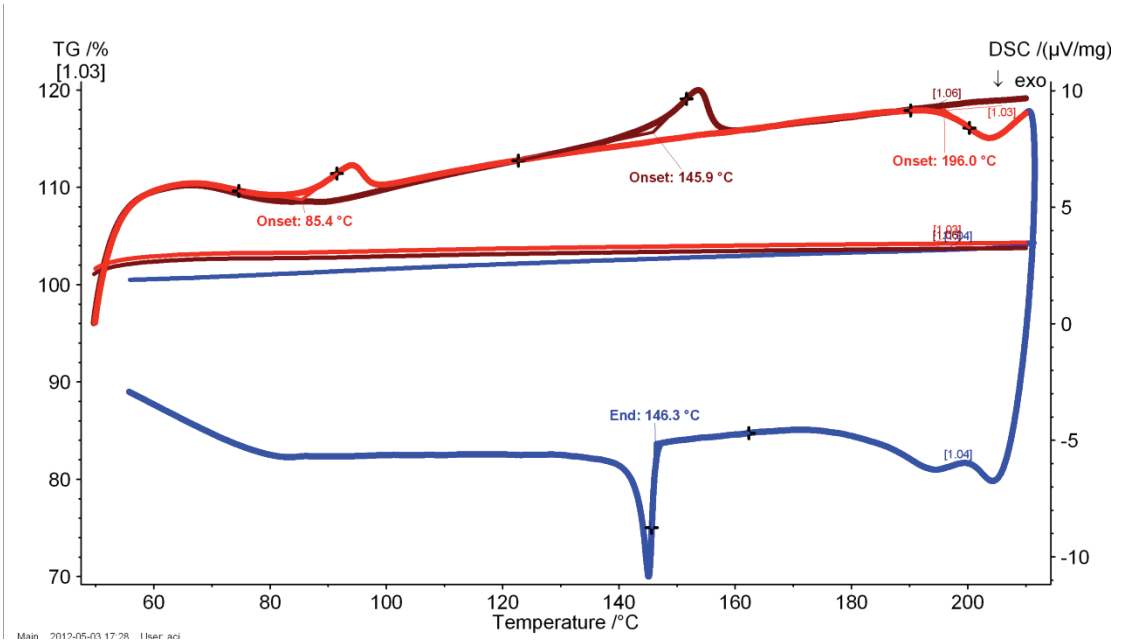

Figure S13. DSC and TGA studies revealing the isomerization of of **5a** to **5b**. DSC: first heating process (top red line), first cooling process (bottom blue line), second heating process (Top wine line). TGA: first heating process (middle red line), first cooling process (middle blue line), second heating process (middle wine line).

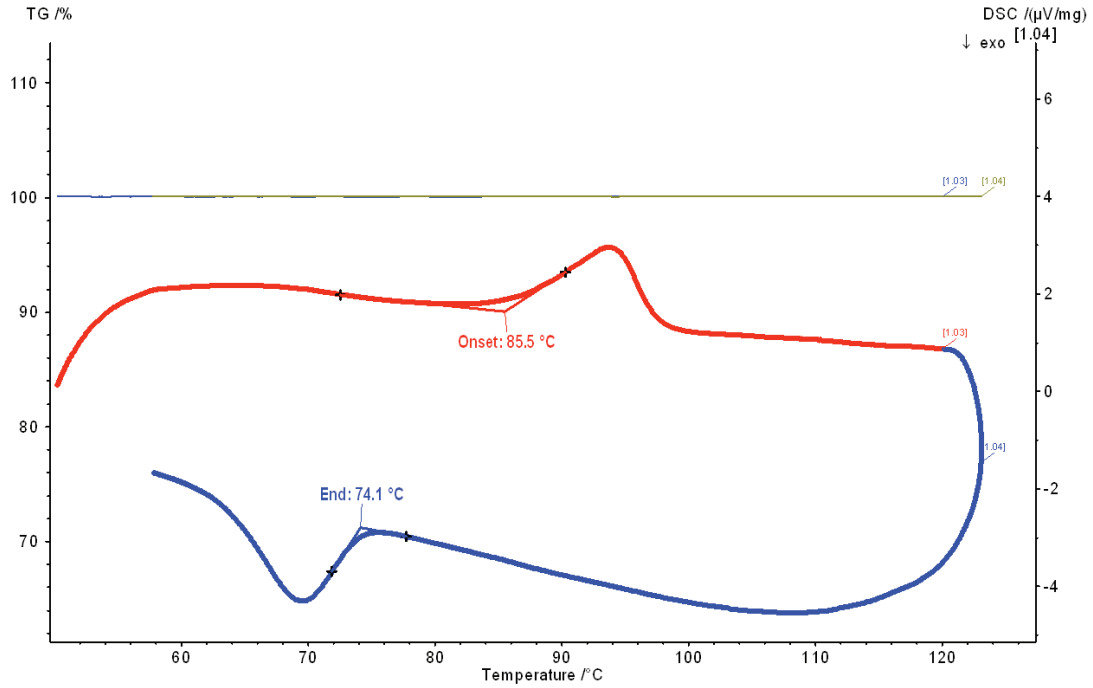

Figure S14. DSC and TGA of complex **5a**. DSC: first heating process (red line), first cooling process (blue line), TGA: first heating process (blue line), first cooling process (yellow line).

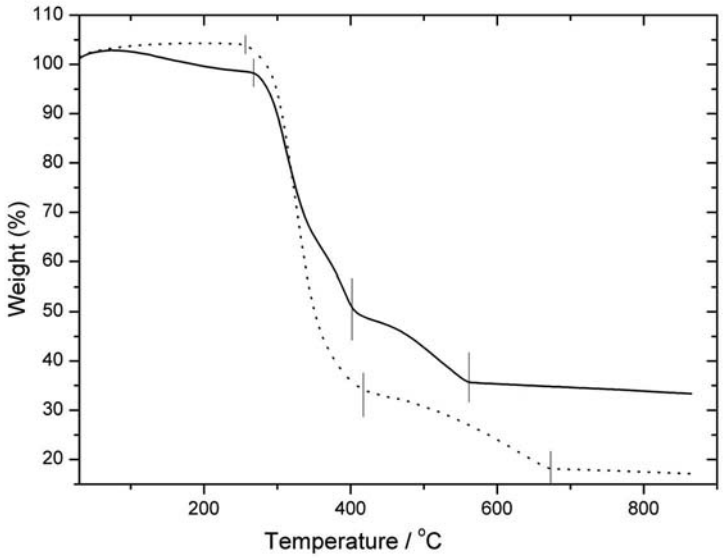

Figure S15. TGA of complexes **5a** (dot line) and **5b** (solid line).

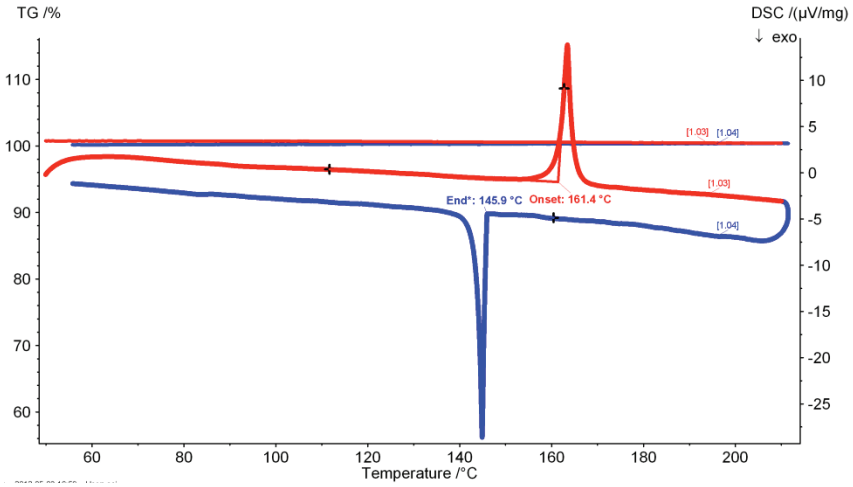

Figure S16. DSC and TGA of complex **5b**. DSC: first heating process (bottom red line), first cooling process (bottom blue line), TGA: first heating process (Top redline), first cooling process (Top blue line).

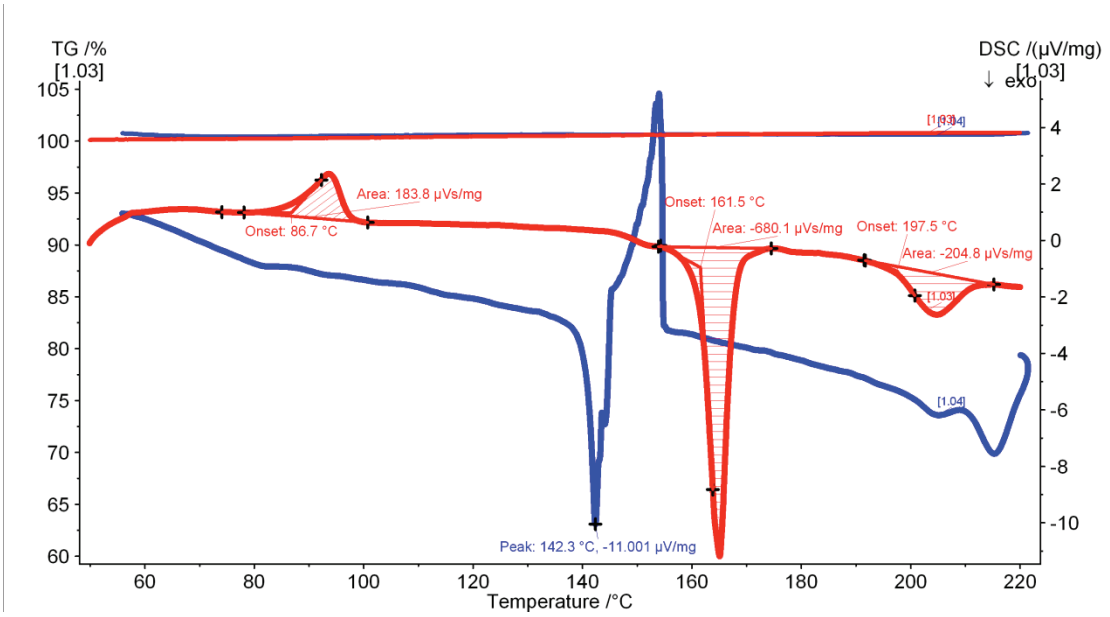

Figure S17. Estimation of enthalpy of isomerization for complexes **5a** to **5b** using DSC. DSC: first heating process (bottom red line), first cooling process (bottom blue line), TGA: first heating process (top redline), first cooling process (top blue line)

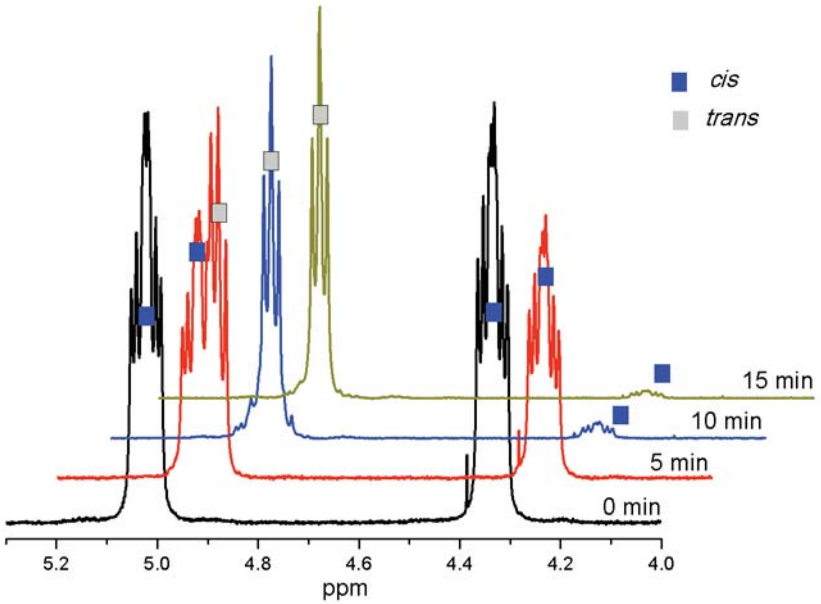

Figure S18. UV irradiation of **5a** to **5b** isomerization in C_6D_6.

Table S1. Crystallographic data for compounds **4a**, **5a**, **5b** and **9b**.

	4a	**5a**	**5b**	**9b**
CCDC	916258	916259	916260	916261
empirical formula	$C_{78}H_{116}F_2N_4Pt$	$C_{78}H_{118}N_4Pt$	$C_{78}H_{118}N_4Pt$	$C_{42}H_{46}N_4Pt$
formula weight ($g \cdot mol^{-1}$)	1342.83	1306.85	1306.84	801.92
temperature (K)	183(2)	183(2)	183(2)	183(2)
wavelength (Å)	0.71073	0.71073	0.71073	0.71073
crystal system, space group	triclinic, $P\bar{1}$	triclinic, $P\bar{1}$	triclinic, $P\bar{1}$	monoclinic, $P\,2_1/c$
a (Å)	8.6169(2)	13.3955(2)	8.6529(1)	11.4673(1)
b (Å)	12.0675(3)	13.4075(2)	9.1139(1)	7.7989(1)
c (Å)	18.5924(4)	21.5535(3)	24.4687(3)	21.7647(3)
α (deg)	89.444(2)	105.270(1)	95.027(1)	90
β (deg)	82.868(2)	100.900(1)	96.004(1)	104.748(1)
γ (deg)	70.201(2)	91.300(1)	108.624(1)	90
volume ($Å^3$)	1803.88(7)	3656.22(9)	1803.51(4)	1882.34(4)
Z, density (calcd) ($Mg \cdot m^{-3}$)	1, 1.236	2, 1.187	1, 1.203	2, 1.415
abs coefficient (mm^{-1})	1.993	1.961	1.988	3.760
$F(000)$	708	1384	692	808
crystal size (mm^3)	0.33 x 0.07 x 0.04	0.41 x 0.09 x 0.07	0.59 x 0.10 x 0.02	0.28 x 0.24 x 0.20
θ range (deg)	2.56 to 28.28	2.51 to 28.28	2.51 to 30.51	2.79 to 30.51
reflections collected	24668	69515	37579	33755
reflections unique	8953 / R_{int} = 0.0382	18144 / R_{int} = 0.0402	10975 / R_{int} = 0.0483	5750 / R_{int} = 0.0297
completeness to θ (%)	99.9	99.9	100.0	99.9
absorption correction	analytical	analytical	analytical	analytical
max/min transmission	0.925 and 0.696	0.900 and 0.620	0.980 and 0.524	0.699 and 0.516
data / restraints / parameters	8243 / 0 / 387	14725 / 88 / 719	10546 / 0 / 378	4416 / 55 / 244
goodness-of-fit on F^2	0.922	0.991	0.964	0.987
final R_1 and wR_2 indices [$I > 2\sigma(I)$]	0.0326, 0.0487	0.0358, 0.0848	0.0330, 0.0560	0.0189, 0.0448
R_1 and wR_2 indices (all data)	0.0363, 0.0492	0.0485, 0.0868	0.0346, 0.0564	0.0290, 0.0462
largest diff. peak and hole ($e \cdot Å^{-3}$)	1.562, -0.944	1.684, -0.753	1.936, -1.040	0.471, -0.876

The unweighted R-factor is $R_1 = \sum(Fo - Fc)/\sum Fo$; $I > 2\,\sigma(I)$ *and the weighted R-factor is* $wR_2 = \{\sum w(Fo^2 - Fc^2)^2/\sum w(Fo^2)^2\}^{1/2}$

Table S2. Selected singlet-singlet (S_0–S_n) and singlet-triplet (S_0–T_m) excited states with TD-DFT/ CPCM (in dichloromethane) vertical excitation energies (nm), transition coefficients, orbitals involved in the transitions, and oscillator strengths *f* for compounds **5a** and **5b** (with $f > 0.10$).

	5a	**5b**
Exp abs l_{max}	285, 300 (sh)	288, 315 (sh)
S_0–S_n	$n = 1$	$n = 1$
	320.0 (0.357)	327.5 (0.238)
	HOMO → LUMO (0.66)	HOMO → LUMO (0.69)
	$n = 2$	$n = 3$
	306.6 (0.380)	301.3 (0.860)
	H-1 → LUMO (0.67)	HOMO→L+1 (0.66)
	$n = 5$	$n = 8$
	291.8 (0.204)	277.8 (0.597)
	HOMO → L+2 (0.64)	H-1 → L+3 (0.64)
	H-1 → L+1 (0.20)	
	$n = 8$	
	282.2 (0.298)	
	H-1 → L+2 (0.64)	
	$n = 9$	
	277.8 (0.326)	
	H-2 → L+2 (0.55)	
	H-2 → LUMO (0.31)	
	$n = 10$	
	277.4 (0.292)	
	HOMO → L+3 (0.49)	
	H-2 → L+1 (0.42)	
Exp em l_{max}	**425**, 447 (sh)	**430**, 451 (sh)
T_1–S_0	431.4	437.5
	HOMO← LUMO (0.438)	HOMO←L+1 (0.614)
	H-1 ← L+3 (0.417)	
T_2–S_0	424.1	417.2
	HOMO ← L+3 (0.479)	H-1 ← L+3 (0.666)
	H-1 ← LUMO (0.390)	H-2 ← L+3 (0.254)
	$p\pi_{alk} \leftarrow \pi_{carb} + \pi_{alk}$	$p\pi_{alk} \leftarrow \pi_{alk}$

Table S3. Frontier orbitals of the DFT optimized ground state and triplet state structures of **5a** and **5b**.

		5a				**5b**			
	MO	Energy (eV)	Composition (%)			Energy (eV)	Composition (%)		
			carbenes	*alkynes*	*Pt*		*carbenes*	*alkynes*	*Pt*
Ground-state	L+3	-0.43	1	98	1	-0.45	0	96	4
	L+2	-0.78	43	49	8	-0.64	90	5	5
	L+1	-0.85	94	0	6	-0.64	5	72	23
	LUMO	-1.08	46	40	14	-0.96	82	7	11
	HOMO	-5.74	0	85	15	-5.52	0	77	23
	H-1	-5.91	3	81	16	-5.69	2	82	16
	H-2	-6.25	19	55	26	-6.39	21	71	8
Triplet-state	SOMO	-3.02	0	95	5	-2.92	0	93	7
	SOMO-1	-5.90	2	85	13	-5.82	2	85	13

Energies and cartesian coordinates of the DFT optimized ground-state structure of 5a

C	-1.52630700	-1.19988900	0.03229500	H	3.47466200	0.95583800	1.71371800
C	-3.05069500	-2.72971400	0.71079000	H	4.49351300	-0.33969300	2.39148100
C	-3.32078000	-2.41158200	-0.62543400	C	1.36630500	-1.95968700	-2.40222000
C	-4.36429500	-3.02028900	-1.31822500	H	2.18841000	-1.89260200	-3.12516500
H	-4.57587100	-2.78223500	-2.35612800	H	0.79019200	-1.03377700	-2.47688800
C	-5.13396400	-3.94914700	-0.62218500	C	0.49930900	-3.18027200	-2.67442100
H	-5.95725100	-4.44326200	-1.13042200	H	-0.34150300	-3.22279200	-1.97489900
C	-4.87240700	-4.25534100	0.72129500	H	1.06795300	-4.11154100	-2.57888400
H	-5.49832800	-4.97998800	1.23442300	C	-1.39131900	1.56554000	0.11428700
C	-3.82398700	-3.65139700	1.41111900	C	-2.25524200	2.43104600	0.21557900
H	-3.62309500	-3.89485800	2.45023800	C	-3.22970400	3.46705000	0.31177300
C	-2.35829200	-0.79390000	-2.28914900	C	-4.53676400	3.19889600	0.76097500
H	-2.34493700	-1.56291500	-3.07272700	H	-4.79438300	2.18178000	1.04528600
H	-1.41540000	-0.24202300	-2.32803200	C	-5.48441700	4.21403600	0.84675100
C	-3.52507400	0.16581300	-2.46845300	H	-6.48796800	3.98444100	1.19821900
H	-3.47461600	0.95583300	-1.71378800	C	-5.15354400	5.52024900	0.48562300
H	-4.49346600	-0.33968500	-2.39158100	C	-3.86158300	5.80122600	0.03878300
C	-1.36632400	-1.95958100	2.40223700	H	-3.59309800	6.81662600	-0.24412300
H	-2.18843400	-1.89243300	3.12517100	C	-2.90990000	4.79066700	-0.04709200
H	-0.79017400	-1.03369100	2.47687200	H	-1.90324000	5.00727400	-0.39392000
C	-0.49938300	-3.18019100	2.67449800	C	1.39137000	1.56552500	-0.11433300
H	-1.06806600	-4.11144000	2.57900900	C	2.25530300	2.43101600	-0.21566900
H	0.34142700	-3.22278000	1.97497800	C	3.22973700	3.46705100	-0.31182600
C	1.52631900	-1.19991800	0.03230500	C	4.53674100	3.19900200	-0.76124800
C	3.32076100	-2.41164100	0.62545700	H	4.79434500	2.18194100	-1.04577100
C	3.05066300	-2.72980800	0.71075600	C	5.48436200	4.21417600	-0.84697400
C	3.82392600	-3.65153700	1.41105600	H	6.48787100	3.98466300	-1.19861500
H	3.62302800	-3.89502400	2.45016800	C	5.15351000	5.52032000	-0.48557800
C	4.87232800	-4.25549100	0.72121300	C	3.86160200	5.80119400	-0.03852000
H	5.49822500	-4.98017400	1.23431900	H	3.59313200	6.81654000	0.24459400
C	5.13389500	-3.94926400	0.62225700	C	2.90995200	4.79060100	0.04730700
H	5.95716700	-4.44338900	1.13050800	H	1.90333200	5.00712600	0.39430400
C	4.36425500	-3.02035900	1.31826800	N	-1.95090400	-1.96728200	1.07241800
H	4.57584000	-2.78227800	2.35616200	N	-2.37345700	-1.47045100	-0.99835300
C	2.35832900	-0.79387600	2.28912300	N	2.37346700	-1.47046800	0.99834900
H	2.34496500	-1.56286400	3.07272600	N	1.95089500	-1.96735400	-1.07240500
H	1.41544800	-0.24197900	2.32799800	Pt	0.00001800	0.14860000	-0.00001600
C	3.52513100	0.16582100	2.46838600	H	-0.09906200	-3.13294200	3.69342500

S22

H	0.09899200	-3.13305800	-3.69335000	H	5.89513400	6.31255300	-0.55265700
H	3.46281600	0.63018000	3.45875500	H	-5.89519300	6.31245600	0.55274000
H	-3.46271600	0.63016900	-3.45882100				

Zero-point correction=	0.674940 (Hartree/Particle)
Thermal correction to Energy=	0.716536
Thermal correction to Enthalpy=	0.717480
Thermal correction to Gibbs Free Energy=	0.593846
Sum of electronic and zero-point Energies=	-1806.635248
Sum of electronic and thermal Energies=	-1806.593652
Sum of electronic and thermal Enthalpies=	-1806.592708
Sum of electronic and thermal Free Energies=	-1806.716342

Toluene: After PCM corrections, the SCF energy is -1807.33072545 a.u.

Dichloromethane: After PCM corrections, the SCF energy is -1807.34544170 a.u.

Energies and cartesian coordinates of the DFT optimized ground-state structure of 5b

C	0.00091900	2.02251200	0.00278900	C	0.00120700	-2.02079100	0.00336500
C	0.24816400	4.16740500	-0.64762500	C	-0.26736300	-4.16252700	0.65609100
C	0.50476400	5.35655400	-1.32448700	C	-0.53431500	-5.34857000	1.33450100
H	0.89828700	5.36468700	-2.33665800	H	-0.92535600	-5.35217700	2.34769700
C	0.23443500	6.54364200	-0.64868800	C	-0.27607300	-6.53883700	0.65947400
H	0.42394100	7.49163700	-1.14431900	H	-0.47310500	-7.48453100	1.15659100
C	-0.27698600	6.54072300	-0.65762200	C	0.23426400	-6.54205700	-0.64725600
H	-0.47448200	7.48653100	-1.15433800	H	0.42339500	-7.49017100	-1.14280600
C	-0.53575300	5.35060300	-1.33270500	C	0.50397500	-5.35512200	-1.32356500
H	-0.92764100	5.35442300	-2.34557300	H	0.89670900	-5.36346600	-2.33604100
C	-0.26819500	4.16440800	-0.65479700	C	0.24791100	-4.16582500	-0.64675700
C	2.00770400	0.00061500	-0.05896900	C	-1.99226300	0.00020400	-0.06253500
C	3.23693000	0.00023100	-0.07482700	C	-3.22108400	-0.00132200	-0.09327700
C	-0.87928100	2.36182100	-2.30353500	C	0.87455600	-2.37090000	-2.29788000
H	-1.37775700	1.40544100	-2.12578200	H	1.37491500	-1.41521000	-2.12200100
H	-1.63845000	3.06900500	-2.65560100	H	1.63247200	-3.08121000	-2.64638800
C	0.25680700	2.21888800	-3.30538400	C	-0.26015100	-2.22723900	-3.30127300
H	0.99431500	1.49757400	-2.93836700	H	-0.99626600	-1.50267900	-2.93784100
H	-0.13366600	1.86157000	-4.26504800	H	0.13228100	-1.87405500	-4.26170500
C	0.87645700	2.37205200	-2.29770600	C	-0.87733600	-2.35953800	2.30481500
H	1.37776400	1.41702100	-2.12092400	H	-1.37593800	-1.40321400	2.12709200
H	1.63380800	3.08299200	-2.64613500	H	-1.63631200	-3.06661500	2.65750600
C	-0.25742700	2.22662800	-3.30177900	C	0.25931700	-2.21637800	3.30600500
H	-0.76866900	3.18057200	-3.47342300	H	0.76739900	-3.17187900	3.47831600
H	-0.99315300	1.50168700	-2.93831200	H	0.99667200	-1.49518800	2.93844400
N	-0.41358500	2.83259800	-1.00812100	N	0.40621300	-2.83587900	-1.00144400
N	0.40674100	2.83737700	-1.00188100	N	-0.41240800	-2.83062700	1.00924300
Pt	0.00684600	0.00087300	-0.00192900	H	0.76481400	3.17441700	3.47775300

S23

H	-0.77065700	-3.18176100	-3.47188800	H	8.56934500	-0.00464300	0.20801700
H	0.13596000	1.87309100	-4.26168900	C	-4.64664900	-0.00207600	-0.12904500
H	-0.13063900	-1.85886500	-4.26580100	C	-5.37165200	1.20485300	-0.14695200
C	4.66285300	-0.00104700	-0.10904300	C	-5.37041500	-1.20975600	-0.14595000
C	5.41827100	-0.00804000	-1.07887000	C	-6.76226000	1.20139600	-0.17900600
C	5.35676100	0.00466000	-1.33396200	H	-4.82437100	2.14373100	-0.13794000
C	6.80889800	-0.00929600	-1.04120500	C	-6.76102800	-1.20775500	-0.17802800
H	4.89623600	-0.01253600	-2.03226400	H	-4.82218500	-2.14807200	-0.13616300
C	6.74732800	0.00330500	-1.36598000	C	-7.46553900	-0.00354700	-0.19400800
H	4.78617700	0.01013800	-2.25871900	H	-7.30156700	2.14587400	-0.19342900
C	7.48259200	-0.00363800	-0.18029100	H	-7.29936700	-2.15279700	-0.19168000
H	7.37107500	-0.01476100	-1.97240600	H	-8.55239300	-0.00411100	-0.21942400
H	7.26159400	0.00774100	-2.32442800				

trans_c2ph_pt.com.log: Zero-point correction= 0.675012 (Hartree/Particle)
trans_c2ph_pt.com.log- Thermal correction to Energy= 0.716934
trans_c2ph_pt.com.log- Thermal correction to Enthalpy= 0.717878
trans_c2ph_pt.com.log- Thermal correction to Gibbs Free Energy= 0.591198
trans_c2ph_pt.com.log- Sum of electronic and zero-point Energies= -1806.649874
trans_c2ph_pt.com.log- Sum of electronic and thermal Energies= -1806.607952
trans_c2ph_pt.com.log- Sum of electronic and thermal Enthalpies= -1806.607008
trans_c2ph_pt.com.log- Sum of electronic and thermal Free Energies= -1806.733689

Dichloromethane: After PCM corrections, the SCF energy is -1807.35087779 a.u.

Toluene: After PCM corrections, the SCF energy is -1807.34031332 a.u.

Energies and cartesian coordinates of the DFT optimized triplet-state structure of 5a

C	1.31191000	-1.39108900	-0.01018700	H	1.55526400	-2.52636200	-3.02290800
C	2.48590600	-3.24223100	-0.58022400	H	0.34468400	-1.41716900	-2.37077700
C	2.92957800	-2.81621200	-0.67783300	C	-0.24012200	-3.50932600	-2.29924500
C	3.91469400	-3.51472500	-1.37253500	H	0.20514100	-4.49738400	-2.14113900
H	4.25625000	-3.19759900	-2.35276900	H	-1.01533800	-3.36208500	-1.54080100
C	4.45358100	-4.64051500	-0.75379000	C	-1.67187200	-0.96340400	-0.00608800
H	5.22613900	-5.20789400	-1.26516000	C	-3.63178600	-1.90637800	-0.63242200
C	4.02557800	-5.05205900	-0.51644100	C	-3.33389400	-2.34829400	-0.66235300
H	4.47568700	-5.92935600	-0.97250500	C	-4.18016400	-3.21553100	-1.34876200
C	3.03072200	-4.36127200	-1.20486300	H	-3.95897300	-3.55251200	-2.35707000
H	2.69871400	-4.68734800	-2.18599100	C	-5.33006000	-3.63801600	-0.68591200
C	2.36248100	-0.91380100	-2.21353700	H	-6.01534600	-4.31380100	-1.18979400
H	2.24543400	-1.60774600	-3.05718900	C	-5.61890500	-3.21198000	-0.61859500
H	1.53636100	-0.19716700	-2.23748000	H	-6.52194600	-3.56702500	-1.10711900
C	3.69042900	-0.17591500	-2.28472400	C	-4.77626300	-2.33675400	-1.29994200
H	3.75026800	0.55996100	-1.47851300	H	-5.00992100	-2.00429500	-2.30658400
H	4.54810200	-0.85300100	-2.21461900	C	-2.53218500	-0.36632200	-2.28081100
C	0.80145600	-2.40139600	-2.23543400	H	-2.64928600	-1.11866400	-3.07258400

H	-1.52375200	0.05238000	-2.34795200
C	-3.56470600	0.74223200	-2.41701200
H	-3.38652800	1.51721900	-1.66658000
H	-4.58870500	0.37126700	-2.30386000
C	-1.47608400	-1.91499800	-2.29181500
H	-2.23381400	-1.77110700	-3.07204700
H	-0.75951800	-1.09265600	-2.37127900
C	-0.78871200	-3.26448700	-2.44160800
H	-0.00131700	-3.38753600	-1.69139800
H	-1.49368200	-4.09575300	-2.33360600
C	1.59270500	1.38400600	-0.17424300
C	2.55782600	2.12895600	-0.31714300
C	3.66148800	3.01620800	-0.47122800
C	4.93779300	2.53661300	-0.82432900
H	5.06980500	1.47017400	-0.98882600
C	6.01246100	3.40790800	-0.96985500
H	6.98899600	3.01564400	-1.24518100
C	5.84277200	4.77786100	-0.76717900
C	4.58334100	5.26808400	-0.41839600
H	4.43993500	6.33463400	-0.26028700
C	3.50543500	4.40188100	-0.27219500
H	2.52411900	4.78208900	-0.00222600
C	-1.12759600	1.76477600	0.06985000
C	-1.85103300	2.79690900	0.23228000
C	-2.59501700	3.91379200	0.41276800
C	-4.06004900	3.86899100	0.48098000
H	-4.54694100	2.90158400	0.38941600
C	-4.78778200	5.00919000	0.66345000
H	-5.87323100	4.95372500	0.71374600
C	-4.14891300	6.27624300	0.79332100
C	-2.72731500	6.35263900	0.73772000
H	-2.24262600	7.32105700	0.84128800
C	-1.96800800	5.23284400	0.55742700
H	-0.88390200	5.28471000	0.51410100
N	1.49778600	-2.34882300	-0.96189200
N	2.19631400	-1.68136500	0.98520800
N	-2.59830800	-1.05933600	-1.00064200
N	-2.13100200	-1.75164100	1.00505700
Pt	0.01509000	0.18212500	-0.03798400
H	-0.72011200	-3.51113000	-3.28437700
H	-0.33050300	-3.33896900	3.43419700
H	-3.47723100	1.19907300	-3.40888200
H	3.75629500	0.35608100	3.24019600
H	-4.74075700	7.17523200	0.93612100
H	6.68353400	5.45757200	-0.88175800

Zero-point correction=	0.670618 (Hartree/Particle)
Thermal correction to Energy=	0.712831
Thermal correction to Enthalpy=	0.713775
Thermal correction to Gibbs Free Energy=	0.588066
Sum of electronic and zero-point Energies=	-1806.535825
Sum of electronic and thermal Energies=	-1806.493612
Sum of electronic and thermal Enthalpies=	-1806.492667
Sum of electronic and thermal Free Energies=	-1806.618377

Dichloromethane: After PCM corrections, the SCF energy is -1807.24050358 a.u.

Energies and cartesian coordinates of the DFT optimized triplet-state structure of 5b

C	0.00527100	-2.02581300	0.01198300
C	-0.25906800	-4.16868600	-0.63707600
C	-0.52602300	-5.35605000	-1.31341800
H	-0.92299700	-5.36164400	-2.32420800
C	-0.26097000	-6.54466800	-0.63848400
H	-0.45797900	-7.49141300	-1.13352200
C	0.25512300	-6.54522500	0.66608600
H	0.44867000	-7.49237400	1.16172500
C	0.52418700	-5.35711300	1.34039300
H	0.92069700	-5.36355400	2.35139600
C	0.26153700	-4.16926900	0.66320000
C	-1.99028100	-0.00016400	0.05210700
C	-3.22044400	-0.00027100	0.05951900
C	0.87807000	-2.37647100	2.31714700
H	1.36260800	-1.41106400	2.15003700
H	1.64606800	-3.07775000	2.66146500
C	-0.25986900	-2.25592900	3.31978700
H	-1.00084100	-1.53293800	2.96290000

H	0.12774800	-1.91097900	4.28505600
C	-0.87618500	-2.37410500	-2.28936200
H	-1.36250900	-1.41056900	-2.11837800
H	-1.64527600	-3.07630700	-2.62956200
C	0.25604900	-2.25290600	-3.29827200
H	0.75788300	-3.21355800	-3.45952300
H	0.99910300	-1.52980400	-2.94603700
N	0.41712900	-2.83841800	1.01652700
N	-0.40901900	-2.83764400	-0.99156100
Pt	0.00848500	0.00001200	0.01089300
C	0.00487700	2.02583300	0.01230100
C	0.26057600	4.16923100	0.66392400
C	0.52286500	5.35701500	1.34136000
H	0.91920800	5.36336800	2.35242900
C	0.25365000	6.54518400	0.66721400
H	0.44691200	7.49229000	1.16304600
C	-0.26223700	6.54474000	-0.63743800
H	-0.45937300	7.49152800	-1.13234300
C	-0.52692800	5.35618000	-1.31261700
H	-0.92374200	5.36186000	-2.32346900
C	-0.25982100	4.16875900	-0.63643600
C	1.97516600	0.00020700	-0.05052600
C	3.24531600	0.00026400	-0.10166500
C	-0.87628300	2.37430300	-2.28911400
H	-1.36234100	1.41058800	-2.11836300
H	-1.64553100	3.07634600	-2.62929300
C	0.25612000	2.25361600	-3.29789500
H	0.99935100	1.53068300	-2.94568600
H	-0.13645100	1.90820600	-4.26104600
C	0.87721600	2.37627100	2.31766300
H	1.36189000	1.41094700	2.15045700
H	1.64509100	3.07759000	2.66217900
C	-0.26082800	2.25543400	3.32014800
H	-0.76372700	3.21611900	3.47770000
H	-1.00168100	1.53242100	2.96306100
N	-0.40943100	2.83774300	-0.99116800
N	0.41638400	2.83835200	1.01705300
H	-0.76263700	-3.21669800	3.47724100
H	0.75767900	3.21444900	-3.45891700
H	-0.13675600	-1.90745400	-4.26131300
H	0.12671700	1.91037500	4.28540700
C	-4.64649800	-0.00046200	0.08773300
C	-5.39652600	0.00392200	-1.10340400
C	-5.34443500	-0.00503600	1.31021800
C	-6.78728300	0.00369700	-1.07100100
H	-4.87091100	0.00752200	-2.05480300
C	-6.73509300	-0.00519200	1.33666300
H	-4.77749000	-0.00845600	2.23717800
C	-7.46539600	-0.00084600	0.14796900
H	-7.34591100	0.00712900	-2.00426800
H	-7.25315800	-0.00876100	2.29299600
H	-8.55220900	-0.00099300	0.17145200
C	4.59843400	0.00040200	-0.15016700
C	5.37230200	-1.25151000	-0.17619100
C	5.37203800	1.25247900	-0.17621400
C	6.73464300	-1.23169900	-0.21133100
H	4.82266500	-2.18897400	-0.16858800
C	6.73438500	1.23295400	-0.21135300
H	4.82220100	2.18982600	-0.16862400
C	7.45568500	0.00070400	-0.22652000
H	7.28662800	-2.16920100	-0.23034900
H	7.28617200	2.17057200	-0.23038300
H	8.54092100	0.00081700	-0.25418600

Energies and cartesian coordinates of the DFT optimized ground-state structure of the carbene ligand

C	0.87108500	-0.06344900	-0.18432600
C	-0.22479800	-0.91660300	0.00672200
N	0.32881700	1.20600200	-0.32822300
N	-1.34660300	-0.09933500	-0.03027000
C	-1.03236300	1.21071700	-0.23471100
C	-2.69649800	-0.61986900	0.12689000
H	-2.75323700	-1.13036500	1.09796600
H	-2.85866400	-1.38271100	-0.64680100
C	1.10763300	2.41670900	-0.50773300
H	0.42403300	3.15736200	-0.93024200
H	1.88952100	2.21912800	-1.25220500
C	2.17359700	-0.55553100	-0.21243300

H	3.02821200	0.09898300	- 0.35998700	H	-4.74814700	-0.01840200	0.16248400
C	-0.05756800	-2.28829900	0.17614200	H	-3.63369200	1.21070300	0.81111000
H	-0.90468700	-2.95256200	- 0.32277000	H	-3.73696600	0.95978300	- 0.93052600
C	2.34308100	-1.92881600	- 0.04256600	C	1.71258000	2.92622000	0.79331600
H	3.34610200	-2.34677200	- 0.05891600	H	2.37632100	2.18299000	1.24869900
C	1.24625900	-2.78124700	0.14958600	H	2.29566400	3.83589000	0.60946500
H	1.41579700	-3.84672400	0.27962700	H	0.92090900	3.16265900	1.51189900
C	-3.76578600	0.45073000	0.03646500				

Zero-point correction=	0.233482 (Hartree/Particle)
Thermal correction to Energy=	0.245347
Thermal correction to Enthalpy=	0.246292
Thermal correction to Gibbs Free Energy=	0.195231
Sum of electronic and zero-point Energies=	-536.222716
Sum of electronic and thermal Energies=	-536.210851
Sum of electronic and thermal Enthalpies=	-536.209907
Sum of electronic and thermal Free Energies=	-536.260967

Toluene: After PCM corrections, the SCF energy is -536.465399740 a.u.

Energies and cartesian coordinates of the DFT optimized ground-state structure of the alkyne ligand

C	1.43042000	1.21684300	0.00001000	H	-0.51273000	2.15446100	0.00006900
C	0.04631700	1.22367600	0.00006700	H	-0.51265900	-2.15450100	0.00005100
C	-0.67479600	-0.00002300	- 0.00007400	H	1.98004200	-2.15397500	0.00003500
C	0.04633500	-1.22368400	- 0.00002400	H	3.21024200	0.00003600	- 0.00005000
C	1.43045400	-1.21682100	- 0.00004500	C	-2.07111400	-0.00000800	- 0.00002200
C	2.12320700	0.00000900	- 0.00006900	C	-3.35497500	0.00000400	0.00000100
H	1.98001600	2.15399100	- 0.00000900				

Zero-point correction=	0.097453 (Hartree/Particle)
Thermal correction to Energy=	0.103412
Thermal correction to Enthalpy=	0.104356
Thermal correction to Gibbs Free Energy=	0.066596
Sum of electronic and zero-point Energies=	-307.219307
Sum of electronic and thermal Energies=	-307.213348
Sum of electronic and thermal Enthalpies=	-307.212404
Sum of electronic and thermal Free Energies=	-307.250163

Toluene: After PCM corrections, the SCF energy is -307.326449134 a.u.

Energies and cartesian coordinates of the DFT optimized ground-state structure of TS1

C	1.61687700	-1.23459300	- 0.13452400	H	3.54718600	-4.02876600	- 2.58602500
C	3.13973500	-2.74051000	- 0.88878200	C	2.69749400	-0.60880400	2.02630900
C	3.56332700	-2.28942600	0.36879900	H	2.80715900	-1.32204400	2.85453200
C	4.72673800	-2.77843400	0.95686400	H	1.73162200	-0.10654400	2.13354000
H	5.05879900	-2.43885400	1.93316800	C	3.82353900	0.41648400	2.03576000
C	5.45603500	-3.72550500	0.24015600	H	3.72522400	1.11843100	1.20334600
H	6.36984200	-4.12702200	0.66927200	H	4.81274400	-0.04801600	1.97421300
C	5.03791900	-4.16611300	- 1.02317000	C	1.16064700	-2.24929700	- 2.35716600
H	5.63417800	-4.90156600	- 1.55602300	H	1.84058100	-2.23689600	- 3.21757300
C	3.87000800	-3.68129500	- 1.60888000	H	0.51943200	-1.36617800	- 2.42711600

C	0.32756300	-3.52253900	-2.32536000
H	0.95269600	-4.41456700	-2.20843800
H	-0.38419800	-3.49038400	-1.49405300
C	-1.63163100	-1.21209600	0.12512500
C	-3.59065400	-2.25905200	-0.34601500
C	-3.15753400	-2.69800800	0.91262700
C	-3.88429900	-3.62833700	1.64968200
H	-3.55378300	-3.96559100	2.62785300
C	-5.05821800	-4.11689300	1.07941100
H	-5.65188500	-4.84458300	1.62564700
C	-5.48501500	-3.69034100	-0.18575900
H	-6.40265400	-4.09526100	-0.60334900
C	-4.75945400	-2.75322900	-0.91911300
H	-5.09817400	-2.42647900	-1.89738800
C	-2.73415000	-0.59375300	-2.02581500
H	-2.82350200	-1.31193900	-2.85225500
H	-1.77792500	-0.07235800	-2.12790400
C	-3.88133200	0.40844300	-2.04940200
H	-3.81011400	1.11533500	-1.21802600
H	-4.86157900	-0.07593600	-1.99917900
C	-1.16777600	-2.19155500	2.36152400
H	-1.84438400	-2.17525200	3.22466600
H	-0.53390500	-1.30178600	2.41826400
C	-0.32809900	-3.46055000	2.34138200
H	0.37807500	-3.43701900	1.50517000
H	-0.95015800	-4.35677100	2.24085200
C	0.81064500	1.85982700	-0.09524400
C	1.77085200	2.65654300	-0.15088900
C	2.84542700	3.55526600	-0.19714000
C	3.27207400	4.13258900	-1.41805000
H	2.73374600	3.88605900	-2.32903000
C	4.35316100	5.00225600	-1.45203700
H	4.65933200	5.43648400	-2.40127900
C	5.04720600	5.32516900	-0.28286800
C	4.64129900	4.76150500	0.92944500
H	5.17312700	5.00658800	1.84635000
C	3.56252200	3.88930400	0.97848900
H	3.25026300	3.45130800	1.92269600
C	-0.78353500	1.86924900	0.04237800
C	-1.74168800	2.66728000	0.10792400
C	-2.80809900	3.57398800	0.17754000
C	-3.17017900	4.19165800	1.39958300
H	-2.58554600	3.97522400	2.28927400
C	-4.24686300	5.06505300	1.46120700
H	-4.50353100	5.52987500	2.41063500
C	-4.99806100	5.35477500	0.31900900
C	-4.65389200	4.75412400	-0.89459700
H	-5.22980500	4.97411100	-1.79101300
C	-3.58132300	3.87615700	-0.97069900
H	-3.31728300	3.40926600	-1.91574600
N	1.95754300	-2.07050200	-1.15751000
N	2.61570900	-1.36812200	0.78787700
N	-2.64371200	-1.34500800	-0.78294700
N	-1.97018400	-2.03051600	1.16306300
Pt	0.00065200	0.01207900	-0.01937400
H	-0.23790900	-3.62503500	-3.25844700
H	0.24360400	-3.54782600	3.27221400
H	-3.83905100	0.97808000	-2.98454200
H	3.78073000	0.98811400	2.96964000
H	-5.83921200	6.04086300	0.37368700
H	5.89230500	6.00776900	-0.31606600

Zero-point correction= 0.671850 (Hartree/Particle)
Thermal correction to Energy= 0.713186
Thermal correction to Enthalpy= 0.714131
Thermal correction to Gibbs Free Energy= 0.591572
Sum of electronic and zero-point Energies= -1806.584307
Sum of electronic and thermal Energies= -1806.542970
Sum of electronic and thermal Enthalpies= -1806.542026
Sum of electronic and thermal Free Energies= -1806.664585

Toluene: After PCM corrections, the SCF energy is -1807.27308773 a.u.

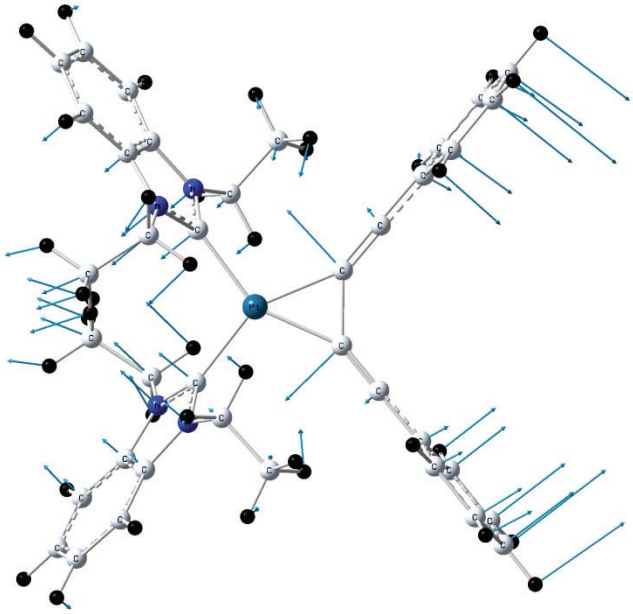

Fig. 1. Displacement vectors corresponding to the negative frequency

```
 Harmonic frequencies (cm**-1):
                      1                      2                      3
                      A                      A                      A
 Frequencies --    -36.4177                4.1648                11.8983
```

Energies and cartesian coordinates of the DFT optimized ground-state structure of cis-1alk

```
 C    -1.97416800    -0.88238400    -0.21589200
 C    -4.12886700    -0.75927800    -0.94157100
 C    -4.13562700    -1.34299600    -0.33407400
 C    -5.32223300    -1.74582100    -0.93988800
 H    -5.33284100    -2.20343300    -1.92488100
 C    -6.50489300    -1.54342000    -0.22782200
 H    -7.44955300    -1.84657300    -0.67073700
 C    -6.49779500    -0.96179000    -1.04625200
 H    -7.43699500    -0.82125400    -1.57405400
 C    -5.30783400    -0.55858200    -1.65318000
 H    -5.30850100    -0.10764600    -2.64133700
 C    -2.35615200    -2.04633700    -1.95534900
 H    -2.99634800    -1.72040300    -2.78476100
 H    -1.34295700    -1.67642600    -2.13825900
 C    -2.34223100    -3.56298100    -1.82582300
 H    -1.65809800    -3.86307200    -1.02557600
 H    -3.33810600    -3.96065100    -1.60191200
 C    -2.34361300     0.10988400    -2.47188100
 H    -2.89134500    -0.35571100    -3.30072600
 H    -1.29050500    -0.16840600    -2.57277400
 C    -2.51434900     1.62251000    -2.48624000
 H    -3.56276900     1.91154500    -2.35325200
 H    -1.92825700     2.08183400    -1.68370600
 C     0.39938500     1.19308400    -0.16335100
 C     1.06334700     3.32194400    -0.22762900
 C     0.59328800     3.25065200    -1.09017900
 C     0.58247500     4.36807600    -1.91962700
 H     0.22152800     4.31689100    -2.94274100
 C     1.05459600     5.56446400    -1.38269100
 H     1.06223500     6.45766900    -2.00115400
 C     1.51768200     5.63819900    -0.06169400
 H     1.87723800     6.58777600    -0.32481900
 C     1.53143500     4.51708100    -0.76612000
 H     1.89761800     4.57804600    -1.78657200
 C     1.39544400     1.65238600    -2.07797400
 H     0.98102100     2.36197200    -2.80600200
 H     0.95986000     0.66728100    -2.26803300
 C     2.91227100     1.57833400    -2.16873700
 H     3.28852600     0.81257100    -1.48352600
 H     3.38553400     2.53595800    -1.92640600
 C    -0.33471700     1.41555700    -2.53306200
 H     0.26336200     1.82957800    -3.35378500
 H    -0.16264100     0.33606700    -2.51002100
 C    -1.81149100     1.73565200    -2.71356300
```

H	-2.40262200	1.28069200	C	5.22669600	-2.20948300
1.91251600			1.18911000		
H	-1.99467400	2.81577600	H	4.70342100	-2.12754800
2.70453900			2.13813300		
C	1.94676600	-1.28066000	N	-2.80336100	-0.49614500
0.06971800			1.23779400		
C	3.14390000	-1.57805200	N	-2.81550700	-1.38956700
0.03197900			0.74425700		
C	4.51564100	-1.95192300	N	0.93094000	2.04691900
0.00054200			0.75604700		
C	5.20761300	-2.07345200	N	0.20431200	1.93506200
1.22251100			1.28938700		
H	4.67077200	-1.88059400	Pt	0.03311400	-0.76431800
2.14736700			0.10559700		
C	6.55009100	-2.43481900	H	-2.16932100	2.03096700
1.24981400			3.44298700		
H	7.06227300	-2.52331900	H	-2.16620600	1.34035000
2.20549500			3.67222500		
C	7.24108200	-2.68401900	H	3.20453600	1.30363100
0.06302300			3.18855000		
C	6.56964500	-2.56922200	H	-1.99516400	-4.01512200
1.15496600			2.76147800		
H	7.09645400	-2.76461500	H	8.29064700	-2.96655400
2.08651600			0.08729300		

Zero-point correction=	0.571242 (Hartree/Particle)
Thermal correction to Energy=	0.606004
Thermal correction to Enthalpy=	0.606948
Thermal correction to Gibbs Free Energy=	0.498591
Sum of electronic and zero-point Energies=	-1499.245884
Sum of electronic and thermal Energies=	-1499.211122
Sum of electronic and thermal Enthalpies=	-1499.210177
Sum of electronic and thermal Free Energies=	-1499.318534

Toluene: After PCM corrections, the SCF energy is -1499.83357086 a.u.

Energies and cartesian coordinates of the DFT optimized ground-state structure of trans-1alk

C	-2.00124700	-0.93554000	H	-3.29312800	-2.47816000
0.00697300			3.24004600		
C	-4.16204400	-0.89246900	H	-1.61334500	-2.67062300
0.69285500			2.69677900		
C	-4.15252100	-1.03984300	C	2.00158100	-0.93518200
0.70265700			0.00677400		
C	-5.33556600	-1.13437400	C	4.15282900	-1.03881400
1.42955200			0.70305100		
H	-5.33389000	-1.23961600	C	4.16241900	-0.89206600
2.51059900			0.69252600		
C	-6.53110400	-1.08352200	C	5.35531800	-0.84300100
0.71337900			1.40784000		
H	-7.47392400	-1.15489700	H	5.36840400	-0.73460500
1.24860100			2.48851600		
C	-6.54058000	-0.94002900	C	6.54096400	-0.93919500
0.68052800			0.68002100		
H	-7.49060500	-0.90348600	H	7.49101700	-0.90271800
1.20644500			1.20589300		
C	-5.35490400	-0.84329300	C	6.53142100	-1.08205900
1.40822500			0.71394900		
H	-5.36793900	-0.73441400	H	7.47421700	-1.15302200
2.48885300			1.24926800		
C	-2.34227100	-1.13373000	C	5.33584400	-1.13280200
2.44606800			1.43006600		
H	-2.97852000	-1.84174900	H	5.33411700	-1.23755400
2.99113300			2.51116100		
H	-1.33376600	-1.55786700	C	2.34248600	-1.13228900
2.39517800			2.44638100		
C	-2.31988500	0.23037000	H	2.97894000	-1.83983900
3.12073000			2.99181500		
H	-1.66173000	0.91156300	H	1.33412700	-1.55678900
2.57105600			2.39562900		
H	-3.32113600	0.67384600	C	2.31961800	0.23211500
3.16196000			3.12041200		
C	-2.37840300	-0.66561400	H	1.66127800	0.91284600
2.45026200			2.57038900		
H	-3.05263000	0.03914100	H	3.32072700	0.67592800
2.95109700			3.16148800		
H	-1.39183300	-0.19627300	C	2.37885400	-0.66634100
2.39267900			2.45015700		
C	-2.31251100	-1.99107800	H	3.05293500	0.03836000
3.19555100			2.95126700		

H	1.39216200	-0.19722400	-2.39284700	H	-2.15054500	6.48736700	-0.01057100
C	2.31334100	-1.99215500	-3.19485800	C	-1.20808800	4.55761000	-0.00633000
H	1.61431700	-2.67165400	-2.69582600	H	-2.14636900	4.00931900	-0.01066700
H	3.29408300	-2.47901000	-3.23908800	N	-2.83664700	-0.81919200	1.08158900
C	-0.00007300	1.17756600	-0.00075800	N	-2.82134400	-1.06638500	-1.07768200
C	-0.00056000	2.40687300	-0.00125500	N	2.82163200	-1.06542900	1.07799700
C	-0.00075600	3.83268300	-0.00090400	N	2.83703900	-0.81918900	-1.08138300
C	1.20638500	4.55792800	0.00490600	Pt	0.00015100	-0.79555100	0.00002700
H	2.14481000	4.00988100	0.00889800	H	-1.96587300	-1.82884200	4.22252100
C	1.20350000	5.94892000	-0.00552000	H	1.96671500	-1.83045900	-4.22191700
H	2.14832800	6.48793100	0.01028500	H	1.94770700	0.13729300	4.14723800
C	-0.00113100	6.65308500	-0.00008400	H	-1.94799600	0.13519000	-4.14753200
C	-1.20557400	5.94860400	-0.00611200	H	-0.00127600	7.74029700	0.00023600

Zero-point correction=	0.571409 (Hartree/Particle)
Thermal correction to Energy=	0.606339
Thermal correction to Enthalpy=	0.607283
Thermal correction to Gibbs Free Energy=	0.496542
Sum of electronic and zero-point Energies=	-1499.253366
Sum of electronic and thermal Energies=	-1499.218437
Sum of electronic and thermal Enthalpies=	-1499.217493
Sum of electronic and thermal Free Energies=	-1499.328233

Toluene: After PCM corrections, the SCF energy is -1499.83730559 a.u.

Energies and cartesian coordinates of the DFT optimized ground-state structure of cis-1carb

Pt	0.42059000	-0.82115100	0.05192100	C	-6.07305100	-1.58164900	0.82498200
C	0.06792700	1.02648200	-0.08334100	H	-7.01129300	-1.66531900	1.36604400
C	2.37942200	-0.74450900	-0.04880300	C	-6.07893800	-1.66106100	-0.57675400
C	-0.17786600	2.22037500	-0.16805200	H	-7.02157700	-1.80502200	-1.09709500
C	3.61071400	-0.77345900	0.05882200	C	-2.18323000	0.52594000	3.00848200
C	-3.71553200	-1.29371900	0.79776000	H	-1.63213600	1.23429700	2.38181800
C	-3.72131800	-1.37416300	-0.60140600	H	-3.24732000	0.78441300	2.97642400
N	-2.39283000	-1.11805000	1.16918400	H	-1.83713000	0.63579900	4.04201800
N	-2.40317300	-1.23098700	-1.00133600	C	-1.79799500	-2.66516100	2.92825200
C	-1.58915000	-1.08149400	0.07533100	H	-1.04303000	-3.21988400	2.36134800
C	-1.94474600	-1.25238800	-2.38318700	H	-2.74150900	-3.21957100	2.87958500
H	-2.65828900	-0.66850000	-2.97557800	H	-1.47691700	-2.62777300	3.97471600
H	-0.98783800	-0.72360500	-2.40023200	C	-0.39874200	3.62609100	0.26350000
C	-1.93486000	-0.89825600	-2.53515400	C	0.68546700	4.52220900	0.22940800
H	-0.86402400	-1.12138100	-2.54106200	C	-1.69796500	4.14964600	0.39203100
H	-2.43721800	-1.63194200	-3.17673100	C	0.47296600	5.89353900	0.32078800
C	-4.89183800	-1.39596300	-1.53679500	H	1.69116900	4.12349400	0.13109900
H	-4.89277800	-1.33051400	-2.62063400	C	-1.90378200	5.52246200	0.48365400
C	-4.90335200	-1.56065100	-1.31460100	H	-2.54099600	3.46423400	0.42021600
H	-4.91307600	-1.62575000	-2.39856800	C	-0.82066300	6.40079400	0.44836700

H	1.32284800	6.57133800	-0.29282400	H	5.22147000	-0.85044000	-2.07235400
H	-2.91531500	5.90929000	-0.58324100	C	7.12998400	-0.87845700	1.29902800
H	-0.98340000	7.47329900	-0.51994100	H	5.18173600	-0.80239200	2.22031300
C	5.03244100	-0.82351400	0.07236800	C	7.84198500	-0.91412800	0.09944000
C	5.76282000	-0.85986800	-1.13056500	H	7.70147500	-0.93027500	-2.05184400
C	5.74041200	-0.83291900	1.28913200	H	7.66156200	-0.88473600	2.24760800
C	7.15238900	-0.90405900	-1.11364000	H	8.92854800	-0.94876900	0.10992000

Zero-point correction= 0.438577 (Hartree/Particle)
Thermal correction to Energy= 0.467394
Thermal correction to Enthalpy= 0.468338
Thermal correction to Gibbs Free Energy= 0.371189
Sum of electronic and zero-point Energies= -1270.320141
Sum of electronic and thermal Energies= -1270.291325
Sum of electronic and thermal Enthalpies= -1270.290380
Sum of electronic and thermal Free Energies= -1270.387529

Toluene: After PCM corrections, the SCF energy is -1270.77820760 a.u.

Energies and cartesian coordinates of the DFT optimized ground-state structure of trans-1carb

Pt	0.03088700	-1.01469800	-0.02890600	H	-1.45256500	2.06838400	-3.25156300
C	-1.94506900	-1.16371900	-0.01096700	H	-0.70158700	0.78186600	-4.21602200
C	2.00960600	-1.11331400	-0.04845800	C	0.85372000	1.03674600	3.22760000
C	-3.16888800	-1.29061700	0.00035800	H	1.54271200	0.35115800	2.72363700
C	3.23610300	-1.21597000	-0.05372400	H	1.34118500	2.01325000	3.32332600
C	0.04959800	3.01575500	-0.63632900	H	0.65620200	0.65245300	4.23422100
C	-0.20470200	2.98162100	0.74101100	C	-4.58242500	-1.47112300	0.01373700
N	0.16734500	1.69623300	-1.04797800	C	-5.14785900	-2.71328200	0.35673200
N	-0.25121100	1.64247500	-1.10039700	C	-5.44649100	-0.41010800	-0.31482400
C	-0.02027000	0.87616500	0.01065400	C	-6.52797800	-2.88405400	0.36932800
C	-0.45131000	1.13672600	2.45291200	H	-4.48831200	-3.53830600	0.61091800
H	-1.16469100	1.80710600	-2.94405100	C	-6.82585500	-0.58741100	-0.29824900
H	-0.93030000	0.15901700	-2.35267300	H	-5.01914700	0.55242800	-0.58260400
C	0.38715900	1.25505500	-2.41992100	C	-7.37421400	-1.82384100	0.04321500
H	0.91696200	0.30051700	-2.35930600	H	-6.94624500	-3.85181000	0.63587300
H	1.06169800	1.98098900	-2.88650800	H	-7.47734000	0.24469400	-0.55489400
C	0.14370900	4.21899100	-1.32890600	H	-8.45259500	-1.96044000	0.05437800
H	0.33270900	4.25032700	-2.39762000	C	4.65305700	-1.36662200	-0.05608900
C	-0.36246600	4.14957600	-1.48079300	C	5.37160400	-1.43354300	1.15220200
H	-0.55083100	4.12824200	-2.54984800	C	5.36767200	-1.45081100	-1.26555300
C	-0.01743800	5.38838600	-0.59052000	C	6.75483000	-1.57680800	1.14777400
H	0.05067400	6.34762400	-1.09561300	H	4.82700800	-1.37408800	2.09045800
C	-0.26534500	5.35432700	-0.78969600	C	6.75096000	-1.59407200	-1.26346100
H	-0.38366300	6.28775200	-1.33245100	H	4.82006400	-1.40523500	-2.20283900
C	-0.91431900	1.11573500	-3.19461800	C	7.45132700	-1.65698200	0.05845800
H	-1.56412000	0.37530400	-2.71684200	H	7.29302600	-1.62787500	2.09129200

H	7.28618700	-1.65892700	2.20782300	H	8.53254100	-1.76978400	0.05937600

Zero-point correction= 0.438644 (Hartree/Particle)
Thermal correction to Energy= 0.467430
Thermal correction to Enthalpy= 0.468374
Thermal correction to Gibbs Free Energy= 0.370065
Sum of electronic and zero-point Energies= -1270.329013
Sum of electronic and thermal Energies= -1270.300227
Sum of electronic and thermal Enthalpies= -1270.299283
Sum of electronic and thermal Free Energies= -1270.397592

Toluene: After PCM corrections, the SCF energy is -1270.79361118 a.u.

Energies and cartesian coordinates of the DFT optimized ground-state structure of Pt-carb2

C	1.98648100	-0.00000300	0.00001800	C	-6.53086900	0.39270000	0.58036500
C	4.15078700	0.39310100	0.58138700	H	-7.47749500	0.69189900	1.02203600
C	4.15080900	-0.39307800	0.58134400	C	-6.53085800	-0.39285000	0.58027400
C	5.33960500	-0.80056800	1.17976600	H	-7.47747800	-0.69207200	1.02194100
H	5.34472400	-1.41291100	2.07697500	C	-5.33958100	-0.80059400	1.17978000
C	6.53087000	-0.39279200	0.58025600	H	-5.34468000	-1.41292100	2.07700000
H	7.47750000	-0.69200500	1.02190900	C	-2.35294900	-1.40034200	2.02075400
C	6.53085400	0.39277000	0.58037500	H	-2.95765200	-1.14412400	2.89990700
H	7.47747000	0.69198700	1.02205500	H	-1.32221900	-1.07818700	2.20303900
C	5.33957900	0.80053600	1.17986500	C	-2.39989000	-2.89384400	1.73287300
H	5.34469400	1.41287900	2.07707600	H	-1.74528000	-3.13068400	0.88780300
C	2.35298700	-1.40044500	2.02071400	H	-3.41440300	-3.23142300	1.49267300
H	2.95770000	-1.14426600	2.89987200	C	-2.35300400	1.40048300	2.02072100
H	1.32225800	-1.07830200	2.20302600	H	-2.95790700	1.14454500	2.89981300
C	2.39993200	-2.89393200	1.73275900	H	-1.32235900	1.07820500	2.20324900
H	1.74529100	-3.13074100	0.88770400	C	-2.39962000	2.89393200	1.73250300
H	3.41443900	-3.23149200	1.49250400	H	-1.74479500	3.13042600	0.88750100
C	2.35296000	1.40043500	2.02072400	H	-3.41402500	3.23165900	1.49206800
H	2.95783300	1.14445900	2.89982600	N	2.82239100	0.60106000	0.90384000
H	1.32230400	1.07816700	2.20321000	N	2.82241500	-0.60113100	0.90378200
C	2.39960400	2.89389200	1.73255800	N	-2.82239600	-0.60109400	0.90378500
H	3.41401900	3.23161900	1.49216900	N	-2.82241300	0.60107500	0.90385200
H	1.74480800	3.13042300	0.88754400	Pt	-0.00000100	0.00001600	0.00002300
C	-1.98648200	-0.00000400	0.00002800	H	2.05107800	3.45544400	2.60688900
C	-4.15079700	-0.39309100	0.58134300	H	-2.05111800	3.45551300	2.60682500
C	-4.15080300	0.39307500	0.58139700	H	-2.05137400	-3.45530800	2.60725800
C	-5.33960600	0.80048600	1.17986800	H	2.05145400	-3.45544200	2.60713100
H	-5.34474000	1.41282600	2.07708000				

Zero-point correction= 0.470141 (Hartree/Particle)
Thermal correction to Energy= 0.497377
Thermal correction to Enthalpy= 0.498321
Thermal correction to Gibbs Free Energy= 0.409011
Sum of electronic and zero-point Energies= -1191.926227
Sum of electronic and thermal Energies= -1191.898992
Sum of electronic and thermal Enthalpies= -1191.898048

Sum of electronic and thermal Free Energies= -1191.987358

Toluene: After PCM corrections, the SCF energy is -1192.40435913 a.u.

Energies and cartesian coordinates of the DFT optimized ground-state structure of alk2

C	0.00015700	1.90115600	-0.00195600	H	2.14968500	5.96456200	-0.03895100
C	0.00033800	0.67986300	-0.00093000	H	0.00010700	7.20980100	0.00245700
C	-0.00033800	-0.67986300	-0.00093000	C	0.00014200	-3.32077000	-0.00091700
C	-0.00015700	-1.90115600	-0.00195600	C	-1.21240900	-4.03373300	-0.02326500
C	-0.00014200	3.32077000	-0.00091700	C	1.21269400	-4.03366900	0.02274900
C	-1.21269400	4.03366900	0.02274900	C	-1.20702100	-5.42370200	-0.02177800
C	1.21240900	4.03373300	-0.02326500	H	-2.14942400	-3.48477600	-0.04133300
C	-1.20702100	5.42368800	0.02381300	C	1.20702100	-5.42368800	0.02381300
H	-2.14971000	3.48462700	0.04017100	H	2.14971000	-3.48462700	0.04017100
C	1.20702100	5.42370200	-0.02177800	C	-0.00004500	-6.12294200	0.00150600
H	2.14942400	3.48477600	-0.04133300	H	-2.14968500	-5.96456200	-0.03895100
C	0.00004500	6.12294200	0.00150600	H	2.14962000	-5.96458400	0.04232200
H	-2.14962000	5.96458400	0.04232200	H	-0.00010700	-7.20980100	0.00245700

Zero-point correction=	0.204221 (Hartree/Particle)
Thermal correction to Energy=	0.217027
Thermal correction to Enthalpy=	0.217971
Thermal correction to Gibbs Free Energy=	0.162209
Sum of electronic and zero-point Energies=	-614.684610
Sum of electronic and thermal Energies=	-614.671805
Sum of electronic and thermal Enthalpies=	-614.670860
Sum of electronic and thermal Free Energies=	-614.726622

Toluene: After PCM corrections, the SCF energy is -614.896801268 a.u.

Energies and cartesian coordinates of the DFT optimized ground-state structure of migr1_ts

Pt	-0.01746500	0.07487100	-0.09232600	C	-1.82866000	-5.03635600	-0.65282300
C	-1.96573700	0.60249700	-0.24749300	C	-3.21494000	-3.08329500	-0.22428300
C	0.13744700	-2.04566200	-0.10114900	C	-2.97451700	-5.81561000	-0.76998200
C	-3.17141900	0.83621700	-0.34366200	H	-0.84408300	-5.48017800	-0.77155500
C	-0.79265700	-2.83794000	-0.24670700	C	-4.35079100	-3.87577900	-0.34591600
C	-4.57059800	1.08689200	-0.45342600	H	-3.29118400	-2.01910700	-0.01279900
C	-5.42987300	0.88650300	-0.64475300	C	-4.23598300	-5.23964400	-0.61764700
C	-5.13534600	1.53694100	-1.66249700	H	-2.88164500	-6.87775600	-0.98163800
C	-6.79592000	1.12662400	-0.53515400	H	-5.33126900	-3.42225100	-0.22543600
H	-5.00647500	0.53981000	-1.58403300	H	-5.12829200	-5.85350500	-0.71008000
C	-6.50196400	1.77368800	-1.76641900	C	3.49774500	-2.25593600	0.61655600
H	-4.48271400	1.69528500	-2.51671000	C	3.51166500	-2.13189300	-0.78702800
C	-7.34096700	1.57066900	-0.66994000	N	2.33693200	-1.66107400	1.07075400
H	-7.43996900	0.96590500	-1.39696400	N	2.35823400	-1.47127600	-1.14937100
H	-6.91601400	2.11996700	-2.71078800	C	1.51858200	-1.25310900	-0.02508000
H	-8.40868700	1.75738600	-0.75368400	C	1.98358700	-1.14937700	-2.50300000
C	-1.94275200	-3.66367000	-0.37795000	H	2.19759000	-2.01765100	-3.14214700

```
 H    0.89778500   -1.00559000   -
2.51265900
 C    1.85675400   -1.75827100
2.43075400
 H    0.99883000   -1.08239700
2.51020100
 H    2.63881400   -1.36922000
3.09815600
 C    4.55394200   -2.85038400
1.29202800
 H    4.55179100   -2.94617300
2.37416800
 C    4.57663900   -2.60721200   -
1.53899100
 H    4.59243200   -2.51322300   -
2.62127400
 C    5.63355000   -3.32792000
0.53209700
 H    6.47132100   -3.79833900
1.03973900
 C    5.64303700   -3.21176100   -
0.85527700
 H    6.48828400   -3.59215100   -
1.42247600
 C    1.45331100   -3.16719900
2.85721800
 H    0.62412200   -3.53563800
2.24683400
 H    2.28713600   -3.87061200
2.76329300
 H    1.13084600   -3.15869900
3.90488200
 C    2.69049000    0.09348600   -
3.03243100
 H    2.45310000    0.96084000   -
2.40804600
 H    3.77805200   -0.03718600   -
3.03028600
 H    2.37431900    0.30462800   -
4.06101000
 C    1.63396700    3.89167800
0.58496100
 C    1.12587200    4.00202600   -
0.71515500
 N    1.33485700    2.60670000
1.01016600
 N    0.54693500    2.77859900   -
1.01221600
 C    0.67423700    1.91807100
0.03823400
 C   -0.18393200    2.49629200   -
2.23923500
 H    0.44527900    2.81076200   -
3.08159500
 H   -0.29482700    1.40939100   -
2.28580100
 C    1.69929400    2.06943900
2.30866000
 H    1.03560400    1.21899000
2.48341400
 H    1.46516500    2.83238900
3.06095700
 C    2.28697500    4.95354200
1.20309400
 H    2.68078000    4.87352900
2.21198000
 C    1.25954700    5.17703900   -
1.44879600
 H    0.86651200    5.26792200   -
2.45692800
 C    2.41893800    6.13204700
0.47104000
 H    2.92303300    6.98275200
0.92092500
 C    1.91683200    6.24057100   -
0.83316000
 H    2.03905700    7.17398400   -
1.37542700
 C    3.16122800    1.65300800
2.37969500
 H    3.36624200    0.85073200
1.66406600
 H    3.83046400    2.49204600
2.16027100
 H    3.39665400    1.28814900
3.38584300
 C   -1.54774900    3.16937100   -
2.27706900
 H   -2.17610500    2.78527400   -
1.46768600
 H   -1.46855400    4.25761100   -
2.18042600
 H   -2.03881200    2.94826300   -
3.23149100

Zero-point correction=                           0.672102 (Hartree/Particle)
Thermal correction to Energy=                    0.713529
Thermal correction to Enthalpy=                  0.714474
Thermal correction to Gibbs Free Energy=         0.591642
Sum of electronic and zero-point Energies=          -1806.576089
Sum of electronic and thermal Energies=             -1806.534662
Sum of electronic and thermal Enthalpies=           -1806.533718
Sum of electronic and thermal Free Energies=        -1806.656549

After PCM corrections, the SCF energy is  -1807.26282663     a.u.
```

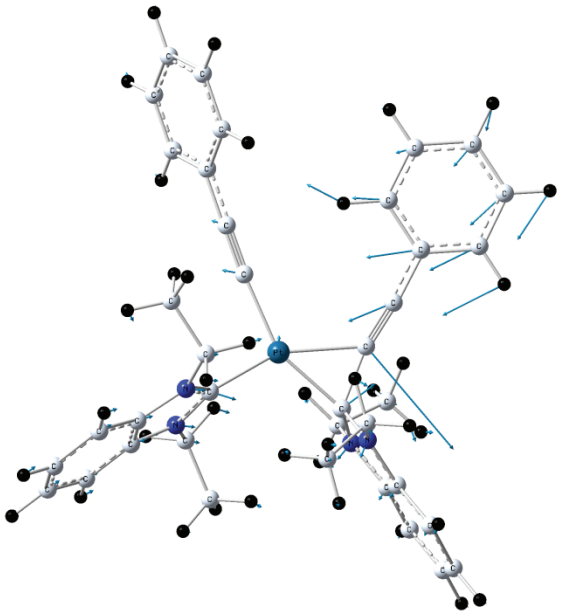

Fig. 2. Displacement vectors corresponding to the negative frequency.

```
Harmonic frequencies (cm**-1):
                      1                      2                      3
                      A                      A                      A
 Frequencies --   -160.1535               10.1900               13.4221
```

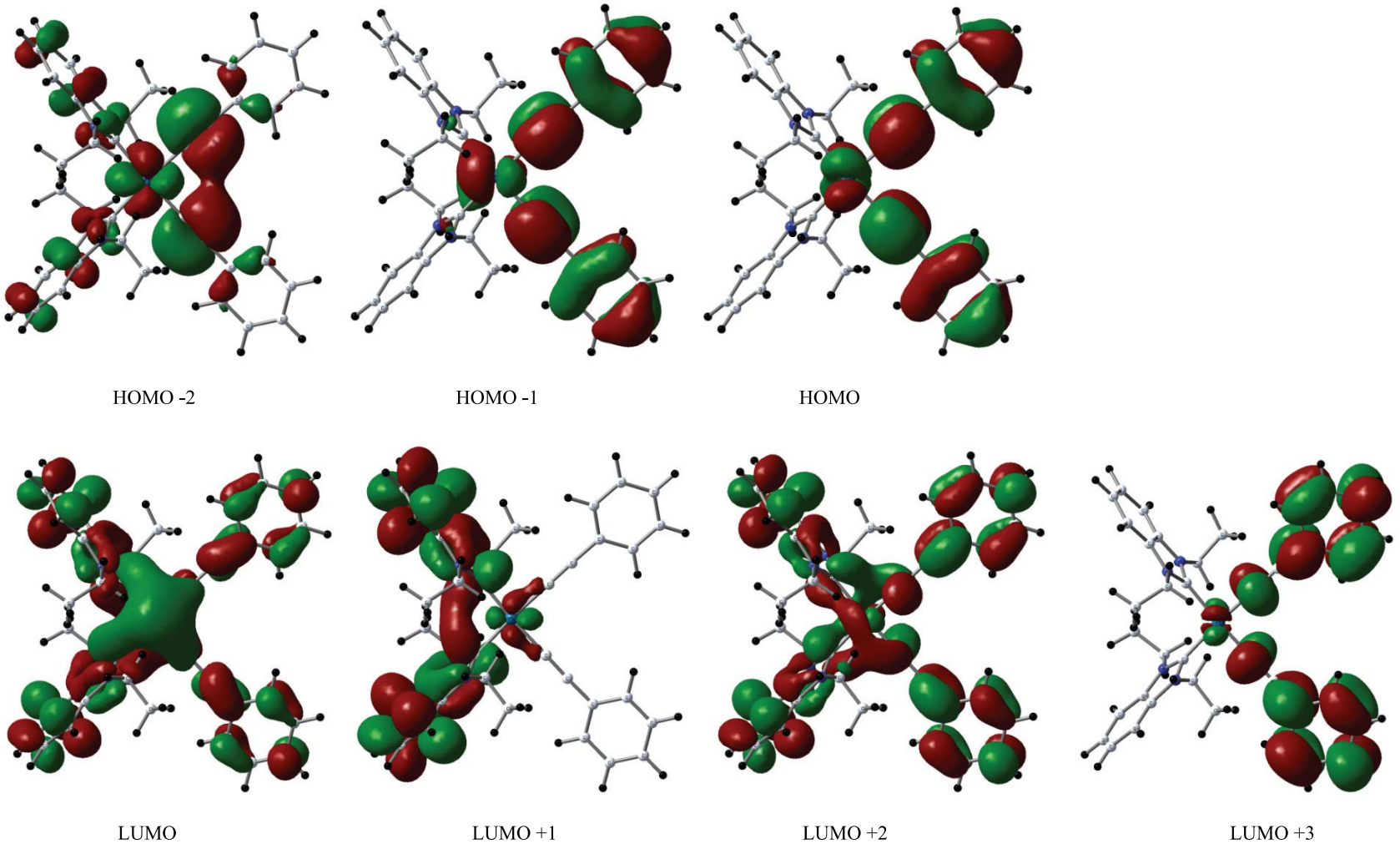

Figure S19. Spatial plots of selected frontier molecular orbitals of the ground-state of **5a**.

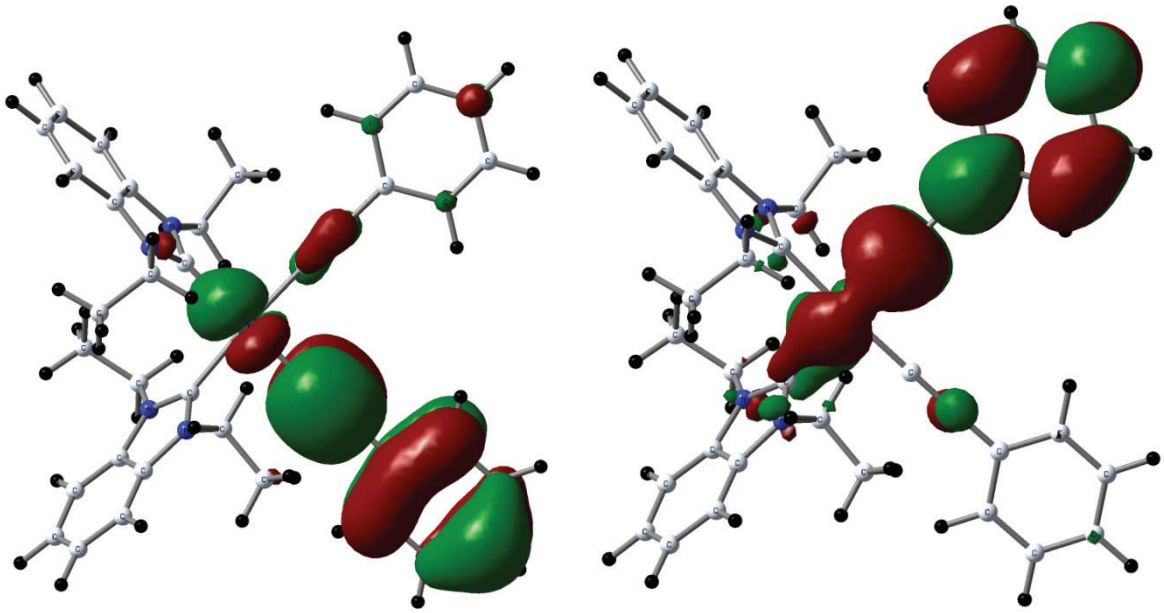

Figure S20. Singly occupied molecular orbitals of the lowest triplet state of **5a**: SOMO -1 (left) and SOMO (right).

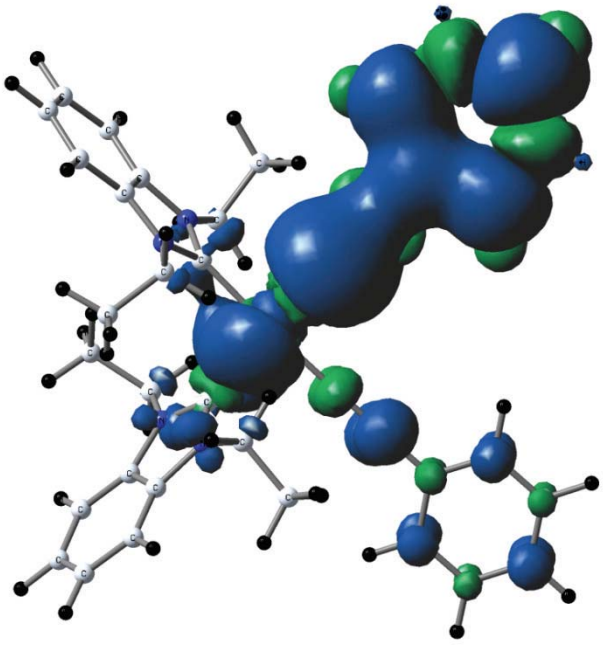

Figure S21. Triplet spin density surface of the lowest triplet state of **5a**. The positive spin densities are shown in blue and the negative ones are in green.

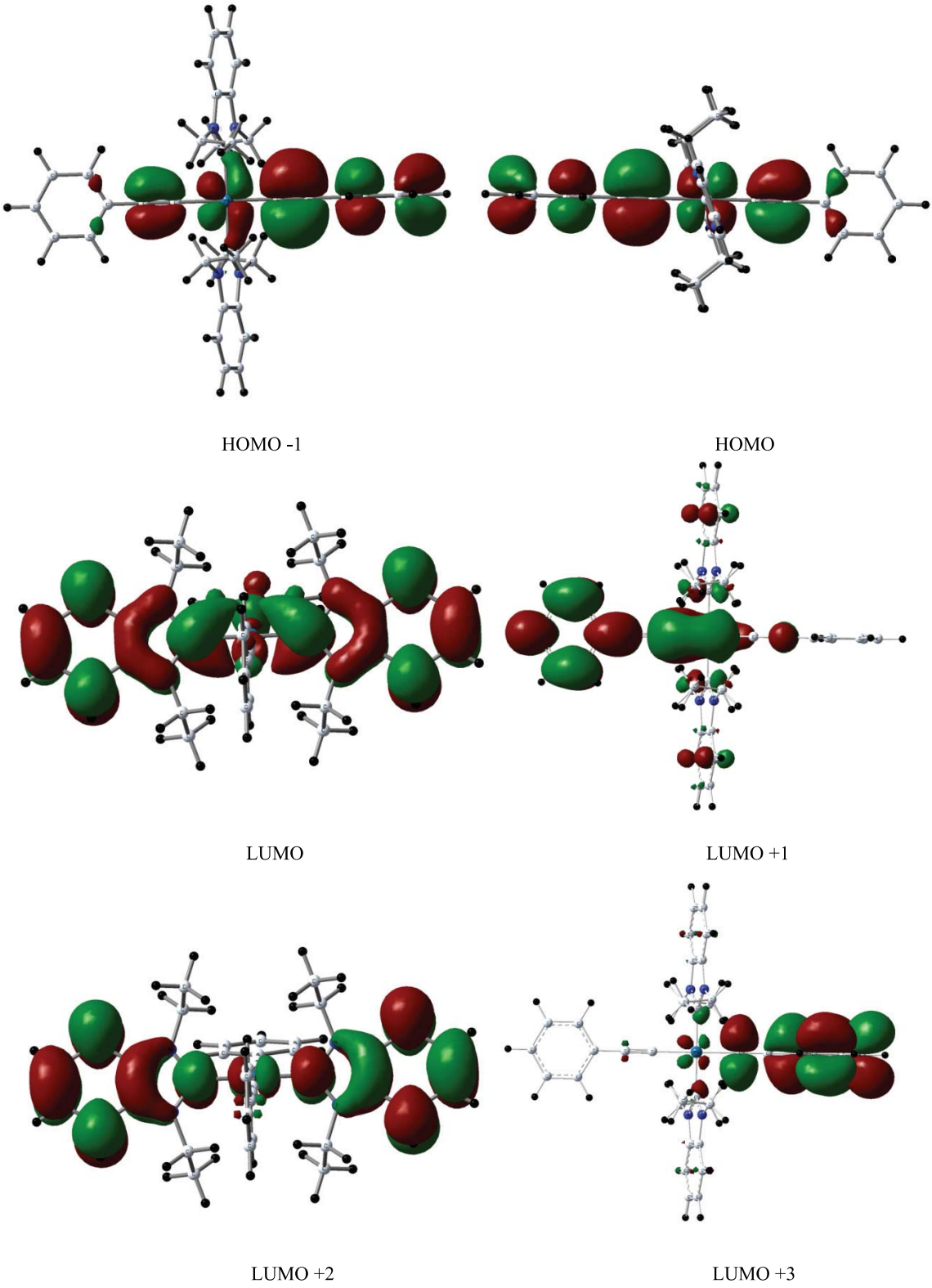

Figure S22. Spatial plots of selected frontier molecular orbitals of the ground-state of **5b**.

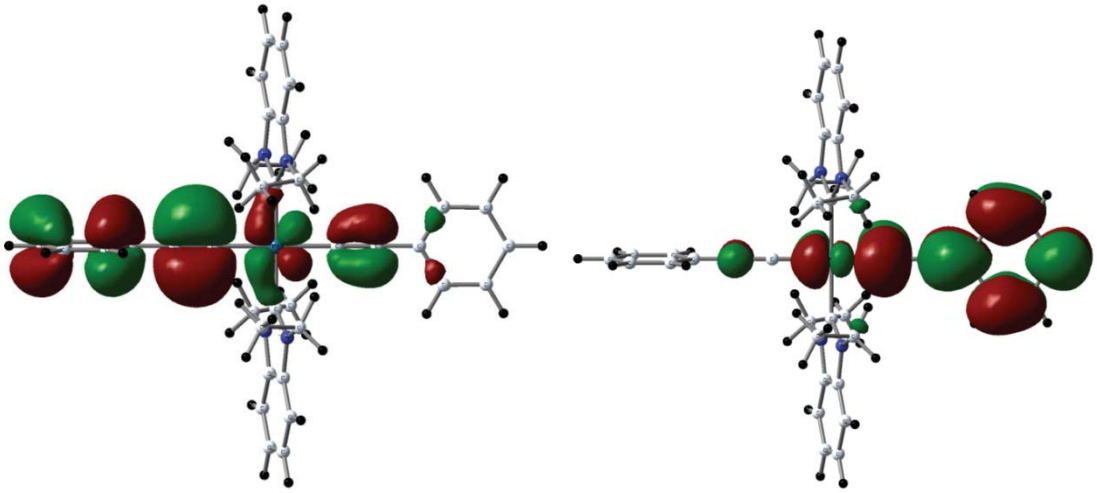

Figure S23. Singly occupied molecular orbitals of the lowest triplet state of **5b**: SOMO -1 (left) and SOMO (right).

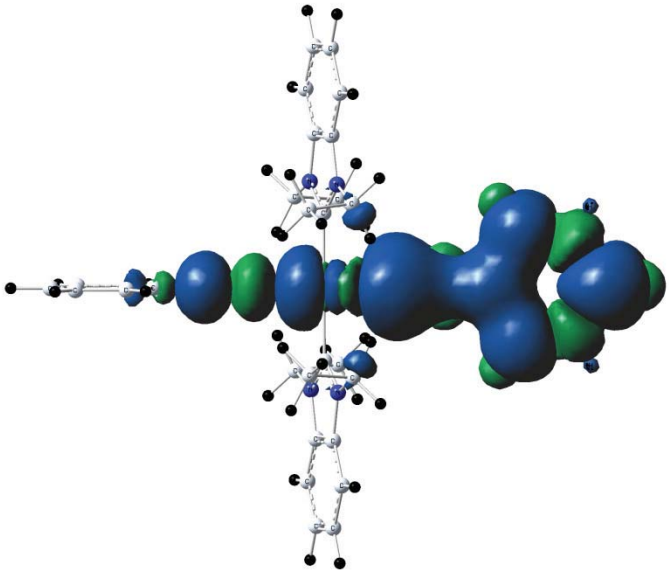

Figure S24. Triplet spin density surface of the lowest triplet state of **5b**.

Tables S4. Energy (eV) and composition (%) of selected frontier orbitals of **5a** and **5b** (ground- and triplet-states).

5a	Energy (eV)		Composition (%)		
			carbenes	*alkynes*	*Pt*
Ground-state	L+3	-0.43	1	98	1
	L+2	-0.78	43	49	8
	L+1	-0.85	94	0	6
	LUMO	-1.08	46	40	14
	HOMO	-5.74	0	85	15
	H-1	-5.91	3	81	16
	H-2	-6.25	19	55	26
Triplet-state	SOMO	-3.02	0	95	5
	SOMO-1	-5.90	2	85	13

Tables S5. Energy (eV) and composition (%) of selected frontier orbitals of **5a** and **5b** (ground- and triplet-states).

5b	Energy (eV)		Composition (%)		
			carbenes	*alkynes*	*Pt*
Ground-state	L+3	-0.45	0	96	4
	L+2	-0.64	5	72	23
	L+1	-0.64	90	5	5
	LUMO	-0.96	82	7	11
	HOMO	-5.52	0	77	23
	H-1	-5.69	2	82	16
	H-2	-6.39	21	71	8
Triplet-state	SOMO	-2.92	0	93	7
	SOMO-1	-5.82	2	85	13

References

[1] S. Fery-Forgues, D. Lavabre, *J. Chem. Educ.* **1999**, *76*, 1260.

[2] M. Hissler, W. B. Connick, D. K. Geiger, J. E. McGarrah, D. Lipa, R. J. Lachicotte, R. Eisenberg, *Inorg. Chem.* **2000**, *39*, 447.

[3] J.-X. Duan, X. Cai, F. Meng, L. Lan, C. Hart, M. Matteucci, *J. Med. Chem.* **2007**, *50*, 1001.

[4] R. H. Pawle, V. Eastman, S. W. Thomas, *J. Mater. Chem.* **2011**, *21*, 14041.

[5] K. Li, Q. Wang, *Chem. Commun.* **2005**, *38*, 4786.

[6] H. V. Huynh, Y. Han, J. H. H. Ho, G. K. Tan, *Organometallics* **2006**, *25*, 3267.

[7] M. J. Frisch, G. W. Trucks, H. B. Schlegel, G. E. Scuseria, M. A. Robb, J. R. Cheeseman, J. A. Montgomery, T. Vreven, K. N. Kudin, J. C. Burant, J. M. Millam, S. S. Iyengar, J. Tomasi, V. Barone, B. Mennucci, M. Cossi, G. Scalmani, N. Rega, G. A. Petersson, H. Nakatsuji, M. Hada, M. Ehara, K. Toyota, R. Fukuda, J. Hasegawa, M. Ishida, T. Nakajima, Y. Honda, O. Kitao, H. Nakai, M. Klene, X. Li, J. E. Knox, H. P. Hratchian, J. B. Cross, V. Bakken, C. Adamo, J. Jaramillo, R. Gomperts, R. E. Stratmann, O. Yazyev, A. J. Austin, R. Cammi, C. Pomelli, J. W. Ochterski, P. Y. Ayala, K. Morokuma, G. A. Voth, P. Salvador, J. J. Dannenberg, V. G. Zakrzewski, S. Dapprich, A. D. Daniels, M. C. Strain, O. Farkas, D. K. Malick, A. D. Rabuck, K. Raghavachari, J. B. Foresman, J. V. Ortiz, Q. Cui, A. G. Baboul, S. Clifford, J. Cioslowski, B. B. Stefanov, G. Liu, A. Liashenko, P. Piskorz, I. Komaromi, R. L. Martin, D. J. Fox, T. Keith, A. Laham, C. Y. Peng, A. Nanayakkara, M. Challacombe, P. M. W. Gill, B. Johnson, W. Chen, M. W. Wong, C. Gonzalez, J. A. Pople, **2003**

[8] C. Adamo, V. Barone, *J. Phys. Chem.* **1999**, *110*, 6158.

[9] T. H. Dunning, P. J. Hay, in *Modern Theoretical Chemistry*, Vol. 3, (Eds: H. F. Schaefer), Plenum, New York **1976.**

[10] R. Dithfie, W. J. Hehre, J. A. Pople, *J. Chem. Phys.* **1972**, *54*, 724.

[11] a) R. E. Stratmann, G. E. Scuseria, M. J. Frisch, *J. Chem. Phys.* **1998**, 109, 8218. b) R. Bauernschmitt, R. Ahlrichs, *Chem. Phys. Lett.* **1996**, *256*, 454. c) M. E. Casida, C. Jamorski, K. C.Casida, D. R. Salahub, *J. Chem. Phys.* **1998**, *108*, 4439.

[12] a) V. Barone, M. J. Cossi, *Phys. Chem. A* **1998**, 102, 1995. b) M. Cossi, N. Rega, G. Scalmani, V. Barone, *J. Comp. Chem.* **2003**, 24, 669.

[13] Xcalibur CCD System; Oxford Diffraction Ltd: Abingdon, Oxfordshire, England, 2007.

[14] R. C. Clark, J. S. Reid, *Acta Cryst.* **1995**, *A51*, 887.

[15] *CrysAlis*^{Pro} (versions 1.171.32.52-55), Oxford Diffraction Ltd, Abingdon, Oxfordshire, England.

[16] G. M. Sheldrick, *Acta Cryst.* **2008**, *A64*, 112.

[17] L. J. Farrugia, *J. Appl. Cryst.* **1999**, *32,* 837.

[18] A. L. Spek, *J. Appl. Cryst.* **2003**, *36*, 7.

Chapter 4 Tuning the Luminescent Properties of Pt(II) Acetylide Complexes through Varying the Electronic Properties of N-Heterocyclic Carbene Ligands

Publication 3. *Inorganic Chemistry,* **2013**, submitted.

Yuzhen Zhang, Jessica Clavadetscher, Michael Bachmann, Olivier Blacque, and KoushikVenkatesan*

Institute of Inorganic Chemistry, University of Zurich, Winterthurerstrasse 190, CH-8057, Zurich, Switzerland

Tuning the Luminescent Properties of Pt(II) Acetylide Complexes Through Varying the Electronic Properties of N-Heterocyclic Carbene Ligands

Yuzhen Zhang, Jessica Clavadetscher, Michael Bachmann, Olivier Blacque and Koushik Venkatesan*

Institute of Inorganic Chemistry, University of Zürich, Winterthurerstrasse 190, CH-8057, Zürich. Switzerland.

ABSTRACT: This paper reports the synthesis, structural characterization, electrochemistry and photophysical investigations of five groups of luminescent Pt(II) alkynyl complexes bearing N-heterocyclic carbene (NHC) ligands with varying electronic properties. Complexes of the type [Pt(**pmdb**)(C≡CR)$_2$] **1a-c**, [Pt(**pm2tz**)(C≡CR)$_2$] **2a-d**, [Pt(**pm3tz**)(C≡CR)$_2$] **3a-c**, [Pt(**ppim**)(C≡CR)$_2$] **4**(**a**, **b**, **e**) and [Pt(**ppbim**)(C≡CR)$_2$] **5**(**a**, **b**, **e**) where pmdb = 1,1'-dipentyl-3,3'-methylene-dibenzimidazoline-2,2'-diylidene, pm2tz = 1,1'-dipentyl-3,3'-methylene-di-1,2,4-triazoline-5,5'-diylidene, pm3tz = 1,1'-dipentyl-3,3'-methylene-di-1,3,4-triazoline-5,5'-diylidene, ppim = 3-pentyl-1-picolylimidazoline-2-ylidene,ppbim = 3-pentyl-1-picolylbenzimidazoline-2-ylidene and R = 4-C_6H_4F, C_6H_5, 4-C_6H_4OMe, $SiMe_3$ and 4-$C_6H_4N(C_6H_5)_2$ were prepared and the consequence of the electronic properties of the NHC ligands on the phosphorescent emission efficiencies were studied. Moreover, the emission quantum efficiencies of the previously reported complexes [Pt(**pmim**)(C≡CR)$_2$] where **pmim** = 1,1'-dipentyl-3,3'-methylene-diimidazoline-2,2'-diylidene and R = 4-C_6H_4F **6a**, C_6H_5 **6b** and 4-C_6H_4OMe **6c** were also recorded in neat solid and in 10 wt% PMMA film. The square planar coordination geometry with the alkynyl ligands in *cis* configuration was corroborated for selected complexes by single crystal X-ray diffraction studies. The observed moderate difference in emission efficiencies of the bis-carbene complexes **6a-c**, **1a-c**, **2a-c** and **3a-c** in conjunction with the decreasing electron-donating nature of the NHC ligands **pmim** > **pmdb** > **pm2tz** ≈ **pm3tz**, can be attributed to the slight modification of the triplet emission parentage among the different complexes. The quantum efficiencies of complexes **4(a**, **b)** and **5(a**, **b)** bearing pyridyl-NHC ligand were significantly low in comparison to the bis-carbene complexes owing to the significant change in the charge transfer character of the triplet manifold. Complexes **4e** and **5e** bearing diarylamine phenylacetylenes display high ϕ_{em} of 27 and 33% in 10 wt% PMMA film, respectively.

Introduction

Platinum(II) triplet emitters have been intensively investigated due to their interesting photophysical properties and their application in OLEDs.[1] In particular, high phosphorescent quantum efficiency combined with microsecond excited state lifetime has been successfully achieved by utilizing cyclometalating ligands as part of the molecular scaffold.[1f,2] Although highly efficient green and red emitters have been achieved and widely explored, stable and highly efficient deep blue emitters based on Pt(II) complexes remain scarce and less explored.[3] Recently, the groups of Strassner,[4] Li[2c,5] and Wang[6] have reported on the development of blue emitters utilizing cyclometalated NHC ligand as part of the coordination sphere of the Pt(II) complexes. The main reason for the high quantum efficiency displayed by the cyclometalated NHC complexes can be ascribed to the strong ligand field (LF) strength that effectively separates the closely associated emitting states and the non-radiative d-d excited states by raising the energy of the non-radiative metal-centered d-d excited states.[1j,7] Around the same time, our group also independently reported the first series of room temperature phosphorescent NHC Pt(II) acetylide [Pt(**pmim**)(C≡CR)$_2$] (**pmim** = 1,1'-dipentyl-3,3'-methylene-diimidazoline-2,2'-diylidene).[8] Some of the complexes displayed deep blue emission in solution albeit with low quantum efficiencies. The quantum efficiencies of the complexes could not be improved by altering the electronic nature of the alkynyl ligands, since the emission energies were significantly affected upon changing the substituents on the alkynyl ligands. Based on these results, it was surmised that employing a strategy that involved the altering of the donor properties of the NHC ligand would allow to tune emission quantum yields of these classes of molecules in the deep blue region without significantly shifting the emission energies. The systematic variation of the NHC donor properties was expected to affect the extent to which the low-lying d-d states are raised in

energy with respect to the emissive states and as a consequence impact the luminescent properties.

In this context, we report the preparation and photophysical investigations of five new groups of complexes [Pt(**pmdb**)(C≡CR)$_2$] **1a-c**, [Pt(**pm2tz**)(C≡CR)$_2$] **2a-d**, [Pt(**pm3tz**)(C≡CR)$_2$] **3a-c**, [Pt(**ppim**)(C≡CR)$_2$] **4(a, b, e)** and [Pt(**ppbim**)(C≡CR)$_2$] **5(a**, **b**, **e)**. The emission properties of the previously reported complexes [Pt(**pmim**)(C≡CR)$_2$] **6a-c** in neat solid and in 10 wt% PMMA film were examined. All five groups of complexes **1-5** were synthesized to assess the effect of the electronic nature of the NHC ligands on the emission quantum yields. Complexes **4e** and **5e** bearing the diarylaminephenylacetylene ligand exhibited green emission with high quantum efficiencies of 27% and 33% in 10 wt% PMMA film. Based on the different emission quantum yields of the above series of complexes bearing electronically different bidentate NHC ligands, the results are suggestive of the significant role of the electronic nature of the NHC ligands on the excited state responsible for the emission.

Results and Discussion

Synthesis and characterization. The precursor complexes **I**, **II** and **III** were prepared by slight modification of previous literature reports.[4a,8,9] The corresponding targeted dialkynyl complexes **1a-c**, **2a-d** and **3a-c** were synthesized in yields of 18-87% by reacting the precursor complexes **I**, **II** and **III** with lithiated acetylenes in dry Et_2O at 45 ^oC in a sealed Schlenk flask (Scheme 1 Left). A different strategy was followed for the synthesis of complexes **4(a, b**, **e)** and **5(a, b, e)**. Treatment of the silver salts of **ppim** and **ppbim** with [Pt(COD)(C≡CR)$_2$] in dichloromethane at room temperature (Scheme 1 Right) gave the corresponding dialkynyl complexes directly in good yields after purification by

chromatography on silica gel.[10] Due to partial decomposition of **4e** and **5e** during column chromatography, there was slight loss of the compounds during purification.

Scheme 1. Synthetic procedure for Pt(II) acetylide complexes bearing different NHC ligands.

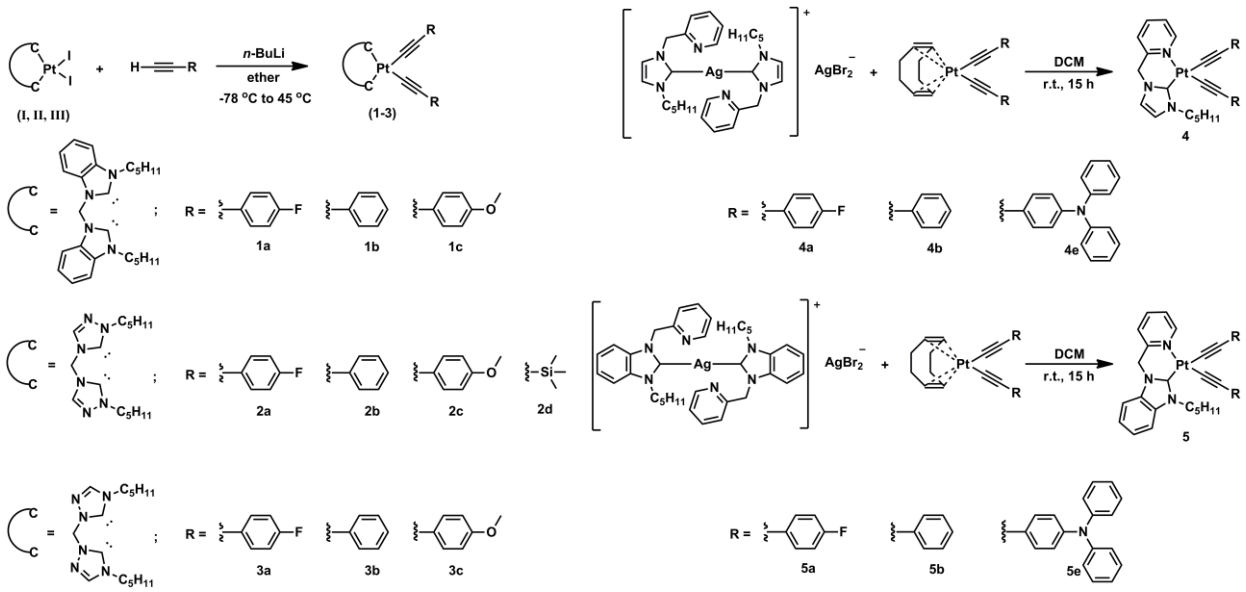

All the prepared complexes were characterized by ^{1}H NMR, ^{13}C NMR, elemental analyses and FT-IR spectroscopy. Single crystal X-ray diffraction studies were carried out for complexes **I**, **1a**, **1b** and **2a**. Although no single crystals suitable for the diffraction studies could be obtained in the case of complexes **3a-3c**, the distinct chemical shifts in the ^{13}C NMR spectra for the N*C*H$_2$N bridging the two triazole units in these complexes provide a strong indication of the structure being different from complexes **2a-2c**. The characteristic resonances observed in the ^{13}C NMR spectra at around 170 ppm for the coordinated carbene ligand and at 102 and 109 ppm for the alkynyl ligand along with the stretching vibration bands at 2100 cm^{-1} in the IR spectra further confirmed the coordination of the acetylide ligand.

Crystal Structure Determination. Single crystals of **I**, **1a**, **1b** and **2a** were obtained by slow evaporation of a mixture of CH_2Cl_2/pentane and the plots of the molecular structures are

shown in Figure 1. The crystallographic details are summarized in Table S1 and selected bond lengths and angles are listed in Table 1. All the four Pt(II) complexes exhibit distorted square planar coordination geometry with two alkynyl ligands disposed *cis* to each other. The dihedral angles of 52.9(2)^{o} for **I**, 40.3 – 42.5^{o} for **1a**, 40.96(4) – 46.20(1)^{o} for **1b**, and 38.9(3) – 42.3(2)^{o} for **2a**, dissecting the NHC plane and the distorted Pt square plane, were found to be strikingly different from each other. The bond length of 1.976(5) Å for the Pt-C_{carb} bond in the precursor complex **I** was found to be shorter than those in **1a** (2.027(6) and 2.033(6) Å) and **1b** (2.0307(6), 2.0327(7), 2.0052(6) and 2.0223(6) Å). The C_{alk}-Pt-C_{alk} angles were found to be strongly varying between the complexes **1a**, **1b** and **2a** which are 86.7(3)^{o} for **1a**, 85.6(3) and 86.68(3)^{o} for **1b**, and 90.4(3)^{o} and 91.8(3)^{o} for **2a**. The smaller C_{alk}-Pt-C_{alk} angle found for **1a** in comparison to **2a** could be attributed to the large extrusion force of **pmdb**.

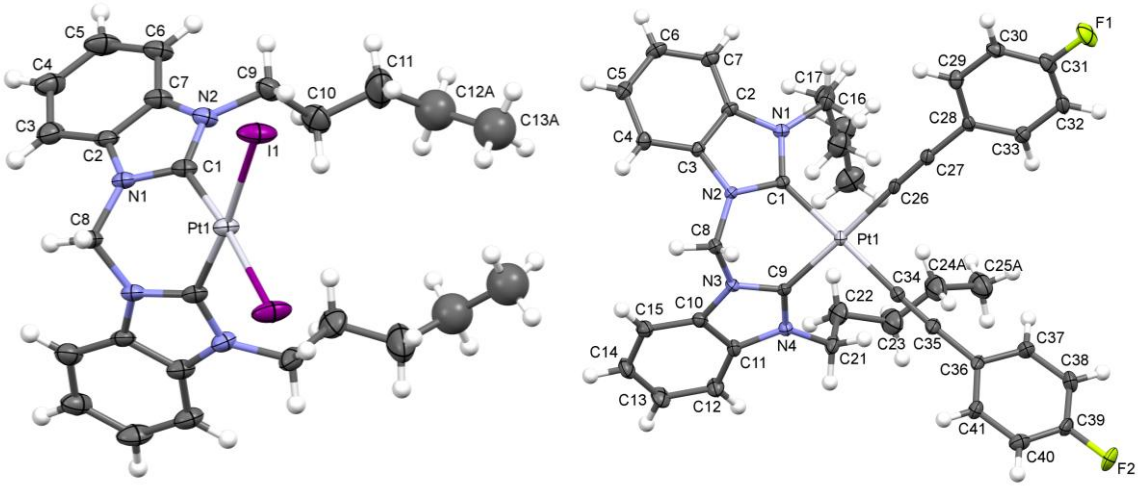

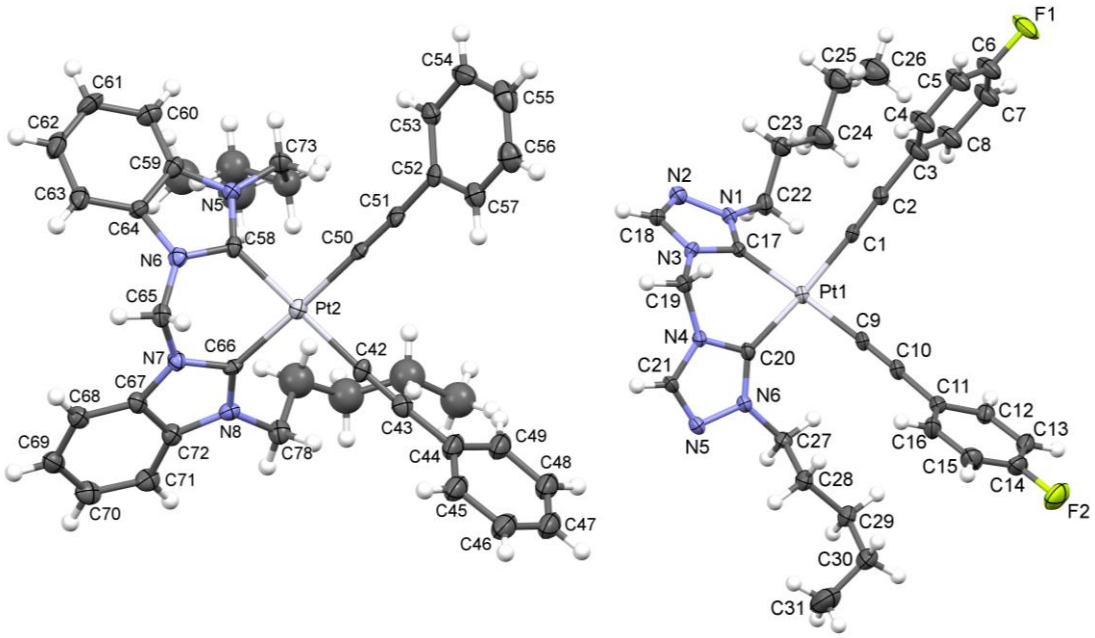

Figure 1. Molecular structures of **I** (top left), **1a** (top right), **1b** (bottom left) and **2a** (bottom right) with a selective atomic numbering scheme. Thermal ellipsoids are drawn at the 30% probability level. Disorders and solvent molecules are omitted for clarity and the hydrogen atoms are presented as white spheres.

Table 1. Selected bond lengths and angles for complexes **I**, **1a**, **1b**, and **2a**.

	bond length (Å)		*bond angle (deg)*
Complex **I**			
C1 – Pt1	1.976(5)	C1 – Pt1 – C1^{i}	83.6(3)^{a}
I1 – Pt1	2.6534(4)	I1 – Pt1 – I1^{i}	89.57(2)
Complex **1a**			
C1 – Pt1	2.027(6)	C1 – Pt1 – C9	85.0(2)
C9 –Pt1	2.033(6)	C1 – Pt1 – C26	93.5(2)
C26 – Pt1	2.013(7)	C9 – Pt1 – C34	94.8(2)
C34 – Pt1	2.008(7)	C26 – Pt1 – C34	86.7(3)
Complex **1b** (two crystallographically independent molecules)			
C1 – Pt1	2.011(10)	C1 – Pt1 – C9	85.6(3)
C9 – Pt1	2.0220(6)	C1 – Pt1 – C17	94.5(3)
C17 – Pt1	2.0307(6)	C9 – Pt1 – C25	94.25(3)
C25 – Pt1	2.0327(7)	C17 – Pt1 – C25	85.63(3)
C42 – Pt2	1.9862(6)	C42 – Pt2 – C50	86.68(3)
C50 – Pt2	2.0114(7)	C42 – Pt2 – C66	94.90(3)
C58 – Pt2	2.0052(6)	C50 – Pt2 – C58	93.12(3)
C66 – Pt2	2.0223(6)	C58 – Pt2 – C66	85.29(2)
Complex **2a** (two crystallographically independent molecules)			

C1 – Pt1	2.006(8)	C1 – Pt1 – C9	90.4(3)
C9 – Pt1	2.000(8)	C1 – Pt1 – C17	91.7(3)
C17 – Pt1	2.022(7)	C9 – Pt1 – C20	92.1(3)
C20 – Pt1	2.018(8)	C17 – Pt1 – C20	85.6(3)
C32 – Pt2	2.026(10)	C32 – Pt2 – C40	91.8(3)
C40 – Pt2	2.008(9)	C32 – Pt2 – C48	91.1(3)
C48 – Pt2	2.014(8)	C40 – Pt2 – C51	91.8(3)
C51 – Pt2	2.020(9)	C48 – Pt2 – C51	85.1(3)

[a]symmetry code: *i* = x, y, −z+3/2.

Photophysical properties. The UV-Vis absorption spectra of complexes **1a-c**, **2a-d** and **3a-c** show absorption bands in the range of 250-295 nm and 300-340 nm with molar extinction coefficients in the range of 10^4 M^{-1} cm^{-1} in dichloromethane except in the case of complex **2d**, which was found to possess low extinction coefficient (Figures 2-4, Figure S1). The absorption maxima of the complexes **1a**, **1b** and **1c** bearing the **pmdb** ligand and electronically different alkynyls display modest bathochromic shifts going from **1a** to **1b**, but a significant shift to lower energy was observed in the case of **1c**. The extent of the observed red shift is consistent with the increasing electron donating nature of the alkynyl in the order F < H < OMe. A strong hypsochromic shift of the absorption band was found for complexes **2b** and **3b** with respect to **1b**. The shifts are consistent with the decreasing electron donating nature of the NHC ligand in the order **pmdb** < **pm2tz** < **pm3tz**.[11] Based on the experimental studies and DFT/TDDFT calculations, the nature of the transitions responsible for the low energy absorption bands in these complexes are assigned to a mixture of metal-perturbed intra-ligand ^{1}ILCT($\pi_{alk}\rightarrow\pi^*_{alk}$), metal-perturbed ligand-to-ligand ^{1}LLCT($\pi_{alk}\rightarrow\pi^*_{carb}$) transition and metal-to-ligand ^{1}MLCT(Pt$\rightarrow\pi^*_{alk}$). In the higher energy part of the absorption spectrum, only one prominent band was observed for complexes **2a-c** and **3a-c** with extinction coefficients of 5 × 10^4 M^{-1} cm^{-1} and the parentage of this band is ascribed to a metal-perturbed intraligand ^{1}ILCT ($\pi_{alk}\rightarrow\pi^*_{alk}$) transition. However, in comparison to the complexes **2a-c** and **3a-c**, complexes **1a-c** showed an additional absorption band at a higher

energy. The origin of the band is assigned to transitions involving a metal-perturbed ^{1}ILCT ($\pi_{alk}\rightarrow\pi^*_{carb}$). Complexes **4b** and **5b** possess a low energy absorption band that is bathochromically shifted by 9 nm (824 cm^{-1}) in comparison of complexes **2b** and **3b** but only 2 nm (177 cm^{-1}) hypsochromic shift than **1b** owing to the influence of NHC-pyridyl ligand (Figures 3 and 4). An additional band appears as a shoulder between the high and low energy absorption bands which is tentatively assigned to intraligand ^{1}IL ($\pi_{pyr}\rightarrow\pi^*_{pyr}$) transition. The absorption spectrum of complexes **4e** and **5e** exhibit one main strong absorption band at 330 nm with extinction coefficients around 6×10^4 M^{-1} cm^{-1} (Figures 3, 4) and the nature of the transition is assigned as a mixture of ^{1}IL, ^{1}LLCT and ^{1}MLCT.

In order to obtain more information on the nature of the charge-transfer state, solvatochromic behavior of the representative molecules **1b**, **2b**, **3b**, **4b** and **5b** in toluene, CH_2Cl_2, THF, CH_3CN and MeOH (Figure 5, Figures S2-S5) was studied. The solvent dependent changes of the lowest-energy absorption maxima were observed for all of the five complexes. They show negative solvatochromic behavior with shifts ranging between 11-27 nm (~ 1039 - 2252 cm^{-1}). Significant shifts were observed particularly for complexes **4b** and **5b** bearing the pyridyl-NHC ligand. The negative solvatochromic behavior indicates a more polar ground state than the excited state.[1k,12] This is further substantiated by the estimation of the dipole moment by TD-DFT calculations for complexes **1b**-**5b**. Similar behavior has been previously reported in the case of metal dithiolate complexes.[12a] Since the evaluated complexes bearing the same alkynyl but different NHC ligand show different extent of shifts, the nature of the charge transfer excitation could be composed of varying degrees of metal perturbed ^{1}LLCT and ^{1}MLCT.

The phosphorescence emission was measured in deaerated dichloromethane at room temperature (r.t.) and only complexes **1a-c**, **2a**, **2c** and **3a-c** exhibited emission (Figures S6-

S8) in solution that can be quenched by oxygen. The emission profiles of the complexes **1a-c** and **3a-c** were broad, structureless and their emission maxima were in the range of 430-450 nm. The emission energy displayed changes reflecting the different electronic properties of the alkynyl ligand (F < H < OMe). Complexes **2b**, **2d**, **4a**, **4b**, **4e**, **5a**, **5b** and **5e** did not display any observable emission in fluid solution at r.t. and the possible reason for this behavior is ascribed to solvent effects and self quenching. At 77K frozen glass state, all complexes exhibit intense and well-structured phosphorescence emission in 2-MeTHF except in the case of complex **2d** for which no noticeable emission was observed (Figures S9-S13). We conclude that the presence of trimethylsilyl group in **2d** leads to an increase in the energy gap of ($\pi_{alk} \rightarrow \pi^*_{alk}$) further resulting in a non-radiative decay of the excited state. The phosphorescence emission maxima for the complexes at 77K were in the range of 430-440 nm with structured bands that are typically characteristic of ^{3}ILCT($\pi_{alk} \rightarrow \pi^*_{alk}$). Complexes **4e** and **5e** display emission at a lower energy around 480 nm consistent with the strong electron donating nature of the diarylaminephenylacetylene. The solid state emission properties of the complexes were investigated in neat solid and in 10 wt% PMMA film. The emission spectra of all the complexes except **2d** are shown in Figures 2-4. In contrast to the moderate to good luminescence observed for the complexes in 10 wt% PMMA, the luminescence was found to be very weak in neat solid. The emission wavelength maxima of the complexes appear quite close in the different measured medium (solution, neat solid, 10% PMMA and 77K frozen matrix), albeit with a small blue shift in the 77K frozen matrix due to the enhanced rigidochromic effect. The strongly correlated emission maxima among the different medium along with the absence of concentration dependent emission wavelength changes is strongly suggestive of low quantum yields in neat solid versus the complexes doped in PMMA could be due to a self-quenching process rather than an excimer formation.[13] And also any Pt···Pt

interactions can be ruled out, since the Pt···Pt distances for the complexes **1a**, **1b** and **2a** were found to be 7.7164 (6), 5.7262(6) and 7.8761(5) Å, respectively.

Due to the weak luminescence in fluid solution, emission quantum yields were not measured in solution and instead measurements were made both in the neat solid and 10 wt% PMMA film. Solid-state quantum yields were also recorded for the previously reported complexes [Pt(pmim)C≡CR] (R = F **6a**, H **6b**, OMe **6c**) by our group for comparison reasons (Table 2). Owing to the strong aggregation of the complexes in the neat solid, the quantum yields were below 1%, but they were found to be as high as 33% in 10 wt% PMMA film. For complexes **1a-c**, **2a-c**, **3a-c** and **6a-c** the quantum yields were in the range of 14 to 33%. It was observed that the complexes **1b**, **2b**, **3b** and **6b** bearing phenylacetylene ligand always displayed lower quantum yields than the rest of the complexes bearing 4-florophenylacetylene (**1a**, **2a**, **3a** and **6a**) and 4-methoxylphenylacetylene (**1c**, **2c**, **3c** and **6c**) as ancillary ligands. While the complexes **4a**, **4b**, **5a** and **5b** exhibited a low quantum yield of 5 to 8%, complexes **4e** and **5e** displayed higher quantum efficiencies of 27% and 33% albeit at lower emission energies due to the electronically different alkynyl ligand. The comparatively low quantum yields of complexes **4a**, **4b**, **5a** and **5b** are tentatively ascribed to the competing non-radiative decay of low-lying d-d states caused by the less strongly electron-donating pyridyl-NHC ligand. Further experimental studies are required to ascertain the nature of the processes contributing to the non-radiative process in these complexes, which is currently in progress.

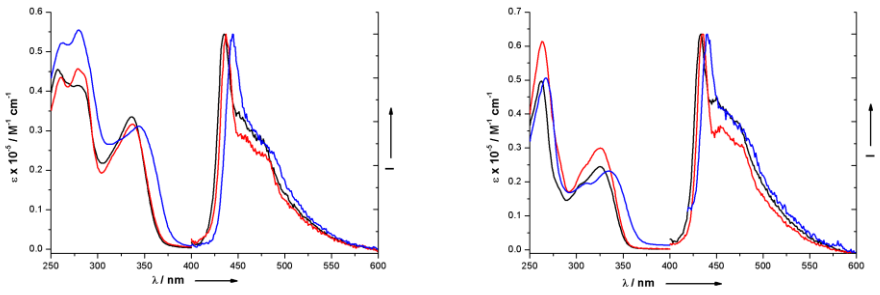

Figure 2. (Left) Electronic absorption spectra of **1a** (black), **1b** (red), **1c** (blue) in DCM, and normalized emission spectra of **1a** (black), **1b** (red), **1c** (blue) in 10wt% PMMA film. (Right) Electronic absorption spectra of **2a** (black), **2b** (red), **2c** (blue) in DCM, and normalized emission spectra of **2a** (black), **2b** (red), **2c** (blue) in 10wt% PMMA film.

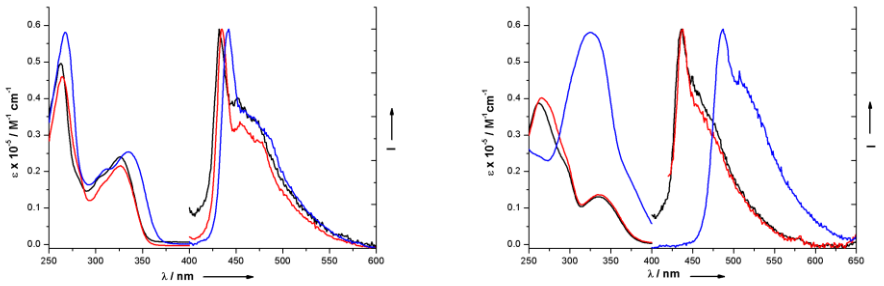

Figure 3. (Left) Electronic absorption spectra of **3a** (black), **3b** (red), **3c** (blue) in DCM, and normalized emission spectra of **3a** (black), **3b** (red), **3c** (blue) in 10wt% PMMA film. (Right) Electronic absorption spectra of **4a** (black), **4b** (red), **4e** (blue) in DCM, and normalized emission spectra of **4a** (black), **4b** (red), **4e** (blue) in 10wt% PMMA film.

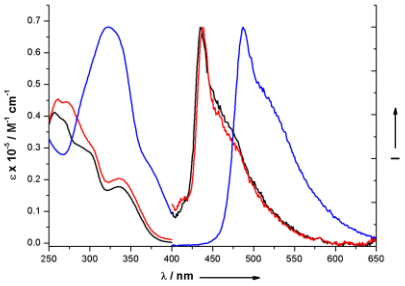

Figure 4. Electronic absorption spectra of **5a** (black), **5b** (red), **5e** (blue) in DCM, and normalized emission spectra of **5a** (black), **5b** (red), **5e** (blue) in 10 wt% PMMA film.

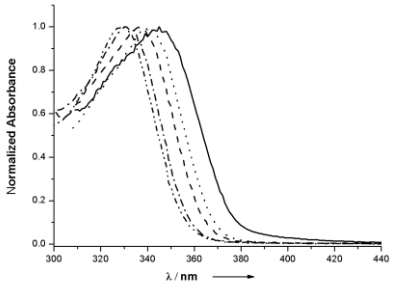

Figure 5. UV-Vis absorption spectra of **1b** in toluene (—), THF (···), CH_2Cl_2 (---), CH_3CN (-·-·-·), and MeOH(-··-··).

Table 2. Photophysical properties of complexes **1a-c**, **2a-d**, **3a-c**, **4(a, b, e)**, **5(a, b, e) and 6a-c**.

	Absorption (CH_2Cl_2)		emission			
complex		medium (T/K)	λ_{max}/nm (τ_0/ μs)	ϕ_{em} (%)	k_r[$\times 10^3$ s^{-1}]	k_{nr}[$\times 10^5$ s^{-1}]
1a	257 (45521), 280 (41444), 337 (33479)	CH_2Cl_2 (298)	436, 523 sh	-		
		glass (77)	433, 450 sh, 475 sh	-		
		solid (298)	435, 451, 467	1.0		
		PMMA (298)	437, 473 (3.50)	19.3	55.1	2.3
1b	261 (43480), 280 (45723), 337 (31660)	CH_2Cl_2 (298)	437, 530 sh	-		
		glass (77)	437, 459 sh, 484 sh	-		
		solid (298)	-	<1		
		PMMA (298)	437, 480 (1.94)	14.6	75.2	4.4
1c	263 (55241), 280 (55483), 344 (31109)	CH_2Cl_2 (298)	445, 541 sh	-		
		glass (77)	437, 455 sh, 476 sh			
		solid (298)	-	<1		
		PMMA (298)	445, 483 sh (2.20)	22.8	103.6	3.5
2a	263 (44668), 326 (24497)	CH_2Cl_2 (298)	437, 533			
		glass (77)	427, 447 sh, 470	-		
		solid (298)	-	<1		
		PMMA (298)	436, 478 (1.23)	17.6	143.1	6.7
2b	263 (61370), 326 (29949)	CH_2Cl_2 (298)	-			

		glass (77)	432, 454 sh, 478 sh	-		
		solid (298)	-	<1		
		PMMA (298)	436, 478 sh (1.47)	14.1	95.9	5.8
2c	267 (50594), 335 (23223)	CH_2Cl_2 (298)	445, 545 sh	-		
		glass (77)	435, 461 sh, 483 sh	-		
		solid (298)	-	<1		
		PMMA (298)	440, 477 sh (0.10)	32.8	3280	67.2
2d	272 (20951), 315 (16973)	CH_2Cl_2 (298)	-	-		
		glass (77)	-	-		
		solid (298)	-	-		
		PMMA (298)	-	-		
3a	263 (49662), 326 (23962)	CH_2Cl_2 (298)	435, 512 sh	-		
		glass (77)	426, 447, 465	-		
		solid (298)	-	<1		
		PMMA (298)	432, 453 sh (0.03)	19.3	6433	268.9
3b	264 (46001), 326 (21497)	CH_2Cl_2 (298)	435, 521 sh			
		glass (77)	432, 453 sh, 475 sh	-		
		solid (298)	-	<1		
		PMMA (298)	435, 457 sh (1.85)	17.7	95.7	4.4
3c	267 (58124), 335 (25367)	CH_2Cl_2 (298)	442, 515 sh	-		
		glass (77)	436, 456 sh, 481 sh	-		
		solid (298)	-	<1		
		PMMA (298)	442, 473 sh (2.9)	28.1	96.9	2.5
4a	262 (38656), 292 (23122), 335 (13123)	CH_2Cl_2 (298)	-	-		
		glass (77)	426, 448 sh, 476 sh	-		
		solid (298)	-	<1		
		PMMA (298)	437, 475 sh (1.56)	5.6	35.9	6.0
4b	265 (40143), 297 (22919), 335 (13640)	CH_2Cl_2 (298)	-	-		
		glass (77)	430, 452, 478	-		
		solid (298)	-	<1		
		PMMA (298)	438, 472 (1.98)	5.0	25.2	4.8
4e	325 (58013), 375 (17303)	CH_2Cl_2 (298)	-	-		

		glass (77)	478, 490 sh, 521 sh	-		
		solid (298)	-	<1		
		PMMA (298)	487, 507 sh (2.16)	26.6	123.1	3.4
5a	257 (41178), 300 (28590), 335 (17794)	CH_2Cl_2 (298)	-	-		
		glass (77)	427, 446, 484 sh	-		
		solid (298)	-	<1		
		PMMA (298)	436, 478 sh (1.82)	7.7	42.3	5.1
5b	261 (46426), 301 (31047), 335 (20351)	CH_2Cl_2 (298)	-	-		
		glass (77)	431, 450 sh, 486 sh	-		
		solid (298)	-	<1		
		PMMA (298)	438, 483 sh (1.94)	8.1	41.7	4.7
5e	322 (68108), 381 (20633)	CH_2Cl_2 (298)	-	-		
		glass (77)	479, 508 sh, 530 sh	-		
		solid (298)	485, 517 sh	1.1		
		PMMA (298)	488, 520 sh (2.59)	32.7	126.2	2.6
6a[a]	264 (48600), 324 (29400)	CH_2Cl_2 (298)	440, 475 sh	-		
		glass (77)	429, 455 sh	-		
		solid (298)	437, 471 sh	2.9		
		PMMA (298)	439, 473 sh (3.02)	18	59.2	2.7
6b[a]	266 (51700), 330 (28600)	CH_2Cl_2 (298)	442, 482 sh	-		
		glass (77)	437, 456 sh,	-		
		solid (298)	439, 478 sh	4.8		
		PMMA (298)	441, 480 sh	17.7		
6c[a]	323 (44600)	CH_2Cl_2 (298)	447, 475 sh	-		
		glass (77)	440, 484 sh	-		
		solid (298)	443, 469 sh	2.0		
		PMMA (298)	445, 473 sh	17.7		

[a]: data from reference 8.

Electrochemical properties

The cyclic voltammetric data for the complexes are listed in Table 3. All the complexes were measured in DCM using 0.1 M [*n*-Bu_4N][PF_6] as supporting electrolyte and ferrocenium/ ferrocene (Fc^+/ Fc) was used as an internal reference for calibration. Although no reduction wave was observed for any of the complexes including complexes **4(a, b, e)** and **5(a, b, e)** bearing pyridyl group in the ligand scaffold on scanning up to -2.18 V in DCM, an irreversible reduction wave was observed in DMF in the range -2.53 - -2.44 V (See supporting information Table S2). This pyridyl ligand based reduction was found to be shifted to more negative potentials in comparison to the polypyridyl Pt(II) acetylide complexes.[12b,14] This observation is similar to the behavior of the previously reported complexes [Pt(**pmim**)($C{\equiv}CR)_2$] and [Pt(phospine)$_2$($C{\equiv}CR)_2$].[15] However, it is quite different to the reported polypyridyl Pt(II) acetylide complexes which have one or more reversible reduction waves attributed to the polypyridyl ligand. Complexes **1a-c**, **2a-d** and **3a-c** displayed only one oxidation wave and the oxidation potential varied depending on both the nature of the alkynyl ligand and the NHC ligand. For example in complexes **1a-c**, the oxidation potential decreased with increasing electron richness of the acetylide. This trend is consistent with the energy of the emission. Comparison of the oxidation potential among the complexes **1a** (+0.77 V), **2a** (+0.80 V) and **3a** (+0.82 V), the potential was found to increase with the decreasing electron-donating character of the NHC ligand in the order **pmdb** < **pm2tz** < **pm3tz**. A significant increase in the oxidation potential of +1.19 V was observed for complex **2d**, strongly indicating a low-lying HOMO and as a result showing no emission in all kind of medium at room temperature. Complexes **4a**, **4b**, **5a** and **5b** also exhibit one oxidative wave at similar potentials in comparison to the other three groups of complexes. Complexes **4e** and **5e** exhibit one irreversible oxidation wave at +0.34 V and +0.24 V and additionally one quasi-reversible wave at +0.56 V and +0.58 V, respectively. However in DMF, two quasi-reversible waves at +0.28 V and +0.44 V were observed for complex **4e** and at +0.29 V and 0.45 V for complex

5e (Table S2**)**. The first oxidation wave was ascribed to the oxidation of C≡CR and the second quasi-reversible waves are likely to be triphenylamine-based oxidation with some mixing of metal-centered character. The strong shifts in the oxidation potential indicate the relative changes in the positions of the HOMO level among the complexes that affects also the emission energies significantly. The complexes with lower oxidation potentials indicate relatively high lying HOMOs and these complexes possess better emission quantum yields.

Table 3. Electrochemical data[a] for complexes **1a-c**, **2a-d**, **3a-c**, **4(a, b, e)** and **5(a, b, e)**.

Complex	E_{ox} (V)
1a	+0.77
1b	+0.76
1c	+0.50
2a	+0.80
2b	+0.75
2c	+0.53
2d	+1.19
3a	+0.82
3b	+0.82
3c	+0.57
4a	+0.73
4b	+0.72
4e	+0.34, +0.56 (quasi-reversible)
5a	+0.77
5b	+0.77
5e	+0.24, +0.58 (quasi-reversible)

[a] Scan rate = 100 mVs^{-1} in 0.1 M [*n*-Bu_4N][PF_6] (Au electrode; E vs Fc^+/ Fc; 20 ^oC; DCM).

DFT and TD-DFT Calculations.

In order to study the luminescent properties of our Pt(II) alkynyl complexes bearing N-heterocyclic carbene ligands, we performed DFT and TD-DFT calculations for **1b** – **5b** (which bear the same phenylacetylide ligand) with the *Gaussian03* program package.[16] The hybrid functional PBE1PBE[17] (also known as PBE0) in conjunction with the Stuttgart/Dresden effective core potentials (SDD) basis set[18] for the Pt center augmented with one *f*-polarization function (exponent = 0.993) and the standard 6-31+G(d) basis set[19] for the

remaining atoms was applied for all calculations. Full geometry optimizations without symmetry constraints were carried out in the gas phase for the singlet ground states (S_0) and the lowest triplet states (T_1). The optimized geometries S_0 and T_1 were confirmed to be potential energy minima by vibrational frequency calculations at the same level of theory, as no imaginary frequency was found. The first 10 singlet-singlet and singlet-triplet transition energies were computed at the optimized S_0 geometries, by using the time-dependent DFT (TD-DFT) methodology.[20] Solvent effects were taken into account using the conductor-like polarizable continuum model (CPCM)[21] with dichloromethane as solvent for single-point calculations on all optimized gas-phase geometries.

The experimental UV–Vis absorption spectra of complexes **1b** – **5b** in dichloromethane at room temperature show absorption bands in the range of 260 – 295 nm and 325 – 340 nm. The absorption maxima experimentally observed in the range 325 – 340 nm for each compound **1b** – **5b** arises from the overlap of the TD-DFT calculated $S_0 \rightarrow S_1$ and $S_0 \rightarrow S_2$ singlet-singlet transitions (Table 4). The one-electron excitations involved in these transitions are HOMO→LUMO and HOMO-1→LUMO. For compounds **1b**, **2b** and **3b**, the analysis of the frontier molecular orbitals reveals that the low energy absorption band corresponds to a mixture of metal-perturbed ligand-to-ligand $^1LL(\pi_{alk} \rightarrow \pi^*_{carb})$ charge transfer and metal-perturbed intra-ligand $^1IL(\pi_{alk} \rightarrow \pi^*_{alk})$ charge transfer (Figure 6, Table 5). For compounds **4b** and **5b**, the LUMO is mainly located on the pyridine ligand (72 – 84%) and shows very small contributions from the carbene ligand (2 – 8%) and the metal center (7 – 9%). In the occupied orbitals HOMO and HOMO-1, the electron density is mainly located on the metal center (13 – 18%) and on one alkynyl ligand: the alkynyl ligand *trans* to the pyridine ring in HOMO (82 – 83%), and the alkynyl ligand *trans* to the carbene in HOMO-1 (70%) (Figure 7, Table 6). Consequently, the origin of the absorption maxima in **4b** and **5b** is clearly different from those in **1b** – **3b** due to the presence of the pyridine ligand and can be assigned to transitions

involving ligand-to-ligand ^{1}LL($\pi_{alk(trans\ to\ pyr)}\rightarrow\pi^*_{pyr}$) and ^{1}LL($\pi_{alk(trans\ to\ carb)}\rightarrow\pi^*_{pyr}$) charge transfers as well as metal-to-ligand ^{1}ML(Pt$\rightarrow\pi^*_{pyr}$) charge transfer. The absorption bands observed at higher energies in the range of 260 – 295 nm are produced from the overlap of two to four significant singlet-singlet transitions with oscillator strength *f* greater than 0.07 (Table 4) involving many frontier orbitals (Figures S14-S18). In all cases, the bands originate with metal-to-ligand ^{1}ML[Pt $\rightarrow\pi^*_{carb}$ (**1b** – **3b**) or Pt$\rightarrow\pi^*_{pyr}$ (**4b** – **5b**)] and ligand-to-ligand ^{1}LL[$\pi_{alk}\rightarrow\pi^*_{carb}$ (**1b**, **5b**), $\pi_{alk}\rightarrow\pi^*_{alk}$ (**2b** – **4b**) or $\pi_{alk}\rightarrow\pi^*_{pyr}$ (**4b** – **5b**)] charge transfers. For compounds **2b** and **3b**, a sizable amount of intra-ligand ^{1}ILCT($\pi_{alk}\rightarrow\pi^*_{alk}$) character can also be deduced from the TD-DFT calculations. The origin of the lowest energy abosprtion bands involving more than one transitions is quite unique and has been only observed in the case of plaintum(II) diimine diacetylide complexes.[12d]

The lowest singlet–triplet vertical excitation ($T_1 - S_0$) energies obtained by TD-DFT on the ground state structures of **1b – 5b** are consistent with the experimental solid state emission properties in 10 wt% PMMA film. The calculated values are slightly underestimated by 8 – 13 nm for **1b** – **3b**, and are in a very good agreement for **4b** – **5b** (Table 4). The promotion of one electron to unoccupied orbitals leads to high-energy electronic excited states, then spin-orbit interaction between excited states operates to induce S→T intersystem crossing to form the corresponding triplet excited states, and geometry relaxation leads to the lowest energy triplet state (emitting state) for which the optimized structure can be determined by DFT calculations. The geometry of the DFT optimized triplet states of **1b** – **5b** corresponds well to the structural distortions expected upon promotion of one electron to the C≡C antibonding or nonbonding LUMO, LUMO+1 and/or LUMO+2 from the C≡C bonding HOMO and/or HOMO-1 (Figures S14-18) as revealed by the contributions of the TD-DFT S_0–T_1 transitions (Table 4). Due to the symmetry of the involved molecular orbitals, the elongation of the C≡C bond associated to the shortening of the Pt–C and C–C_{Ph} bonds occurs only for one alkynyl

ligand. Indeed, the Pt–C bond lengths vary from 1.983 – 1.986 Å in the ground states to 1.926 – 1.939 Å in the triplet states (maximum deviation of 0.060 Å for **4b**), the C≡C bond lengths increase from 1.226 – 1.228 Å to 1.266 – 1.273 Å (maximum deviation of 0.046 Å for **2b** and **3b**), while the C–C_{Ph} bond lengths decrease from 1.424 – 1.425 Å to 1.356 – 1.370 Å (maximum deviation of 0.069 Å for **3b**). The second alkynyl ligand remains almost unchanged, the average variation of the corresponding Pt–C, C≡C, and C–C_{Ph} bond distances is 0.003 Å with a maximum deviation of 0.012 Å for the Pt–C bond length in **4b** (alkynyl *trans* to pyridine ligand). For the unsymmetric molecules **4b** and **5b**, it is important to note that the ^{3}ILCT is likely to take place from the alkynyl *cis* to the pyridine ligand. The spin density plots, which take into account the electron density on all α and β singly occupied orbitals of the triplet states, confirm the assumptions described above and visually identify the phosphorescence of our molecules (Figure 8). The emitting states of compounds **1b** – **3b** are very similar showing ^{3}ILCT($\pi_{alk}\rightarrow\pi^*_{alk}$) and ^{3}MLCT(Pt$\rightarrow\pi^*_{alk}$) characters, while the presence of the pyridine ligand in **4b** – **5b** reduces the contribution of the metal center and increases the participation of the N-heterocyclic carbene ligands through metal-perturbed ^{3}LLCT($\pi_{pyr}\rightarrow\pi^*_{alk}$) and ^{3}ILCT($\pi_{alk}\rightarrow\pi^*_{alk}$) characters (Tables 5 – 6).

Table 4. Selected singlet-singlet (S_0–S_n) and singlet-triplet (S_0–T_1) excited states with TD-DFT/CPCM (in dichloromethane) vertical excitation energies (nm), transition coefficients, orbitals involved in the transitions, and oscillator strengths *f* for compounds **1b – 5b** (with *f*> 0.07).

	1b	**2b**	**3b**	**4b**	**5b**
exp abs λ_{max} [a]	337, 280, 261	326, 263	326, 264	335, 297, 265	335, 301, 261
S_0–S_n	*n* = 1	*n* = 1	*n* = 1	*n* = 1	*n* = 1
	352 (*f* = 0.258)	336 (*f* = 0.149)	336 (0.121)	376 (0.093)	372 (0.158)
	H-1→LUMO (0.69)	HOMO→LUMO (0.69)	HOMO→LUMO (0.69)	HOMO→LUMO (0.57)	H-1→LUMO (0.54)
				H-1→LUMO (0.42)	HOMO→LUMO (0.45)
	n = 2	*n* = 2	*n* = 2	*n* = 2	*n* = 2
	347 (*f* = 0.285)	329 (*f* = 0.290)	327 (0.229)	362 (0.172)	365 (0.202)
	HOMO→LUMO (0.69)	H-1→LUMO (0.70)	H-1→LUMO (0.70)	H-1→LUMO (0.56)	HOMO→LUMO (0.52)
	n = 4	*n* = 4	*n* = 3	*n* = 3	*n* = 3
	309 (*f* = 0.274)	295 (*f* = 0.223)	300 (0.075)	326 (0.099)	327 (0.082)
	H-3→LUMO (0.68)	H-3→LUMO (0.68)	H-2→LUMO (0.69)	H-2→LUMO (0.68)	H-2→LUMO (0.67)
	n = 6	*n* = 6	*n* = 4	*n* = 5	*n* = 5
	295 (*f* = 0.317)	282 (*f* = 0.514)	292 (0.242)	308 (0.323)	315 (0.560)
	H-1→L+1 (0.68)	HOMO→L+1 (0.55)	H-3→LUMO (0.68)	HOMO→L+1 (0.57)	H-1→L+1 (0.65)
				H-1→L+1 (0.37)	
	n = 7		*n* = 6	*n* = 8	*n* = 8
	290 (*f* = 0.256)		277 (*f* = 0.544)	303 (0.389)	300 (0.085)
	HOMO→L+1 (0.68)		HOMO→L+1 (0.53)	HOMO→L+2 (0.55)	H-1→L+2 (0.58)
				H-1→L+2 (0.39)	HOMO→L+2 (0.39)
	n = 8		*n* = 9		
	287 (*f* = 0.129)		266 (*f* = 0.412)		
	HOMO→L+2 (0.61)		HOMO→L+2 (0.63)		
exp emiss λ_{max} [b]	437, 480sh	436, 478sh	435, 457sh	438, 472sh	438, 483sh
T_1–S_0	429	424	422	437	438
	HOMO←LUMO (0.40)	H-1←LUMO (0.41)	H-1←LUMO (0.36)	HOMO←L+2 (0.37)	H-1←LUMO (0.28)
	HOMO←L+2 (0.34)	HOMO←L+1 (0.38)	HOMO←L+1 (0.38)	HOMO←L+1 (0.22)	H-1←L+1 (0.27)
				H-1←L+2 (0.22)	HOMO←LUMO (0.26)

[a] in dichloromethane [b] 10 wt% PMMA film.

Table 5. Frontier orbitals of the DFT optimized ground state S_0 and triplet state T_1 structures of **1b** – **3b**: energy levels and compositions.

		1b				**2b**				**3b**			
	MO	Energy (eV)	Composition (%)			Energy (eV)	Composition (%)			Energy (eV)	Composition (%)		
			carbene	*alkynes*	*Pt*		*carbene*	*alkynes*	*Pt*		*carbene*	*alkynes*	*Pt*
Ground-state	L+2	-0.57	36	**60**	5	-0.45	29	**64**	7	-0.49	18	**80**	2
	L+1	-0.92	**94**	4	3	-0.48	3	**94**	3	-0.51	10	**86**	4
	LUMO	-1.51	**62**	18	20	-1.35	**42**	30	28	-1.34	**42**	30	28
	HOMO	-5.83	2	**91**	7	-5.90	3	**84**	13	-5.90	3	**84**	13
	H-1	-5.83	7	**79**	14	-5.91	1	**94**	5	-5.93	2	**94**	4
	H-2	-6.42	7	**72**	21	-6.51	4	**74**	22	-6.50	4	**72**	24
	H-3	-6.49	16	**53**	31	-6.62	10	**58**	32	-6.64	9	**58**	34
Triplet-state	α-HOMO	-3.05	13	**73+2**	12	-3.14	9	**79+1**	11	-3.15	8	**80+1**	11
	Spin densities[a]	-	6	**76+3**	15	-	3	**81+3**	13	-	2	**82+4**	12

[a] Sum of Mulliken spin densities per fragment (given in %).

131

Table 6. Frontier orbitals of the DFT optimized ground state S_0 and triplet state T_1 structures of **4b** – **5b**: energy levels and compositions.

		4b						**5b**					
	MO	Energy (eV)	Composition (%)					Energy (eV)	Composition (%)				
			carb	*pyr*	alk_{carb}	alk_{pyr}	*Pt*		*carb*	*pyr*	alk_{carb}	alk_{pyr}	*Pt*
Ground-state	L+2	-0.84	3	**45**	39	3	8	-0.94	2	**90**	0	2	1
	L+1	-0.99	5	**57**	19	1	12	-1.21	**49**	20	17	0	11
	LUMO	-1.71	2	**84**	4	1	7	-1.76	8	**72**	6	0	9
	HOMO	-5.80	1	1	2	**83**	14	-5.83	0	1	4	**82**	13
	H-1	-5.85	9	0	**70**	3	18	-5.92	8	0	**70**	5	17
	H-2	-6.42	2	3	4	**56**	35	-6.48	2	3	4	**57**	34
	H-3	-6.66	3	4	**71**	9	13	-6.70	1	5	**72**	9	14
Triplet-state	α-HOMO	-2.94	5	19	**64**	0	12	-3.02	8	**11**	**67**	**0**	12
	Spin densities[a]	-	1	11	**71**	1	16	-	0	8	**73**	2	17

[a] Sum of Mulliken spin densities per fragment (given in %).

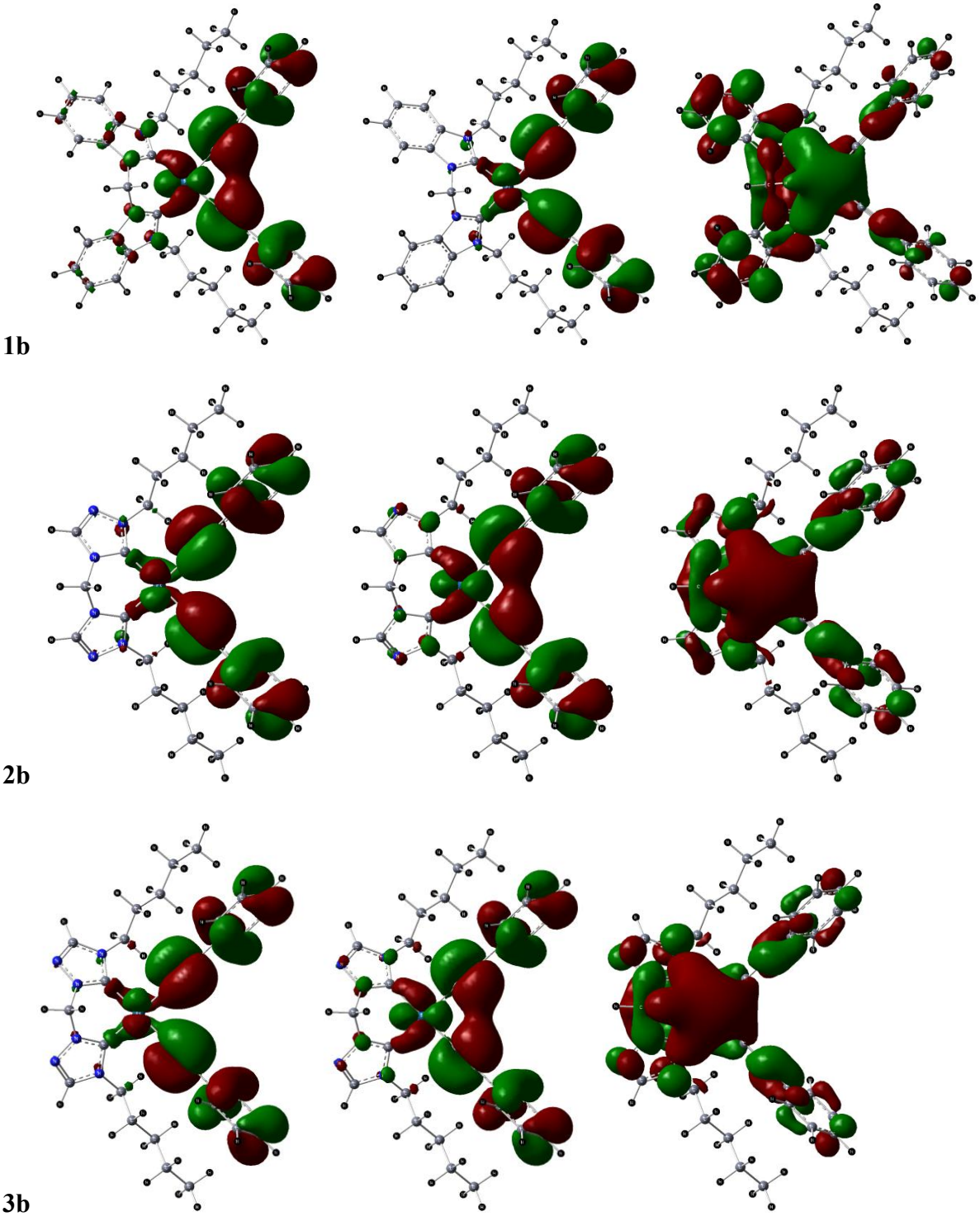

Figure 6. Spatial plots of selected frontier orbitals of the optimized ground states of **1b** – **3b**.

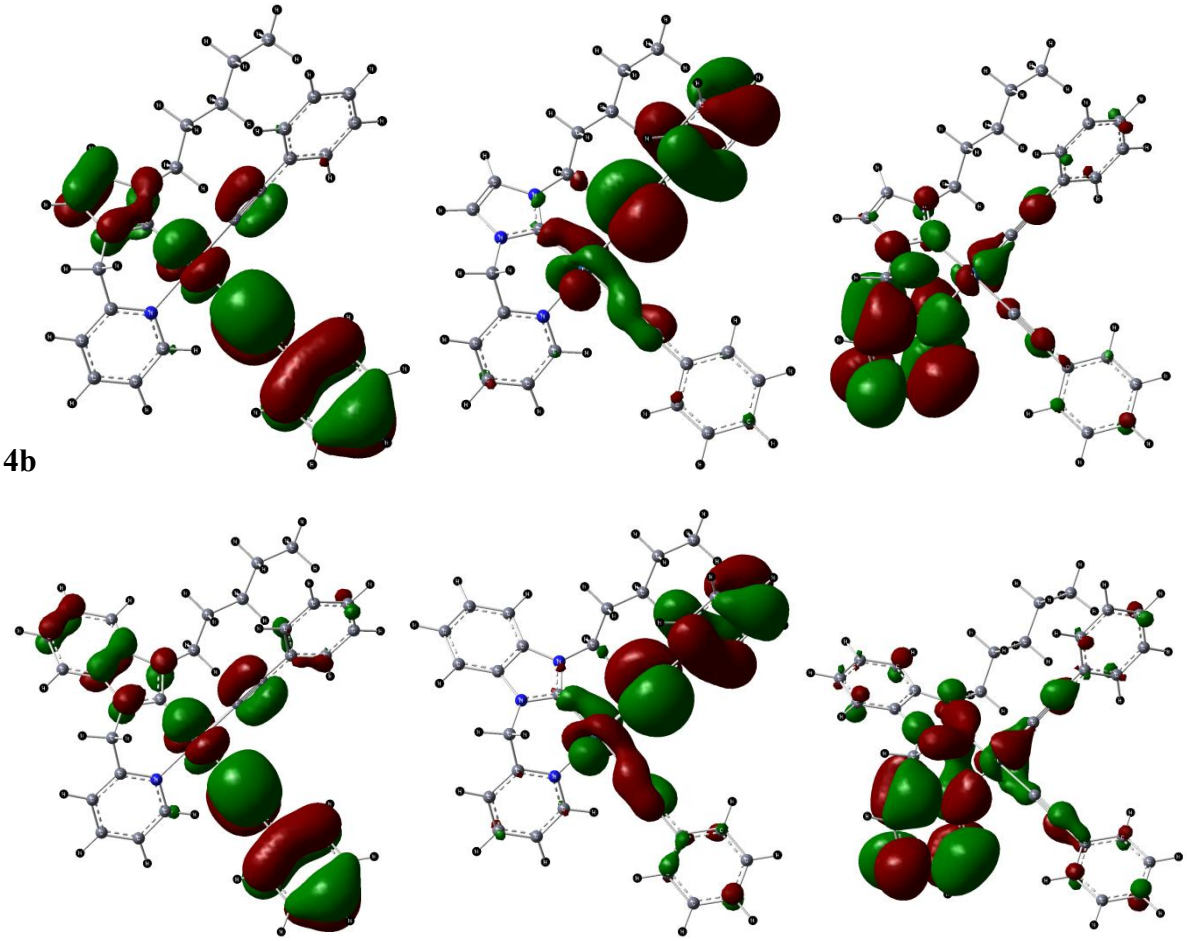

Figure 7. Spatial plots of selected frontier orbitals of the optimized ground states of **4b**– **5b**.

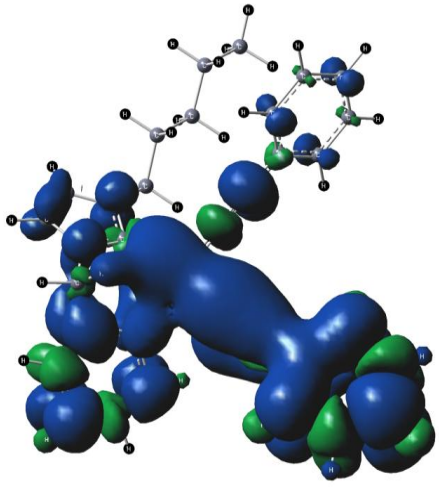

4b

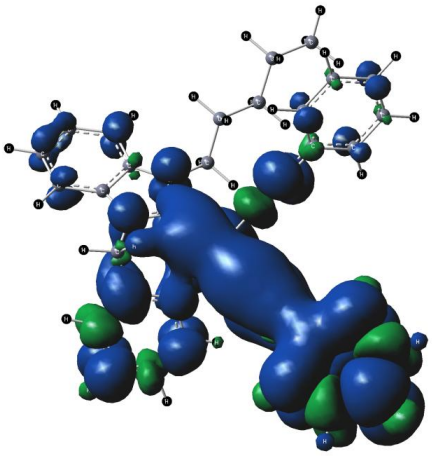

5b

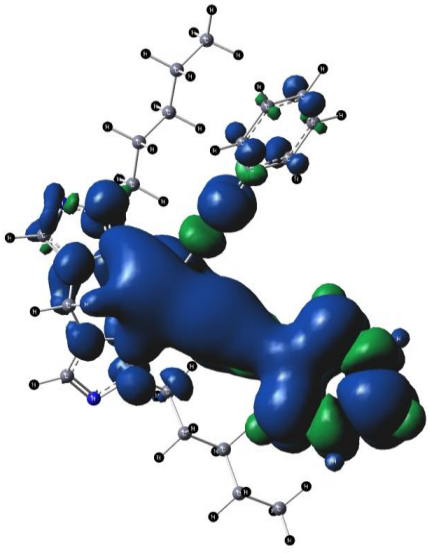

2b

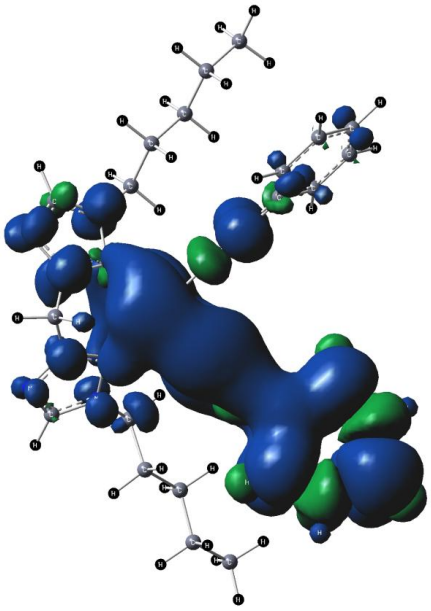

3b

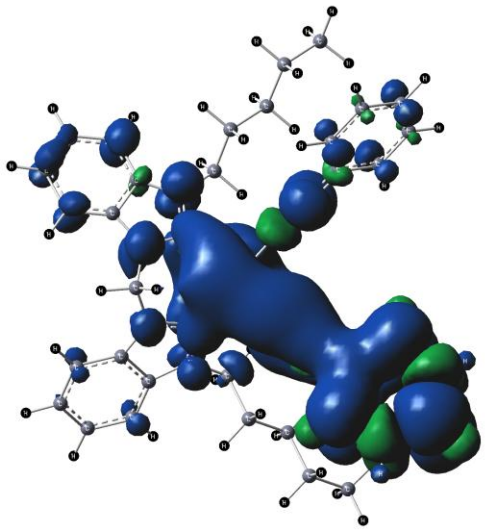

1b

Figure 8. Spin density surfaces for the optimized triplet states of **1b** – **5b** (the positive spin densities are shown in blue and the negative ones are in green).

Conclusions.

This paper reports the influence of the different electronic properties of the chelated NHC ligands on the luminescent quantum yields of Pt(II) bisacetylide complexes. For this purpose five new groups of complexes were prepared. Structural, electrochemical and detailed photophysical investigations of the new complexes were carried out along with DFT and TD-DFT calculations. Most of the newly synthesized complexes displayed deep blue emission in the solid-state with varying emission efficiencies that was found to be influence by the electronic nature of the NHC and alkynyl ligands. The nature of the emission is ascribed to originate from predominantly metal perturbed ^{3}LLCT($\pi_{alk}\rightarrow\pi^*_{alk}$) in case of the bis NHC complexes and an admixture of metal perturbed ^{3}LLCT($\pi_{alk}\rightarrow\pi^*_{alk}$) and ^{3}MLCT (Pt$\rightarrow\pi^*_{alk}$) in the complexes bearing pyridyl-NHC ligands. The results from the studies suggest a moderate electronic influence of the bis NHC ligands on the emission quantum yields and a strong influence exerted by the pyridyl NHC

ligand. The resulting photophysical behavior of the complexes are strongly suggestive of the significant impact, the electronic properties of the NHC ligands bear on the excited states of the Pt(II) acetylide complexes. This work provides a further impetus to the development of highly efficient deep blue emitters based on Pt(II) acetylide complexes with novel chelating NHC ligands.

Experimental Section

General procedure: All manipulations requiring inert atmosphere were carried out using standard schlenk techniques under dinitrogen. ^{1}H, $^{13}C\{^{1}H\}$ and ^{19}F NMR spectra were recorded on Bruker 400 MHz and 500 MHz or Varian 200 MHz and 300 MHz spectrometers. Chemical shifts (δ) are reported in parts per million (ppm) referenced to tetramethylsilane (δ 0.00) ppm using the residual protio solvent peaks as internal standards (^{1}H NMR experiments) or the characteristic resonances of the solvent nuclei (^{13}C NMR experiments). ^{19}F NMR was referenced to $CFCl_3$ (δ 0.00) ppm. Coupling constants (*J*) are quoted in Hertz (Hz) and the following abbreviations are used to describe the signal multiplicities: s (singlet); d (doublet); t (triplet); q (quartet); m (multiplet). Proton and carbon assignments have been made using routine one and two dimensional NMR spectroscopies where appropriate. Infra-red (IR) spectra were recorded on a Perkin-Elmer 1600 Fourier Transform spectrophotometer using KBr pellet with frequencies (ν_{max}) quoted in wavenumbers (cm^{-1}). Elemental microanalysis was carried out with Leco CHNS-932 analyzer. Mass spectra were run on a Finnigan-MAT-8400 mass spectrometer. TLC analysis was performed on precoated Merck Silica Gel60F254 slides and visualized by luminescence quenching either at (short wavelength) 254 nm or (long wavelength) 365 nm. Chromatographic purification of products was performed on a short column (Length 15.0 cm: diameter 1.5 cm) using silica gel 60, 230–400 mesh using a forced flow of eluent. UV-Vis

absorption measurements were carried out on a Perkin-Elmer Lambda 19 UV-Vis spectrophotometer. Emission spectra were acquired on Perkin Elmer spectrophotometer using 450W Xenon lamp excitation by exciting at the longest-wavelength absorption maxima with the excitation slit width 5 nm and emission slit width 10 nm. All samples for emission spectra were degassed by at least three freeze-pump-thaw cycles in an anaerobic cuvette and were pressurized with N_2 following each cycle. 77 K emission spectra were acquired in frozen 2-methyltetrahydrofuran (2-MeTHF) glass. Luminescence quantum yields ϕ_{em} of the complexes in solution was determined at 298 K (estimated uncertainty ± 15%) using standard methods, wavelength-integrated intensities (I) of the corrected emission spectra was compared to iso-absorptive spectra of quinine sulfate standard (ϕ_{ref} = 0.55 in 1N H_2SO_4 air-equilibrated solution) and was corrected for solvent refractive index. Absolute quantum yields were measured in neat solid and thin films using an integrating sphere on the Edinburgh spectrophotometer FLS920. YAG:Ce (powder) was used as a calibration reference with ϕ_{em} = 97%. Phosphorescent lifetimes in thin films were measured on the Edinburgh laser flash photolysis spectrophotometer LP920 with a Nd:YAG 355 nm laser as an excitation source fitted with a single monochromator. Cyclic voltamograms were measured with a Methrom 757 VA Computrace with a glassy carbon electrode (d = 2mm) or a gold electrode with a Pt counter electrode versus Ag/AgCl reference electrode.

All starting materials were purchased from commercial sources and used as received unless stated otherwise. The solvents used for synthesis were of analytical grade. The ligands 1,1'-dipentyl-3,3'-methylene-dibenzolimidazolium diiodide [**pmdb**H_2]I_2,[9b] 1,1'-dipentyl-3,3'-methylene-di-1,**2**,4-triazolium dibromide [**pm2tz**H_2]Br_2,[9b] 1,1'-dipentyl-3,3'-methylene-di-1,**3**,4-triazolium diiodide [**pm3tz**H_2]I_2,[22] precursors *bis*-(N-pentyl-N'-picolylimidazolin-2-

ylidene)silver dibromoargentate [(**ppim**)$_2$Ag] {AgBr$_2$] and *bis*-(N-pentyl-N'-picolylbenzimidazolin-2-ylidene)silver dibromoargentate [(**ppbim**)$_2$Ag] {AgBr$_2$] were synthesized by reported literatures.[10]

[pmdbH$_2$]I$_2$. 1-pentylbenzimidazole (2.14 g, 11.37 mmol) dissolved in 5 mL THF was mixed with methylene iodide (1.52 g, 0.46 mL, 5.68 mmol) and the mixture was heated at 110 ^{o}C for 3 days in an autoclave. The resulting product was washed with cold THF (five times) to give a yellow solid. Yield: 1.17 g, 32%. ^{1}H NMR (300 MHz, d$_6$-DMSO, 300 K): δ (ppm) = 10.25 (s, 2H, NC*H*N), 8.37 (m, 2H, benzimidazole), 8.17 (m, 2H, benzimidazole), 7.78 (m, 4H, benzimidazole), 7.36 (s, 2H, NC*H*$_2$N), 4.56 (m, 4H, NC*H*$_2$CH$_2$), 1.91 (m, 4H, NCH$_2$C*H*$_2$), 1.33 (m, 8H, C*H*$_2$C*H*$_2$CH$_3$), 0.87 (m, 6H, CH$_2$C*H*$_3$). ^{13}C{^{1}H} NMR (125.8 MHz, CD$_2$Cl$_2$, 300 K): 143.7, 143.6, 131.1, 130.5, 127.5, 127.2, 144.2, 113.6, 55.2, 47.3, 28.1, 27.8, 21.7, 13.8. ESI^{+} MS *m/z*: 517.2 [M-I]$^{+}$ (M = C$_{25}$H$_{34}$I$_2$N$_4$). Anal. Calc. for C$_{25}$H$_{34}$I$_2$N$_4$: C, 46.60; H, 5.32; N, 8.69 found: C, 46.31; H, 5.48; N, 8.41

[pm2tzH$_2$]Br$_2$. The procedure was adopted similar to [pmdbH$_2$]I$_2$. A white compound was obtained. Yield: 46%. ^{1}H NMR (500 MHz, CD$_2$Cl$_2$, 300 K): δ (ppm) = 11.72 (s, 2H, triazole), 10.35 (s, 2H, triazole), 7.94 (s, 2H, NC*H*$_2$N), 4.47 (m, 4H, NC*H*$_2$CH$_2$), 2.06 (m, 4H, NCH$_2$C*H*$_2$), 1.44 (m, 8H, C*H*$_2$C*H*$_2$CH$_3$), 0.91 (m, 6H, C*H*$_3$). ^{13}C{^{1}H} NMR (125.8 MHz, CD$_2$Cl$_2$, 300 K): 145.2, 144.2 (C of triazole), 55.9 (N*C*H$_2$N), 53.8, 28.8, 28.6, 22.6, 14.1 (C of (*C*H$_2$)$_4$*C*H$_3$). Anal. Calc. for C$_{15}$H$_{28}$Br$_2$N$_6$ · 0.2 H$_2$O: C, 39.45; H, 6.29; N, 18.40 found: C, 39.54; H, 6.22; N, 18.09.

[Pt(pmdb)I$_2$] I. [pmdbH$_2$]I$_2$ (1.01 g, 1.57 mmol) dissolved in DMSO (20 mL) was added to platinum(II) acetylacetonate (0.62 g, 1.57 mmol) dissolved in DMSO (20 mL) at 100 ^{o}C during 18h by a syringe pump. The reaction mixture was stirred at 110 ^{o}C for additional 2h after

completion of addition. After removing solvent *in vacuo*, the resulting product was purified by column chromatography over silica gel using acetone/ hexane (v/v 1:2) as the eluent. The pure product was isolated as white powder. Yield: 565 mg, 43%. ^{1}H NMR (500 MHz, CD_2Cl_2, 300 K): δ (ppm) = 7.30 (d, 2H, ^{3}J = 10.0 Hz, benzimidazole), 7.19 (d, 2H, ^{3}J = 10.0 Hz, benzimidazole), 7.10 (dt, 4H, benzimidazole), 6.38 (d, 1H, ^{2}J = 15.0 Hz, NC*H*HN), 6.03 (d, 1H, ^{2}J = 15.0 Hz, NCH*H*N), 4.91 (m, 2H, NC*H*HCH$_2$), 4.05 (m, 2H, NCH*H*CH$_2$), 1.65 (m, 4H, NCH$_2$C*H*$_2$), 1.12 (m, 8H, C*H*$_2$C*H*$_2$CH$_3$), 0.73 (t, 6H, CH$_2$C*H*$_3$). ^{13}C{^{1}H} NMR (125.8 MHz, CD_2Cl_2, 300 K): 162.3 (*C*=Pt), 134.1, 132.3, 124.4, 124.2, 112.6, 110.8 (C on benzimidazole), 57.6 (N*C*H$_2$N), 50.1, 29.6, 29.3, 23.4, 14.6 (C on (CH$_2$)$_4$CH$_3$). ESI^{+} MS *m/z*: 860.0 [M + Na]$^{+}$ (M = $C_{25}H_{32}I_2N_4Pt$). Anal. Calc. for $C_{25}H_{32}I_2N_4Pt$: C, 35.86; H, 3.85; N, 6.69 found: C, 36.14; H, 3.87; N, 6.59. IR (cm^{-1}): 2955.07, 2928.53, 1423.90, 1391.27, 747.74.

[Pt(pm2tz)Br$_2$] II. Platinum(II) acetylacetonate (1.39 g, 3.25 mmol) was dissolved in DMSO (20 mL) and heated to 100 ^{o}C. [pm2tzH$_2$]Br$_2$ (1.63 g, 3.25 mmol) dissolved in DMSO (20 mL) was added during 18h with a syringe pump. The reaction solution was stirred at 100 ^{o}C additionally for another 2h. After removing solvent *in vacuo*, the resulting product was purified by washing twice with water and twice with MeOH. The pure compound was isolated as white powder. Yield: 1.71 g, 82%. ^{1}H NMR (500 MHz, d$_6$-DMSO, 300 K): δ (ppm) = 8.79 (s, 2H, triazole), 6.40 (d, 1H, ^{2}J = 15.0 Hz, NC*H*HN), 6.07 (d, 1H, ^{2}J = 15.0 Hz, NCH*H*N), 4.75 (m, 2H, NC*H*HCH$_2$), 4.30 (m, 2H, NCH*H*CH$_2$), 1.80 (m, 4H, NCH$_2$C*H*$_2$), 1.20 (m, 8H, C*H*$_2$C*H*$_2$CH$_3$), 0.83 (t, 6H, CH$_2$CH$_3$). ^{13}C{^{1}H} NMR (125.8 MHz, d$_6$-DMSO, 300 K): 147.5 (*C*=Pt), 142.7 (C on triazole), 58.6 (N*C*H$_2$N), 51.8, 28.7, 27.7, 21.5, 13.7 (C on (CH$_2$)$_4$CH$_3$). Anal. Calc. for $C_{15}H_{26}Br_2N_6Pt$: C, 27.92; H, 4.06; N, 13.02 found: C, 27.84; H, 4.05; N, 12.88. IR (ATR, cm^{-1}): 2957, 2860, 1617, 1467, 1358, 823.

[Pt(pm3tz)I_2] III. Platinum(II) acetylacetonate (0.72 g, 1.83mmol) was dissolved in DMSO (5 mL) and heated to 100 °C. [pm3tzH_2]I_2 (1.00 g, 1.83 mmol) dissolved in DMSO (20 mL) was added during 18h with a syringe pump. The reaction mixture was stirred at 100 °C for another 2h. After removal of the solvent *in vacuo*, the resulting product was purified by column chromatography using DCM/ EtOAc (v/v 19:1) as the eluent. Yield: 309 mg, 22%. ^{1}H NMR (400 MHz; CD_2Cl_2, 300 K): δ (ppm) = 8.05 (s, 2H, triazole), 6.53 (d, 1H, ^2J = 16.0 Hz, NC*H*HN), 6.07 (d, 1H, ^2J = 16.0 Hz, NCH*H*N), 4.95 (m, 2H, NC*H*HCH_2), 4.23 (m, 2H, NCH*H*CH_2), 1.95 (m, 4H, NCH$_2$C*H*$_2$), 1.38 (m, 8H, C*H*$_2$C*H*$_2$CH$_3$), 0.94 (t, 6H, CH$_2$C*H*$_3$). ^{13}C{^{1}H} NMR (100.6 MHz, CD_2Cl_2, 300 K): 155.6 (*C*=Pt), 143.2 (C on triazole), 66.2 (N*C*H$_2$N), 50.3, 29.8, 28.3, 22.1, 13.6 (C of $(CH_2)_4CH_3$). ESI$^+$ MS *m/z*: 612.2 [M-I]$^+$ (M = $C_{15}H_{26}N_6I_2Pt$); Anal. Calc. for $C_{15}H_{26}N_6I_2Pt$: C, 24.37; H, 3.54; N, 11.37 found: C, 24.21; H, 3.43; N, 11.20. IR (ATR, cm^{-1}): 2955.3, 2929.1, 1618.9, 1535.4, 1461.9, 820.1.

General procedure for the synthesis of 1a-c, **2a-c and 3a-c**. 2.1 equiv. of the acetylene ligand was dissolved in dry diethyl ether (20 mL) and cooled to -78 °C. 2 equiv. of *n*-butyllithium (1.6 M in hexane) was added and stirred for 30 min at -78 °C, and the temperature of the reaction was raised to -30 °C and stirred at this temperature for 30 min. Then the solution was transferred to a schlenk flask containing the precursor suspended in dry ether at -78 °C. The mixture was then heated to 45 °C and stirred additionally for another 4h. The reaction was quenched with water and washed with brine. The organic layer was separated and the aqueous layer was extracted three times with dichloromethane (15 mL). The organic layer was separated, dried over $MgSO_4$ and concentrated *in vacuo*. The resulting product was purified by column chromatography over silica gel with a suitable eluent.

[Pt(pmdb)(C≡CC$_6$H$_4$F)$_2$] 1a. A light yellow compound was obtained. Eluent: acetone/ hexane (v/v 1:3.5). Yield: 61%. ^{1}H NMR (400 MHz, CD_2Cl_2, 300 K): δ (ppm) = 7.61 (d, 2H, ^3J = 7.47 Hz, benzimidazole), 7.54 (d, 2H, ^3J = 7.6 Hz, benzimidazole), 7.42-7.31 (m, 4H, benzimidazole, 4H, phenyl), 6.91 (t, 4H, ^3J = 8.8 Hz, phenyl), 6.98 (quart., 2H, ^2J = 13.4, NC*H*$_2$N), 5.48-5.41 (m, 2H, NC*H*HCH$_2$), 4.48-4.41 (m, 2H, NCH*H*CH$_2$), 1.96-1.88 (m, 4H, NCH$_2$C*H*$_2$), 1.40-1.18 (m, 8H, C*H*$_2$C*H*$_2$CH$_3$), 0.80 (t, 6H, ^3J = 6.8 Hz, CH$_2$C*H*$_3$). ^{13}C{^{1}H} NMR (100.6 MHz, CD_2Cl_2, 300 K): 178.5 (*C*=Pt), 161.0 (d, $^1J_{F\text{-}C}$ = 243.6 H$_Z$), 134.7, 133.0, 125.2, 124.2, 124.1, 115.1, 114.9, 112.1, 109.6 (C on benzimidazole), 108.4, 104.6 (Pt-*C*≡*C*), 56.5 (N*C*H$_2$N), 48.3, 30.1, 29.4, 22.8, 14.1 (C on (CH$_2$)$_4$CH$_3$). ^{19}F NMR (188.3 MHz, CD_2Cl_2, 300 K): δ (ppm) = -117.2. Anal. Calc. for $C_{41}H_{40}F_2N_4Pt$: C, 59.92; H, 4.91; N, 6.82 found: C, 59.82; H, 4.88; N, 6.78. IR (ATR, cm^{-1}) ν(C≡C) = 2103.

[Pt(pmdb)(C≡CC$_6$H$_5$)$_2$] 1b. A light yellow compound was obtained. Eluent: acetone/ hexane (v/v 1:3.5). Yield: 56%. ^{1}H NMR (400 MHz, CD_2Cl_2, 300 K): δ (ppm) = 7.62 (d, 2H, ^3J = 7.6 Hz, benzimidazole), 7.44 (d, 2H, ^3J = 7.8 Hz, benzimidazole), 7.39-7.31 (m, 4H, benzimidazole, 4H, phenyl), 7.22 (t, 4H, ^3J = 7.6 Hz, phenyl), 7.11 (t, 2H, ^3J = 7.6 Hz, phenyl), 6.48 (quat., 2H, ^2J = 13.2 Hz, NC*H*$_2$N), 5.58-5.51 (m, 2H, NC*H*HCH$_2$), 4.44-4.37 (m, 2H, NCH*H*CH$_2$), 1.96-1.88 (m, 4H, NCH$_2$C*H*$_2$), 1.44-1.18 (m, 8H, C*H*$_2$C*H*$_2$CH$_3$), 0.81 (t, 6H, ^3J = 7.2 Hz, CH$_2$C*H*$_3$). ^{13}C{^{1}H} NMR (100.6 MHz, CD_2Cl_2, 300 K): 178.7 (*C*=Pt), 134.8, 133.3, 131.7, 129.3, 128.4, 125.5, 124.2 (C on phenyl), 112.2, 109.4 (C on benzimidazole), 105.8 (Pt-*C*≡*C*), 56.9 (N*C*H$_2$N), 48.4, 30.3, 29.6, 22.9, 14.3 (C on (CH$_2$)$_4$CH$_3$). Anal. Calc. for $C_{41}H_{42}N_4Pt$: C, 62.66; H, 5.39; N, 7.13 found: C, 62.81; H, 5.56; N, 6.95. IR (ATR, cm^{-1}) ν(C≡C) = 2105.

[Pt(pmdb)(C≡CC$_6$H$_4$OCH$_3$)$_2$] 1c. A light yellow compound was obtained. Eluent: ether acetate/ DCM (v/v 2:18). Yield: 79%. ^{1}H NMR (500 MHz, CD_2Cl_2, 300 K): δ (ppm) = 7.60 (d,

2H, ^{3}J = 8.0 Hz, benzimidazole), 7.46 (d, 2H, ^{3}J = 8.0 Hz, benzimidazole), 7.41-7.33 (m, 4H, benzimidazole), 7.30 (d, 4H, ^{3}J = 9.0 Hz, phenyl), 6.77 (d, 4H, ^{3}J = 10.0 Hz, phenyl), 6.45 (q, 2H, ^{2}J = 13.5 Hz, NCH_2N), 5.59-5.53 (m, 2H, NCHHCH$_2$), 4.44-4.38 (m, 2H, NCHHCH$_2$), 3.77 (s, 6H, OCH_3), 1.97-1.87 (m, 4H, NCH$_2$CH_2), 1.40-1.19 (m, 8H, CH_2CH_2CH$_3$), 0.81 (t, 6H, ^{3}J = 7.0 Hz, CH$_2$CH_3). ^{13}C{^{1}H} NMR (125.8 MHz, CD_2Cl_2, 300 K): 179.0 (*C*=Pt), 157.9, 134.9, 133.3, 132.8, 124.2, 124.1, 122.2, 121.9, 113.9 (C on phenyl), 112.2, 109.8 (C on benzimidazole), 109.4, 103.1 (Pt-*C*≡*C*), 100.1, 56.8 (N*C*H$_2$N), 55.7, 48.4, 30.3, 29.6, 23.0, 14.3 (C on (CH$_2$)$_4$CH$_3$). Anal. Calc. for $C_{43}H_{46}N_4O_2Pt$: C, 61.05; H, 5.48; N, 6.62 found: C, 61.14; H, 5.46; N, 6.55. IR (ATR, cm^{-1}) ν(C≡C) = 2105.

[Pt(pm2tz)(C≡CC$_6$H$_4$F)$_2$] 2a. Alight yellow compound was obtained. Eluent: acetone/ hexane (v/v 1:2). Yield: 51%. ^{1}H NMR (500 MHz, CD_2Cl_2, 300 K): δ (ppm) = 8.26 (s, 2H, triazole), 7.25 (t, 4H, ^{3}J = 8.0 Hz, phenyl), 6.90 (t, 4H, ^{3}J = 8.0 Hz, phenyl), 6.19 (s, 2H, NCH_2N), 4.96-4.53 (m, 4H, NCH_2CH$_2$), 1.88 (s, 4H, NCH$_2$CH_2), 1.22-1.15 (m, 8H, CH_2CH_2CH$_3$), 0.78 (t, 6H, ^{3}J = 6.5 Hz CH_3). ^{13}C{^{1}H} NMR (125.8 MHz, CD_2Cl_2, 300 K), δ (ppm) = 167.7 (Pt=*C*), 162.0 (C $^{1}J_{F\text{-}C}$ = 240 Hz, C-F), 140.4 (C on triazole), 133.1, 132.4, 124.0, 115.4, 115.3, 114.8 (C on the phenyl), 108.0, 102.4 (Pt-*C*≡*C*), 58.7 (C on NCH$_2$N), 52.7, 30.4, 29.2, 28.9, 28.6, 22.9, 14.2 (C on (CH$_2$)$_4$CH$_3$). ^{19}F NMR (188.3 MHz, CD_2Cl_2, 300 K): δ (ppm) = -116.2. ESI^{+} MS *m/z*: 724.2 [M]$^{+}$ (M = $C_{31}H_{34}F_2N_6Pt$); Anal. Calc. for $C_{31}H_{34}F_2N_6Pt$: C, 51.45; H, 4.74; N, 11.61 found: C, 51.31; H, 4.74; N, 11.45. IR (ATR, cm^{-1}) ν(C≡C) = 2109.

[Pt(pm2tz)(C≡CC$_6$H$_4$)$_2$] 2b. Alight yellow compound was obtained. Eluent: DCM/ EtOAc (v/v 19:1). Yield: 60%. ^{1}H NMR (400 MHz, CD_2Cl_2, 300 K): δ (ppm) = 8.26 (s, 2H, triazole), 7.27 (d, 4H, ^{3}J = 8.0 Hz, phenyl), 7.20 (t, 4H, ^{3}J = 7.6 Hz, phenyl), 7.12 (t, 2H, ^{3}J = 6.8 Hz, phenyl) 6.20 (s, 2H, NCH_2N), 4.91-4.59 (m, 4H, NCH_2CH$_2$), 1.92-1.84 (m, 4H, NCH$_2$CH_2),

1.26-1.18 (m, 8H, CH_2CH_2CH$_3$), 0.78 (t, 6H, ^3J = 6.8 Hz, CH_3). ^{13}C{^{1}H} NMR (100.6 MHz, CD_2Cl_2, 300 K), δ (ppm) = 168.7 (Pt=*C*), 140.6 (C on triazole), 131.6, 128.7, 128.5, 125.9 (C on the phenyl), 109.7, 103.9 (Pt-*C* ≡ *C*), 59.1 (C on NCH$_2$N) 30.3, 29.2, 22.9, 14.2 (C on (CH$_2$)$_4$CH$_3$). ESI$^+$ MS *m/z*: 688.3 [M]$^+$ (M = $C_{31}H_{36}N_6Pt$); Anal. Calc. for $C_{31}H_{36}N_6Pt$: C, 54.10; H, 5.28; N, 12.22 found: C, 53.98; H, 5.32; N, 12.09. IR (ATR, cm^{-1}) ν(C≡C) = 2110.

[Pt(pm2tz)(C≡CC$_6$H$_4$OCH$_3$)$_2$] 2c. A white compound was obtained. Eluent: acetone/ hexane (v/v 1:2). Yield: 21%. ^{1}H NMR (500 MHz, CD_2Cl_2, 300 K): δ (ppm) = 8.49 (s, 2H, triazole), 7.16 (d, 4H, ^3J = 10.0 Hz, phenyl), 6.74 (t, 4H, ^3J = 10.0 Hz, phenyl), 5.32 (s, 2H, NCH_2N), 4.89-4.56 (m, 4H, NCH_2CH$_2$), 3.74 (s, 6H, OCH_3), 1.95-1.80 (m, 4H, NCH$_2$CH_2), 1.24-1.16 (m, 8H, CH_2CH_2CH$_3$), 0.78 (t, 6H, ^3J = 6.5 Hz CH_3). ^{13}C{^{1}H} NMR (125.8 MHz, CD_2Cl_2, 300 K), δ (ppm) = 168.0 (Pt=*C*), 158.3, 141.4 (C on triazole), 132.4, 120.8, 114.3, (C on the phenyl), 109.7, 101.8 (Pt-*C*≡*C*), 59.4 (C on N*C*H$_2$N) 55.7 (O*C*H$_3$), 53.1, 30.4, 29.9, 29.2, 29.0, 22.8, 14.3 (C of (CH$_2$)$_4$CH$_3$). ESI$^+$ MS *m/z*: 749.2 [M]$^+$ (M = $C_{33}H_{40}N_6O_2Pt$). $C_{33}H_{40}N_6O_2Pt$: C, 53.00; H, 5.39; N, 11.24 found: C, 52.86; H, 5.65; N, 11.21. IR (ATR, cm^{-1}) ν(C≡C) = 2113.

[Pt(pm2tz)(C≡CSi(CH$_3$)$_3$)$_2$] 2d. A white color compound was obtained after washing twice with pentane. Single crystal was obtained from the slow evaporation of dichloromethane and methanol. Yield: 18%. ^{1}H NMR (400 MHz, CD_2Cl_2, 300 K): δ (ppm) = 8.68 (s, 2H, triazole), 7.26 (s, 1H, NC*H*HN), 5.82 (s, 1H, NCH*H*N), 5.43 (s, 2H, NCH*H*CH$_2$), 4.18-4.06 (m, 2H, NC*H*HCH$_2$), 1.84-1.77 (m, 4H, NCH$_2$CH_2), 1.36-1.24 (m, 8H, CH_2CH_2CH$_3$), 0.87 (t, ^3J = 7.2 Hz 6H, CH_3), -0.07 (m, 18H, Si(CH_3)$_3$). ^{13}C{^{1}H} NMR (100.6 MHz, CD_2Cl_2, 300 K): δ (ppm) = 168.2 (Pt=*C*), 141.8 (C on triazole), 125.3, 114.5 (Pt-*C*≡*C*), 59.2 (N*C*H$_2$N), 53.3 (N*C*H$_2$CH$_2$), 30.6, 29.1 22.9, 14.2 (C on (CH$_2$)$_4$CH$_3$) 1.1 (Si(*C*H$_3$)$_3$). ESI$^+$ MS *m/z*: 679.3 [M]$^+$ (M =

$C_{25}H_{44}N_6PtSi_2$). Anal. Calc. for $C_{25}H_{44}N_6PtSi_2$: C, 44.16; H, 6.52; N, 12.36 found: C, 44.16; H, 6.38; N, 12.16. IR (ATR, cm^{-1}) ν(C≡C) = 2035.

[Pt(pm3tz)(C≡C$C_6H_4F)_2$] 3a. A light yellow compound was obtained. Eluent: DCM/ EtOAc (v/v 19:1). Yield: 87%. ^{1}H NMR (400 MHz, CD_2Cl_2, 300 K): δ (ppm) = 8.01 (s, 2H, triazole), 7.32-7.28 (m, 4H, phenyl), 6.92 (t, 4H, ^3J = 8.8 Hz, phenyl), 6.28 (s, 2H, NCH_2N), 4.74-4.65 (m, 4H, NC$H_2$$CH_2$), 1.89 (m, 4H, NCH_2CH_2), 1.43-1.15 (m, 8H, CH_2C$H_2$$CH_3$), 0.81 (t, 6H, ^3J = 8.0 Hz, CH_3). ^{13}C{^{1}H} NMR (100.6 MHz, CD_2Cl_2, 300 K): δ (ppm) = 170.4 (Pt=*C*), 161.9, 143.3 (C on triazole), 133.2, 115.4, 115.2 (C on the phenyl), 108.3, 102.0 (Pt-*C*≡*C*), 66.8 (C of N*C*H_2N), 49.4, 31.4, 29.2, 22.9, 14.2 (C of $(CH_2)_4CH_3$). ^{19}F NMR (376.5 MHz, CD_2Cl_2, 300 K): δ (ppm)= -116.9. Anal. Calc. for $C_{31}H_{34}F_2N_6Pt \cdot 0.2\ CH_3C(O)OC_2H_5$: C, 51.54; H, 4.87; N, 11.27 found: C, 51.77; H, 4.98; N, 11.08. IR (ATR, cm^{-1}) ν(C≡C) = 2117.

[Pt(pm3tz)(C≡C$C_6H_5)_2$] 3b. A light yellow compound was obtained. Eluent: DCM/ EtOAc (v/v 19:1). Yield: 64%. ^{1}H NMR (400 MHz, CD_2Cl_2, 300 K): δ (ppm) = 8.00 (s, 2H, triazole), 7.33 (d, 4H, ^3J = 7.2 Hz, phenyl), 7.21 (t, 4H, ^3J = 8.0 Hz, phenyl), 7.11 (t, 2H, ^3J = 7.2 Hz, phenyl), 6.34 (s, 2H, NCH_2N), 4.78-4.68 (m, 4H, NC$H_2$$CH_2$), 1.93-1.86 (m, 4H, NCH_2CH_2), 1.29-1.23 (m, 8H, CH_2C$H_2$$CH_3$), 0.81 (t, 6H, ^3J = 7.2 Hz, CH_3). ^{13}C{^{1}H} NMR (100.6 MHz, CD_2Cl_2, 300 K): δ (ppm) = 170.4 (Pt=*C*), 143.3 (C on triazole), 131.6, 128.9, 128.4, 125.7 (C on the phenyl), 109.7, 102.8 (Pt-*C*≡*C*), 66.9 (C of N*C*H_2N) 49.4, 31.4, 29.2, 22.8, 14.2 (C of $(CH_2)_4CH_3$). Anal. Calc. for $C_{31}H_{36}N_6Pt$: C, 54.14; H, 5.28; N, 12.22; found: C, 54.04; H, 5.32; N, 12.19. IR (ATR, cm^{-1}) ν(C≡C) = 2107.

[Pt(pm3tz)(C≡C$C_6H_4OCH_3$)$_2$] 3c. A light yellow compound was obtained. Eluent: DCM/ EtOAc (v/v 18:2). Yield: 37%. ^{1}H NMR (400 MHz, CD_2Cl_2, 300 K): δ (ppm) = 7.99 (s, 2H, triazole), 7.27 (d, 4H, ^3J = 8.8 Hz, phenyl), 6.76 (t, 4H, ^3J = 8.8 Hz, phenyl), 6.27 (s, 2H, NCH_2N), 4.94 (m, 1H, NCH_2CH$_2$), 4.79-4.69 (m, 2H, NCH_2CH$_2$), 4.20-4.13 (m, 1H, NCH_2CH$_2$), 3.77 (s, 6H, OCH_3), 1.94-1.84 (m, 4H, NCH$_2$CH_2), 1.37-1.21 (m, 8H, CH_2CH_2CH$_3$), 0.82 (t, 6H, ^3J = 7.2 Hz, CH_3). ^{13}C{^{1}H} NMR (100.6 MHz, CD_2Cl_2, 300 K), δ (ppm) = 170.6 (Pt=*C*), 158.1 143.3 (C of triazole), 132.8, 121.4, 114.0, (C on the phenyl), 109.0, 100.1 (Pt-*C*≡*C*), 66.8 (C of N*C*H$_2$N), 55.7 (O*C*H$_3$), 49.1, 31.5, 29.4, 22.8, 14.2 (C of (CH$_2$)$_4$CH$_3$). Anal. Calc. for $C_{33}H_{40}N_6O_2Pt$: C, 53.00; H, 5.39; N, 11.24 found: C, 53.09; H, 5.53; N, 11.19. IR (ATR, cm^{-1}) ν(C≡C) = 2109.

General procedure for the synthesis of 4a, **4b**, **4e**, **5a**, **5b**, and **5e**. 1 equiv. of the silver salt was dissolved in dry DCM and was added dropwise to a DCM solution of [Pt(COD)(C≡CR)$_2$] and stirred for 15 h with exclusion of light. The mixture was filtered through Celite to remove the silver salts and the obtained residue was purified by column chromatography over silica gel with a suitable eluent.

[Pt(ppim)(C≡CC_6H_4F)$_2$] 4a. A light yellow compound was obtained. Eluent: Et$_2$O/ EtOAc (v/v 19:1). Yield: 60%; ^{1}H NMR (400 MHz, CD_2Cl_2, 300 K): δ (ppm) = 9.62 (d, 1H, ^3J = 6.2 Hz, pyridine), 7.92 (t, 1H, ^3J = 6.8 Hz, pyridine), 7.52 (d, 1H,^3J = 7.6 Hz, pyridine), 7.39 (dt, 1H, ^3J = 7.6 Hz, pyridine), 7.35-7.27 (m, 4H, phenyl), 7.09 (s, 1H, imidazole), 6.95 (s, 1H, imidazole), 6.94-6.89 (m, 4H, phenyl), 5.28-5.16 (m, 2H, NCH_2C), 4.60-4.49 (m, 2H, NCH_2CH$_2$), 1.88-1.81 (m, 2H, NCH$_2$CH_2), 1.55 (s, 2H, CH$_2$), 1.23-1.19 (m, 2H, CH_2CH$_3$), 0.77 (t, 3H, ^3J = 6.8 Hz, CH_3). ^{13}C{^{1}H} NMR (100.6 MHz, CD_2Cl_2, 300 K), δ (ppm) = 169.8 (Pt=*C*), 162.5 160.1 (*C*-F), 156.4, 153.4, 139.3, 133.3, 126.0 125.0 (pyridine), 120.6 (imidazole), 115.1 (phenyl), 103.0,

101.6 (*C*≡*C*), 56.3 (C of N*C*H_2N), 54.5, 31.6, 29.4, 27.5, 22.9, 14.4 (C of $(CH_2)_4CH_3$). ^{19}F NMR (188.3 MHz, CD_2Cl_2, 300 K):δ (ppm) = -116.8, -117.4. ESI$^+$ MS *m/z*: 663.1 $[M]^+$ (M = $C_{30}H_{27}F_2N_3Pt$). Anal. Calc. for $C_{30}H_{27}N_3F_2Pt \cdot Et_2O$: C, 55.58; H, 4.80; N, 5.72 found: C, 55.38; H, 4.41; N, 6.00. IR (ATR, cm^{-1}) ν(C≡C) = 2121, 2106.

[Pt(ppim)(C≡CC_6H_5)$_2$] 4b. A light yellow compound was obtained. Eluent: DCM/ EtOAc (v/v 19:1). Yield: 35%; ^{1}H NMR (400 MHz, CD_2Cl_2, 300 K): δ (ppm) = 9.66 (d, 1H, ^3J = 5.6 Hz, pyridine), 7.92 (t, 1H, ^3J = 8.0 Hz, pyridine), 7.51 (d, 1H, ^3J = 7.6 Hz, pyridine), 7.41-7.38 (m, 1H, pyridine), 7.38-7.31 (m, 4H, phenyl), 7.21 (t, 4H, ^3J = 7.6 Hz, phenyl), 7.13-7.08 (m, 2H, phenyl, 1H, imidazole), 6.95 (s, 1H, imidazole), 5.29-5.13 (m, 2H, NCH_2C), 4.64-4.5 (m, 2H, NCH_2CH_2), 1.89-1.81 (m, 2H, NCH_2CH_2), 1.27-1.19 (m, 4H, CH_2CH_2CH_3), 0.77 (t, 3H, ^3J = 6.8 Hz, CH_3). ^{13}C{^{1}H} NMR (100.6 MHz, CD_2Cl_2, 300 K), δ (ppm) = 169.9 (Pt=*C*), 158.3, 156.4, 139.3, 132.0, 131.8, 130.7, 129.3, 128.4, 126.0, 125.7, 125.4 (phenyl), 124.9 (pyridine), 121.1, 120.5 (imidazole), 111.0, 105.5, 104.4 (*C*≡*C*), 55.5 (C of N*C*H_2N), 51.0, 31.6, 31.2, 29.4, 22.9, 14.2 (C of $(CH_2)_4CH_3$). ESI$^+$ MS *m/z*: 627.3 $[M]^+$ (M = $C_{30}H_{29}N_3Pt$). Anal. Calc. for $C_{30}H_{29}N_3Pt$: C, 57.50; H, 4.66; N, 6.71 found: C, 57.77; H, 4.72; N, 6.58. IR (ATR, cm^{-1}) ν(C≡C) = 2117, 2101.

[Pt(ppim)(C≡CC_6H_4N(C_6H_5)$_2$)$_2$] 4e. A brown compound was obtained. Eluent: DCM/ EtOAc (v/v 19:1), slight decomposition was observed on silica gel during column chromatography. Yield: 17%. ^{1}H NMR (500 MHz, CD_2Cl_2, 300 K): δ (ppm) = 9.64 (d, 1H, ^3J = 5.6 Hz, pyridine), 7.91 (t, 1H, ^3J = 7.6 Hz, pyridine), 7.52 (d, 1H,^3J = 7.6 Hz, pyridine), 7.38 (t, 1H, ^3J = 7.5 Hz, pyridine), 7.26 -7.19 (m, 4H, phenyl, 8H, *o*-phenyl N), 7.11 (s, 1H, imidazole), 7.06-7.04 (m, 8H, *m*-phenyl N), 7.00-6.95 (m, 4H, *p*-phenyl N), 6.94 (s, 1H, imidazole), 6.92-6.89 (m, 4H,

phenyl), 5.36-5.08 (m, 2H, NC*H*$_2$C), 4.59-4.52 (m, 2H, NC*H*$_2$CH$_2$), 1.89-1.83 (m, 2H, NCH$_2$C*H*$_2$), 1.28-1.17 (m, 4H, C*H*$_2$C*H*$_2$CH$_3$), 0.78 (t, 3H, ^3J = 7.0 Hz, C*H*$_3$). ^{13}C{^{1}H} NMR (125.8 MHz, CD_2Cl_2, 300 K): δ (ppm) = 170.1 (Pt=*C*), 156.5, 153.4, 148.4, 145.6, 145.3, 139.2, 132.8, 132.6, 129.7, 126.0, 124.5, 123.1 (pyridine), 122.9, 121.0 (phenyl), 120.5 (imidazole), 115.0, 105.2, 104.1 (*C*≡*C*), 78.3, 56.9 (C of N*C*H$_2$N), 51.0, 31.7, 29.4, 23.0, 14.4 (C of (CH$_2$)$_4$CH$_3$). ESI$^+$MS *m/z*: 960.3 [M]$^+$ (M = $C_{54}H_{47}N_5Pt$). Anal. Calc. for $C_{54}H_{47}N_5Pt$: C, 67.49; H, 4.93; N, 7.29 found: C, 67.86; H, 4.90; N, 7.24. IR (ATR, cm^{-1}) ν(C≡C) = 2110.

[Pt(ppbim)(C≡CC$_6$H$_4$F)$_2$] 5a. A light yellow compound was obtained. Eluent: Hexane/ EtOAc (v/v 12:8). Yield: 79%. ^{1}H NMR (400 MHz, CD_2Cl_2, 300 K): δ (ppm) = 9.60 (d, 1H, ^3J = 6.8 Hz, pyridine), 7.92 (t, 1H, ^3J = 7.6 Hz, pyridine), 7.63-7.57 (m, 2H, benzimidazole), 7.49-7.47 (m, 1H, pyridine), 7.42-7.40 (m, 1H, pyridine), 7.39-7.35 (m, 4H, phenyl), 7.33-7.28 (m, 2H, benzimidazole), 6.92 (t, 4H, ^3J = 8.8 Hz, phenyl), 5.55-5.46 (m, 2H, NC*H*$_2$C), 4.99-4.79 (m, 2H, NC*H*$_2$CH$_2$), 2.00-1.93 (m, 2H, NCH$_2$C*H*$_2$), 1.34-1.27 (m, 4H, C*H*$_2$C*H*$_2$CH$_3$), 0.77 (t, 3H, ^3J = 7.2 Hz, C*H*$_3$). ^{13}C{^{1}H} NMR (100.6 MHz, CD_2Cl_2, 300 K): δ (ppm) = 179.1 (Pt=*C*), 162.6 160.1 (*C*-F), 156.3, 153.3, 139.5, 134.8, 133.7, 133.4, 126.1 125.1 (pyridine), 124.1, 115.4, 115.2 (phenyl), 112.2, 110.2 (benzimidazole), 104.3, 103.7 (*C*≡*C*), 78.2, 52.4 (C of N*C*H$_2$N), 48.4, 30.2, 29.7, 22.9, 14.3 (C of (CH$_2$)$_4$CH$_3$). ^{19}F NMR (188.3 MHz, CD_2Cl_2, 300 K): δ (ppm) = -117.3, -117.2. ESI$^+$ MS *m/z*: 761.2 [M + CHCl]$^+$ (M = $C_{34}H_{29}F_2N_3Pt$). Anal. Calc. for $C_{34}H_{29}F_2N_3Pt$ 0.5 hexane: C, 58.80; H, 4.80; N, 5.56; found: C, 58.81; H, 4.50; N, 5.41. IR (ATR, cm^{-1}) ν(C≡C) = 2121, 2108.

[Pt(ppbim)(C≡CC$_6$H$_5$)$_2$] 5b. A light yellow compound was obtained. Eluent: DCM/ EtOAc (v/v 19:2). Yield: 57%. ^{1}H NMR (400 MHz, CD_2Cl_2, 300 K): δ (ppm) = 9.64 (d, 1H, ^3J = 5.6 Hz, pyridine), 7.93 (t, 1H, ^3J = 7.6 Hz, pyridine), 7.62-7.57 (m, 2H, benzimidazole), 7.48 (d, 1H,^3J =

7.6 Hz, pyridine), 7.43-7.41 (m, 1H, pyridine), 7.39-7.37 (m, 4H, phenyl), 7.35-7.33 (m, 2H benzimidazole), 7.22 (t, 4H, ^{3}J = 7.6 Hz, phenyl), 7.14-7.08 (m, 2H, phenyl), 5.57-5.47 (m, 2H, NCH_2C), 5.05-4.78 (m, 2H, NCH_2CH$_2$), 2.00-1.93 (m, 2H, NCH$_2$CH_2), 1.35-1.25 (m, 4H, CH_2CH_2CH$_3$), 0.77 (t, 3H, ^{3}J = 7.2 Hz, CH_3). ^{13}C{^{1}H} NMR (100.6 MHz, CD_2Cl_2, 300 K), δ (ppm) = 179.4 (Pt=*C*), 156.5, 153.3, 139.6, 134.9, 133.7, 132.1, 131.8, 129.2, 128.8, 128.4, 126.1, 125.8, 125.6, 125.1 (phenyl), 124.1 (pyridine), 115.7, 112.2, 110.2 (benzimidazole), 105.7, 105.1 (*C*≡*C*), 52.4 (C of N*C*H$_2$N), 48.3, 30.3, 29.7, 22.9, 14.3 (C of (CH$_2$)$_4$CH$_3$). ESI$^+$ MS *m/z*: 725.1 [M + CHCl]$^+$ (M = $C_{34}H_{31}N_3Pt$). Anal. Calc. for $C_{34}H_{31}N_3Pt$: C, 60.35; H, 4.62; N, 6.21 found: C, 60.71; H, 4.73; N, 6.03. IR (ATR, cm^{-1}) ν(C≡C) = 2121, 2106.

[Pt(ppbim)(C≡CC$_6$H$_4$N(C$_6$H$_5$)$_2$)$_2$] 5e. A brown compound was obtained. Eluent: DCM/ EtOAc (v/v 19:2), slight decomposition on silica gel during column chromatography. Yield: 25%. ^{1}H NMR (400 MHz, CD_2Cl_2, 300 K): δ (ppm) = 9.67 (d, 1H, ^{3}J = 6.0 Hz, pyridine), 7.92 (t, 1H, ^{3}J = 7.5 Hz, pyridine), 7.63-7.57 (m, 2H, benzimidazole), 7.48 (d, 1H, ^{3}J = 7.8 Hz, pyridine), 7.41-7.34 (m, 1H, pyridine, 2H, benzimidazole), 7.28-7.21 (m, 12H, *o*-phenyl, *m*-phenyl, N), 7.07-7.04 (m, 8H, phenyl, N), 7.01-6.96 (m, 4H, phenyl, N), 6.92 (d, 4H, ^{3}J = 9.0 Hz, *o*-phenyl), 5.54-5.48 (m, 2H, NCH_2C), 4.95-4.84 (m, 2H, NCH_2CH$_2$), 2.04-1.95 (m, 2H, NCH$_2$CH_2), 1.37-1.30 (m, 2H, CH$_2$CH_2CH$_3$), 1.25-1.18 (m, 2H, CH_2CH$_2$CH$_3$), 0.80 (t, 3H, ^{3}J = 7.2 Hz, CH_3). ^{13}C{^{1}H} NMR (100.6 MHz, CD_2Cl_2, 300 K): δ (ppm) = 179.3 (Pt=*C*), 156.8, 153.3, 148.3, 148.2, 145.7, 145.4, 139.4, 134.8, 133.7, 132.8, 132.6, 129.7, 129.6, 126.1, 125.0, 124.9, 124.6, 124.4 (pyridine), 124.3, 124.2, 124.0, 123.9, 123.8, 123.5, 123.1, 122.9, 114.9, 112.2, 110.16 (benzimidazole), 105.3, 104.8, 78.0, 52.3, 48.4, 30.2, 29.7, 22.9, 14.4 ((*C*H$_2$)$_4$*C*H$_3$). ESI$^+$ MS *m/z*: 1011.3 [M]$^+$ (M = $C_{58}H_{49}N_5Pt$). Anal. Calcd. For $C_{58}H_{49}N_5Pt$: C, 68.90; H, 4.88; N, 6.93 found: C, 68.89; H, 4.80; N, 6.89. IR (ATR, cm^{-1}) ν(C≡C) = 2108.

X-ray diffraction analyses. Single-crystal X-ray diffraction data were collected at 183(2) K on an *Agilent Technologies Xcalibur Ruby* area-detector diffractometer using a single wavelength Enhance X-ray source with Mo K_α radiation (λ = 0.71073 Å)[23] from a micro-focus X-ray source and an *Oxford Instruments Cryojet XL* cooler. The selected suitable single crystals were mounted using polybutene oil on a flexible loop fixed on a goniometer head and immediately transferred to the diffractometer. Pre-experiment, data collection, data reduction and analytical absorption correction[24] were performed with the program suite *CrysAlisPro*.[25] Using *Olex2*,[26] the structure was solved by direct methods using *SHELXS97*[27] and refined with the *SHELXL2013*[27] program package by full-matrix least-squares minimization on F^2. *PLATON*[28] was used to check the results of the X-ray analyses. Crystal data for **I**: $C_{25}H_{32}I_2N_4Pt.(CH_2Cl_2)_{0.333}.(CH_4O)_{0.333}$ (M = 876.42), hexagonal, space group $P6_3/m$ (no. 176), a = 17.5075(2) Å, c = 16.9453(2) Å, V = 4498.09(12) Å^3, Z = 6, T = 183(2) K, μ(Mo Kα) = 6.819 mm^{-1}, D_{calc} = 1.941 g/mm^3, 48697 reflections measured ($5.238 \leq 2\Theta \leq 56.55$), 3858 unique ($R_{int}$ = 0.0409) which were used in all calculations. The final R_1 was 0.0391 ($I > 2\sigma(I)$) and wR_2 was 0.1063 (all data). Crystal data for **1a**: $C_{42}H_{46}F_2N_4PtO_2$ (M = 871.92), orthorhombic, space group $Pca2_1$ (no. 29), a = 13.7433(2) Å, b = 21.0614(3) Å, c = 13.18580(10) Å, V = 3816.67(8) Å^3, Z = 4, T = 183(2) K, μ(Mo Kα) = 3.727 mm^{-1}, D_{calc} = 1.517 g/mm^3, 34854 reflections measured ($5.77 \leq 2\Theta \leq 56.562$), 9470 unique ($R_{int}$ = 0.0498) which were used in all calculations. The final R_1 was 0.0347 ($I > 2\sigma(I)$) and wR_2 was 0.0653 (all data). Crystal data for **1b**: $C_{85}H_{91}N_8Pt_2Cl$ (M = 1650.28), monoclinic, space group $P2_1/c$ (no. 14), a = 16.9885(7) Å, b = 25.6500(8) Å, c = 19.5345(9) Å, β = 114.494(5)°, V = 7746.2(6) Å^3, Z = 4, T = 183(2) K, μ(Mo Kα) = 3.691 mm^{-1}, D_{calc} = 1.415 g/ mm^3, 60100 reflections measured ($5.468 \leq 2\Theta \leq 52.744$), 15828 unique ($R_{int}$ = 0.0863) which were used in all

calculations. The final R_1 was 0.0701 ($I > 2\sigma(I)$) and wR_2 was 0.1628 (all data). Crystal data for **2a**: $C_{65}H_{80}N_{12}F_4Pt_2O_3$ (M = 1543.59), triclinic, space group $P\bar{1}$ (no. 2), a = 13.8528(6) Å, b = 15.5714(5) Å, c = 17.8630(6) Å, α = 82.817(3)°, β = 69.071(4)°, γ = 73.626(3)°, V = 3451.7(2) Å^3, Z = 2, T = 183(2) K, μ(Mo Kα) = 4.110 mm^{-1}, D_{calc} = 1.485 g/mm^3, 34609 reflections measured ($5.086 \leq 2\Theta \leq 50.7$), 12649 unique ($R_{int}$ = 0.0646) which were used in all calculations. The final R_1 was 0.0539 ($I > 2\sigma(I)$) and wR_2 was 0.1247 (all data). For more details about the data collection and refinements parameters, see the Crystallographic Information files (Supporting Information). CCDC-950233 (for **I**), CCDC-950234 (for **1a**), CCDC-950235 (for **1b**) and CCDC-950236 (for **2a**) contain the supplementary crystallographic data (excluding structure factors) for this paper. These data can be obtained free of charge from The Cambridge Crystallographic Data Centre via www.ccdc.cam.ac.uk/data_request/cif.

ASSOCIATED CONTENT

Supporting Information. X-ray crystallographic data for complexes **I**, **1a**, **1b** and **2a** in CIF format, electronic absorption spectra of complexes **2b-5b** in different solvents, **2d** in CH_2Cl_2, emission spectra of complexes **1a-c**, **2a**, **2c** and **3a-3c** at r.t. in solution, emission spectra of complexes **1a-1c**, **2a-2c**, **3a-3c**, **4a**, **4b**, **4e**, **5a**, **5b** and **5e** at 77K, crystal data and refinement details of complexes **I**, **1a**, **1b** and **2b**, cartesian coordinates and energies for all optimized molecules and spatial plots of selected frontier orbitals of the optimized ground state of **1b-5b**. This material is available free of charge via the Internet at http://pubs.acs.org.

AUTHOR INFORMATION

Corresponding Author

*Email: venkatesan.koushik@aci.uzh.ch

Authors Contributions

The manuscript was written through contributions of all authors. All authors have given approval to the final version of the manuscript.

Notes

The authors declare no competing interests.

Funding

This work was supported by the Swiss National Science Foundation (Grant no. 200021_135488) and University of Zürich.

Acknowledgements

K.V. is grateful to Prof. H. Berke and Prof. R. Alberto for their generous support.

References

(1) (a) Baldo, M. A.; O'Brien, D. F.; You, Y.; Shoustikov, A.; Sibley, S.; Thompson, M. E.; Forrest, S. R. *Nature* **1998**, *395*, 151. (b) Thompson, M. *MRS Bull.* **2007**, *32*, 694. (c) Xiang, H.-F.; Lai, S.-W.; Lai, P. T.; Che, C.-M. In *Highly Efficient OLEDs with Phosphorescent Materials*; Wiley-VCH Verlag GmbH & Co. KGaA: 2008, p 259. (d) Yersin, H.; Finkenzeller, W. J. In *Highly Efficient OLEDs with Phosphorescent Materials*; Wiley-VCH Verlag GmbH & Co. KGaA: 2008, p 1. (e) Yersin, H.; Rausch, A. F.; Czerwieniec, R.; Hofbeck, T.; Fischer, T. *Coord. Chem. Rev*. **2011**, *255*, 2622. (f) Balzani, V.; Campagna, S.; Williams, J. A. G. In *Photochemistry and Photophysics of Coordination Compounds II*; Springer Berlin Heidelberg: 2007; Vol. 281, p 205. (g) Chi, Y.; Chou, P.-T. *Chem. Soc. Rev.* **2010**, *39*, 638. (h) Wong, W.-Y.; Ho, C.-L. *Acc. Chem. Res.* **2010**, *43*, 1246. (i) Currie, M. J.; Mapel, J. K.; Heidel, T. D.; Goffri, S.; Baldo, M. A. *Science* **2008**, *321*, 226. (j) Wong, W.-Y.; Harvey, P. D. *Macromol. Rapid Commun.* **2010**, *31*, 671. (k) Chan, C.-W.; Cheng, L.-K.; Che, C.-M. *Coord. Chem. Rev*. **1994**, *132*, 87. (l) Lu, W.; Mi, B.-X.; Chan, M. C. W.; Hui, Z.; Che, C.-M.; Zhu, N.; Lee, S.-T. *J. Am. Chem. Soc*. **2004**, *126*, 4958.

(2) (a) Li, K.; Guan, X.; Ma, C.-W.; Lu, W.; Chen, Y.; Che, C.-M. *Chem. Comm.* **2011**, *47*, 9075. (b) Wang, Z.; Turner, E.; Mahoney, V.; Madakuni, S.; Groy, T.; Li, J. *Inorg. Chem.* **2010**, *49*, 11276. (c) Hang, X.-C.; Fleetham, T.; Turner, E.; Brooks, J.; Li, J. *Angew. Chem. Int. Ed*. **2013**, *52*, 6753. (d) Han, J.; Chen, X.; Shen, L.; Chen, Y.; Fang, W.; Wang, H. *Chem.–Eur. J.* **2011**, *17*, 13971. (e) Rochester, D. L.; Develay, S.; Zalis, S.; Williams, J. A. G. *Dalton Trans.*

2009, 1728. (f) Hanson, K.; Roskop, L.; Djurovich, P. I.; Zahariev, F.; Gordon, M. S.; Thompson, M. E. *J. Am. Chem. Soc*. **2010**, *132*, 16247.

(3) (a) Tsuboyama, A.; Iwawaki, H.; Furugori, M.; Mukaide, T.; Kamatani, J.; Igawa, S.; Moriyama, T.; Miura, S.; Takiguchi, T.; Okada, S.; Hoshino, M.; Ueno, K. *J. Am. Chem. Soc*. **2003**, *125*, 12971. (b) Yang, C.-H.; Tai, C.-C.; Sun, I. W. *J. Mater. Chem.* **2004**, *14*, 947. (c) Tamayo, A. B.; Alleyne, B. D.; Djurovich, P. I.; Lamansky, S.; Tsyba, I.; Ho, N. N.; Bau, R.; Thompson, M. E. *J. Am. Chem. Soc*. **2003**, *125*, 7377. (d) Tsuzuki, T.; Shirasawa, N.; Suzuki, T.; Tokito, S. *Adv. Mater.* **2003**, *15*, 1455.

(4) (a) Unger, Y.; Zeller, A.; Ahrens, S.; Strassner, T. *Chem. Comm.* **2008**, 3263. (b) Unger, Y.; Meyer, D.; Molt, O.; Schildknecht, C.; Münster, I.; Wagenblast, G.; Strassner, T. *Angew. Chem. Int. Ed*. **2010**, *49*, 10214. (c) Unger, Y.; Meyer, D.; Strassner, T. *Dalton Trans.* **2010**, *39*, 4295. (d) Tronnier, A.; Strassner, T. *Dalton Trans.* **2013**, *42*, 9847.

(5) (a) Yang, X.; Wang, Z.; Madakuni, S.; Li, J.; Jabbour, G. E. *Adv. Mater.* **2008**, *20*, 2405. (b) Fleetham, T.; Wang, Z.; Li, J. *Org. Electron.* **2012**, *13*, 1430.

(6) Hudson, Z. M.; Sun, C.; Helander, M. G.; Chang, Y.-L.; Lu, Z.-H.; Wang, S. *J. Am. Chem. Soc*. **2012**, *134*, 13930.

(7) (a) Sajoto, T.; Djurovich, P. I.; Tamayo, A.; Yousufuddin, M.; Bau, R.; Thompson, M. E.; Holmes, R. J.; Forrest, S. R. *Inorg. Chem.* **2005**, *44*, 7992. (b) Yam, V. W.-W. *Acc. Chem. Res.***2002**, *35*, 555. (c) Baggaley, E.; Weinstein, J. A.; Williams, J. A. G. *Coord*. *Chem*. *Rev*. **2012**, *256*, 1762. (d) Kalionowski, J.; Fattori, V.; Cocchi, M.; Williams, J. A. G. *Coord*. *Chem*. *Rev*. **2011**, *255*, 2401.

(8) Zhang, Y.; Garg, J. A.; Michelin, C.; Fox, T.; Blacque, O.; Venkatesan, K. *Inorg. Chem.* **2011**, *50*, 1220.

(9) (a) Unger, Y.; Zeller, A.; Taige, M. A.; Strassner, T. *Dalton Trans.* **2009**, 4786. (b) Muehlhofer, M.; Strassner, T.; Herdtweck, E.; Herrmann, W. A. *J. Organomet. Chem.* **2002**, *660*, 121.

(10) (a) Jahnke, M. C.; Pape, T.; Hahn, F. E. *Z. Naturforsch., B: Chem. Sci.* **2010**, 341. (b) Tanase A. D., Herdtweck, E., Herrmann, W. A., Kuehn, F. E. *Heterocycles* **2007**, *73*, 651.

(11) Gusev, D. G. *Organometallics* **2009**, *28*, 6458.

(12) (a) Vanhelmont, F. W.; M.; Johnson, R. C.; Hupp, J. T. *Inorg. Chem.* **2000**, *39*, 1814. (b) Hissler, M.; Connick, W. B.; Geiger, D. K.; McGarrah, J. E.; Lipa, D.; Lachicotte, R. J.; Eisenberg, R. *Inorg. Chem.* **2000**, *39*, 447. (c) Wadas, T. J.; Chakraborty, S.; Lachicotte, R. J.; Wang, Q.-M.; Eisenberg, R. *Inorg. Chem.* **2005**, *44*, 2628. (d) Hua, F.; Kinayyigit, S,; Cable, J. R.; Castellano, F. N. *Inorg*. *Chem*. **2006**, *45*, 4304. (e) McGarrah, J. E.; Hupp, J. T.; Smirnov, S. N. *J*. *Phys*. *Chem*. *A* **2009**, *113*, 6430.

(13) (a) Farley, S. J.; Rochester, D. L.; Thompson, A. L.; Howard, J. A. K.; Williams, J. A. G. *Inorg. Chem.* **2005**, *44*, 9690. (b) Lai, S.-W.; Chan, M. C.-W.; Cheung, T.-C.; Peng, S.-M.; Che, C.-M. *Inorg. Chem.* **1999**, *38*, 4046. (c) Connick, W. B.; Geiger, D.; Eisenberg, R. *Inorg. Chem.* **1999**, *38*, 3264.

(14) (a) Yang, Q.-Z.; Wu, L.-Z.; Wu, Z.-X.; Zhang, L.-P.; Tung, C.-H. *Inorg. Chem.* **2002**, *41*, 5653. (b) Wen, H.-M.; Wu, Y.-H.; Fan, Y.; Zhang, L.-Y.; Chen, C.-N.; Chen, Z.-N. *Inorg. Chem.* **2010**, *49*, 2210.

(15) (a) Chan, C. K. M.; Tao, C.-H.; Tam, H.-L.; Zhu, N.; Yam, V. W.-W.; Cheah, K.-W. *Inorg. Chem.* **2009**, *48*, 2855. (b) Tao, C.-H.; Zhu, N.; Yam, V. W.-W. *Chem.–Eur. J.* **2005**, *11*, 1647.

(16) Frisch, M. J.; Trucks, G. W.; Schlegel, H. B.; Scuseria, G. E.; Robb, M. A.; Cheeseman, J. R.; Montgomery, J. A.; Vreven, T.; Kudin, K. N.; Burant, J. C.; Millam, J. M.; Iyengar, S. S.; Tomasi, J.; Barone, V.; Mennucci, B.; Cossi, M.; Scalmani, G.; Rega, N.; Petersson, G. A.; Nakatsuji, H.; Hada, M.; Ehara, M.; Toyota, K.; Fukuda, R.; Hasegawa, J.; Ishida, M.; Nakajima, T.; Honda, Y.; Kitao, O.; Nakai, H.; Klene, M.; Li, X.; Knox, J. E.; Hratchian, H. P.; Cross, J. B.; Bakken, V.; Adamo, C.; Jaramillo, J.; Gomperts, R.; Stratmann, R. E.; Yazyev, O.; Austin, A. J.; Cammi, R.; Pomelli, C.; Ochterski, J. W.; Ayala, P. Y.; Morokuma, K.; Voth, G. A.; Salvador, P.; Dannenberg, J. J.; Zakrzewski, V. G.; Dapprich, S.; Daniels, A. D.; Strain, M. C.; Farkas, O.; Malick, D. K.; Rabuck, A. D.; Raghavachari, K.; Foresman, J. B.; Ortiz, J. V.; Cui, Q.; Baboul, A. G.; Clifford, S.; Cioslowski, J.; Stefanov, B. B.; Liu, G.; Liashenko, A.; Piskorz, P.; Komaromi, I.; Martin, R. L.; Fox, D. J.; Keith, T.; Laham, A.; Peng, C. Y.; Nanayakkara, A.; Challacombe, M.; Gill, P. M. W.; Johnson, B.; Chen, W.; Wong, M. W.; Gonzalez, C.; Pople, J. A. Gaussian 03 (Gaussian, Inc., Wallingford, CT, 2003).

(17) Adamo, C.; Barone, V. J. *Chem. Phys.* **1999**, *110*, 6158.

(18) Dunning Jr, T. H.; Hay, P. J. Modern Theoretical Chemistry; Schaefer, H. F., III, Ed.; Plenum: New York, 1976; Vol. 3, p 1.

(19) Ditchfield, R.; Hehre, W. J.; Pople, J. A. *J. Chem. Phys*. **1971**, *54*, 724.

(20) (a) Stratmann, R. E.; Scuseria, G. E.; Frisch, M. J. *J. Chem. Phys.* **1998**, *109*, 8218. (b) Bauernschmitt, R.; Ahlrichs, R. *Chem. Phys. Lett.* **1996**, *256*, 454. (c) Casida, M. E.; Jamorski, C.; Casida, K. C.; Salahub, D. R. *J. Chem. Phys.* **1998**, *108*, 4439.

(21) (a) Barone, V.; Cossi, M. *J. Phys. Chem. A* **1998**, *102*, 1995. (b) Cossi, M.; Rega, N.; Scalmani, G.; Barone, V. *J. Comp. Chem.* **2003**, *24*, 669.

(22) Diez-Barra, E.; de la Hoz, A.; Rodriguez-Curiel, R.; Tejeda, J. *Tetrahedron* **1997**, *53*, 2253.

(23) Agilent Technologies (formerly Oxford Diffraction), Yarnton, Oxfordshire, England, 2012.

(24) Clark, R. C.; Reid, J. S. *Acta Crystallogr., Sect. A.* **1995**, *51*, 887.

(25) CrysAlisPro Version 1.171.36.20, Agilent Technologies, Yarnton, Oxfordshire, England, 2012.

(26) Dolomanov, O. V.; Bourhis, L. J.; Gildea, R. J.; Howard, J. A. K.; Puschmann, H. *J. Appl. Cryst.* **2009**, *42*, 339.

(27) Sheldrick, G. M. *Acta Crystallogr., Sect. A.* **2008**, *64*, 112.

(28) Spek, A. L. *J. Appl. Crystallogr.* **2003**, *36*, 7.

Table of Content graphic

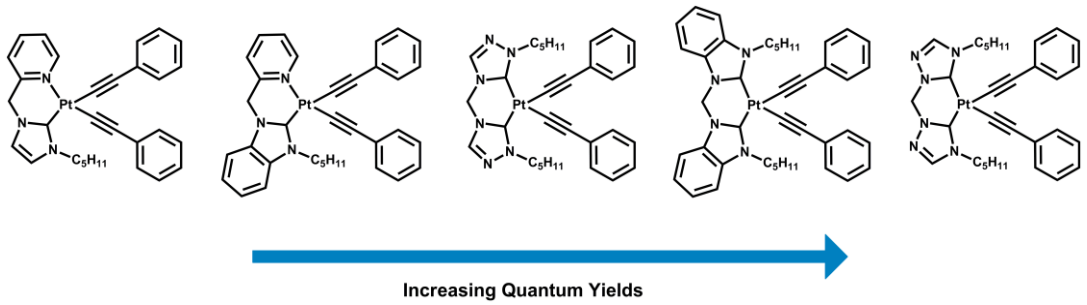

Table of Content (Synopsis)

A series of Pt(II) bis acetylide complexes bearing electronically different chelating NHC ligands were investigated. The varying extent of the quantum efficiencies of the deep blue emission of the different complexes is strongly suggestive of the impact of the NHC ligand on the triplet manifold.

Supporting Information

Tuning the Luminescent Properties of Pt(II) Acetylide Complexes Through Varying the Electronic Properties of N-Heterocyclic Carbene Ligands

*Yuzhen Zhang, Jessica Clavadetscher, Michael Bachmann, Olivier Blacque and Koushik Venkatesan**

Institute of Inorganic Chemistry, University of Zürich, Winterthurerstrasse 190, CH-8057, Zürich, Switzerland

Table of Contents

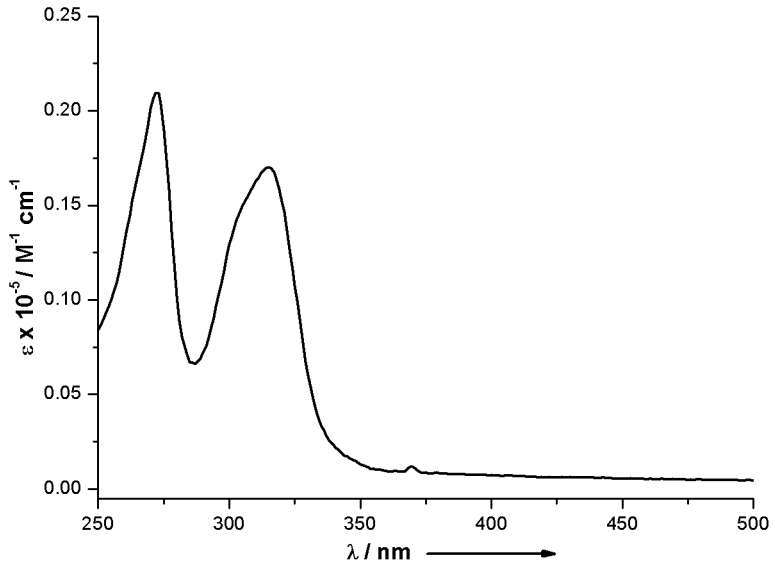

Figure S1. Electronic absorption spectrum of complex **2d** in CH_2Cl_2.

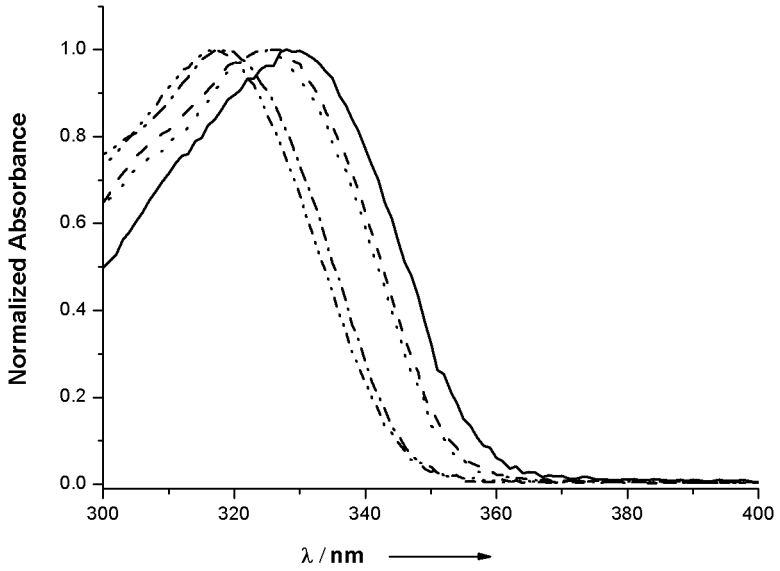

Figure S2. UV-Vis absorption spectra of **2b** in toluene (—), THF (···), CH_2Cl_2 (---), CH_3CN (-·-·-·), and MeOH(-··-··)

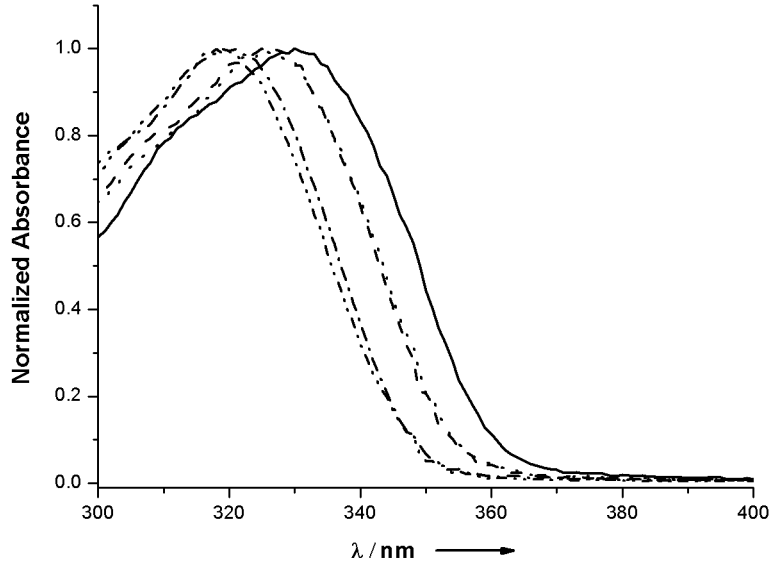

Figure S3. UV-Vis absorption spectra of **3b** in toluene (—), THF (···), CH_2Cl_2 (---), CH_3CN (-·-·-·), and MeOH(-··-··)

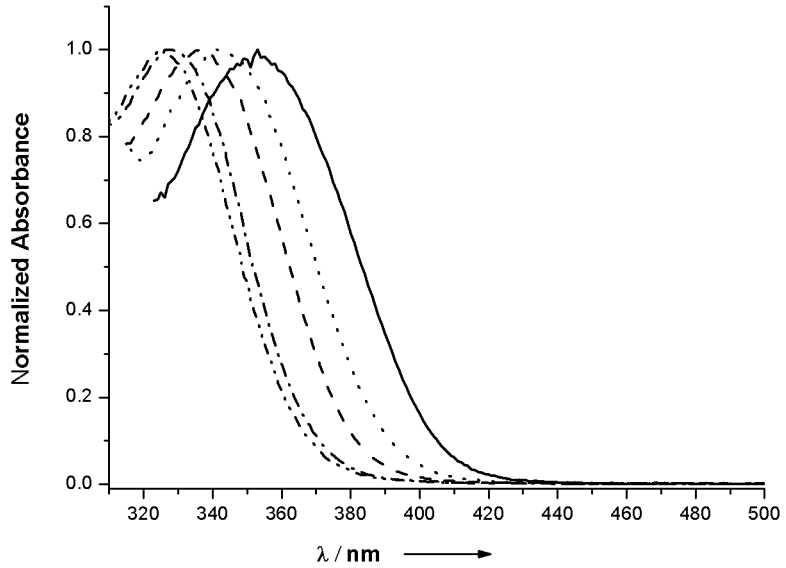

Figure S4. UV-Vis absorption spectra of **4b** in toluene (—), THF (···), CH_2Cl_2 (---), CH_3CN (-·-·-·), and MeOH(-··-··)

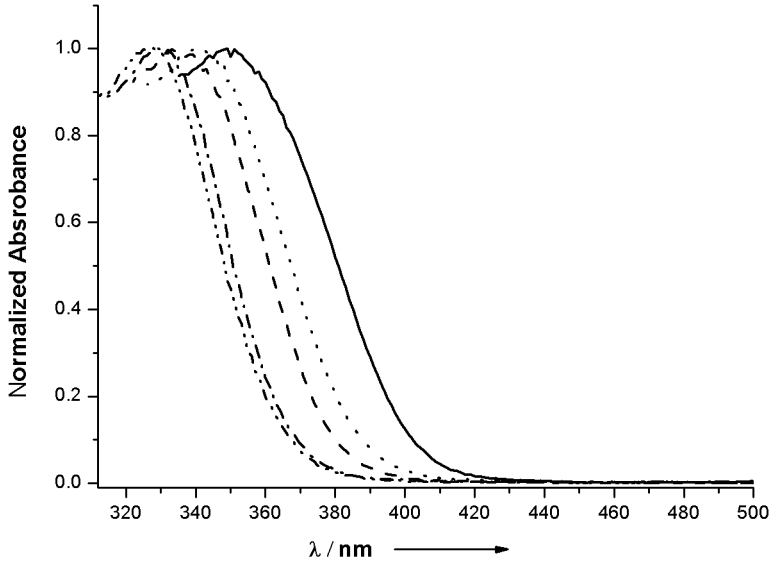

Figure S5. UV-Vis absorption spectra of **5b** in toluene (—), THF (···), CH_2Cl_2 (---), CH_3CN (-·-·-·), and MeOH(-··-··)

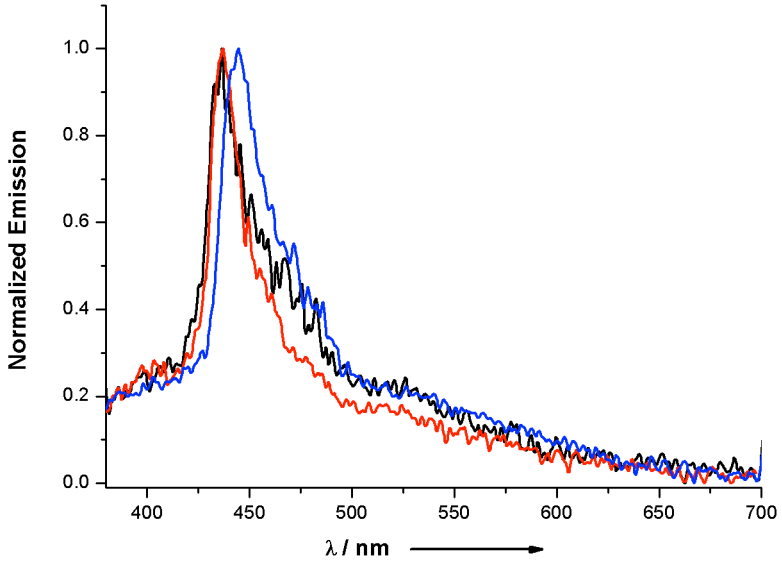

Figure S6. Normalized emission spectra of complexes **1a** (black), **1b** (red) and **1c** (blue) in degassed CH_2Cl_2.

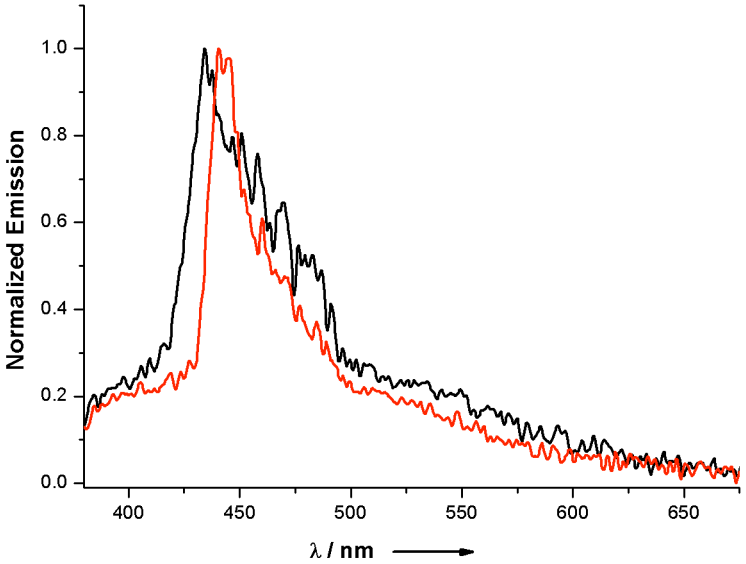

Figure S7. Normalized emission spectra of complexes **2a** (black) and **2c** (red) in degassed CH_2Cl_2.

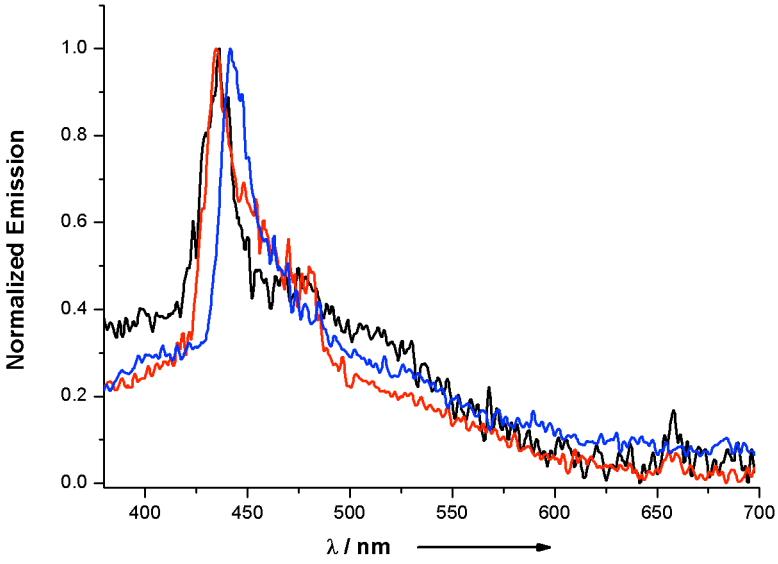

Figure S8. Normalized emission spectra of complexes **3a** (black), **3b** (red) and **3c** (blue) in degassed CH_2Cl_2.

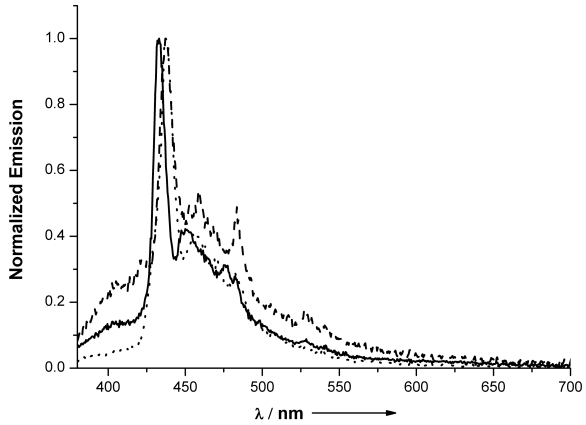

Figure S9. Normalized emission spectra of complexes **1a** (—), **1b** (- - -) and **1c** (···) in 2-MeTHF at 77 K.

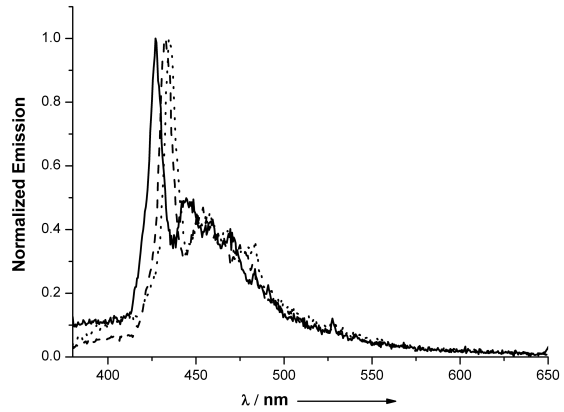

Figure S10. Normalized emission spectra of complexes 2**a** (—), **2b** (- - -) and **2c** (···) in 2-MeTHF at 77 K.

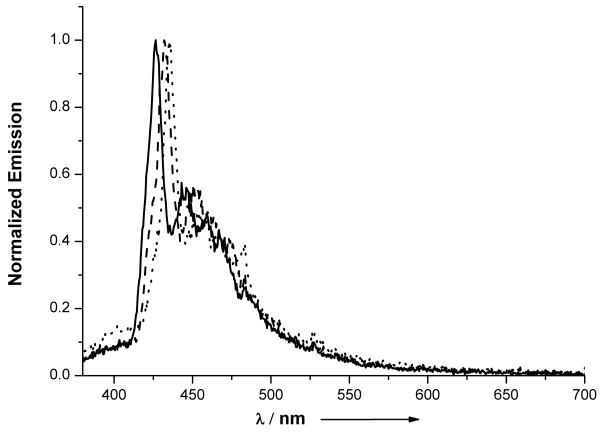

Figure S11. Normalized emission spectra of complexes 3**a** (—), **3b** (- - -) and **3c** (···) in 2-MeTHF at 77 K.

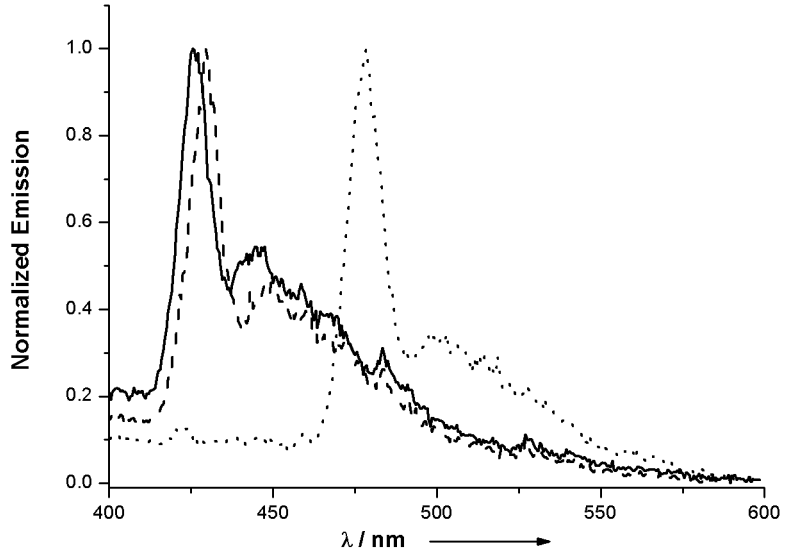

Figure S12. Normalized emission spectra of complexes **4a** (—), **4b** (- - -) and **4e** (···) in 2-MeTHF at 77 K.

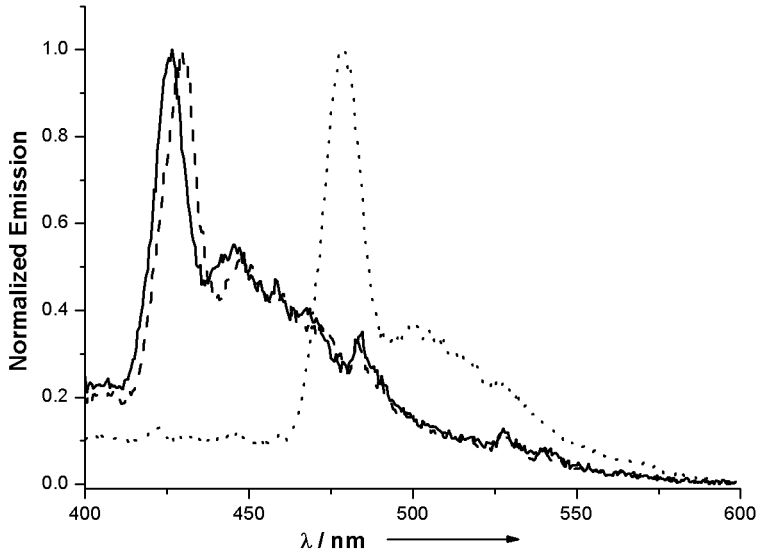

Figure S13. Normalized emission spectra of complexes 5**a** (—), **5b** (- - -) and **5e** (···) in 2-MeTHF at 77 K.

Table S1. Crystal data and structure refinement for **I**, **1a**, **1b**, and **2b**.

	I	**1a**	**1b**	**2a**
CCDC number	950233	950234	950235	950236
Empirical formula	$C_{25}H_{32}I_2N_4Pt$ $.(CH_2Cl_2)_{0.333}.(CH_4O)_{0.333}$	$C_{42}H_{46}F_2N_4PtO_2$	$C_{85}H_{91}N_8Pt_2Cl$	$C_{65}H_{80}N_{12}F_4Pt_2O_3$
Formula weight	876.42	871.92	1650.28	1543.59
Temperature/K	183(2)	183(2)	183(2)	183(2)
Crystal system	hexagonal	orthorhombic	monoclinic	triclinic
Space group	$P6_3/m$	$Pca2_1$	$P2_1/c$	P-1
a/Å	17.5075(2)	13.7433(2)	16.9885(7)	13.8528(6)
b/Å	17.5075(2)	21.0614(3)	25.6500(8)	15.5714(5)
c/Å	16.9453(2)	13.18580(10)	19.5345(9)	17.8630(6)
α/°	90	90	90	82.817(3)
β/°	90	90	114.494(5)	69.071(4)
γ/°	120	90	90	73.626(3)
Volume/$Å^3$	4498.09(12)	3816.67(8)	7746.2(6)	3451.7(2)
Z	6	4	4	2
$\rho_{calc}mg/mm^3$	1.941	1.517	1.415	1.485
m/mm^{-1}	6.819	3.727	3.691	4.110
F(000)	2484.0	1752.0	3320.0	1540.0
Crystal size/mm^3	0.26 × 0.10 × 0.05	0.16 × 0.15 × 0.09	0.34 × 0.13 × 0.07	0.31 × 0.09 × 0.03
2Θ range for data collection	5.238 to 56.55°	5.77 to 56.562°	5.468 to 52.744°	5.086 to 50.7°
Index ranges	-23 ≤ h ≤ 23, -23 ≤ k ≤ 22, -22 ≤ l ≤ 22	-18 ≤ h ≤ 17, -28 ≤ k ≤ 28, -17 ≤ l ≤ 17	-21 ≤ h ≤ 20, -32 ≤ k ≤ 28, -24 ≤ l ≤ 22	-16 ≤ h ≤ 16, -18 ≤ k ≤ 18, -21 ≤ l ≤ 21
Reflections collected	48697	34854	60100	34609
Independent reflections	3858[R(int) = 0.0409]	9470[R(int) = 0.0498]	15828[R(int) = 0.0863]	12649[R(int) = 0.0646]
Data/restraints/parameters	3858/10/167	9470/155/517	15828/149/518	12649/229/758
Goodness-of-fit on F^2	1.120	1.014	1.034	1.044
Final R indexes [I>=2σ (I)]	R_1 = 0.0391, wR_2 = 0.1024	R_1 = 0.0347, wR_2 = 0.0579	R_1 = 0.0701, wR_2 = 0.1433	R_1 = 0.0539, wR_2 = 0.1091
Final R indexes [all data]	R_1 = 0.0467, wR_2 = 0.1063	R_1 = 0.0580, wR_2 = 0.0653	R_1 = 0.1091, wR_2 = 0.1628	R_1 = 0.0879, wR_2 = 0.1247
Largest diff. peak/hole / e $Å^{-3}$	1.50/-1.73	1.38/-0.66	1.95/-1.81	1.66/-1.14
Flack parameter	n/a	-0.020(4)	n/a	n/a

Table S2. Electrochemical data[a] for complexes **4(a, b, e)** and **5(a, b, e)**.

Complex	E_{ox} (V)	E_{Red} (V)
4a	-	-2.49
4b	-	-2.49
4e	+0.28, +0.44 quasi reversible	-2.53
5a	-	-2.44
5b	-	-2.44
5e	+0.29, +0.45 quasi reversible	-2.45

[a] Scan rate = 100 mVs^{-1} in 0.1 M [*n*-Bu_4N][PF_6] (Glassy carbon electrode; E vs Fc^+/ Fc; 20 ^oC; DMF).

Energies and cartesian coordinates of the DFT optimized ground-state structure of 1b

C	-2.56141100	2.42376700	6.77489900
C	-2.56141100	2.42376700	-6.77489900
C	-0.87833600	1.90295600	4.94583900
C	-0.87833600	1.90295600	-4.94583900
C	-1.55507900	1.41955300	6.22545800
C	-1.55507900	1.41955300	-6.22545800
C	0.76587900	1.43078900	3.10489000
C	0.76587900	1.43078900	-3.10489000
C	-5.24729500	0.04839300	4.32298700
C	-5.24729500	0.04839300	-4.32298700
C	0.14308200	0.91263700	4.39536100
C	0.14308200	0.91263700	-4.39536100
C	-4.28151300	0.19190900	3.33210100
C	-4.28151300	0.19190900	-3.33210100
C	-5.18101100	-1.01180100	5.22805000
C	-5.18101100	-1.01180100	-5.22805000
C	-3.21605800	-0.72279500	3.22623500
C	-3.21605800	-0.72279500	-3.22623500
C	-2.21023600	-0.56763300	2.22922000
C	-2.21023600	-0.56763300	-2.22922000
C	-1.33583700	-0.43071100	1.37890400
C	-1.33583700	-0.43071100	-1.37890400
C	-4.13666500	-1.93175100	5.12880200
C	-4.13666500	-1.93175100	-5.12880200
C	1.56489300	-0.18550500	1.37879700
C	1.56489300	-0.18550500	-1.37879700
C	-3.16460600	-1.79020600	4.14358800
C	-3.16460600	-1.79020600	-4.14358800
C	2.91547500	-1.67925500	0.00000000
H	-2.08252500	3.38377500	7.00766000
H	-2.08252500	3.38377500	-7.00766000
H	-0.39151000	2.87310700	5.13529400
H	-3.03324500	2.05473800	7.69275900
H	-3.35886900	2.61499500	6.04684700
H	-0.39151000	2.87310700	-5.13529400
H	-3.03324500	2.05473800	-7.69275900
H	-3.35886900	2.61499500	-6.04684700
H	1.27280100	2.39152300	3.26751600
H	-1.64716600	2.08409800	4.18127800
H	1.27280100	2.39152300	-3.26751600
H	-1.64716600	2.08409800	-4.18127800
H	-6.06193300	0.76650200	4.38601000
H	-0.78881700	1.21030300	6.98683300
H	-6.06193300	0.76650200	-4.38601000
H	-0.78881700	1.21030300	-6.98683300
H	-0.00951600	1.57422800	2.34851700
H	-0.00951600	1.57422800	-2.34851700
H	-4.33901500	1.01163900	2.62095300
H	-4.33901500	1.01163900	-2.62095300
H	-2.06311500	0.46738100	6.02282500
H	-2.06311500	0.46738100	-6.02282500
H	0.91874200	0.71917800	5.14948700
H	0.91874200	0.71917800	-5.14948700
H	-0.34714400	-0.04327300	4.17762400

H	-0.34714400	-0.04327300	-4.17762400
H	-4.07914300	-2.76658900	5.82376500
H	-4.07914300	-2.76658900	-5.82376500
H	-2.35324700	-2.50909500	4.06482700
H	-2.35324700	-2.50909500	-4.06482700
H	3.92474200	-2.09213900	0.00000000
H	2.18589600	-2.49405200	0.00000000
N	1.74040200	0.51462000	2.52333000
N	1.74040200	0.51462000	-2.52333000
N	2.72865200	-0.87602700	1.18618300
N	2.72865200	-0.87602700	-1.18618300
Pt	0.08435300	-0.26721900	0.00000000
H	-5.93930400	-1.12299600	-5.99916200
H	-5.93930400	-1.12299600	5.99916200
C	3.00714600	0.28984500	3.04899700
C	3.00714600	0.28984500	-3.04899700
C	3.65470100	0.80003400	-4.17103700
H	3.16530100	1.49976800	-4.84095400
C	4.96060500	0.37587600	-4.40241100
H	5.49515300	0.75297100	-5.26954300
C	5.59839900	-0.52962500	-3.54266000
H	6.61645500	-0.84217100	-3.75664800
C	4.95389000	-1.03678600	-2.41704800
C	3.65470100	0.80003400	4.17103700
C	4.96060500	0.37587600	4.40241100
H	5.49515300	0.75297100	5.26954300
C	5.59839900	-0.52962500	3.54266000
H	6.61645500	-0.84217100	3.75664800
C	4.95389000	-1.03678600	2.41704800
H	3.16530100	1.49976800	4.84095400
H	5.45731200	-1.73681000	1.75624400
H	5.45731200	-1.73681000	-1.75624400
C	3.65176400	-0.60578500	-2.18460900
C	3.65176400	-0.60578500	2.18460900

Zero-point correction= 0.741434 (Hartree/Particle)
Thermal correction to Energy= 0.784877
Thermal correction to Enthalpy= 0.785821
Thermal correction to Gibbs Free Energy= 0.659508
Sum of electronic and zero-point Energies= -1923.163648
Sum of electronic and thermal Energies= -1923.120205
Sum of electronic and thermal Enthalpies= -1923.119261
Sum of electronic and thermal Free Energies= -1923.245574

Energies and cartesian coordinates of the DFT optimized ground-state structure of 2b

C	-7.34721100	1.40089300	1.91422600
C	7.34658700	1.40120600	1.91483000
C	-5.31630700	-0.08697500	1.57458700
C	5.31594700	-0.08695300	1.57491600
C	-6.62031400	0.43906100	0.98159200
C	6.62003000	0.43915500	0.98215600
C	-3.28379700	-1.53442700	1.26185000
C	3.28363500	-1.53458600	1.26192100
C	-4.35026800	4.49793000	0.43049900
C	4.35058800	4.49765900	0.43006600
C	-4.58278900	-1.04393900	0.64005800
C	4.58272300	-1.04409700	0.64033700
C	-3.36893400	3.51531200	0.51177800
C	3.36916600	3.51513000	0.51134600
C	-5.22167400	4.53934800	-0.65864200
C	5.22212600	4.53887300	-0.65897600
C	-3.23929200	2.54159100	-0.49701800
C	3.23957300	2.54128800	-0.49734300
C	-2.24338400	1.52579900	-0.41067700
C	2.24357700	1.52558800	-0.41095000
C	-1.38242600	0.65537500	-0.32947800
C	1.38255000	0.65524300	-0.32963200
C	-5.09927500	3.58579000	-1.66972900
C	5.09978200	3.58519300	-1.66995600
C	-1.38308600	-2.24203800	-0.21738800
C	1.38300400	-2.24210200	-0.21744600
C	-4.12330700	2.59733600	-1.59150700
C	4.12373400	2.59681700	-1.59172300
C	-2.23830300	-4.25934900	-0.63226600
C	2.23818000	-4.25941900	-0.63235600
C	-0.00008100	-3.66611600	-1.67403800

H	-7.59544900	0.91955300	2.86897100
H	7.59459800	0.92005200	2.86972900
H	-5.52850100	-0.59153900	2.53023000
H	-8.28242900	1.75957600	1.46900900
H	-6.72587400	2.27782300	2.13227400
H	5.52798100	-0.59138300	2.53066600
H	8.28190100	1.75988900	1.46981500
H	6.72511500	2.27812200	2.13255000
H	-3.46997900	-2.06894700	2.20029200
H	-4.66012800	0.76357800	1.80735600
H	3.46967000	-2.06914000	2.20037400
H	4.65962100	0.76355600	1.80743900
H	-4.43143700	5.24144400	1.22030100
H	-7.27749300	-0.40878000	0.73805200
H	4.43172000	5.24126500	1.21978500
H	7.27736900	-0.40863900	0.73888400
H	-2.60503800	-0.69938300	1.44870200
H	2.60487900	-0.69952700	1.44871300
H	-2.68298100	3.48995200	1.35423700
H	2.68310800	3.48991900	1.35372300
H	-6.40075600	0.94768200	0.03313700
H	6.40063200	0.94762700	0.03358500
H	-5.22197100	-1.90422400	0.39989400
H	5.22202100	-1.90436100	0.40041400
H	-4.34446300	-0.53055700	-0.29987700
H	4.34456900	-0.53084400	-0.29971300
H	-5.76797300	3.61337100	-2.52725300
H	5.76858700	3.61261600	-2.52740100
H	-4.02484500	1.85830400	-2.38242000
H	-2.34048700	-5.25874300	-1.03205700
H	2.34034800	-5.25880700	-1.03216600
H	4.02531900	1.85769000	-2.38255500
H	-0.00011600	-4.70121200	-2.02244600
H	-0.00008700	-2.98401900	-2.52908900
N	-2.56250000	-2.45079200	0.38670900
N	2.56240700	-2.45089100	0.38666200
N	-1.18269500	-3.42688700	-0.87964300
N	1.18258000	-3.42693800	-0.87970400
Pt	-0.00000100	-0.76333200	-0.23900100
H	5.98562100	5.31028000	-0.72176400
H	-5.98510000	5.31082300	-0.72142300
N	3.10215500	-3.67806400	0.14053200
N	-3.10228800	-3.67794800	0.14057400

Zero-point correction= 0.623133 (Hartree/Particle)
Thermal correction to Energy= 0.661082
Thermal correction to Enthalpy= 0.662026
Thermal correction to Gibbs Free Energy= 0.545160
Sum of electronic and zero-point Energies= -1648.369851
Sum of electronic and thermal Energies= -1648.331903
Sum of electronic and thermal Enthalpies= -1648.330958
Sum of electronic and thermal Free Energies= -1648.447824

Energies and cartesian coordinates of the DFT optimized ground-state structure of 3b

C	-1.49112400	1.82202300	7.32511100
C	-1.49112400	1.82202300	-7.32511100
C	0.03446900	1.51946400	5.31747000
C	0.03446900	1.51946400	-5.31747000
C	-0.52522800	0.89748700	6.59352500
C	-0.52522800	0.89748700	-6.59352500
C	1.52566800	1.24356600	3.30773900
C	1.52566800	1.24356600	-3.30773900
C	-4.44959500	0.47185100	4.39308400
C	-4.44959500	0.47185100	-4.39308400
C	1.00921000	0.60103300	4.58725400
C	1.00921000	0.60103300	-4.58725400
C	-3.46420600	0.57068600	3.41595800
C	-3.46420600	0.57068600	-3.41595800
C	-4.54243700	-0.66854400	5.19186100
C	-4.54243700	-0.66854400	-5.19186100
C	-2.53914400	-0.47232400	3.21758800
C	-2.53914400	-0.47232400	-3.21758800
C	-1.51704400	-0.37068400	2.22963700
C	-1.51704400	-0.37068400	-2.22963700
C	-0.63672000	-0.28637000	1.37857200
C	-0.63672000	-0.28637000	-1.37857200
C	-3.63784700	-1.71349900	5.00048200

C	-3.63784700	-1.71349900	-5.00048200
C	2.27078000	-0.20417300	1.37910300
C	2.27078000	-0.20417300	-1.37910300
C	-2.64718000	-1.61868900	4.02830400
C	-2.64718000	-1.61868900	-4.02830400
C	3.75475300	-1.61316600	0.00000000
H	-1.00357800	2.76286500	7.61143100
H	-1.00357800	2.76286500	-7.61143100
H	0.53328500	2.47028200	5.56300300
H	-1.87601700	1.35484000	8.23877300
H	-2.35119200	2.06826900	6.69110500
H	0.53328500	2.47028200	-5.56300300
H	-1.87601700	1.35484000	-8.23877300
H	-2.35119200	2.06826900	-6.69110500
H	2.03684900	2.19153700	3.51657900
H	-0.79778600	1.76590300	4.64359900
H	2.03684900	2.19153700	-3.51657900
H	-0.79778600	1.76590300	-4.64359900
H	-5.15556500	1.28848600	4.52719800
H	0.30525100	0.62616200	7.26228900
H	-5.15556500	1.28848600	-4.52719800
H	0.30525100	0.62616200	-7.26228900
H	0.70031700	1.43407000	2.61818800
H	0.70031700	1.43407000	-2.61818800
H	-3.40012100	1.45378900	2.78574300
H	-3.40012100	1.45378900	-2.78574300
H	-1.03978200	-0.03828500	6.33744100
H	-1.03978200	-0.03828500	-6.33744100
H	1.84935700	0.34982200	5.25226600
H	1.84935700	0.34982200	-5.25226600
H	0.50785700	-0.33806900	4.32317700
H	0.50785700	-0.33806900	-4.32317700
H	-3.70630100	-2.61094100	5.61130200
H	-3.70630100	-2.61094100	-5.61130200
H	-1.94704900	-2.43576600	3.87507700
H	-1.94704900	-2.43576600	-3.87507700
H	4.82159300	-1.83313400	0.00000000
H	3.16803300	-2.53671900	0.00000000
N	2.46628800	0.38357000	2.59079700
N	2.46628800	0.38357000	-2.59079700
N	3.44428300	-0.84065600	1.18010200
N	3.44428300	-0.84065600	-1.18010200
Pt	0.78831100	-0.20644500	0.00000000
H	-5.31633400	-0.74464700	-5.95158900
H	-5.31633400	-0.74464700	5.95158900
N	4.35488900	-0.69066900	2.17735100
N	4.35488900	-0.69066900	-2.17735100
C	3.72093900	0.06035000	3.02937000
C	3.72093900	0.06035000	-3.02937000
H	4.13615300	0.39868200	-3.96798800
H	4.13615300	0.39868200	3.96798800

Zero-point correction= 0.623225 (Hartree/Particle)
Thermal correction to Energy= 0.661156
Thermal correction to Enthalpy= 0.662100
Thermal correction to Gibbs Free Energy= 0.545258
Sum of electronic and zero-point Energies= -1648.374484
Sum of electronic and thermal Energies= -1648.336553
Sum of electronic and thermal Enthalpies= -1648.335609
Sum of electronic and thermal Free Energies= -1648.452451

Energies and cartesian coordinates of the DFT optimized ground-state structure of 4b

C	-6.93082500	0.47024300	-1.54289200
C	-4.70063500	-0.73202900	-1.35213500
C	-6.00713100	-0.35813000	-0.65770800
C	-2.46986600	-1.89096000	-1.18447200
C	3.70030500	5.52893500	-0.45588100
C	-4.39948300	3.90354800	-0.22592400
C	-3.78017500	-1.57563500	-0.47608600
C	2.88744200	4.40369100	-0.37109800
C	-3.29630300	3.07069700	-0.38167100
C	5.08275300	5.41643000	-0.30168200
C	-5.17357800	3.84337100	0.93370900
C	3.44124100	3.13200000	-0.12904900
C	-2.94129000	2.14813600	0.62179000
C	2.60474600	1.98094800	-0.04725000
C	-1.81810900	1.28746900	0.45738100

C	1.84939900	1.01514900	0.02136400
C	-0.84606400	0.55617600	0.30455600
C	5.64515400	4.16316900	-0.05827000
C	-4.82926700	2.93967800	1.93942700
C	-0.40185300	-2.29695000	0.16269900
C	4.83661100	3.03435000	0.02805000
C	-3.72977900	2.10052600	1.78772300
C	1.35988200	-3.36702800	1.48678900
H	-7.20029400	-0.07293800	-2.45794000
H	-4.92454700	-1.27402400	-2.28463800
H	-7.86018800	0.72629000	-1.02123000
H	-6.44811200	1.40901500	-1.83950100
H	-2.64952900	-2.42698200	-2.12529300
H	-4.17476300	0.18788600	-1.64342500
H	3.25146000	6.50196000	-0.64241100
H	-4.65370700	4.60979000	-1.01326500
H	-6.52534500	-1.27433700	-0.33724900
H	-1.92894200	-0.96879200	-1.40805500
H	1.81074800	4.48926600	-0.48787300
H	-2.68736600	3.12518100	-1.28020800
H	-5.77511700	0.20647700	0.25530000
H	-4.29114100	-2.50777200	-0.19178000
H	-3.54817800	-1.03425500	0.44923200
H	6.72120900	4.06509800	0.06769700
H	-5.42055000	2.88948300	2.85114700
H	5.27502700	2.05933400	0.22512000
H	-3.45877000	1.40158700	2.57476300
H	1.53250300	-4.34936300	1.93305600
H	1.30256100	-2.62308000	2.29078600
N	-1.57389800	-2.71012200	-0.37391200
N	0.08407500	-3.39643500	0.79678800
Pt	0.69305900	-0.59414900	0.09279500
H	-6.03313100	4.49795100	1.05467700
H	5.71564900	6.29797400	-0.36819900
C	-1.81142600	-4.03795600	-0.07707800
C	-0.76109300	-4.47841900	0.65945600
N	2.40069900	-1.83777200	-0.09803600
C	2.49408800	-3.01079600	0.55912500
C	3.40296700	-1.46858300	-0.91231400
C	3.59779000	-3.84396000	0.41280400
C	4.53286200	-2.25319300	-1.10715500
H	3.27995800	-0.50099400	-1.38764100
C	4.63623900	-3.46364400	-0.43293200
H	3.64009400	-4.78030200	0.96180500
H	5.31383100	-1.90587300	-1.77610800
H	5.50650900	-4.10169800	-0.55956800
H	-2.69895600	-4.55213300	-0.41434600
H	-0.55327700	-5.44424200	1.09558000

Zero-point correction= 0.520576 (Hartree/Particle)
Thermal correction to Energy= 0.552592
Thermal correction to Enthalpy= 0.553536
Thermal correction to Gibbs Free Energy= 0.451239
Sum of electronic and zero-point Energies= -1442.147562
Sum of electronic and thermal Energies= -1442.115546
Sum of electronic and thermal Enthalpies= -1442.114602
Sum of electronic and thermal Free Energies= -1442.216899

Energies and cartesian coordinates of the DFT optimized ground-state structure of 5b

C	-5.27782400	4.18637300	-1.69830300
C	-3.98329100	2.01381200	-1.45826400
C	-4.95614400	2.99256600	-0.80685600
C	-2.68182100	-0.12968000	-1.26324700
C	6.26631000	3.35937500	-0.52057600
C	-1.52188800	5.92394800	-0.00404000
C	-3.65027900	0.82002600	-0.56888100
C	5.00600100	2.77538600	-0.45200300
C	-0.96723300	4.66358100	-0.20075700
C	7.41073200	2.60476700	-0.25932900
C	-2.29814700	6.18698900	1.12539400
C	4.86057700	1.41511600	-0.11946700
C	-1.18152000	3.62825400	0.72976300
C	3.56786100	0.81856900	-0.05180200
C	-0.62433400	2.33366100	0.52212000
C	2.43980900	0.33707700	0.00618200
C	-0.13850800	1.22456700	0.33231500
C	7.28149500	1.25634200	0.07451400

C	-2.51199200	5.17316100	2.05977800
C	-1.11436000	-1.49592000	0.12152500
C	6.02329600	0.66708500	0.14442600
C	-1.96394500	3.90897600	1.86631300
C	-0.06077000	-3.27753600	1.43338200
H	-5.72407400	3.86625000	-2.64881600
H	-4.40690700	1.66084500	-2.41215400
H	-5.98352200	4.86960500	-1.21189500
H	-4.37030100	4.75694600	-1.92918800
H	-3.10551900	-0.50625900	-2.20399700
H	-3.05322300	2.54402300	-1.70698300
H	6.35645800	4.41230400	-0.77779200
H	-1.34207700	6.70908800	-0.73512900
H	-5.88528800	2.46373300	-0.54690000
H	-1.74776600	0.38902800	-1.49135000
H	4.11334200	3.36170700	-0.65095600
H	-0.35452300	4.46142600	-1.07526900
H	-4.52451900	3.34926400	0.13783600
H	-4.57367600	0.29254400	-0.29092800
H	-3.18205900	1.16959100	0.35893200
H	8.16705800	0.66068000	0.28483400
H	-3.10887100	5.36904000	2.94784200
H	5.92225200	-0.38155400	0.41217800
H	-2.12641300	3.12171200	2.59791800
H	-0.36696600	-4.22180500	1.88830500
H	0.24414900	-2.59081000	2.23254000
N	-2.32399900	-1.28649600	-0.45141100
N	-1.20043600	-2.70514400	0.74429800
Pt	0.65248800	-0.52097600	0.07156000
H	-2.72751700	7.17397300	1.27854700
H	8.39455500	3.06446500	-0.31264600
C	-3.17197500	-2.35832200	-0.20769500
C	-4.48244300	-2.61865800	-0.60017200
H	-5.04690800	-1.91220700	-1.20071600
C	-5.04428400	-3.82455400	-0.18949700
H	-6.06534200	-4.05925400	-0.47643600
C	-4.32137600	-4.74022700	0.58876800
H	-4.79315700	-5.66961700	0.89484100
C	-3.00868200	-4.48416400	0.97681000
H	-2.45613700	-5.20113400	1.57722000
C	-2.44739900	-3.28026000	0.56150500
N	1.56286600	-2.42243000	-0.16250400
C	1.10117200	-3.50212500	0.49875400
C	2.60914700	-2.56559000	-0.99201900
C	1.68159700	-4.75596500	0.34351800
C	3.23439600	-3.78915800	-1.19696400
H	2.94885100	-1.65358500	-1.47144800
C	2.76580100	-4.90647200	-0.51679900
H	1.28523900	-5.60339800	0.89543400
H	4.07762500	-3.84944900	-1.87761100
H	3.23232900	-5.87853100	-0.65097200

Zero-point correction= 0.568049 (Hartree/Particle)
Thermal correction to Energy= 0.602731
Thermal correction to Enthalpy= 0.603675
Thermal correction to Gibbs Free Energy= 0.495711
Sum of electronic and zero-point Energies= -1595.577018
Sum of electronic and thermal Energies= -1595.542336
Sum of electronic and thermal Enthalpies= -1595.541392
Sum of electronic and thermal Free Energies= -1595.649356

Energies and cartesian coordinates of the DFT optimized triplet-state structure of 1b

C	-6.62390652	2.88174122	2.65883820
C	6.92820254	1.94804415	2.43742119
C	-4.89467937	1.12438809	2.04147116
C	4.97479738	0.42485803	1.87394014
C	-6.15608949	1.87165215	1.61764012
C	6.29342448	1.02918408	1.40004111
C	-3.18115024	-0.63696105	1.48364911
C	3.01953023	-1.07248508	1.36389710
C	-2.81945822	6.01581947	-0.83013806
C	4.44393234	5.03267139	0.32007302
C	-4.42344534	0.10663801	1.00720308
C	4.33426533	-0.50243504	0.84581106
C	-2.10844316	4.86807738	-0.58845804
C	3.42757226	4.08905232	0.42862403
C	-4.13192632	5.95817948	-1.35642310

C	5.36782140	4.96102038	-0.72352706
C	-2.68894721	3.56479327	-0.86174807
C	3.31258526	3.04169823	-0.50633104
C	-1.98763216	2.42508019	-0.61309005
C	2.28175118	2.06544616	-0.39527303
C	-1.27474310	1.39622411	-0.38211703
C	1.40147711	1.21372109	-0.30519202
C	-4.71659636	4.70246836	-1.64780813
C	5.26220240	3.93317930	-1.66136413
C	-1.55155512	-1.50531512	-0.20192002
C	1.19232509	-1.69658613	-0.23145002
C	-4.03060431	3.53755627	-1.41544411
C	4.25071332	2.98412123	-1.55581512
C	-0.29487902	-2.92268822	-1.72966113
H	-6.84949351	2.39270518	3.61503228
H	7.13748955	1.41136511	3.37193126
H	-5.08015039	0.61810205	3.00178323
H	-7.52941558	3.40474326	2.33063218
H	-5.85285944	3.63878528	2.84673322
H	5.14367239	-0.12340501	2.81468621
H	7.87362363	2.36788618	2.07486616
H	6.26324646	2.78714122	2.67528521
H	-3.38020326	-1.16208709	2.42802819
H	-4.08940331	1.85011814	2.22608717
H	3.17719824	-1.63874312	2.29259718
H	4.27208633	1.23709109	2.10896516
H	-2.36903418	6.98290852	-0.61963305
H	-6.95915952	1.14637809	1.42006511
H	4.51404135	5.83244844	1.05407408
H	6.99421455	0.22018202	1.14506109
H	-2.35784018	0.06261300	1.65477513
H	2.31602718	-0.26251102	1.57166112
H	-1.09734308	4.90142138	-0.19336001
H	2.70557521	4.14795332	1.23891909
H	-5.96423543	2.38921219	0.66796805
H	6.11601649	1.59209812	0.47404204
H	-5.23235640	-0.60491105	0.78992206
H	5.03081939	-1.31313610	0.59007805
H	-4.18150032	0.61396505	0.06551801
H	4.12723832	0.05189400	-0.07681301
H	-5.71935945	4.66385436	-2.06741516
H	5.97278143	3.87112830	-2.48261719
H	-4.47011234	2.57272820	-1.65302513
H	4.16633832	2.18698317	-2.28984318
H	-0.36947503	-3.91583630	-2.17333817
H	-0.26045702	-2.16349717	-2.51967920
N	-2.69256521	-1.62015712	0.52930904
N	2.35944318	-1.96098815	0.41777603
N	-1.44941311	-2.67687620	-0.90180007
N	0.90832007	-2.83578822	-0.94212807
Pt	-0.07779401	-0.11359001	-0.23574402
H	6.15957449	5.70134446	-0.80700506
H	-4.68540736	6.87354552	-1.54456812
C	-3.29330725	-2.85293322	0.31485702
C	2.79541922	-3.24818425	0.14295001
C	3.89374830	-3.97569230	0.59557604
H	4.61574335	-3.54583527	1.28254910
C	4.03199431	-5.28278740	0.12960401
H	4.87897837	-5.87670946	0.46133304
C	3.10539924	-5.84389344	-0.75774906
H	3.24683225	-6.86373754	-1.10412309
C	1.99902915	-5.12065740	-1.20420809
C	-4.43990534	-3.43522426	0.84847606
C	-4.75797737	-4.72527937	0.42585303
H	-5.64641343	-5.20913640	0.82156206
C	-3.95807431	-5.40832341	-0.49887004
H	-4.23734732	-6.41139349	-0.80854206
C	-2.80593022	-4.82880137	-1.02953808
H	-5.06366939	-2.91107722	1.56580712
H	-2.18868217	-5.36952143	-1.74129313
H	1.28178110	-5.56742245	-1.88692015
C	1.85988414	-3.81893829	-0.73356206
C	-2.48811419	-3.54336827	-0.60316504

Energies and cartesian coordinates of the DFT optimized triplet-state structure of 2b

C	-7.49272359	1.36128710	2.01695415

C	7.31079055	1.07437708	2.04306816
C	-5.42204344	-0.05080200	1.59536212
C	5.23961140	-0.33366903	1.61693313
C	-6.81579752	0.33939003	1.11118408
C	6.55709049	0.19208601	1.05467408
C	-3.38584926	-1.49289812	1.22776610
C	3.16821024	-1.70542513	1.22441210
C	-3.03064323	5.27169340	-0.38352203
C	4.41489634	4.35459833	0.51645304
C	-4.72191336	-1.03369308	0.66211605
C	4.48382934	-1.22149509	0.63320005
C	-2.27119218	4.13551532	-0.29403702
C	3.39869726	3.40717726	0.58933304
C	-4.40851034	5.20326940	-0.71073805
C	5.31959943	4.34202734	-0.54603004
C	-2.86305822	2.82364722	-0.52831504
C	3.26518925	2.41585919	-0.40205803
C	-2.11441316	1.69655513	-0.42054403
C	2.23425617	1.43517011	-0.33065503
C	-1.34629411	0.68756605	-0.30796902
C	1.35339910	0.58150305	-0.27862802
C	-5.00784138	3.94250530	-0.96081707
C	5.19534940	3.36985226	-1.53914412
C	-1.51707411	-2.22054117	-0.28680402
C	1.24177310	-2.31222018	-0.27757002
C	-4.27588233	2.78796621	-0.88009407
C	4.18406732	2.41732119	-1.46966911
C	-2.41282219	-4.22633733	-0.68445205
C	2.04232016	-4.34597733	-0.73669206
C	-0.18006101	-3.66535428	-1.75680714
H	-7.59592258	0.97753008	3.03974624
H	7.55071560	0.52701904	2.96377523
H	-5.50221342	-0.48948504	2.60186120
H	-8.49543463	1.61609213	1.65495713
H	-6.90954354	2.28879918	2.06705316
H	5.43735143	-0.89392507	2.54427820
H	8.25287565	1.43863911	1.61713712
H	6.71190854	1.95022015	2.32084818
H	-3.52521127	-2.01229015	2.18341317
H	-4.80596937	0.85385707	1.69990913
H	3.33737926	-2.28352017	2.14065217
H	4.60384735	0.51880804	1.89576814
H	-2.57170120	6.24119749	-0.20421802
H	-7.43973459	-0.56308604	1.03813908
H	4.49945334	5.11103239	1.29355810
H	7.19093053	-0.65662405	0.75802406
H	-2.70389021	-0.65234405	1.37976511
H	2.50998919	-0.86284007	1.44752811
H	-1.21399509	4.17839532	-0.04901200
H	2.69124621	3.42053926	1.41428411
H	-6.74503551	0.74489206	0.09188901
H	6.35092848	0.76391406	0.13984901
H	-5.35939642	-1.91100115	0.48950304
H	5.09938839	-2.08729416	0.35387903
H	-4.54619535	-0.56288704	-0.31412902
H	4.26591133	-0.65763105	-0.28224402
H	-6.06174349	3.89557830	-1.22622409
H	5.89070144	3.35481126	-2.37551918
H	-4.72988936	1.82245014	-1.08379509
H	-2.53528919	-5.22541940	-1.07925108
H	2.11440716	-5.34054443	-1.15461509
H	4.08425431	1.66408813	-2.24689517
H	-0.21347602	-4.68711736	-2.14091817
H	-0.16230201	-2.94648923	-2.58515720
N	-2.69766621	-2.41059118	0.33351203
N	2.42909018	-2.56450920	0.31085602
N	-1.34974210	-3.41121826	-0.95252807
N	1.00531508	-3.48461727	-0.95862907
Pt	-0.08786301	-0.78201106	-0.25732302
H	6.11093146	5.08541539	-0.60138505
H	-5.00022739	6.11142048	-0.77766506
N	2.92960122	-3.80116429	0.03629000
N	-3.25795825	-3.63090728	0.09835001

Zero-point correction= 0.619230 (Hartree/Particle)
Thermal correction to Energy= 0.657675
Thermal correction to Enthalpy= 0.658620
Thermal correction to Gibbs Free Energy= 0.539739

Sum of electronic and zero-point Energies= -1648.272821
Sum of electronic and thermal Energies= -1648.234376
Sum of electronic and thermal Enthalpies= -1648.233432
Sum of electronic and thermal Free Energies= -1648.352313

Energies and cartesian coordinates of the DFT optimized triplet-state structure of 3b

C	-7.39167148	1.50266397	1.98740465
C	7.26717015	1.19564973	1.95441467
C	-5.36722449	0.02241015	1.58219790
C	5.22494827	-0.26207806	1.56122763
C	-6.75696153	0.43453100	1.10489594
C	6.53117673	0.27732328	0.98585778
C	-3.37752925	-1.49045318	1.23534675
C	3.18619729	-1.69535855	1.20578808
C	-3.03887530	5.24556284	-0.32276918
C	4.39171493	4.35471547	0.52612977
C	-4.70401555	-1.00352200	0.66820926
C	4.48505408	-1.18504667	0.59810468
C	-2.28158441	4.10928956	-0.23210079
C	3.38953261	3.39325465	0.60978166
C	-4.40179881	5.18565611	-0.71402580
C	5.26238586	4.37675165	-0.56421185
C	-2.85923985	2.80104222	-0.52944816
C	3.23629440	2.42222144	-0.39874472
C	-2.11495623	1.67288466	-0.41676042
C	2.21948453	1.42742474	-0.31770876
C	-1.35031512	0.66202268	-0.29446900
C	1.34863981	0.56348916	-0.26144404
C	-4.98514297	3.93076739	-1.03133840
C	5.11802028	3.42518477	-1.57446069
C	-1.50844684	-2.25304631	-0.27891336
C	1.24058876	-2.33884686	-0.27545506
C	-4.25553927	2.77588933	-0.95128410
C	4.12053984	2.45892776	-1.49472425
C	-0.18014983	-3.74980944	-1.70979414
H	-7.48894945	1.15515222	3.02365035
H	7.51776024	0.67378224	2.88699661
H	-5.44366583	-0.38430031	2.60244738
H	-8.39268158	1.77241555	1.63200720
H	-6.78325412	2.41491111	1.99723789
H	5.43410577	-0.79726322	2.50096573
H	8.20187953	1.56800513	1.51971533
H	6.65156043	2.06588447	2.21185182
H	-3.52319355	-1.98232493	2.20548600
H	-4.72523984	0.91186644	1.64990269
H	3.37513657	-2.24905554	2.13432739
H	4.57079089	0.58221533	1.82018555
H	-2.59095882	6.21021866	-0.09554684
H	-7.40680944	-0.45210822	1.06927971
H	4.49107508	5.09575433	1.31623220
H	7.18246755	-0.56444290	0.70700943
H	-2.68087359	-0.65972732	1.37542807
H	2.51578604	-0.86213533	1.42775979
H	-1.23635795	4.14661329	0.06062502
H	2.70738361	3.38101834	1.45586625
H	-6.68941803	0.80660952	0.07305814
H	6.31289281	0.82496676	0.05936693
H	-5.38292396	-1.85628511	0.51821503
H	5.13332426	-2.03127200	0.32433982
H	-4.52071023	-0.56324421	-0.32023595
H	4.24510135	-0.64444351	-0.32547489
H	-6.02433653	3.89142992	-1.35085843
H	5.78569055	3.43799088	-2.43311679
H	-4.69510239	1.81724831	-1.21189819
H	4.00364414	1.72296459	-2.28602324
H	-0.21207284	-4.80605228	-1.97361635
H	-0.16914816	-3.11856322	-2.60614821
N	-2.70624773	-2.43633841	0.34979979
N	2.45334970	-2.58137958	0.30530891
N	-1.34417518	-3.43182664	-0.92007036
N	1.00743722	-3.49959612	-0.93318511
Pt	-0.08715714	-0.80820221	-0.24359916
H	6.04218229	5.13152141	-0.62827078
H	-4.99206135	6.09460746	-0.78175070
N	-2.33918546	-4.33628909	-0.72232236
N	1.97748256	-4.44153736	-0.79596144
C	-3.16053683	-3.69211456	0.05294376

C	2.84875158	-3.84373286	-0.03722215
H	3.77405730	-4.29342056	0.29418464
H	-4.08894217	-4.10055977	0.42604684

Zero-point correction= 0.619294 (Hartree/Particle)
Thermal correction to Energy= 0.657781
Thermal correction to Enthalpy= 0.658725
Thermal correction to Gibbs Free Energy= 0.539460
Sum of electronic and zero-point Energies= -1648.276654
Sum of electronic and thermal Energies= -1648.238167
Sum of electronic and thermal Enthalpies= -1648.237223
Sum of electronic and thermal Free Energies= -1648.356487

Energies and cartesian coordinates of the DFT optimized triplet-state structure of 4b

C	-6.87947103	0.47171372	-1.56511744
C	-4.67002070	-0.76039976	-1.32704259
C	-5.98409334	-0.36545995	-0.65929258
C	-2.45782629	-1.94720431	-1.11367805
C	3.50329665	5.58326533	-0.17658158
C	-4.27867718	3.98671919	-0.31240053
C	-3.76408991	-1.58629104	-0.41947917
C	2.72657518	4.44716382	-0.17985529
C	-3.18813726	3.13729978	-0.46681359
C	4.90719062	5.49048760	-0.08855629
C	-5.07516708	3.91489162	0.83135105
C	3.33675159	3.14653867	-0.09668349
C	-2.86800128	2.18651058	0.52226911
C	2.56969374	2.00816443	-0.10894703
C	-1.75579113	1.31143528	0.36116686
C	1.85090317	0.96566962	-0.12261274
C	-0.79622906	0.56070355	0.21610555
C	5.52676968	4.22800393	-0.00253143
C	-4.76656307	2.98219230	1.82223098
C	-0.36128005	-2.29896332	0.21147979
C	4.77117156	3.07724332	-0.00464177
C	-3.67964628	2.12678864	1.67196686
C	1.44422504	-3.30030534	1.52857816
H	-7.13415388	-0.06934959	-2.48559383
H	-4.88408440	-1.32255413	-2.24976250
H	-7.81764980	0.73781646	-1.06462468
H	-6.38042540	1.40510949	-1.85186717
H	-2.64501254	-2.53384363	-2.02250311
H	-4.13565790	0.14997379	-1.63280540
H	3.03134014	6.56049791	-0.23922394
H	-4.50722979	4.71302726	-1.08925182
H	-6.52050190	-1.27295778	-0.34440333
H	-1.91616152	-1.04115997	-1.39406466
H	1.64387839	4.50380667	-0.24242233
H	-2.56519130	3.19711886	-1.35541885
H	-5.76184175	0.20028477	0.25552706
H	-4.28964117	-2.49940697	-0.10235138
H	-3.52651980	-1.01573245	0.48678588
H	6.60971536	4.16371186	0.06785622
H	-5.37645741	2.92165821	2.72091961
H	5.23733176	2.09876862	0.06614113
H	-3.43649994	1.40518608	2.44759292
H	1.61695364	-4.24588968	2.04779386
H	1.41601776	-2.48439497	2.26697978
N	-1.56037653	-2.72032404	-0.26260145
N	0.12910015	-3.35896908	0.90014650
Pt	0.74731974	-0.60451709	0.00519485
H	-5.92548849	4.58159642	0.95093963
H	5.51172644	6.39317175	-0.08409049
C	-1.80485129	-4.02054264	0.12613831
C	-0.73574855	-4.42811116	0.85847785
N	2.41047864	-1.87545940	-0.19078691
C	2.51619571	-3.04488645	0.51766736
C	3.39187140	-1.60556864	-1.09538598
C	3.56146159	-3.93185517	0.32150981
C	4.46814547	-2.43682868	-1.31343934
H	3.27373052	-0.67684885	-1.64248223
C	4.57177268	-3.64482659	-0.59954365
H	3.58936336	-4.84758265	0.90734077
H	5.21687699	-2.14751925	-2.04497319
H	5.39958971	-4.32850719	-0.75743213
H	-2.70800098	-4.54327173	-0.15142140
H	-0.52678875	-5.36772504	1.34786686

Zero-point correction= 0.516164 (Hartree/Particle)
Thermal correction to Energy= 0.547763
Thermal correction to Enthalpy= 0.548707
Thermal correction to Gibbs Free Energy= 0.447448
Sum of electronic and zero-point Energies= -1442.055712
Sum of electronic and thermal Energies= -1442.024113
Sum of electronic and thermal Enthalpies= -1442.023169
Sum of electronic and thermal Free Energies= -1442.124428

Energies and cartesian coordinates of the DFT optimized triplet-state structure of 5b

C	-4.82049337	4.69371636	-1.66043013
C	-3.76612829	2.39314819	-1.42809011
C	-4.59640735	3.48502827	-0.75926206
C	-2.70068821	0.11864801	-1.23051010
C	6.39269549	2.92714023	-0.13276301
C	-0.79139906	6.04263246	-0.09304001
C	-3.52623527	1.18782009	-0.52463904
C	5.11351139	2.42199419	-0.13479101
C	-0.39035103	4.72708036	-0.30153602
C	7.50450858	2.06376016	-0.04329100
C	-1.51501212	6.38941649	1.04875908
C	4.88867738	1.00068508	-0.05093100
C	-0.70910205	3.71986329	0.63003705
C	3.61730628	0.49024304	-0.06785501
C	-0.30680502	2.37015518	0.41832403
C	2.43363419	0.03719100	-0.09004801
C	0.03348200	1.20478509	0.24274202
C	7.30982655	0.67012405	0.04595800
C	-1.83352414	5.40291940	1.98278415
C	-1.24512309	-1.39882611	0.13167101
C	6.04045648	0.13959901	0.04366000
C	-1.43921311	4.08468331	1.77810414
C	-0.35278503	-3.26119725	1.44933711
H	-5.33628439	4.41067934	-2.58719620
H	-4.26812233	2.07058216	-2.35420818
H	-5.42730643	5.45802241	-1.16128209
H	-3.86572630	5.15718039	-1.93676415
H	-3.20332825	-0.22572502	-2.14465616
H	-2.79626722	2.81350622	-1.72982913
H	6.54933052	4.00092631	-0.19701002
H	-0.53460504	6.80415350	-0.82610106
H	-5.56673241	3.06719724	-0.45224803
H	-1.72411613	0.52116404	-1.50965412
H	4.24839833	3.07538024	-0.19801802
H	0.17701101	4.45839634	-1.18878209
H	-4.08945432	3.80558229	0.16064201
H	-4.48863235	0.77144106	-0.19549601
H	-2.98393123	1.50136512	0.37522903
H	8.17112364	0.01067800	0.11846401
H	-2.39256919	5.66262541	2.87900022
H	5.87904747	-0.93206407	0.11598201
H	-1.68328513	3.31811625	2.50895819
H	-0.74990306	-4.14191732	1.95772415
H	0.06284601	-2.57372320	2.20175717
N	-2.44695519	-1.05076808	-0.40103503
N	-1.45051411	-2.57382920	0.78750106
Pt	0.62903905	-0.62890705	0.00008800
H	-1.82505514	7.41879256	1.21029009
H	8.51099366	2.47255719	-0.03954600
C	-3.40327826	-2.00671716	-0.09893201
C	-4.75047037	-2.11735216	-0.43721603
H	-5.24998040	-1.36366211	-1.03776708
C	-5.43530139	-3.23774625	0.02709500
H	-6.48742848	-3.35506126	-0.21671402
C	-4.79650037	-4.21559232	0.80311206
H	-5.36317041	-5.07493739	1.15038209
C	-3.44733326	-4.11194732	1.13415909
H	-2.95763123	-4.87983238	1.72564613
C	-2.76218621	-2.99376423	0.66627405
N	1.28596610	-2.61887120	-0.22194702
C	0.70708805	-3.64810628	0.46586104
C	2.26053418	-2.93128423	-1.11493609
C	1.07990008	-4.96747338	0.26507402
C	2.69148621	-4.22219332	-1.33936210
H	2.68899321	-2.08930016	-1.64699312
C	2.09179316	-5.28295841	-0.64305605

H	0.58019804	-5.74818443	0.83307306
H	3.48389927	-4.39616534	-2.06110816
H	2.39778319	-6.31154150	-0.80583906

Zero-point correction= 0.563709 (Hartree/Particle)
Thermal correction to Energy= 0.598835
Thermal correction to Enthalpy= 0.599779
Thermal correction to Gibbs Free Energy= 0.489725
Sum of electronic and zero-point Energies= -1595.485007
Sum of electronic and thermal Energies= -1595.449881
Sum of electronic and thermal Enthalpies= -1595.448937
Sum of electronic and thermal Free Energies= -1595.558991

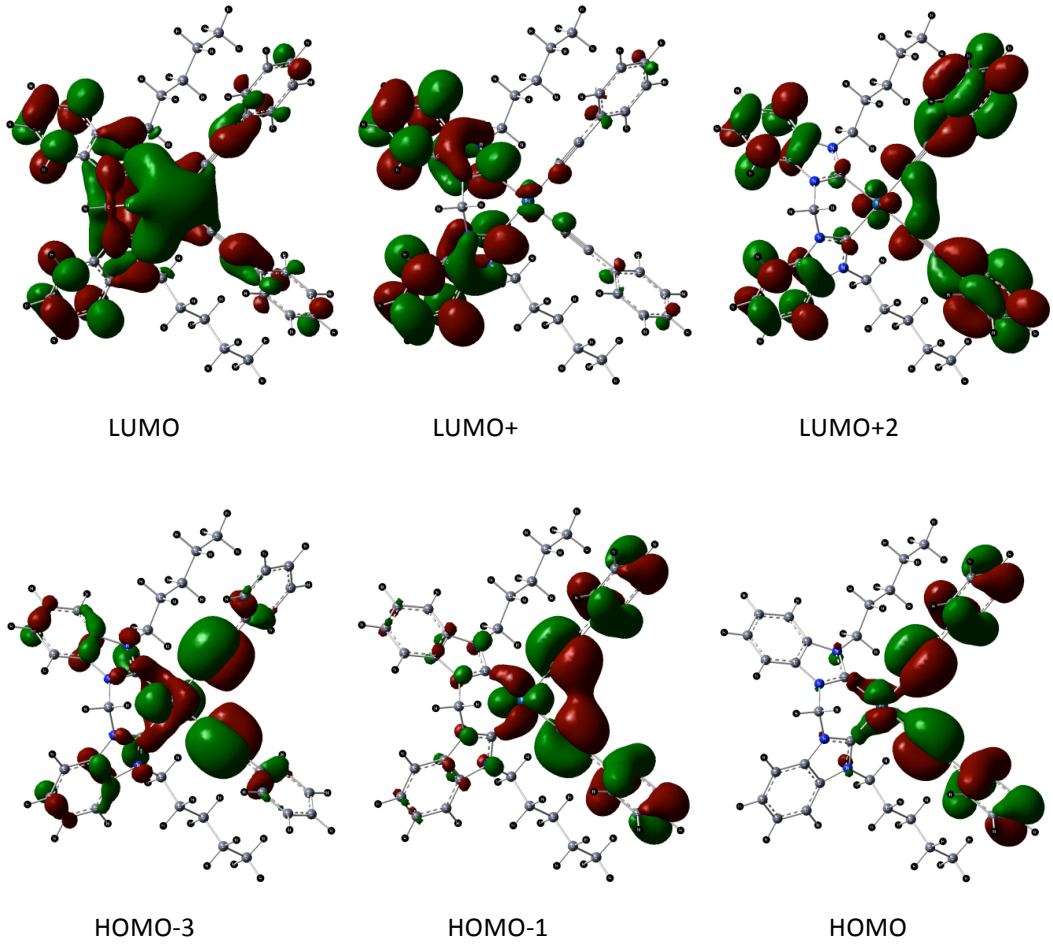

Figure S14. Spatial plots of selected frontier orbitals of the optimized ground state of **1b**.

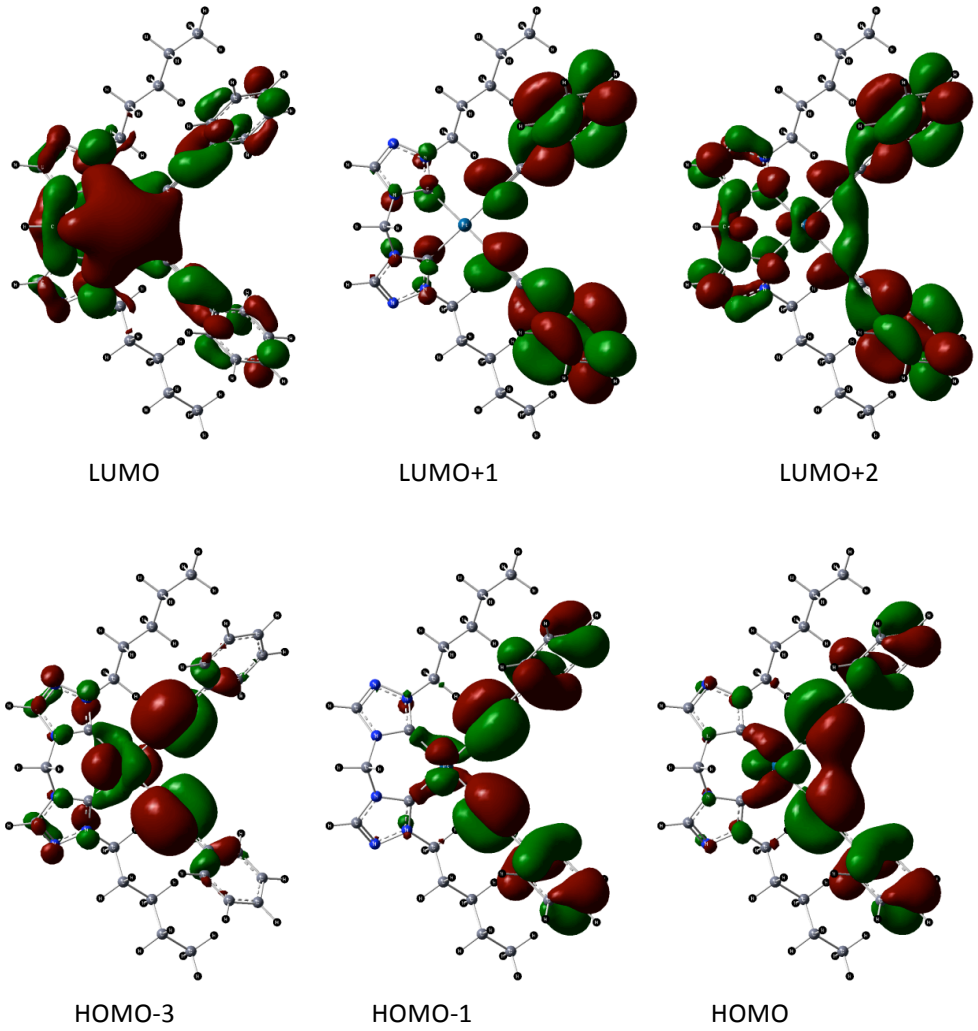

Figure S15. Spatial plots of selected frontier orbitals of the optimized ground state of **2b**.

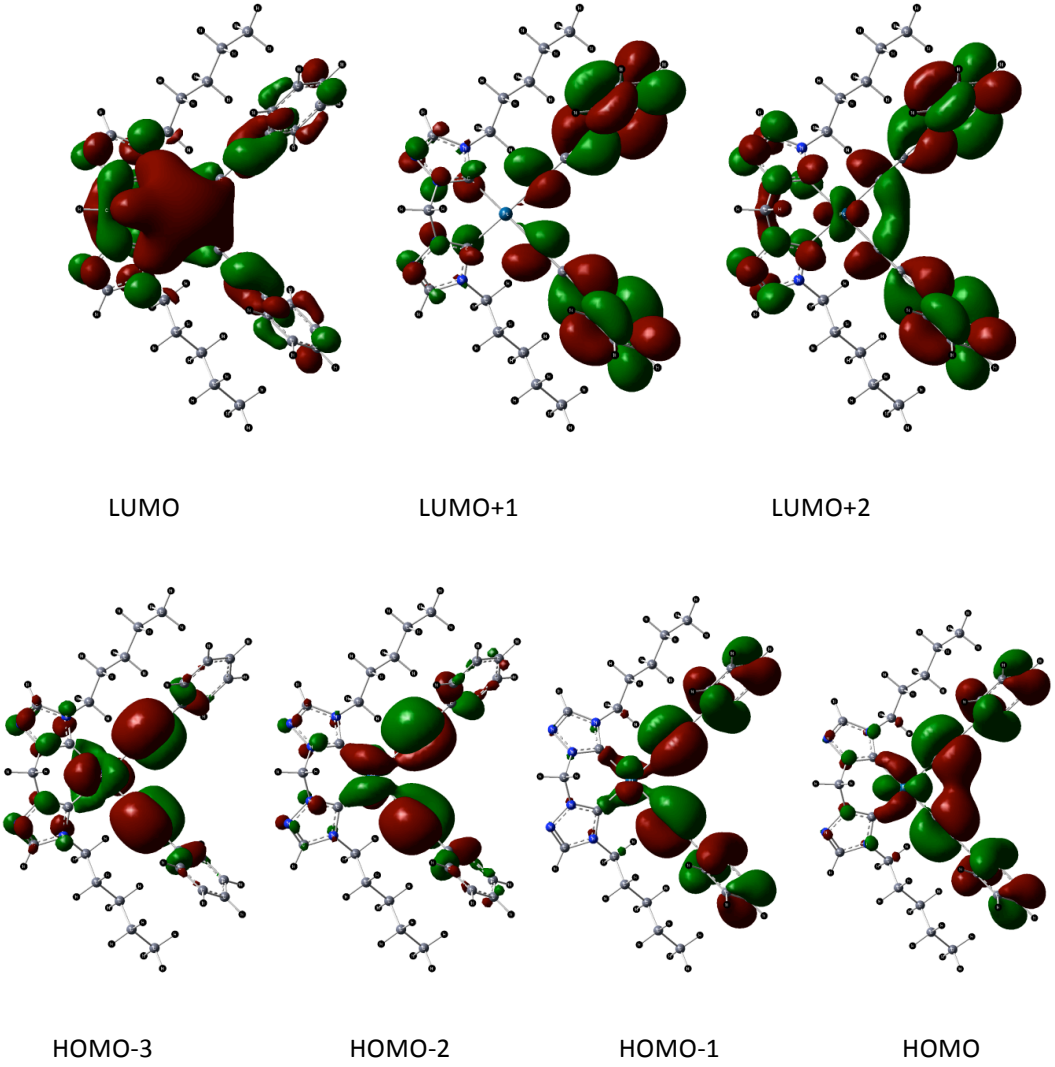

Figure S16. Spatial plots of selected frontier orbitals of the optimized ground state of **3b**

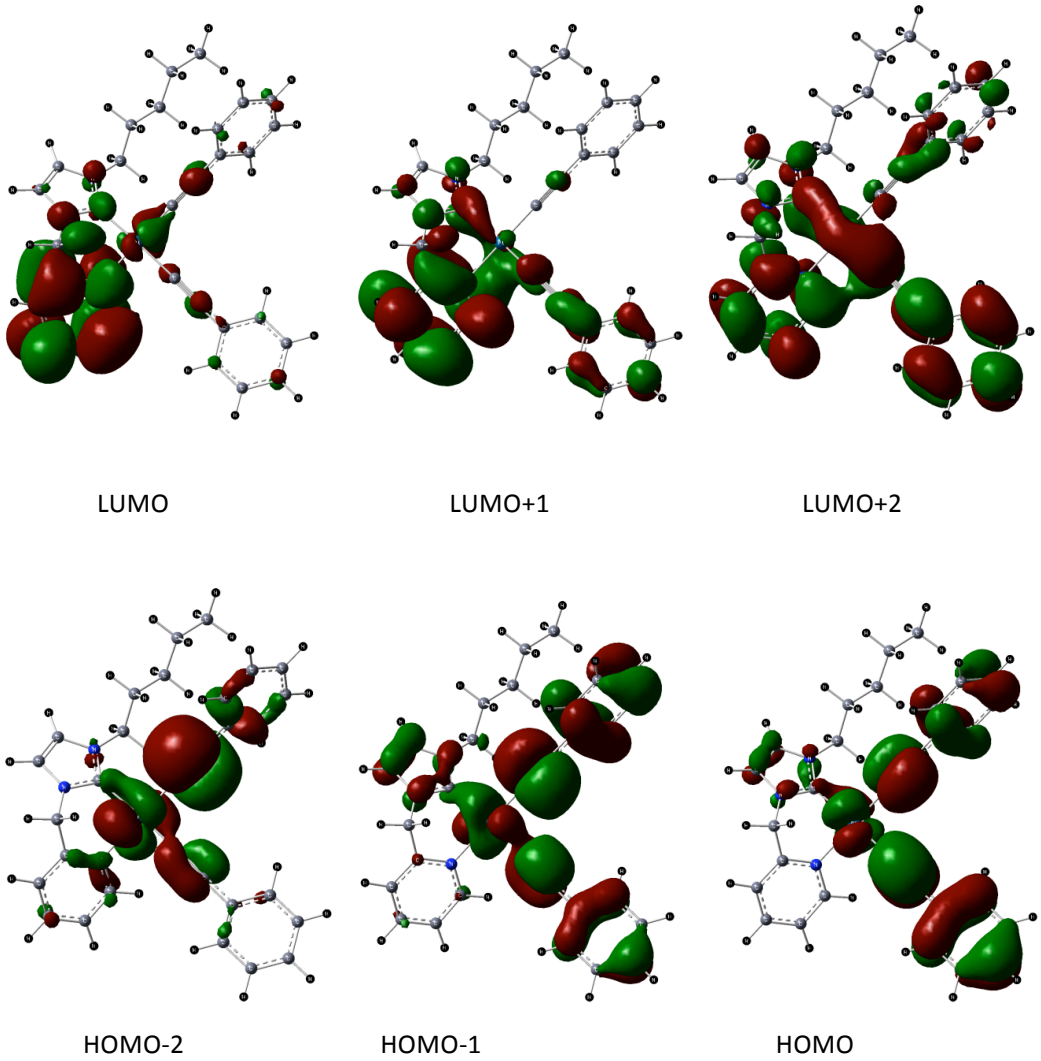

Figure S17. Spatial plots of selected frontier orbitals of the optimized ground state of **4b**

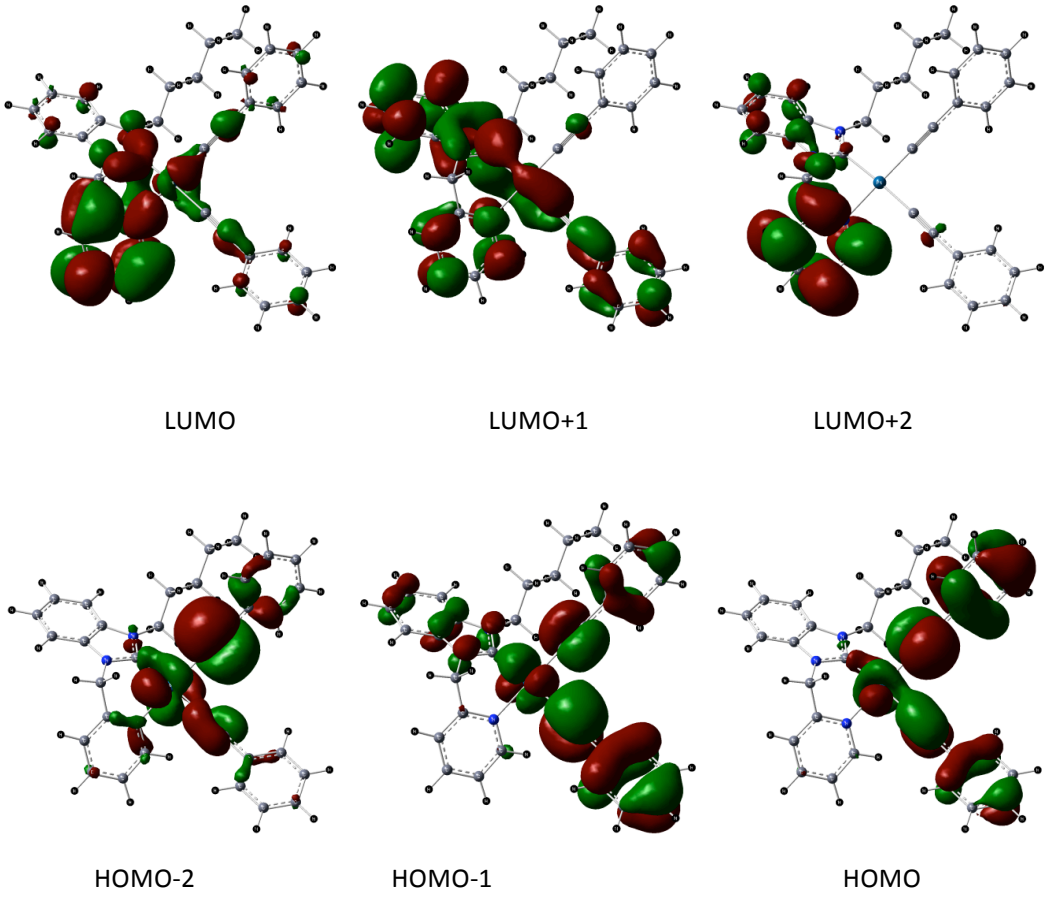

Figure S18. Spatial plots of selected frontier orbitals of the optimized ground state of **5b**

Chapter 5 Rational Design of Highly Efficient Deep Blue Emitting N-Heterocyclic Carbene Pt(II) Acetylide Complexes

5.1 Abstract

A series of *cis* and *trans* N-heterocyclic carbene Pt(II) acetylide complexes [Pt(**pimi**)$_2$(C≡CC_6H_4F)$_2$] (**1**), [Pt(**pimi**)$_2$(C≡CC_6H_5)$_2$] (**2**), [Pt(**ptrz**)$_2$(C≡C-C_6H_4F)$_2$] (**3**) and [Pt(**ptrz**)$_2$(C≡C-C_6H_5)$_2$] (**4**) (**pimi** = N,N'-dipentyl-imidazoline-2-ylidene and **ptrz** = N,N'-dipentyl-trizoline-2-ylidene) were prepared and detailed photophysical properties of the complexes were examined. NHC ligands **pimi** and **ptrz** with varying electronic properties were utilized to efficiently harvest the triplet emission by pushing the relatively low-lying non-radiative metal d-d state to higher energy levels. Single crystal X-ray diffraction studies of **1a**, **2a** and **4a** were carried out and the photophysical and electrochemical experimental observations are indicative of the metal perturbed ^{3}IL charge transition. In all cases, the *trans* isomers were found to exhibit higher quantum yields than the corresponding *cis* isomers except in the case of complex **2**. Additionally, complex **2'** bearing NHC ligands with dodecyl chains were synthesized to confirm this behavior. Spin coated films of 2 wt% and 10 wt% complexes in PMMA showed significant increase in quantum yields of all the *cis* and *trans* complexes. Among all the complexes, **3b** and **4b** exhibited the highest quantum yield of 80%. The observation of self-quenching behavior of complex **2a'** at high concentrations (1 x 10^{-3} M^{-1}) in fluid solution and the significant increase in quantum yields in the PMMA film in comparison to the neat solid is strongly suggestive of molecular aggregation being a primary factor contributing to the lower quantum yields observed in the neat solid.

5.2 Introduction

Since the report of [Pt(phen)(C≡C-C_6H_5)$_2$] (phen = phenanthroline) as a triplet emitter,[1] significant research efforts has been focused towards the development of square planar Pt(II) complexes due to their extensive applications in the fields of phosphorescent organic light-emitting diodes (OLEDs),[2-6] non-linear optical (NLO) materials,[7-9] chemosensors[10, 11] and other electroluminescent technologies. Design and synthesis of highly emissive Pt(II) phosphors have relied on the effective use of strong field ligands such as phosphine and polypyridine in order to elicit control and tune the luminescence efficiency by raising the low lying metal d-d states.[4, 12-14] In addition, cyclometalated aromatic ligands have also been used to harvest luminescence through the formation of strong metal-carbon bonds and supplying close-lying π-π* transitions a common strategy.[15] Polypyridine and phosphine ligated Pt(II) complexes bearing strong σ-donor ligands such as acetylene have been explored and investigated as triplet emitters during the past two decades.[5, 8, 13, 16-25] Recently, the groups of Strassner, Li and Wang reported cyclometalated NHC Pt(II) phosphors that exhibit high quantum efficiency at high emission energies that have benefited from the strong ligand field strength of NHC which raises the low-lying non-radiative d-d states to higher energy levels.[3, 4, 26, 27] Besides the electronic properties of the ligand, molecular configurations of the emitters also strongly dictate the phosphorescence emission efficiency. For example, the facial (*fac*) isomer of the Ir(ppy)$_3$ octahedral complex display strikingly a high quantum yield of 40% in comparison to the 3.6% of the meridional (*mer*) isomer.[28] This difference has been attributed to the efficient bond breaking process in the excited state that serves as an emission quencher for the meridional isomer. Although molecular aggregation are

known to induce new emission characteristics in certain cases of square planar Pt(II) complexes, it can also quench the emission in most of the cases. Recently, a series of *trans* and *cis* blue emitters of [Pt(**dbim**)$_2$(C≡C-R)$_2$] bearing NHC ligand have been reported by our group. Although the thermodynamically stable *trans* NHC Pt(II) acetylide complex displayed a 80% quantum yield in a 10 wt% PMMA film, further improvement of the quantum yields was expected by tuning the electronic properties of the NHC ligand.

To this end we report the preparation of a series of *cis* and *trans* complexes of the type [Pt(**pimi**)$_2$(C≡CC$_6$H$_4$F)$_2$] (**1**), [Pt(**pimi**)$_2$(C≡CC$_6$H$_5$)$_2$] (**2**), [Pt(**ptrz**)$_2$(C≡C-C$_6$H$_4$F)$_2$] (**3**) and [Pt(**ptrz**)$_2$(C≡C-C$_6$H$_5$)$_2$] (**4**). All the complexes were characterized and the photophysical investigations revealed intense blue ^{3}IL emission both in fluid solution and solid state. The *trans* complexes displayed higher quantum yield than the corresponding *cis* isomers both in solution and in neat solid except in the case of complexes **2a** and **2b**. To ascertain the isolated behavior of complex **2**, complexes **2a'** and **2b'** bearing dodecyl chains on the NHC ligand were synthesized and characterized. The quantum yields for all the complexes were also evaluated in 10 wt% and 2 wt% PMMA film and drastic improvement in emission quantum yield was observed in comparison to solution and neat solid. The self-quenching behavior of complex **2a'** along with the increased quantum efficiencies upon doping in a film are highly indicative of molecular aggregation in neat solid. The 80% quantum yield of *trans* complexes **3b** and **4b** in 2 wt% PMMA film are as high as reported *trans* [Pt(**ibim**)$_2$(C≡C-C$_6$H$_5$)$_2$]. OLED fabrication using complex **3b** is currently being carried out in the labs of Prof. Trisha Andrew (University of Wisconsin-Madison) to obtain the external quantum efficiency. The modularity of the structure with tunable

emission properties along with the good quantum yield of *trans* complexes at high emission energies makes them a potential emitter material for light emitting applications.

5.3 Results and Discussion

Synthesis and characterization. The *cis* complexes were synthesized by treating [(COD)Pt(C≡C-R)$_2$] (R= C_6H_4F and C_6H_5) with 3.0 equiv. NHC ligands ([dpimH]I, [ddimH]I and [dptzH]I) and 3.0 equiv. *t*-BuOK in dry THF at 80 ^oC. While the yields of the complexes **1a**, **2a** and **2a'** bearing imidazoline-2-ylidene are low to moderate, the yields of complexes **3a** and **4a** bearing trizoline-2-ylidene ligand were 83% and 79%, respectively. *Trans* complexes **1b**, **2b'** and **3b** were obtained by heating the corresponding *cis* isomer in a schlenk tube to 180 ^oC for 1 h under an N_2 atmosphere. The yields of the three complexes were in the range of 66-80%. However, this synthetic approach did not lead to the *trans* complex **4b** and also the DSC studies on the complex of **4a** did not indicate any peaks corresponding to the isomerization process. The same behavior was also observed in the case of complex **2a** and no *trans* isomer **2b** could be obtained just by heating the complex. In view of this unsuccessful approach, *trans* complexes **2b** and **4b** were obtained by reacting the corresponding *cis* isomers **2a** and **4a** with [(COD)Pt(C≡CC_6H_5)$_2$] in THF at 80 ^oC. The *trans* isomers **2b** and **4b** could be obtained in an yield of 25% and 66%, respectively. All the complexes were purified by column chromatography on silica gel with a suitable eluent.

All the *cis* and *trans* complexes were characterized by ^1H NMR, ^{13}C NMR, IR, ESI-MS and elemental analysis. The *cis* and the *trans* isomers of **1a**, **1b**, **2a**, **2b** and **2a'**, **2b'** were easily distinguished by their characteristic resonances as two sets of multiplet between 4.4 ppm and 3.9 ppm for the *cis* isomers and only one multiplet

around 4.5 ppm for *trans* isomers in the ^{1}H NMR spectrum. However, complexes **3a**, **3b** and **4a**, **4b** could not be differentiated by ^{1}H NMR and ^{13}C NMR studies, since both the isomers showed nearly similar resonances. The UV-Vis studies (low energy absorption for *trans*) and the difference in the characteristic IR stretching vibrations between the two isomers support the existence of the *cis* and *trans* isomers.

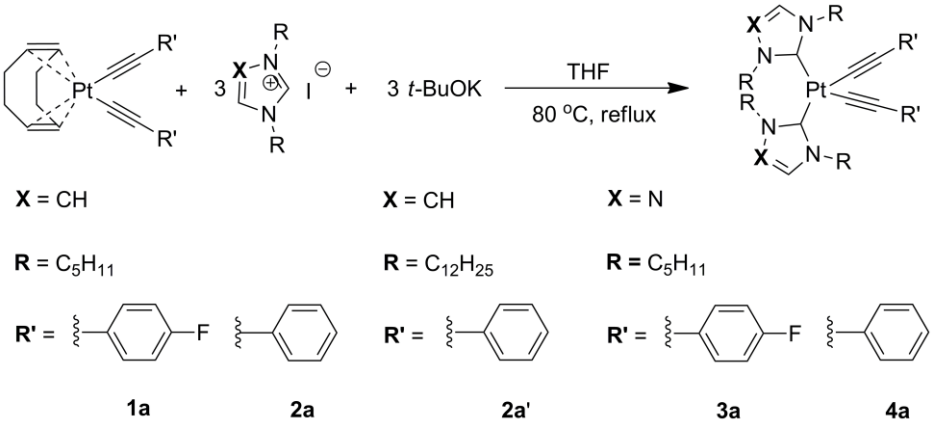

Scheme 1. Synthetic of *cis* complexes **1a**-**4a**.

Single Crystal X-ray Diffraction Studies. Single crystals of **1a** and **2a** suitable for X-ray diffraction studies were grown by slow evaporation of a concentrated solution of the complexes in a mixture of pentane and dichloromethane and crystals of **4a** was obtained by slow evaporation of a concentrated solution of the complex in ethyl acetate. The structures of complexes **1a**, **2a** and **4a** were determined by X-ray crystallography and their ORTEP drawings are depicted in Figure 1. Crystallographic parameters are summarized in Table S1 and selected bond lengths and angles are listed in Table 1. The Pt(II) centers of all the three complexes show a distorted square planar environment, a characteristic of these class of complexes. The C-C bond lengths of 1.215(4) Å for **1a**, 1.199(9) Å for **2a** and 1.189(8) Å for **4a** coroborate the triple bond nature. The Pt-C_{carb} distances in complex **4a** (2.026(6) Å) is shorter than **2a** (2.038(6) Å and 2.036(7)Å) is indicative of a stronger bond between the **ptrz**

ligand and the platinum centre in comparison to the **pimi** complex. And in comparison between complexes **1a** and **2a** bearing the same **pimi** ligand, the Pt-C_{alk} distances are slightly shorter in Pt-C≡CC_6H_4F than in the case of Pt-C≡CC_6H_5.The phenylacetylene and the carbene ligands are disposed perpendicular to the plane of the Pt with the dihedral angle between plane of phenylacetylene and Pt square plane being 74.8(1)^o and 78.7(1)^o for complex **1** and 73.9 (1)^o and 73.4 (1)^o for complex **1a**. Although the

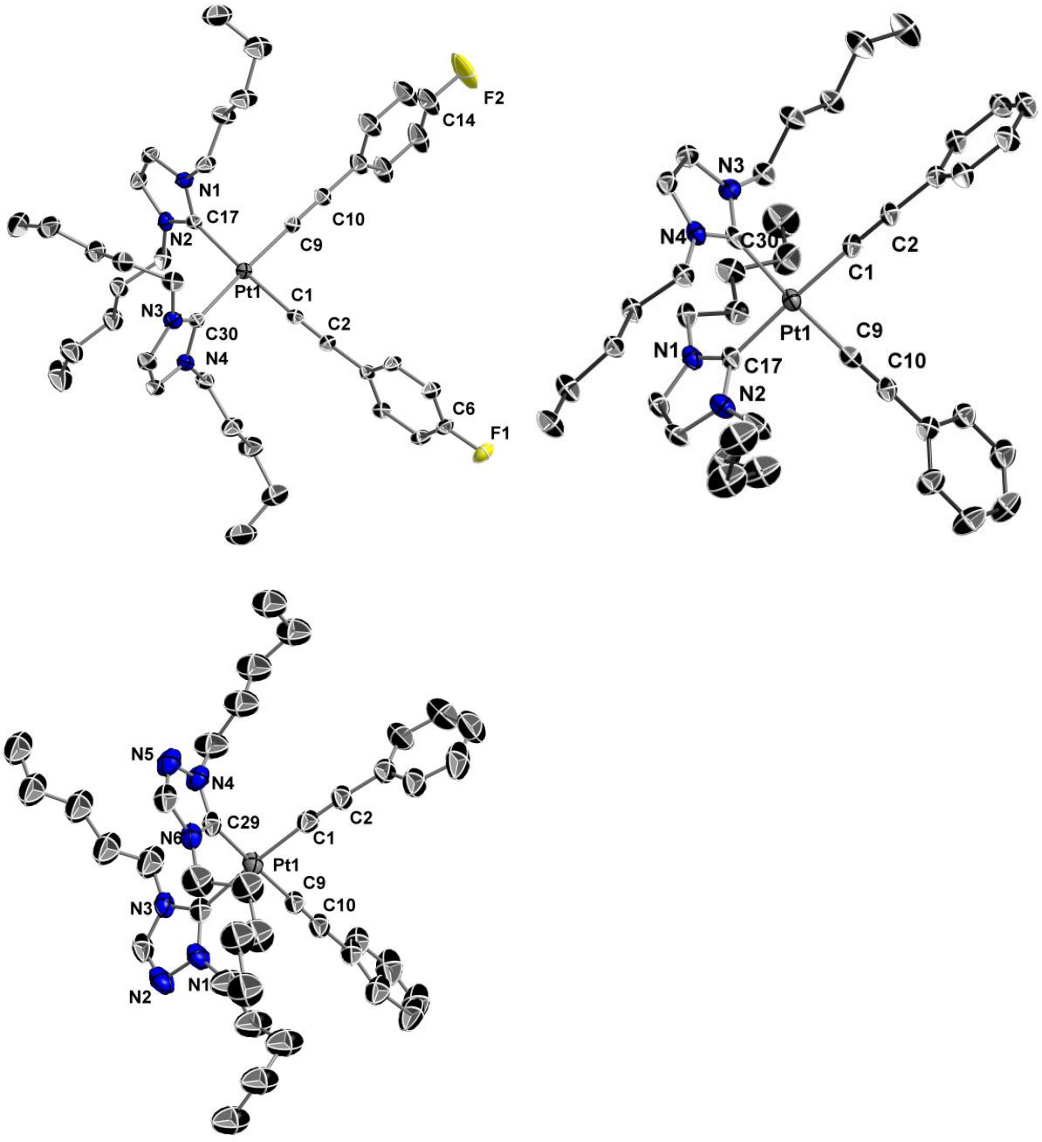

Figure 1. Molecular structures of **1a** (top left), **2a** (top right) and **4a** (bottom left) with a selective atomic numbering scheme. Thermal ellipsoids are drawn at the 30% probability level. Disorders, hydrogen atoms and solvent molecules are omitted for clarity.

photophysical properties were found to be strongly affected by molecular aggregation in the neat solid, no Pt···Pt or π-π interaction was evident from the single crystal structures.

Table 1. Selected Bond Distances (Å) and Angles (deg) of complexes **1a**, **2a** and **3a**

	Distance (Å)		Angle (deg)
Complex **1a**			
C(1)-Pt(1)	1.999(3)	C(9)-Pt(1)-C(1)	89.77(11)
C(9)-Pt(1)	1.996(3)	C(9)-Pt(1)-C(17)	87.23(11)
C(17)-Pt(1)	2.035(3)	C(1)-Pt(1)-C(30)	87.38(11)
C(30)-Pt(1)	2.036(3)	C(17)-Pt(1)-C(30)	95.62(11)
Complex **2a**			
C(1)–Pt(1)	2.007(7)	C(1)-Pt(1)-C(9)	88.8(2)
C(9)–Pt(1)	2.008(7)	C(1)-Pt(1)-C(30)	88.0(2)
C(17)–Pt(1)	2.038(6)	C(9)-Pt(1)-C(17)	89.5(3)
C(30)–Pt(1)	2.036(7)	C(30)-Pt(1)-C(17)	93.8(2)
Complex **4a**			
C(1)-Pt(1)	2.001(7)	C(1)-Pt(1)-C(9)	89.3(2)
C(9)-Pt(1)	2.002(6)	C(1)-Pt(1)-C(29)	89.2(2)
C(17)-Pt(1)	2.026(6)	C(9)-Pt(1)-C(17)	85.8(2)
C(29)-Pt(1)	2.026(6)	C(29)-Pt(1)-C(17)	95.6(2)

UV-Vis Absorption and Emission. The UV-Vis absorption spectra of all the ten complexes in methylene chloride (DCM) at room temperature are illustrated in Figure 2 and Figure S1. The absorption patterns for all the ten complexes are similar with one intense band in the range 284-300 nm and an additional shoulder band (low energy absorption bands) between 300-310 nm. In comparison to the previously reported *cis* and *trans* complexes [Pt(**dbim**)$_2$(C≡C-R)$_2$] (dbim = N,N'-didodecyl-benzimidazoline-2-ylidene), the molar absorption coefficient (ε) for the intense absorption bands at the higher energy are slightly lower in the range of 2.5 × 10^4 to 6.5 × 10^4 M^{-1} cm^{-1}. These intensive bands (< 300 nm) are assignable to acetylide based π→π* intraligand transitions ^{1}LLCT ($\pi_{alk}\rightarrow\pi^*_{alk}$).[29] The low energy

absorption bands which are less intense and have molar extinction coefficients in the range of 2.0 × 10^4 to 4.0 × 10^4 M^{-1} cm^{-1}can be assigned to an admixture of metal-perturbed ligand-to-ligand ^{1}LLCT ($\pi_{alk}\rightarrow\pi^*_{carb}$) and metal-to-ligand ^{1}MLCT (5d(Pt)$\rightarrow\pi^*_{carb}$) transition. Complexes **2a** and **2a'** bearing different alkyl chains on the **pimi** ligand exhibit similar absorption bands at the same wavelength maxima, except that **2a'** possesses a higher molar extinction coefficient (Figure S1). In comparison between the *cis* and *trans* isomers, the *trans* isomers always exhibit a few nm red shift of the low energy band than the *cis* isomers and the reason for this observation is tentatively ascribed to the higher symmetry of the *trans* complexes leading to the decrease of the HOMO-LUMO gap. The UV-Vis spectra of complexes **1** and **2** display a blue shift by few nm in comparison to the complexes **3a**, **4a**, **3b** and **4b** reflecting the stronger electron donor nature of the **pimi** carbene with respect to the **ptrz** carbene. While the *cis* complexes were found to display a small solvatochromic behavior, due to the poor solubility of the *trans* isomer in CH_3CN and MeOH, solvatochromic studies could not be carried out for the *trans* isomers.

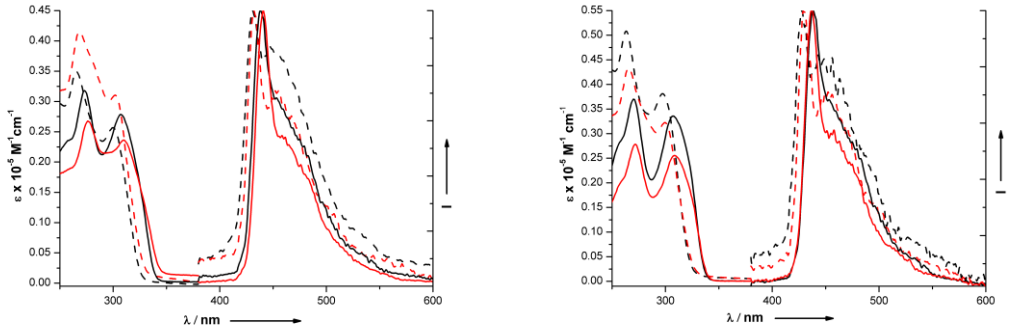

Figure 2. (Left) Electronic absorption and normalized emission spectra of **1a** (black dot), **1b** (black solid), **2a** (red dot), **2b** (red solid) in CH_2Cl_2 at RT. (Right) Electronic absorption and normalized emission spectra of **3a** (black dot), **3b** (black solid), **4a** (red dot) and **4b** (red solid) in CH_2Cl_2 at RT.

The luminescent properties of *cis* and *trans* isomers **1**-**4** in solution, neat solid and PMMA film at room temperature are summarized in table 2 and the emission spectra in degassed DCM of complexes **1**-**4** are shown in Figure 1 and Figure S1. Upon excitation of the low energy bands (297 nm -310 nm), all the ten complexes displayed a deep blue emission with the λ_{max} in the range 428–441 nm at 298 K. The excited state lifetimes of all the ten complexes were recorded in DCM at 298 K and were found to be between 593 ns and 2647 ns. The large stokes shifts together with the lower microsecond-range lifetimes strongly support the triplet nature of the excited state. The emission wavelength of the *cis* complexes **1a**, **2a**, **3a** and **4a** shift hypsochromically with the decreasing electron withdrawing nature (F > H) of the substituents on the alkynes. A similar behavior was also observed in the case of the *trans* isomers **1b**, **2b**, **3b** and **4b** respectively. Comparison of the emission maxima among the *cis* isomers **1a**, **2a**, **3a** and **4a** bearing the same acetylide unit but different NHC, complexes **1a** and **2a** showed a 2 nm bathochromic shift than **3a** and **4a** due to the stronger electron donating nature of **pimi** than the **ptrz** ligand which was also observed in the case of the *trans* complex. The emission maxima of the *trans* complexes were found to be blue shifted by about 8-10 nm in comparison with the corresponding *cis* isomers, which could be attributed to the higher symmetry of the *trans* isomer resulting in the decrease of the HOMO-LUMO gap. Complexes **2a** and **2a'** bearing different alkyl chains on the **pimi** ligand exhibited the same maxima emission wavelength at the 432 nm and the *trans* isomers showed only a negligible difference between the two complexes. Along with the UV-Vis studies, we can conclude that the alkyl chain does not significantly influence the photophysical properties in solution. Emission spectra of complexes measured in 2-MeTHF at 77 K

are shown in Figure S2-S4. Unlike the broad and unsymmetrical emission profile in solid-state and solution at room-temperature, emission with a rigidochromic shift and resolvable vibronic components was clearly evident at 77 K. In comparison to the emission in solution at room temperature, the emission wavelength maxima were shifted by 1-6 nm to the blue, except in complex **3b,** which showed a 12 nm red shift.

The emission spectra of all the complexes in neat solid and 10 wt% PMMA film are illustrated in Figure 3 and Figure S5. The emission wavelength maxima of the complexes in 10 wt% PMMA displayed a small shift of 0-4 nm shift than the corresponding emission in solution. The emission spectra of the complexes in the neat solid revealed the shoulder peak to be rather broad in some cases, while in other an additional second peak,, which is strongly indicative of molecular aggregation. This aggregation behavior was also found to affect the quantum yields of the complexes in the neat solid significantly. Based on the photophysical behavior properties of these complexes and previous DFT-TDFFT studies, the parentage of the emission of all the complexes is tentatively assigned to an admixture of metal perturbed ligand-to-ligand

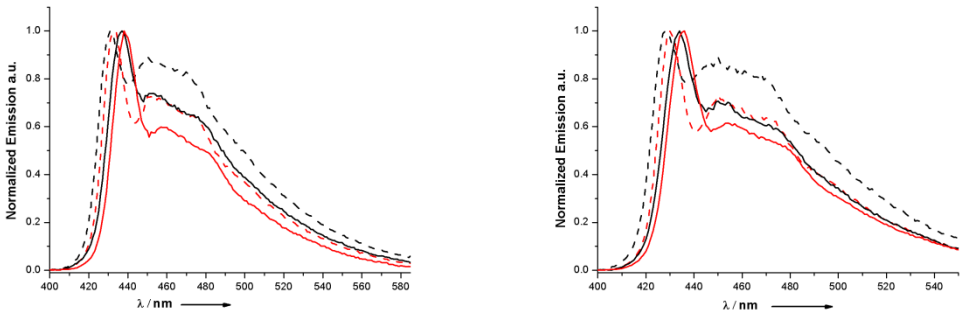

Figure 3. (Left) Normalized emission spectra of **1a** (black dot), **1b** (black solid), **2a** (red dot), **2b** (red solid) in 10 wt% PMMA film at RT. (Right) Normalized emission spectra of **3a** (black dot), **3b** (black solid), **4a** (red dot) and **4b** (red solid) in 10 wt% PMMA film at RT.

charge transfer ^{3}LLCT($\pi_{alk}\rightarrow\pi^*_{alk}$) and a metal to ligand charge transfer ^{3}MLCT(Pt(5d)$\rightarrow\pi^*_{alk}$) transitions.[29]

The solid state quantum yields of the *trans* isomers were found to be higher than the *cis* isomers in all cases except for complex **2**. In order to explain this behavior, complexes **2a'** and **2b'** bearing dodecyl chains were synthesized to rule out the effect of the chain length on the solid state quantum yields. Even the data support the observed behavior of **2a** and **2b** in the solid state as an independent case, the measurement of the quantum yields were obtained using 10 wt% and 2 wt% complex doped PMMA. The quantum yields of the complexes at 10 wt% PMMA are almost a magnitude to several magnitudes higher than in neat solid state and solution state. However, in comparison to 10 wt% PMMA film, the complexes at 2 wt% PMMA film exhibited higher quantum efficiencies except in the case of **4a** and **2b**. While the low quantum yield in the fluid state can be ascribed to the non-radiative decay of the excited states caused by the rotation of the ligands and floppy nature of the alky chain,, the low quantum yield in neat solid to the molecular aggregation. The self-quenching behavior was observed in complexes **2a'** even in solution. As shown in Figure 4, with increments in concentration from 1 x 10 $^{-5}$ M to 1 x 10 $^{-3}$ M lead to gradual decrease in emission intensity. Although the self-quenching behavior in square-planar Pt(II) complexes is quite common, this is the first time we observed in the NHC Pt(II) acetylide complexes.[22, 25, 30]

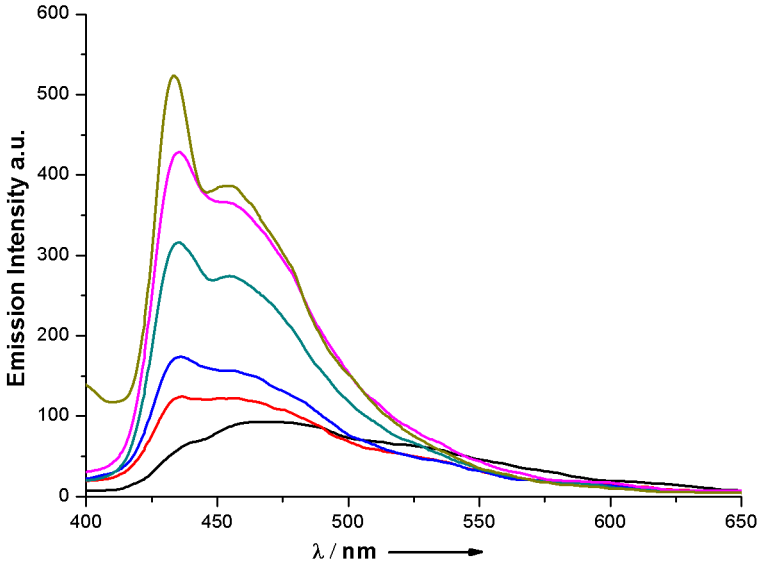

Figure 4. Emission spectra of complex **2a'** in 10^{-5} M (--), 5 x 10^{-5} M (--), 10^{-4} M (--), 2.5 x 10^{-4} M (--), 5 x 10^{-4} M (--) and 10^{-3} M (--) in DCM at RT.

Table 2. Photophysical Properties of Complexes **1a-4a** and **1b-4b.**

	Room temperature solution (CH_2Cl_2)							77 K glass	10% PMMA		2% PMMA
	Absorption λ_{max}[nm] (ε_{max}/[$dm^3\,mol^{-1}cm^{-1}$])	Emission λ_{max}[nm]	τ [ns]	ϕ_{em}% (298 K) CH_2Cl_2	Solid	k_r [s^{-1}] $\times 10^3$	k_{nr} [s^{-1}] $\times 10^5$	(2-MeTHF) λ[nm]	Emission λ_{max}[nm]	ϕ_{em}% 298 K	ϕ_{em}% 298 K
1a	265 (34919), 300 (25676)	430, 446 sh	601	0.8	0.4	13.3	16.5	428, 444 sh	431, 450, 471 sh	42	48
2a	268 (41540), 302 (31031)	432, 455 sh	593	0.9	20	15.1	16.6	423, 450 sh	433, 451, 474 sh	39	59
2a'	268 (62329), 302 (46667)	432, 453 sh	740	1.0	0.7	13.5	13.4	432, 452 sh	432, 453, 473 sh	36	63
3a	283 (50851), 297 (38118)	428, 449 sh	601	0.9	0.3	14.9	16.4	426, 442 sh	428, 450, 468 sh	57	78
4a	265 (43336), 300 (32246)	430, 452 sh	507	0.8	0.2	15.8	19.6	427, 445 sh	430, 450, 470 sh	48	42
1b	273 (31799), 307 (27852)	438, 454 sh	1788	1.4	23	7.8	5.5	425, 444 sh	437, 454, 476 sh	58	58
2b	276 (26759), 310 (23613)	440, 462 sh	1973	2.8	3	14.2	4.9	438, 458 sh	438, 459, 482 sh	58	54
2b'	277 (40118), 310 (36102)	441, 472 sh	2647	1.3	0.2	4.9	3.7	435, 459 sh	439, 457, 481 sh	24	61
3b	270 (37017), 307 (33571)	438, 454 sh	978	1.7	21	17.4	10.1	450, 465 sh	434, 451, 474 sh	57	80
4b	272 (27844), 309 (25554)	437, 460 sh	938	1.6	19	17.0	10.5	425, 442 sh	436, 455, 475 sh	54	80

Electrochemistry. All the *cis* and *trans* complexes **1-4** were investigated by cyclic voltammetry in DCM using 0.1 M [*n*-Bu_4N][PF_6] as supporting electrolyte. The results are summarized in table 3 with the potentials given relative to Fc^+/Fc couple used as an internal standard and the CV figure of complexes 1a and 1b is illustrated in Figure 5. The *cis* complexes **1a-4a** show only one irreversible oxidation wave in the range of +0.67 V to +0.84 V, while the *trans* isomers **1b**-**4b** exhibit one quasireversible oxidation wave. The electrochemical behavior of the *cis* complexes are similar to the analogues previously reported, but the *trans* complexes display electrochemical behavior different than the previously reported *trans* isomers. The substituent changes on the alkyne strongly affect the oxidation potential of the complexes. The *trans* isomers **3b** and **4b** exhibit a similar quasi-reversible oxidation wave at +0.73 V and +0.70 V and the similar behavior is also observed for *trans* isomers **1b** and **2b** which exhibit quasirevesible oxidation wave at +0.60 V and +0.57 V, respectively. Consistent with the more electron donating nature of the **pimi**, complexes **1** and **2** possess lower oxidative potentials than the corresponding **ptrz** based complexes due to the stronger electron donating property of **pimi**. Since the *trans* isomers possess a lower HOMO-LUMO gap than corresponding *cis* isomers (observed in emission studies), this is also reflected in the *trans* isomers having lower oxidation potential than the *cis* isomers for all the complexes. Based on the earlier literature reports on Pt(II) complexes, the oxidation waves observed for the *cis* and

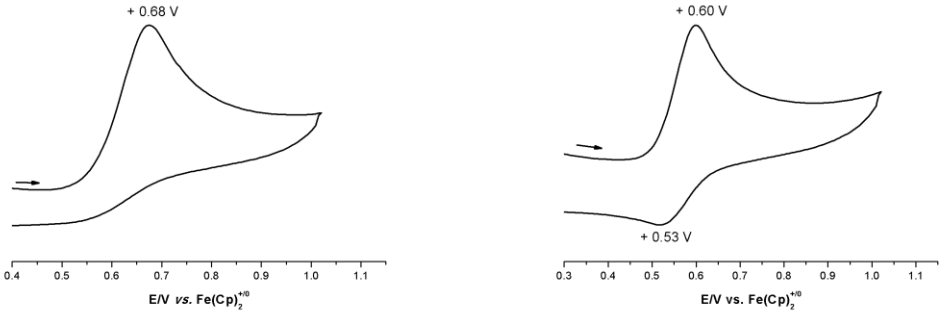

Figure 5. CV of **1a** (left) and **1b** (right) in 0.1 M [*n*-Bu_4N][PF_6] with Fc^+/Fc and internal standard. Au electrode; sacan rate = 100 mV/s; 20 ^oC CH_2Cl_2.

trans complexes are tentatively assigned to the oxidation of the alkynyl ligand rather than to a Pt(II)/Pt(III) process due to the process occurs at a low potential (< +1.0 V).

Table 3. Electrochemical Potentials for **1a**-**4a** and **1b**-**4b**.[a]

Complex	E_{ox} *(V)*
1a	+0.68
2a	+0.67
2a'	+0.74
3a	+0.84
4a	+0.79
1b	+0.60/ +0.53
2b	+0.57/ +0.48
2b'	+0.60/ +0.54
3b	+0.73/ +0.66
4b	+0.70/ +0.65

5.4 Conclusions

The present work describes the synthesis and photophysical investigation of a series of *cis* and *trans* N-heterocyclic Pt(II) acetylide complexes [Pt(**pimi**)$_2$($C\equiv CC_6H_4F$)$_2$] (**1**), [Pt(**pimi**)$_2$($C\equiv CC_6H_5$)$_2$] (**2**), [Pt(**ptrz**)$_2$($C\equiv C$-C_6H_4F)$_2$] (**3**)

and [Pt(**ptrz**)$_2$(C≡C-C$_6$H$_5$)$_2$] (**4**). These complexes exhibit intense emission in the range of 425-450 nm in 10 wt% and 2 wt% PMMA film. The quantum yields of the *trans* complexes **3** and **4** were found to be as high as 80% when doped into a 2 wt% PMMA film. Experimental investigations suggest the presence of self-quenching of the emission process in complex **2a'** at high concentrations in fluid solution. Through these experimental investigations, we also conclude that these molecules show strong aggregation in the neat solid, which results in low qauntum yields in neat solid. Given the high quantum efficiency of 80% for complexes **3b** and **4b** in the deep blue region, testing of the complex in an OLED set-up is ongoing in collaboration with the group of Prof. Trisha Andrew at the University of Wisconsin-Madison.

5.5 Experimental Section

General procedure: All manipulations requiring inert atmosphere were carried out using standard schlenk techniques under dinitrogen. ^{1}H, ^{13}C{^{1}H} and ^{19}F NMR spectra were recorded on Bruker AV2-300 (300 MHz) or AV-500 (500 MHz) spectrometers. Chemical shifts (δ) are reported in parts per million (ppm) referenced to tetramethylsilane (δ 0.00) ppm using the residual protio solvent peaks as internal standards (^{1}H NMR experiments) or the characteristic resonances of the solvent nuclei (^{13}C NMR experiments). ^{19}F NMR was referenced to $CFCl_3$ (δ 0.00) ppm. Coupling constants (*J*) are quoted in Hertz (Hz) and the following abbreviations are used to describe the signal multiplicities: s (singlet); d (doublet); t (triplet); q (quartet); m (multiplet); dm (doublet of multiplet). Proton and carbon assignments have been made using routine one and two dimensional NMR spectroscopes where appropriate. Infra-red (IR) spectra were recorded on a Perkin-Elmer 1600 Fourier Transform spectrophotometer using KBr pellet with frequencies (ν_{max}) quoted in wavenumbers

(cm^{-1}). Elemental microanalysis was carried out with Leco CHNS-932 analyzer. Mass spectra were run on a Finnigan-MAT-8400 mass spectrometer. TLC analysis was performed on precoated Merck Silica Gel60F_{254} slides and visualized by luminescence quenching either at (short wavelength) 254 nm or (long wavelength) 365 nm. Chromatographic purification of products was performed on a short column (Length 15.0 cm: diameter 1.5 cm) using silica gel 60, 230–400 mesh using a forced flow of eluent. UV-vis measurements were carried out on a Perkin-Elmer Lambda 19 UV/VIS spectrophotometer. Emission spectra were acquired on Perkin Elmer spectrophotometer using 450W Xenon lamp excitation by exciting at the longest-wavelength absorption maxima. All samples for emission spectra were degassed by at least three freeze-pump-thaw cycles in an anaerobic curette and were pressurized with N_2 following each cycle. 77 K emission spectra were acquired in frozen 2-methyltetrahydrofuran (2-MeTHF) glass. Luminescence quantum yields of (ϕ) was determined at 298 K (estimated uncertainty ± 15%) using standard methods, wavelength-integrated intensities (I) of the corrected emission spectra was compared to iso-absorptive spectra of quinine sulfate standard (ϕ_r = 0.55 in 1N H_2SO_4 air-equilibrated solution) and was corrected for solvent refractive index.[31] Absolute quantum yields were measured in the solid-state using an integrating sphere from Edinburgh Instruments. YAG:Ce (powder) was used as a calibration reference with ϕ_{em} = 97%.

All starting materials were purchased from commercial sources and used as received unless stated otherwise. The solvents used for synthesis were of analytical grade. The compounds [CODPt(C≡C$C_6H_4F)_2$], [CODPt(C≡C$C_6H_5)_2$],[32] [dpimH]I, [ddimH]I and [dptzH]I were prepared according to literature methods.[33]

General procedure for the synthesis of complexes 1a-4a: All manipulations were performed under N_2 atmosphere. 3 equiv. of N,N'-dipentyl-imidazolium iodide (N,N'-dipentyl-imidazolium iodide for **2a'** and **2b'** and N,N'-dipentyl-imidazolium iodide for **3a** and **4a**), 3 equiv. of *t*-BuOK and 1 equiv. of [Pt(COD)(C≡C-R)$_2$]were dissolved in dry THF (15 mL). The reaction mixture was stirred under reflux condition (75^{o}C) for 12-16 h. After the reaction mixture was allowed to cool down to room temperature, H_2O (10 mL) was added. The product was extracted with CH_2Cl_2 (3 × 15 mL) and the organic layer was separated and dried over $MgSO_4$. The solvent was evaporated to dryness in vacuo and the compound was purified by column chromatography over silica gel.

***Cis*-[Pt(dpim)$_2$(C≡CC$_6$H$_4$F)$_2$]** (**1a**). Hexane/ CH_2Cl_2 (1:4 v/v) was used as a eluent. Yield: 63%. ^{1}H NMR (400 MHz, CD_2Cl_2, 20 ^{o}C): δ (ppm) = 7.17 (t, 4H, ^3J = 8.0 Hz, phenyl), 6.89 (d, 4H, ^3J = 8.0 Hz, imidazole), 6.78 (t, 4H, ^3J = 8.0 Hz, Phenyl), 4.49 (m, 4H, NCH*H*CH$_2$), 3.92 (m, 4H, NC*H*HCH$_2$), 1.80 (m, 4H, NCH$_2$CH*H*CH$_2$), 1.60 (m, 4H, NCH$_2$CH*H*CH$_2$), 1.26 (m, 16H, CH$_2$C*H*$_2$C*H*$_2$CH$_3$), 0.84 (t, 6H, CH$_2$C*H*$_3$); ^{13}C{^{1}H} NMR (100.6 MHz, CD_2Cl_2, 20 ^{o}C), δ (ppm) = 169.8 (*C*=Pt), 159.6 (d, $^1J_{F\text{-}C}$ = 240.0 Hz, *C*-F), 132.8 (d, phenyl), 126.1 (d phenyl), 120.4 (s, imidazole), 114.6 (d, phenyl), 105.3, 104.1 (*C*≡*C*-Pt), 51.8, 31.4, 29.5, 23.2, 14.1((CH$_2$)$_4$CH$_3$); ^{19}F NMR (188.3 MHz, CD_2Cl_2, 25 ^{o}C): δ (ppm) = -118.4. ESI$^+$ MS *m/z* : 849.4 (M$^+$); IR (ATR, cm^{-1}) $\nu_{C\equiv C}$ = 2103; Elemental analysis calcd (%) for $C_{42}H_{56}F_2N_4Pt$: C 59.35, H 6.64, N 6.59; found: C 59.54, H 6.49, N 6.61.

***Cis*-[Pt(dpim)$_2$(C≡CC$_6$H$_5$)$_2$]** (**2a**). EtOAc/ Hexane (8:12 v/v) was used as a eluent. Yield: 49%. ^{1}H NMR (500 MHz, CD_2Cl_2, 20 ^{o}C): δ (ppm) = 7.17 (d, 4H, ^3J = 10.0 Hz, Phenyl), 7.07 (t, 4H, ^3J = 5.0 Hz, phenyl), 6.93 (t, 2H, ^3J = 5.0 Hz,phenyl),

6.85 (s, 4H, imidazole), 4.48 (m, 4H, NCH*H*CH_2), 3.91 (m, 4H, NC*H*HCH_2), 1.83 (m, 4H, NCH_2CH*H*), 1.57 (m, 4H, NCH_2C*H*H), 1.21 (m, 16H, CH_2C*H*$_2C$*H*$_2CH_3$), 0.83 (t, 12H, CH_2C*H*$_3$); $^{13}C\{^1H\}$ NMR (125.8 MHz, CD_2Cl_2, 20^oC), δ (ppm) = 169.5 (C=Pt), 131.0, 129.3, 127.6, 124.2 (C on Phenyl ring), 119.5 (C on imidazole), 106.1, 105.7 (C≡C), 50.5, 30.1, 29.0, 22.5, 13.7 (C on $(CH_2)_4CH_3$); ESI^+ MS *m/z*: 813.4 (M^+); IR (ATR, cm^{-1}) $\nu_{C\equiv C}$ = 2097; Elemental analysis calcd (%) for $C_{42}H_{58}N_4Pt$: C 61.97, H 7.18, N 6.88; found: C 62.32, H 7.01, N 6.91.

***Cis*-[Pt(ddim)$_2$(C≡CC_6H_5)$_2$]** (**2a'**). EtOAc/ Hexane (6:14 v/v) was used as a eluent. Yield: 33%. ^1H NMR (400 MHz, CD_2Cl_2, 20 ^oC): δ (ppm) = 7.18 (d, 4H, ^3J = 8.0 Hz, Phenyl), 7.09 (t, 4H, ^3J = 4.0 Hz, phenyl), 6.98 (t, 2H, ^3J = 4.0 Hz,phenyl), 6.86 (s, 4H, imidazole), 4.45 (m, 4H, NCH*H*CH_2), 3.96 (m, 4H, NC*H*HCH_2), 1.79 (m, 4H, NCH_2CH*H*), 1.56 (m, 4H, NCH_2C*H*H), 1.27 (m, 72H, $CH_2(CH_2)_9CH_3$), 0.84 (t, 12H, ^3J = 4.0 Hz, CH_2C*H*$_3$); $^{13}C\{^1H\}$ NMR (100.6 MHz, CD_2Cl_2, 20^oC), δ (ppm) = 170.1 (C=Pt), 131.5, 129.9, 128.1, 124.7 (C on Phenyl ring), 120.0 (C on imidazole), 106.6, 106.2 (C≡C), 51.9, 32.4, 30.9, 30.16, 30.15, 30.11, 30.10, 29.99, 29.86, 27.42, 23.18, 14.35 (C on $(CH_2)_{11}CH_3$); ESI^+ MS *m/z*:1206.6(M^+); IR (ATR, cm^{-1}) $\nu_{C\equiv C}$ = 2100; Elemental analysis calcd (%) for $C_{70}H_{114}N_4Pt$: C 69.67, H 9.52, N 4.64; found: C 69.46, H 9.44, N 4.51.

***Cis*-[Pt(dptz)$_2$(C≡CC_6H_4F)$_2$]** (**3a**). EtOAc/ CH_2Cl_2 (1:19 v/v) was used as eluent. Yield: 83%. ^1H NMR (400 MHz, CD_2Cl_2, 20 ^oC): δ (ppm) = 8.0 (s, 2H, triazole), 7.25 (t, 4H, ^3J = 8.0 Hz, phenyl), 6.91 (t, 4H, Phenyl), 4.51 (m, 4H, NCH_2CH_2), 4.20 (m, 4H, NCH_2CH_2), 1.92 (m, 8H, NCH_2CH_2), 1.39 (m, 16H, $CH_2CH_2CH_2CH$), 0.92 (t, 6H, CH_2CH_3); $^{13}C\{^1H\}$ NMR (100.6 MHz, CD_2Cl_2, 20 ^oC), δ (ppm) =171.44 (*C*=Pt), 159.3 (d, $^1J_{F\text{-}C}$= 240.4 Hz, *C*-F), 141.7 (triazole), 132.6 (d, phenyl), 124.9 (d phenyl),

114.6 (d, phenyl), 104.7, 101.9 (*C*≡*C*-Pt),52.6, 48.7 (N*C*H_2), 29.8, 29.1 (NCH_2*C*H_2), 28.8, 28.7 (NCH_2CH_2*C*H_2), 22.4, 22.3 (N$CH_2CH_2CH_2$*C*H_2), 13.7, 13.6 (*C*H_3),^{19}F NMR (188.3 MHz, CD_2Cl_2, 25 ^{o}C): δ (ppm)= -119.0. ESI$^+$ MS *m/z*: 851.4 (M^+); IR(ATR, cm^{-1}) $\nu_{C\equiv C}$ = 2111; Elemental analysis calcd (%) for $C_{40}H_{54}F_2N_4Pt$: C 56.39, H 6.39, N 9.86; found: C 56.70, H 6.28, N 9.81.

***Cis*-[Pt(dptz)$_2$(C≡CC_6H_5)$_2$]** (**4a**). EtOAc/ Hexane (8:12 v/v) was used as a eluent. Yield: 79%. ^{1}H NMR (500 MHz, CD_2Cl_2, 20 ^{o}C): δ (ppm) = 7.87 (s, 2H, triazole), 7.17 (t, 4H, ^3J = 5.0 Hz, phenyl), 7.08 (t, 4H, ^3J = 5.0 Hz,phenyl), 6.97 (s, 4H, triazole), 4.45 (m, 4H, NCH*H*CH_2), 4.12 (m, 4H, NC*H*HCH_2), 1.81 (m, 8H, NCH_2C*H*$_2$), 1.21 (m, 16H, NCH_2C*H*$_2$C*H*$_2$$CH_3$), 0.82 (t, 12H, CH_2C*H*$_3$); ^{13}C{^{1}H} NMR (125.8 MHz, CD_2Cl_2, 20^{o}C), δ (ppm) = 172.2 (*C*=Pt),142.2 (triazole), 131.7, 129.3, 127.3, 125.2 (C on phenyl ring), 106.7, 103.3 (*C*≡*C*), 53.1, 49.3 (N*C*H_2), 30.4, 29.7 (NCH_2*C*H_2), 29.4, 29.3 (NCH_2CH_2*C*H_2), 23.0, 22.9 (N$CH_2CH_2CH_2$*C*H_2), 14.3, 14.2 (*C*H_3), ESI$^+$ MS *m/z*: 810.4 (M^+); IR (ATR, cm^{-1}) $\nu_{C\equiv C}$ = 2118, 2108; Elemental analysis calcd (%) for $C_{40}H_{56}N_4Pt$: C 58.88, H 6.92, N 10.30; found: C 58.99, H 6.94, N 10.21.

General procedure for the synthesis of *trans* complexes. 1b, 2b' and **3b**: *cis* complexes (**1a** and **3a**) were heated to 200 ^{o}C in a sealed schlenk flask for 1 h (0.5 h for **2a'**), and then corresponding *trans* complexes were obtained and purified by silica gel chromatography column with proper eluent. Complexes **2b** and **4b** were obtained by heating corresponding *cis* complexes (1.0 equiv.) and [Pt(COD)(C≡CC_6H_5)] (1.0 equiv.) in THF to 80 ^{o}C for 1 day. (Note: The Rf value of chromatography are the same for **3a** and **3b**, **4a** and **4b**)

***Trans*-[Pt(dpim)$_2$(C≡CC$_6$H$_4$F)$_2$]** (**1b**). EtOAc/ CH_2Cl_2 (1:19 v/v) was used as the eluent. Yield: 80%. ^{1}H NMR (500 MHz, CD_2Cl_2, 20 ^{o}C): δ (ppm) = 7.04 (q, 4H, ^3J = 4.0 Hz, phenyl), 6.99 (s, 4H, imidazole), 6.83 (t, 4H, phenyl), 4.50 (t, 8H, ^3J =8.0 Hz, NCH_2), 2.14 (m, 8H, NCH_2CH_2), 1.45 (m, 16H, $CH_2CH_2CH_2CH_3$), 0.93 (t, 6H, ^2J = 8.0 Hz, CH_2CH_3); ^{13}C{^{1}H} NMR (100.6 MHz, CD_2Cl_2, 20 ^{o}C), δ (ppm) =167.8 (C=Pt), 158.4 (d, $^1J_{F-C}$= 240.0 Hz, *C*-F), 132.1 (d, phenyl), 126.3 (d, phenyl), 119.7 (s, imidazole), 114.5 (d, phenyl), 107.3, 103.8 (*C*≡*C*-Pt), 50.8, 30.4, 29.1, 22.5, 13.8 ($(CH_2)_4CH_3$); ^{19}F NMR (188.3 MHz, CD_2Cl_2, 25 ^{o}C): δ (ppm) = -118.5. ESI$^+$ MS *m/z* : 849.4 (M^+); IR (ATR, cm^{-1}) $\nu_{C\equiv C}$ = 2091; Elemental analysis calcd (%) for $C_{42}H_{56}F_2N_4Pt$: C 59.35, H 6.64, N 6.59; found: C 59.02, H 6.48, N 6.50.

***Trans*-[Pt(dpim)$_2$(C≡CC$_6$H$_5$)$_2$]** (**2b**). CH_2Cl_2/ Hexane (18:2 v/v) was used as eluent. Yield: 25%. ^{1}H NMR (400 MHz, CD_2Cl_2, 20 ^{o}C): δ (ppm) = 7.12 (t, 4H, ^3J = 4.0 Hz, Phenyl), 7.10 (t, 4H, ^3J = 4.0 Hz, phenyl), 7.03 (t, 2H, ^3J = 4.0 Hz, phenyl), 6.99 (s, 4H, imidazole), 4.52 (m, 4H, NCH_2CH_2), 2.12 (m, 8H, NCH_2CH_2), 1.44 (m, 16H, $CH_2CH_2CH_2CH_3$), 0.96 (t, 12H, CH_2CH_3); ^{13}C{^{1}H} NMR (125.8 MHz, CD_2Cl_2, 20^{o}C), δ (ppm) = 169.8 (C=Pt), 130.7, 129.6, 127.5, 123.9 (phenyl), 119.6 (C on imidazole), 106.4, 105.2 (C≡C), 50.8, 30.4, 29.1, 22.5, 13.8 (C on $(CH_2)_4CH_3$); ESI$^+$ MS *m/z*: 813.4 (M^+); IR (ATR, cm^{-1}) $\nu_{C\equiv C}$ = 2090; Elemental analysis calcd (%) for $C_{42}H_{58}N_4Pt$: C61.97, H 7.18, N 6.88; found: C 62.26, H 7.10, N 6.89.

***Trans*-[Pt(ddim)$_2$(C≡CC$_6$H$_5$)$_2$]** (**2b'**). CH_2Cl_2/ Hexane (16:4 v/v) was used as a eluent. Yield: 68%.^{1}H NMR (500 MHz, CD_2Cl_2, 20 ^{o}C): δ (ppm) = 7.12 (d, 4H, ^3J = 5.0 Hz, Phenyl), 7.09 (t, 4H, ^3J = 5.0 Hz, phenyl), 7.03 (t, 2H, ^3J = 4.0 Hz, phenyl), 6.99 (s, 4H, imidazole), 4.50 (m, 4H, ^3J = 10.0 Hz, NCH_2CH_2), 2.12 (m, 8H, NCH_2CH_2), 1.48 (m, 8H, $NCH_2CH_2CH_2$),1.28 (m, 64H, $CH_2(CH_2)_8CH_3$) 0.92 (t, 12H,

CH_2CH_3); $^{13}C\{^1H\}$ NMR (100.6 MHz, CD_2Cl_2, 20°C), δ (ppm) = 169.9 (C=Pt), 130.8, 129.6, 127.6, 124.0 (phenyl), 119.7 (C on imidazole), 107.8, 105.3 (C≡C), 50.95, 31.94, 30.80, 29.78, 29.75, 29.72, 29.69, 29.62, 29.38, 27.13, 22.70, 13.87 (C on $(CH_2)_{11}CH_3$); ESI^+ MS *m/z*: 1205.6(M^+); IR (ATR, cm^{-1}) $\nu_{C\equiv C}$ = 2090; Elemental analysis calcd (%) for $C_{70}H_{114}N_4Pt$: C 69.67, H 9.52, N 4.64; found: C 69.20, H 9.22, N 4.26.

***Trans*-[Pt(dptz)$_2$(C≡CC$_6$H$_4$F)$_2$]** (**3b**). EtOAc/ CH_2Cl_2 (1:19 v/v) was used as eluent. Yield: 66%.^{1}H NMR (500 MHz, CD_2Cl_2, 20 °C): δ (ppm) = 7.86 (s, 2H, triazole), 6.96 (t, 4H, ^3J = 8.0 Hz, phenyl), 6.71 (t, 4H, phenyl), 4.54 (t, 4H, NCH_2CH_2), 4.40 (m, 4H, NCH_2CH_2), 2.08 (m, 8H, NCH_2CH_2), 1.35 (m, 16H, $CH_2CH_2CH_2CH_3$), 0.83 (t, 6H, CH_2CH_3); $^{13}C\{^1H\}$ NMR (125.8 MHz, CD_2Cl_2, 20 °C), δ (ppm) =171.3 (*C*=Pt), 159.3 (d, $^1J_{F\text{-}C}$= 244.0 Hz, *C*-F), 141.7 (triazole), 132.3 (d, phenyl), 125.1 (d, phenyl), 114.6 (d, phenyl), 104.2, 103.6 (*C*≡*C*-Pt),52.7, 48.7 (NCH_2), 30.0, 29.4 (NCH_2CH_2), 28.9, 28.8 ($NCH_2CH_2CH_2$), 22.4, 22.3 ($NCH_2CH_2CH_2CH_2$), 13.8, 13.7 (CH_3),^{19}F NMR (188.3 MHz, CD_2Cl_2, 25 °C): δ (ppm)= -119.2. ESI^+ MS *m/z*: 851.4 (M^+); IR(ATR, cm^{-1}) $\nu_{C\equiv C}$ = 2106.7; Elemental analysis calcd (%) for $C_{40}H_{54}F_2N_4Pt$: C 56.39, H 6.39, N 9.86; found: C 56.42, H 6.26, N 9.71.

***Trans*-[Pt(dptz)$_2$(C≡CC$_6$H$_5$)$_2$]** (**4b**). EtOAc/ CH_2Cl_2 (1:19 v/v) was used as eluent. Yield: 66%. ^{1}H NMR (400 MHz, CD_2Cl_2, 20 °C): δ (ppm) = 7.91 (s, 2H, triazole), 7.03 (m, 10H, phenyl), 4.60 (t, 4H, NCH_2CH_2), 4.47 (m, 4H, NCH_2CH_2), 2.08 (m, 8H, NCH_2CH_2), 1.34 (m, 16H, $CH_2CH_2CH_2CH_3$), 0.84 (t, 6H, CH_2CH_3); $^{13}C\{^1H\}$ NMR (100.6 MHz, CD_2Cl_2, 20 °C), δ (ppm) = 171.8 (*C*=Pt), 142.2 (triazole), 131.3, 129.5, 128.1, 125.0 (phenyl), 106.2, 105.0 (*C*≡*C*-Pt),53.4, 49.2 (NCH_2), 30.5,

29.9 ($NCH_2\mathit{C}H_2$), 29.4, 29.3 ($NCH_2CH_2\mathit{C}H_2$), 23.0, 22.9 ($NCH_2CH_2CH_2\mathit{C}H_2$), 14.3, 14.2 ($\mathit{C}H_3$). IR (ATR, cm^{-1}) $\nu_{C\equiv C}$ = 2104; Elemental analysis calcd (%) for $C_{40}H_{56}F_2N_6Pt$: C 58.88, H 6.92, N 10.30; found: C 58.82, H 6.90, N 10.21.

5.6 References

[1] C.-W. Chan, L.-K. Cheng, C.-M. Che, *Coord. Chem. Rev.*, **1994**, *132*, 87.

[2] H. Yersin, A. F. Rausch, R. Czerwieniec, T. Hofbeck, T. Fischer, *Coord. Chem. Rev.*, **2011**, *255*, 2622.

[3] Y. Unger, D. Meyer, O. Molt, C. Schildknecht, I. Münster, G. Wagenblast, T. Strassner, *Angew. Chem. Int. Ed.*, **2010**, *49*, 10214.

[4] Z. M. Hudson, C. Sun, M. G. Helander, Y.-L. Chang, Z.-H. Lu, S. Wang, *J. Am. Chem. Soc.*, **2012**, *134*, 13930.

[5] H.-F. Xiang, S.-W. Lai, P. T. Lai, C.-M. Che, in *Highly Efficient OLEDs with Phosphorescent Materials*, Wiley-VCH Verlag GmbH & Co. KGaA, **2008**, pp. 259.

[6] H. Yersin, W. J. Finkenzeller, in *Highly Efficient OLEDs with Phosphorescent Materials*, Wiley-VCH Verlag GmbH & Co. KGaA, **2008**, pp. 1.

[7] R. Zieba, C. Desroches, F. Chaput, M. Carlsson, B. Eliasson, C. Lopes, M. Lindgren, S. Parola, *Adv. Funct. Mate.*, **2009**, *19*, 235.

[8] C. K. M. Chan, C.-H. Tao, H.-L. Tam, N. Zhu, V. W.-W. Yam, K.-W. Cheah, *Inorg. Chem.*, **2009**, *48*, 2855.

[9] R. Liu, Y. Li, Y. Li, H. Zhu, W. Sun, *J. Phys. Chem. A*, **2010**, *114*, 12639.

[10] Z. M. Hudson, C. Sun, K. J. Harris, B. E. G. Lucier, R. W. Schurko, S. Wang, *Inorg. Chem.*, **2011**, *50*, 3447.

[11] S. W. Thomas, K. Venkatesan, P. Mueller, T. M. Swager, *J. Am. Chem. Soc.*, **2006**, *128*, 16641.

[12] T. Sajoto, P. I. Djurovich, A. Tamayo, M. Yousufuddin, R. Bau, M. E. Thompson, R. J. Holmes, S. R. Forrest, *Inorg. Chem.*, **2005**, *44*, 7992.

[13] V. W.-W. Yam, *Acc. Chem, Res.*, **2002**, *35*, 555.

[14] V. Balzani, S. Campagna, J. A. G. Williams, in *Photochemistry and Photophysics of Coordination Compounds II, Vol. 281*, Springer Berlin Heidelberg, **2007**, pp. 205.

[15] Y. Chi, P.-T. Chou, *Chem. Soc. Rev.*, **2010**, *39*, 638.

[16] A. Y.-Y. Tam, W. H. Lam, K. M.-C. Wong, N. Zhu, V. W.-W. Yam, *Chem.–Eur. J.*, **2008**, *14*, 4562.

[17] T. Yasuda, I. Yamaguchi, T. Yamamoto, *Adv. Mater.*, **2003**, *15*, 293.

[18] C.-H. Tao, N. Zhu, V. W.-W. Yam, *Chem.–Eur. J.*, **2005**, *11*, 1647.

[19] A. J. Lees, M. Muro, A. Rachford, X. Wang, F. Castellano, in *Photophysics of Organometallics, Vol. 29*, Springer Berlin Heidelberg, pp. 1.

[20] J. Schneider, P. Du, P. Jarosz, T. Lazarides, X. Wang, W. W. Brennessel, R. Eisenberg, *Inorg. Chem.*, **2009**, *48*, 4306.

[21] J. E. McGarrah, R. Eisenberg, *Inorg. Chem*, **2003**, *42*, 4355.

[22] W. B. Connick, D. Geiger, R. Eisenberg, *Inorg, Chem.*, **1999**, *38*, 3264.

[23] M. Hissler, W. B. Connick, D. K. Geiger, J. E. McGarrah, D. Lipa, R. J. Lachicotte, R. Eisenberg, *Inorg. Chem.*, **2000**, *39*, 447.

[24] P. Jarosz, K. Lotito, J. Schneider, D. Kumaresan, R. Schmehl, R. Eisenberg, *Inorg. Chem.*, **2009**, *48*, 2420.

[25] S.-W. Lai, M. C.-W. Chan, T.-C. Cheung, S.-M. Peng, C.-M. Che, *Inorg. Chem.*, **1999**, *38*, 4046.

[26] X. Yang, Z. Wang, S. Madakuni, J. Li, G. E. Jabbour, *Adva. Mater.*, **2008**, *20*, 2405.

[27] X.-C. Hang, T. Fleetham, E. Turner, J. Brooks, J. Li, *Angew. Chem. Int. Ed.*,

2013, *52*, 6753.

[28] A. B. Tamayo, B. D. Alleyne, P. I. Djurovich, S. Lamansky, I. Tsyba, N. N. Ho, R. Bau, M. E. Thompson, *J. Am. Chem. Soc.*, **2003**, *125*, 7377.

[29] Y. Zhang, J. A. Garg, C. Michelin, T. Fox, O. Blacque, K. Venkatesan, *Inorg. Chem.*, **2011**, *50*, 1220.

[30] S. J. Farley, D. L. Rochester, A. L. Thompson, J. A. K. Howard, J. A. G. Williams, *Inorg. Chem.*, **2005**, *44*, 9690.

[31] S. Fery-Forgues, D. Lavabre, *J. Chem. Edu.* **1999**, *76*, 1260.

[32] M. Herberhold, T. Schmalz, W. Milius, B. Wrackmeyer, *J. Organomet. Chem.*, **2002**, *641*, 173.

[33] Y. Han, H. V. Huynh, G. K. Tan, *Organometallics* **2007**, *26*, 4612.

Supporting Information

Rational Design of Highly Efficient Deep Blue Emitting N-Heterocyclic Carbene Pt(II) Acetylide Complexes

*Yuzhen Zhang, Olivier Blacque and Koushik Venkatesan**

Institute of Inorganic Chemistry, University of Zürich, Winterthurerstrasse 190, CH-8057, Zürich, Switzerland

Table of Contents

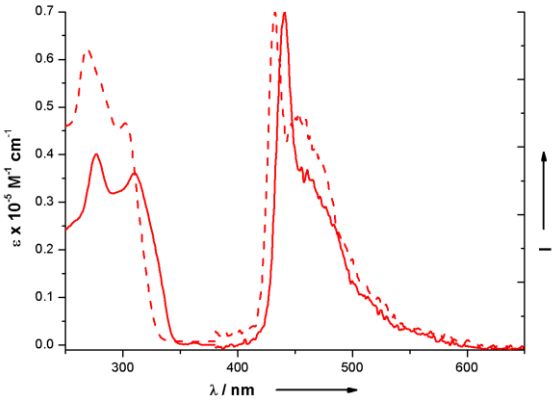

Figure S1. Electronic absorption spectra (left) and normalized emission spectra (right) of **2a** (red dash), **2b** (red solid) in CH_2Cl_2 at RT.

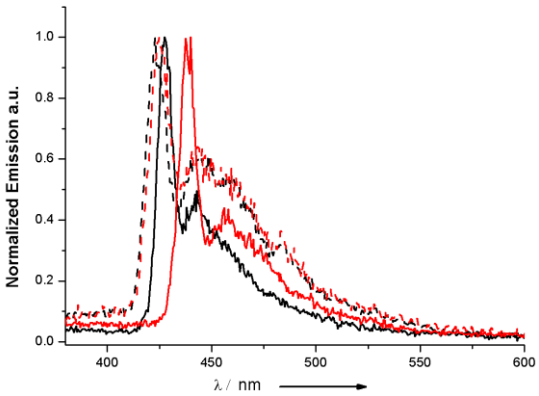

Figure S2. Normalized emission spectra of **1a** (black dash), **1b** (black solid), **2a** (red dash), **2b** (red solid) in 2-MeTHF at 77 K.

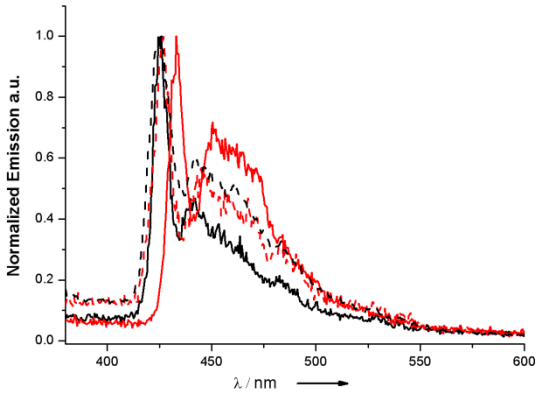

Figure S3. Normalized emission spectra of **3a** (black dash), **3b** (black solid), **4a** (red dash), **4b** (red solid) in 2-MeTHF at 77 K.

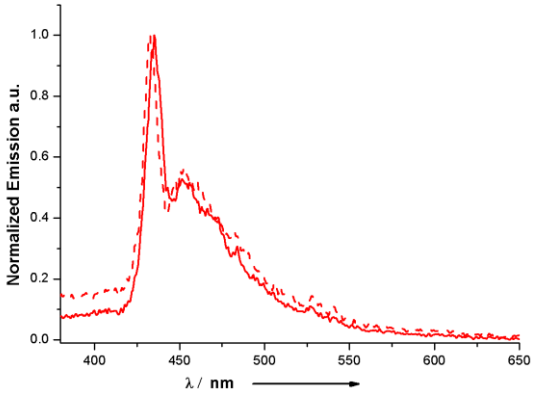

Figure S4. Normalized emission spectra of **2a'** (red dash), **2b'** (red solid) in 2-MeTHF at 77 K.

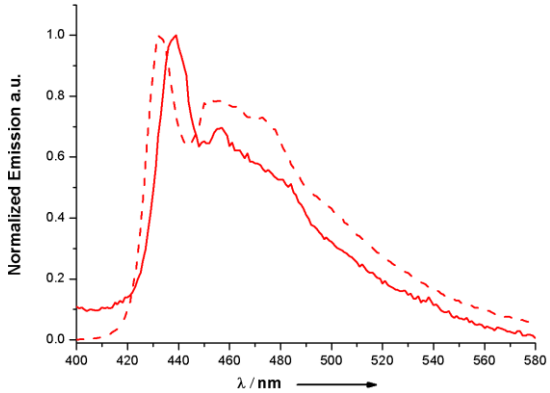

Figure S5. Normalized emission spectra of **2a'** (red dash), **2b'** (red solid) in 10 wt% PMMA film at RT.

Table S1. Crystal data and structure refinement for **1a**, **2a**, and **4a**.

	1a	**2a**	**4a**
CCDC number			
Empirical formula	$C_{42}H_{56}F_2N_4Pt.\ (CH_2Cl_2)_1$	$C_{42}H_{46}F_2N_4PtO_2$	$C_{85}H_{91}N_8Pt_2Cl$
Formula weight	934.92	898.94	1650.28
Temperature/K	183(2)		183(2)
Crystal system	triclinic	orthorhombic	monoclinic
Space group	P-1	$Pca2_1$	$P2_1/c$
a/Å	12.8898(3)	13.7433(2)	16.9885(7)
b/Å	14.8898(3)	21.0614(3)	25.6500(8)
c/Å	15.3277(4)	13.18580(10)	19.5345(9)
α/°	62.146(2)	90	90
β/°	68.512(2)	90	114.494(5)
γ/°	65.835(2)	90	90
Volume/$Å^3$	2192.22(8)	3816.67(8)	7746.2(6)
Z	2	4	4
$\rho_{calc}mg/mm^3$	1.416	1.517	1.415
m/mm^{-1}	63.364	3.727	3.691
F(000)	948	1752.0	3320.0
Crystal size/mm^3	0.42 × 0.36 × 0.18	0.16 × 0.15 × 0.09	0.34 × 0.13 × 0.07
2Θ range for data collection	2.76 to 30.51°	5.77 to 56.562°	5.468 to 52.744°
Index ranges	-17 ≤ h ≤ 17, -21 ≤ k ≤ 21, -21 ≤ l ≤ 21	-18 ≤ h ≤ 17, -28 ≤ k ≤ 28, -17 ≤ l ≤ 17	-21 ≤ h ≤ 20, -32 ≤ k ≤ 28, -24 ≤ l ≤ 22
Reflections collected	39450	34854	60100
Independent reflections	13378[R(int) = 0.0369]	9470[R(int) = 0.0498]	15828[R(int) = 0.0863]
Data/restraints/parameters	11898/123/474	9470/155/517	15828/149/518
Goodness-of-fit on F^2	1.087	1.014	1.034
Final R indexes [I>=2σ (I)]	R_1 = 0.0314, wR_2 = 0.0772	R_1 = 0.0347, wR_2 = 0.0579	R_1 = 0.0701, wR_2 = 0.1433
Final R indexes [all data]	R_1 = 0.0389, wR_2 = 0.0824	R_1 = 0.0580, wR_2 = 0.0653	R_1 = 0.1091, wR_2 = 0.1628
Largest diff. peak/hole / e $Å^{-3}$	1.826/-1.205	1.38/-0.66	1.95/-1.81
Flack parameter	n/a	-0.020(4)	n/a

Summary

Since the discovery of electroluminescence in inorganic SiC at 1907, it takes around 80 years to accomplish the commercialization of electroluminescent displays (ELDs). As the organic light-emitting diodes (OLEDs), in short 30 years, it almost achieved the same success as ELDs. But due to the difficulty of producing efficient and durable triplet blue emitters, the real commercialization of OLEDs especial PhOLEDs still has a long way to go. In recent ten years, the research and innovation of triplet blue emitters have gained a boom and most of the researches are focused on cyclometalated Ir(III) complexes. Although these cyclometalated Ir(III) emitters can reach as high as 19.2% external quantum efficiency, there is still certain space to improve. Recently, the triplet emitters based on Cu, Zn and Pt have been reported and due to the poor properties of Cu and Zn emitters, Pt emitters attracted much more attentions because of their comparable efficiencies to Ir(III) complexes. This thesis demonstrated the approach of synthesizing non-cyclometalated N-heterocyclic carbene Pt(II) acetylide triplet blue emitters.

The phoshine and polypyridyl Pt(II) acetylide emitters have been profoundly investigated due to their interesting properties and potential application in chemsesor solar cell and OLEDs. These complexes normally exhibited low energy emission in solution or neat solid with moderate to low quantum efficiencies. With the intent of producing triple blue emitters, we firstly introduced stronger ligand filed (LF) strength fragment NHC into this system to push the low-lying d-d excited state to high energy level. Acetylene is also important not only to create strong metal-ligand interaction via pπ - dπ overlap with Pt, but also afford the duty as chromophor. The first group bis *N*-heterocyclic carbene platinum(II) complexes, [(pmim)Pt(C≡C-R)$_2$] (R = C_6H_5 (**2**), C_6H_4OMe (**3**), $C_6H_2(OMe)_3$ (**4**), $C_6H_4NMe_2$ (**5**), C_4H_3S (**6**), $C_6H_4C{\equiv}CC_6H_5$ (**7**), 1-pyrenyl (**8**), and C_6H_4F (**9**) were successfully synthesized stating from precursor (pmim)PtI_2 **1** (pmim = 1,1'-dipentyl-3,3'-methylene-diimidazoline-2,2'-diylidene). Among those emitters, complexes **2**, **3**, **4**, **5** and **9** exhibited triplet blue emissions in the range of 429-454 nm and the emissions could be tuned by the electronic properties of substitutes on phenylacetylene. The solution quantum yields were measured for

complexes **2-9** and complex **5** exhibited as high as 3.4%. TD-DFT and DFT calculations performed on model molecule **5** exhibited the predominantly metal-perturbed ligand-to-ligand ^{3}LLCT ($\pi_{alk} \rightarrow \pi^*_{alk}$) character and to a lesser extent the ^{3}MLCT (5d $\rightarrow \pi^*_{alk}$).

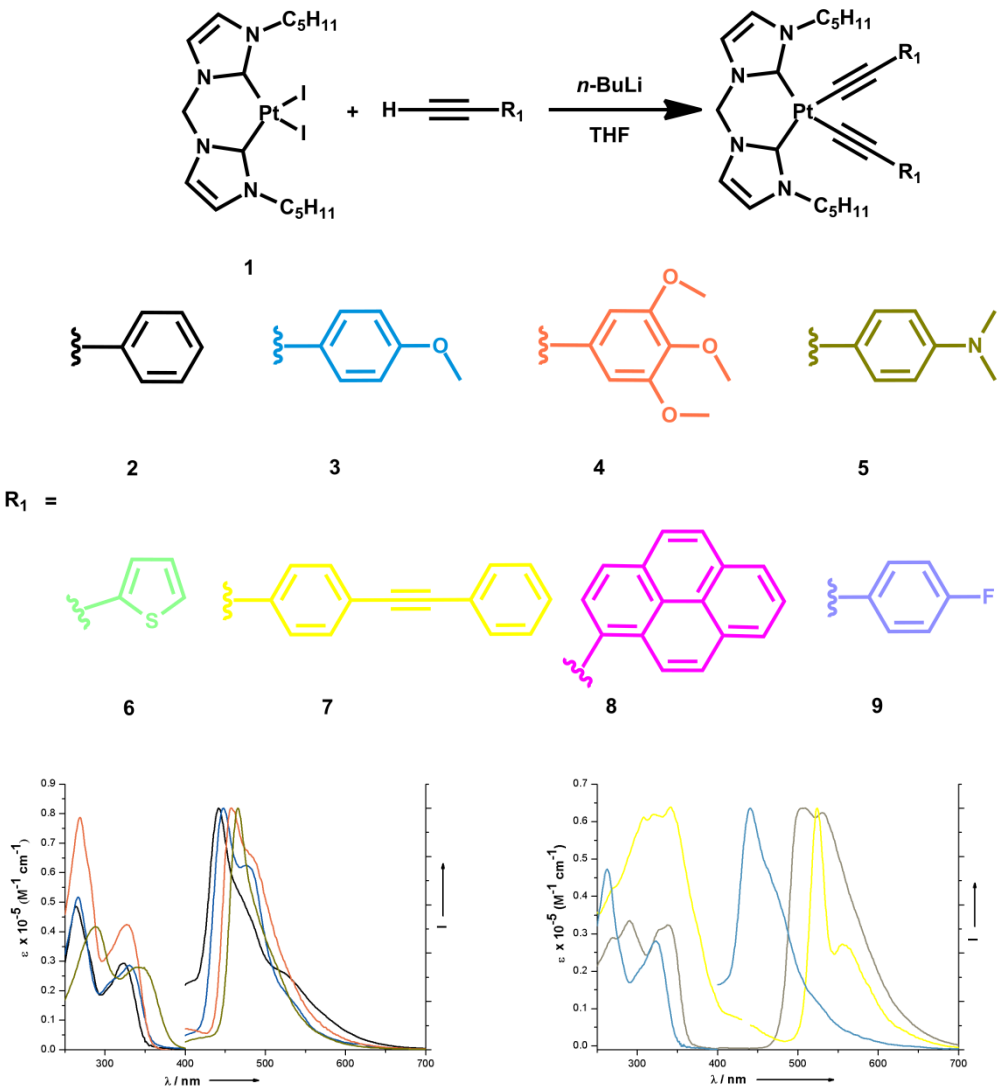

Figure 1. Synthetic process of complexes **2-9** and UV-Vis and emission in degassed DCM at RT.

Inspired by the blue emission of the bis NHC Pt(II) acetylide complexes, we speculated that the mono NHC Pt(II) acetylide complexes could also be emissive and moreover the variety of coordination patterns (*cis* and *trans*) could influence the photophysical properties. In this project a series of *cis* and *trans* NHC Pt(II) acetylide

complexes namely [Pt(**dbim**)$_2$(C≡C-R)$_2$] (dbim = N,N'-didodecyl-benzimidazoline-2-ylidene) [R = C_6H_4F (**13**), C_6H_5 (**14**), $C_6H_2(OMe)_3$ (**15**), C_4H_3S (**16**), and $C_6H_4C{\equiv}CC_6H_5$ (**17**)] and [Pt(**ibim**)$_2$(C≡C-C_6H_5)$_2$] (**18**) (ibim = N,N'-diisopropyl-benzimidazoline-2-ylidene) were synthesized and the photophysical properties were investigated for all of the complexes. All of the *cis* and *trans* complexes **13a**, **13b**, **14a**, **14b**, **15a**, **15b**, **18a**, and **18b** exhibited blue emission in the range of 429-454 nm with the highest quantum yield of 80% for complex **18b** in 10 wt% PMMA film. Beyond the investigation of photophyscial properties, the mechanistic study of *cis* to *trans* isomerization were also performed on the representative complexes 14a and 14b. The study results indicated the *cis* to *trans* isomerization in reaction condition concerning a precursor [Pt(COD)(C≡CC_6H_5)$_2$] catalyzed process, while under the heating and UV-irridation conditions, the process concerned a Pt(0) isolable catalyzed mechanism. DFT and TD-DFT calculations were performed for both the triplet emission and the mechanistic investigation. The results support the emission origin of ^{3}LLCT characters and the Pt(0) catalyzed *cis* to *trans* isomerization.

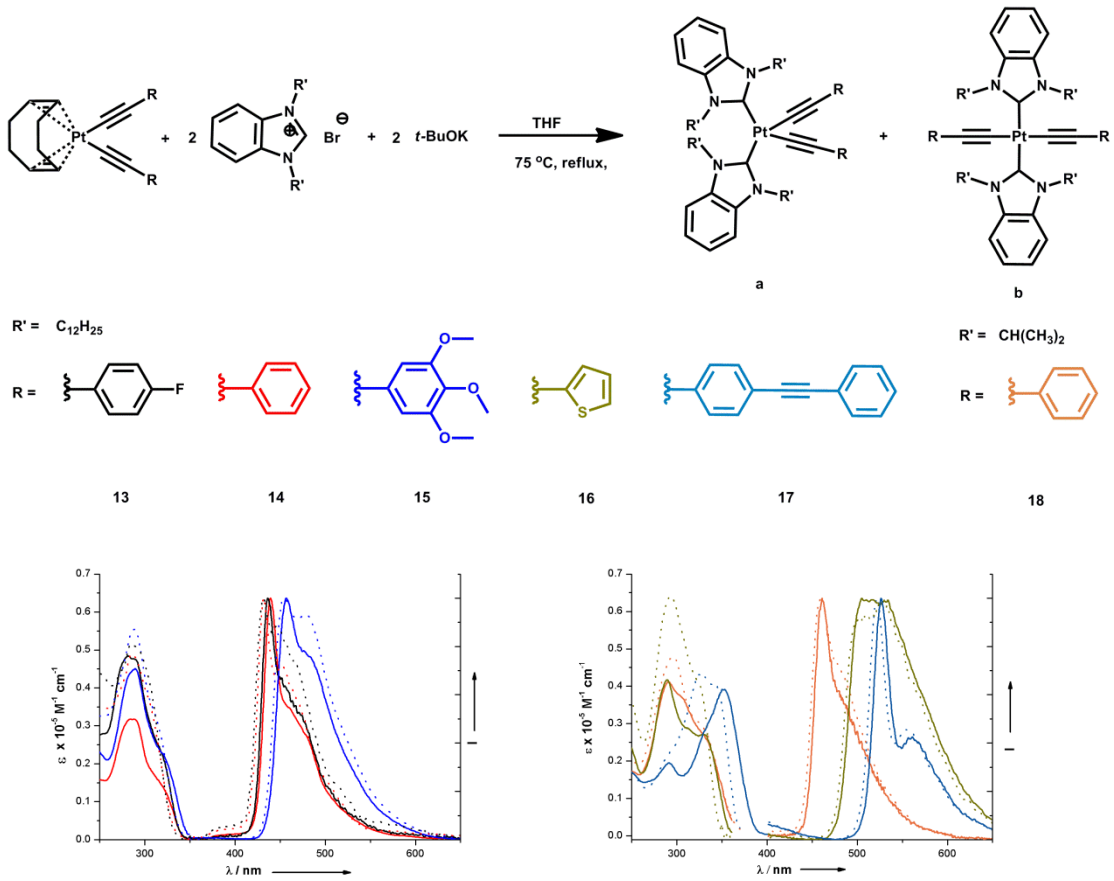

Figure 2. Synthetic process of complexes **13-18** and UV-Vis and emission in degassed DCM at RT.

As the NHC ligand is crucial for harvesting the triplet blue emission on Pt(II) acetylide complexes, we hypothesized that the photophyscial properties especially the quantum yield could be influenced by the electronic effects of NHC. With this intent we synthesized five groups of bis NHC Pt(II) acetylide emitters [Pt(**pmdb**)(C≡CR)$_2$] **22a-c**, [Pt(**pm2tz**)(C≡CR)$_2$] **23a-d**, [Pt(**pm3tz**)(C≡CR)$_2$] **24a-c** [Pt(**ppim**)(C≡CR)$_2$] **25**(**a**, **b**, **e**) and [Pt(**ppbim**)(C≡CR)$_2$] **26**(**a**, **b**, **e**) where pmdb = 1,1'-dipentyl-3,3'-methylene-dibenzimidazoline-2,2'-diylidene, pm2tz = 1,1'-dipentyl-3,3'-methylene-di-1,2,4-trizoline-5,5'-diylidene, pm3tz = 1,1'-dipentyl-3,3'-methylene-di-1,3,4-trizoline-5,5'-diylidene, ppim = 3-pentyl-1-picolylimidazoline-2-ylidene, ppbim = 3-pentyl-1-picolylbenzimidazoline -2-ylidene and R = 4-C_6H_4F, C_6H_5, 4-C_6H_4OMe, $SiMe_3$ and 4-$C_6H_4N(C_6H_5)_2$ with the electron donating properties in order of **pmim** > **pmdb** > **dm2tz** > **dm3tz** > **ppim** > **ppbim**.

All of the five group complexes bearing the 4-fluorophenylacetylene, phenylacetylene and 4-methoxylphenylacetylene exhibited blue emission in the range of 426-437 nm in 10 wt% PMMA film. The quantum yields of all the complexes were measured and the complexes **26b** and **27b** exhibited low quantum efficiencies comparing with complexes **23b**, **24b** and **25b** bearing the same phenylacetylene. This result indicated the electronic effects of NHC to the efficiencies of triplet emission.

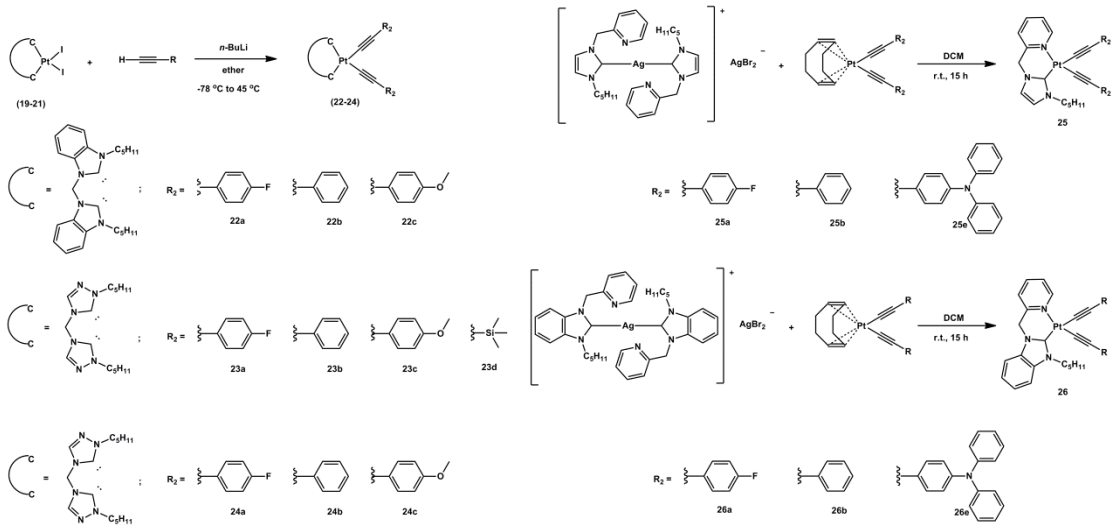

Figure 3. Synthetic process of complexes **22-26**.

Electronic effects of NHC can influence the quantum efficiencies of the triplet emitters, and the proper tuning of NHC ligands in accordance with proper geometry can provide the possibility of design high quantum efficient blue triplet emitters. In the last chapter, we designed and synthesized a series of *cis* and *trans* mono NHC Pt(II) acetylide complexes [Pt(**pimi**)$_2$(C≡CC_6H_4F)$_2$] **26(a,b)**, [Pt(**pimi**)$_2$(C≡CC_6H_5)$_2$] **27(a,b)**, [Pt(**dimi**)$_2$(C≡CC_6H_5)$_2$] **28(a,b)**, [Pt(**ptrz**)$_2$(C≡C-C_6H_4F)$_2$] **29(a,b)** and [Pt(**ptrz**)$_2$(C≡C-C_6H_5)$_2$] **30(a,b)** (**pimi** = N,N'-dipentyl-imidazoline-2-ylidene, **dimi** = N,N'-didodecyl-imidazoline-2-ylidene and **ptrz** = N,N'-dipentyl-trizoline-2-ylidene). All of the *cis* and *trans* complexes were well characterized and they all exhibited triple blue emission in the range of 428-439 nm in 10 wt% PMMA film. The quantum yields were recorded for all the complexes and the *trans* isomers **31b** and **32b** exhibited the quantum yield of 80% in 2% PMMA.

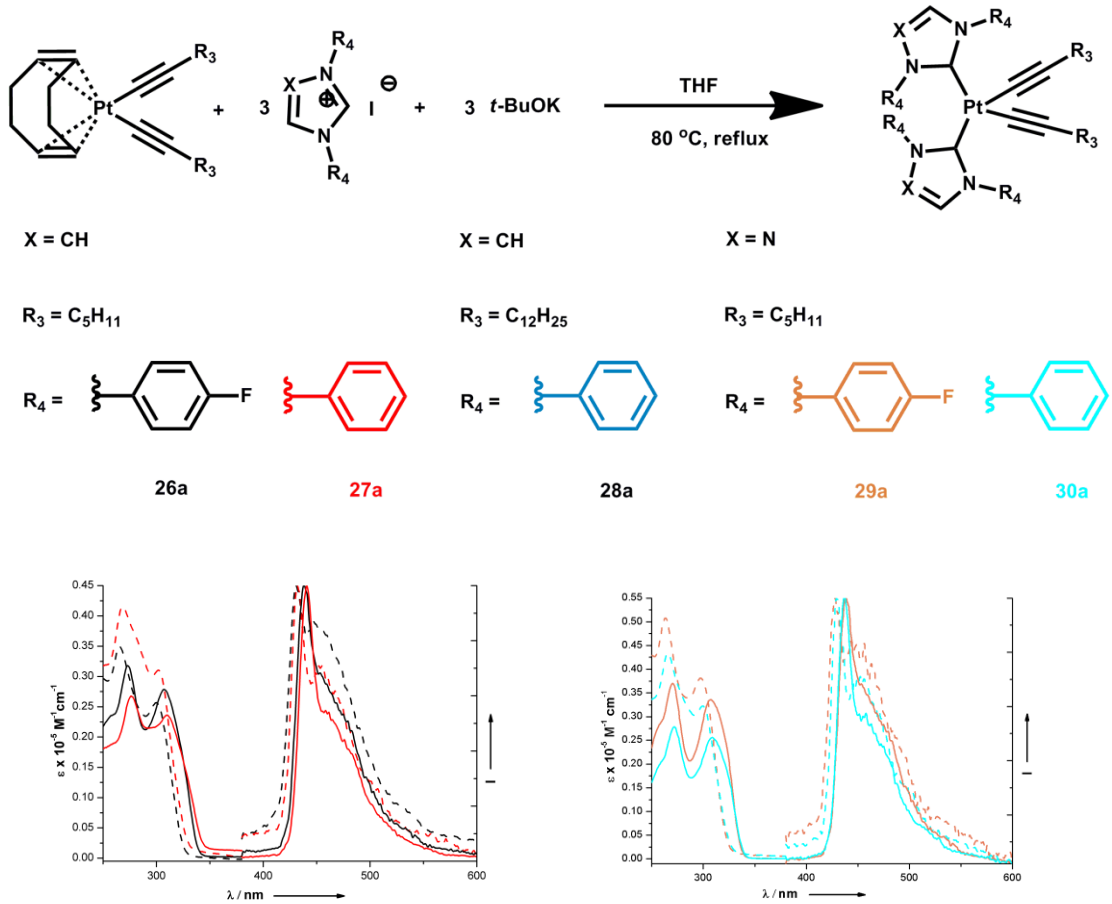

Figure 4. Synthetic process of complexes **26-30** and UV-Vis and emission in degassed DCM at RT.

ABSTRACT

The research into phosphorescent organic light-emitting devices (PhOLEDs) as a viable technology for the development of energy efficient displays and lighting is currently progressing at a rapid pace. Inspite of the increasing demand for the triplet blue emitters to enable the commercialization of the PHOLED technology, highly efficient and stable triplet blue emitters remains scarce. This thesis focuses on the design, syntheses and investigation of triplet blue emitters based on non-cyclometalated Pt(II) complexes. Based on our first report on the bis-N-heterocyclic carbenes (NHC) Pt(II) acetylide triple blue emitters with the wavelength emission maxima hovering in the range 426-454 nm and emission quantum yields around 12%, we pursued a follow-up strategy of varying the electronic properties of NHC to achieve improvements in quantum efficiencies. Since this strategy resulted only in modest improvements, the approach to utilize monodentate NHC ligands was pursued that resulted in the formation of *cis* and *trans* NHC Pt(II) acetylide complexes with significantly high quantum efficiencies as high as 80% for a deep blue triplet emitter. The successful accomplishment of highly emissive deep blue materials based on an ingenuous approach in this thesis opens broad avenues for the rapid development of new class of deep blue triplet emitters with high quantum efficiencies devoid of cyclometalation.

Zusammenfassung

Die Forschung nach phosphoreszenten organischen lichtemmitierenden Geräten (engl. phosphorescent organic light-emitting devices, PhOLEDs) als brauchbare Technologie für die Entwicklung energieeffizienter Displays und Beleuchtung schreitet gegenwärtig rasch fort. Trotz der zunehmenden Nachfrage nach blau-emittierenden Emittern, um die PhOLED-Technolgie kommerziell sinnvoll zu machen, sind hoch effiziente und stabile Triplett-Emitter rar. Die vorliegende Arbeit behandelt das Design, die Synthese und die Untersuchung von blau-emittierenden nicht-cyclometallierten Pt(II)-komplexen als Triplett-Emitter. Basierend auf unseren ersten Berichten über bis-N-heterocyclischen-Carben (NHC) Pt(II)-acetylid-Triplett-Emitter mit Emissionsmaxima in Bereich zwischen 426 und 454 nm und Quantenausbeuten um 12%, folgten wir einer Strategie die elektronischen Eigenschaften des NHC zu varieren, um höhere Quantenausbeuten zu erreichen. Da diese Strategie nur geringfügige Steigerungen der Quantenausbeuten zur Folge hatte, wurde ein neuer Ansatz verfolgt, welcher zur Bildung von *cis*- und *trans*- NHC Pt(II)-acetylid-komplexen mit signifikant höheren Quantenausbeuten von bis zu 80% als tiefblauer Triplett-Emitter führte.

Die erfolgreiche Darstellung stark emittierender tiefblauer Materialien durch eine schlichte Herangehensweise in der vorliegenden Arbeit, eröffnet einen breiten Weg für eine schnelle Entwicklung einer neuen Klasse von tiefblauen Triplett-Emmittern mit hohen Quantenausbeuten ohne Cyclometallierung.

Acknowledgments

I am indebted to many people who supported me throughout the four years and contributed a lot to this dissertation work. I would like to take this opportunity to acknowledge and extend my sincere gratitude to you.

I would like to thank Dr. Koushik Venkatesan, for offering me the precious opportunity to do my PhD study here. Koushik gave me an interesting project and he also gave me the consistent support and supervision throughout the whole duration of my PhD study. He introduced me to the field of organometallic chemistry and also also cultivated my scientific literacy. I real appreciate all what he has done for me.

I would like to thank Prof. Heinz Berke for his general support. It is because of his encouragement during one of his presentations, I made the decision to go abroad and start my PhD study. I also thank the constructive suggestions during my PhD study.

I would like to thank Prof. Roger Alberto for his valuable support and agreeing to be a co-referee of this dissertation.

I would like to extend my special thanks to the people below:

Dr. Olivier Blacque for great help with all the DFT calculations and XRD structure determination.

Dr. Ferdinand Wild for MS, TGA and DSC measurements.

Dr. Thomas Fox for performing fantastic NMR measurement.

Dr. Heinz Spring for elemental analysis.

Dr. Jae Kyoung Pak, Susanna Sprokkereef, Nathalie Fichter and Ramona Erni for their help with the administrative tasks, Dr. Manfred Jöhri for computer related assistance and Hanspeter Stalder for technical support.

Dr. Jai Anand Garg, Michael Koch, Alexander Szentkuti, Michael Bachmann, Jessica Clavadetscher, Lubin Ni, Yunjun Shen, Dr. Yanfeng Jiang, Rajesh Kunjanpillai, Dr. Rajkumar Jana, Franziska Lissel, Dr. Ying Zhou, Dr. Chunfang Jiang, Dr. Yan Li, Dr. Xianghua Yang, Dr. Hailin Dong, Dr. Samir Barman. Gabriele Grieco, Pascal Plüss, Subrata Chakraborty and Hongfei Liu for discussions, good suggestions and great help for various measurements.

I would like to thank our collaborators, Prof Rainer Winter and Prof. Jeschke Gunnar.
I would like to thank Prof. Zilu Chen and Prof. Fupei Liang for their great support.

Financial support from UZH and ACI is gratefully acknowledged.

In the end I would like to thank my wife Chuanli Nie and my son Xiuning Zhang, my parents Laifeng Zhang and Ziyun Qiao for their constant love and support. I really appreciate their great patience and understanding. Without their support I wouldn’t have been able to accomplish this work.

List of metal complexes

- [Pt(pmim)$(I)_2$]
- [Pt(pmim)$(C\equiv C\text{-}C_6H_5)_2$]
- [Pt(pmim)$(C\equiv C\text{-}C_6H_4OMe)_2$]
- [Pt(pmim)$(C\equiv C\text{-}C6H_2(OMe)_3)_2$]
- [Pt(pmim)$(C\equiv C\text{-}C_6H_4N(Me)_2)_2$]
- [Pt(pmim)$(C\equiv C\text{-}C_4H_3S)_2$]
- [Pt(pmim)$(C\equiv C\text{-}C_6H_4C\equiv C\text{-}C_6H_5)_2$]
- [Pt(pmim)$(C\equiv C\text{-Pyrenyl})_2$]
- [Pt(pmim)$(C\equiv C\text{-}C_6H_4F)_2$]
- [Pt(COD)$(C\equiv C\text{-}C_6H_4F)_2$]
- [Pt(COD)$(C\equiv C\text{-}C_6H_2(OMe)_3)_2$]
- [Pt(COD)$(C\equiv C\text{-}C_4H_3S)_2$]
- *cis*-[Pt$(dbim)_2(C\equiv C\text{-}C_6H_4F)_2$]
- *trans*-[Pt$(dbim)_2(C\equiv C\text{-}C_6H_4F)_2$]
- *cis*-[Pt$(dbim)_2(C\equiv C\text{-}C_6H_5)_2$]
- *trans*-[Pt$(dbim)_2(C\equiv C\text{-}C_6H_5)_2$]
- *cis*-[Pt$(dbim)_2(C\equiv C\text{-}C_6H_2(OMe)_3)_2$]
- *trans*-[Pt$(dbim)_2(C\equiv C\text{-}C_6H_2(OMe)_3)_2$]
- *cis*-[Pt$(dbim)_2(C\equiv C\text{-}C_4H_3S)_2$]
- *trans*-[Pt$(dbim)_2(C\equiv C\text{-}C_4H_3S)_2$]
- *cis*-[Pt$(dbim)_2(C\equiv C\text{-}C_6H_4C\equiv C\text{-}C_6H_5)_2$]
- *trans*-[Pt$(dbim)_2(C\equiv C\text{-}C_6H_4C\equiv C\text{-}C_6H_5)_2$]
- *cis*-[Pt$(ibim)_2(C\equiv C\text{-}C_6H_5)_2$]
- *trans*-[Pt$(ibim)_2(C\equiv C\text{-}C_6H_5)_2$]
- [Pt(pmdb)$(I)_2$][a]
- [Pt(pm2tz)$(Br)_2$][a]
- [Pt(pm3tz)I_2]
- [Pt(pmdb)$(C\equiv C\text{-}C_6H_4F)_2$][a]
- [Pt(pmdb)$(C\equiv C\text{-}C_6H_5)_2$][a]
- [Pt(pmdb)$(C\equiv C\text{-}C_6H_4OMe)_2$][a]
- [Pt(pm2tz)$(C\equiv C\text{-}C_6H_4F)_2$][a]
- [Pt(pm2tz)$(C\equiv C\text{-}C_6H_5)_2$]
- [Pt(pm2tz)$(C\equiv C\text{-}C_6H_4OMe)_2$][a]
- [Pt(pm2tz)$(C\equiv C\text{-Si}(Me)_3)_2$][a]
- [Pt(pm3tz)$(C\equiv C\text{-}C_6H_4F)_2$]
- [Pt(pm3tz)$(C\equiv C\text{-}C_6H_5)_2$]
- [Pt(pm3tz)$(C\equiv C\text{-}C_6H_4OMe)_2$]
- [Pt(ppim)$(C\equiv CC_6H_4F)_2$]
- [Pt(ppim)$(C\equiv CC_6H_5)_2$]
- [Pt(ppim)$(C\equiv CC_6H_4N(C_6H_5)_2)_2$]
- [Pt(ppbim)$(C\equiv CC_6H_4F)_2$]

- [Pt(ppbim)(C≡CC_6H_5)$_2$]
- [Pt(ppbim)(C≡CC_6H_4N(C_6H_5)$_2$)$_2$]
- *cis*-[Pt(dpim)$_2$(C≡CC_6H_4F)$_2$]
- *trans*-[Pt(dpim)$_2$(C≡CC_6H_4F)$_2$]
- *cis*-[Pt(dpim)$_2$(C≡CC_6H_5)$_2$]
- *trans*-[Pt(dpim)$_2$(C≡CC_6H_5)$_2$]
- *cis*-[Pt(ddim)$_2$(C≡CC_6H_5)$_2$]
- *trans*-[Pt(ddim)$_2$(C≡CC_6H_5)$_2$]
- *cis*-[Pt(dptz)$_2$(C≡CC_6H_4F)$_2$]
- *trans*-[Pt(dptz)$_2$(C≡CC_6H_4F)$_2$]
- *cis*-[Pt(dptz)$_2$(C≡CC_6H_5)$_2$]
- *trans*-[Pt(dptz)$_2$(C≡CC_6H_5)$_2$]

[a] The first synthesis was accomplished by Jessica Clavadetscher.

Yuzhen Zhang
Institute of Inorganic Chemistry, University of Zurich, Winterthurerstrasse 190,
CH-8057 Zurich, Switzerland

Tel.: +41-788306590, yuzhen.zhang.sh@gmail.com; yuzhen.zhang@aci.uzh.ch

Personal information

Date of Birth:	Apr. 29, 1982
Native Place:	Shandong Province
Nationality:	Chinese
Gender:	Male
Marital Status:	Married

Education

Sep. 2009 – Aug. 2013

Ph.D. Institute of Inorganic chemistry , University of Zurich, Switzerland

Doctoral Thesis

Synthesis and Photophysical Investigations of Novel Deep Blue Triplet Emitters Based on N-Heterocyclic Carbene Pt(II) Acetylide Complexes for Light Emitting Devices

Advisor: Dr. Koushik Venkatesan

Sep. 2004 – Jul. 2007

M.Sc. in inorganic chemistry, Faculty of Chemistry and pharmacy, Guangxi Normal University, Guilin, China

Master Thesis

Synthesis of Nickel(II) Complexes Containing NH Functionality and Their Applications in Asymmetric Catalysis

Advisor: Prof. Dr. Zi-Lu Chen

Sep. 2000 – Jul. 2004

Bachelor in chemistry, Department of Chemistry, Linyi Normal University, Linyi, China

Sep. 1997 – Jul. 2000

High School Student, Pingyi NO. 1 Middle School, Shandong Province, China

Working Experience

Jul. 2007 – Aug. 2009

Chemical Inspector, Guangxi Zhuang Autonomous Region Institute for the Prevention and Treatment of Occupational Diseases, Guangxi, China

Publications

1. **Yuzhen Zhang**, Jai Anand Garg, Clement Michelin, Thomas Fox, Olivier Blacque, and Koushik Venkatesan. Synthesis and Luminescent Properties of *cis* Bis-N-Heterocyclic Carbene Platinum(II) Bis-Arylacetylide Complexes. *Inorg. Chem.*, **2011**, *50*, 1220–1228
2. **Yuzhen Zhang**, Olivier Blacque, and Koushik Venkatesan. Highly Efficient Deep Blue Emitters Based on *cis* and *trans* N-Heterocyclic Carbene Pt(II) Acetylide Complexes: Syntheses, Photophysical Properties and Mechanistic Studies. *Chem.-Eur. J.*, **2013**, *19*, 15689-15701.
3. **Yuzhen Zhang**, Jessica Clavadetscher, Michael Bachmann, Olivier Blacque, and Koushik Venkatesan. Tuning the Luminescence Properties of Pt(II) Acetylide Complexes through Varying the Donor Properties of N-Heterocyclic Carbene Ligands. **2013**, **Submitted**.
4. **Yuzhen Zhang**, Olivier Blacque, and Koushik Venkatesan. Rational Design of Highly Efficient Deep Blue Emitting N-Heterocyclic Carbene Pt(II) Acetylide Complexes. **2013**, **Manuscript under preparation**.
5. **Yuzhen Zhang**, Olivier Blacque, Jeschke Gunnar, Rainer F. Winter, and Koushik Venkatesan. Electronic Coupling in Mixed-Valence *cis* and *trans* N-Heterocyclic Carbene Pt(II) Triarylamine Acetylide Complexes. **2013**, **Manuscript under preparation**.
6. Zilu Chen, Mulan Zeng, **Yuzhen Zhang,** Zhong Zhang, and Fupei Liang. Preparation and Structures of A Series of Phosphorus-free Nickel(II) Diamine Complexes and Their Applications in Hydrogenation of Acetonphenoe. *Appl. Organometal. Chem.*, **2010**, *24*, 625-630.